

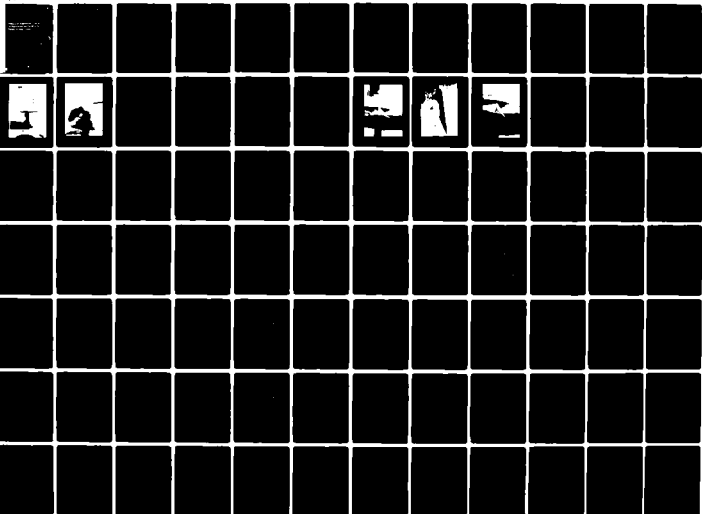
AD-A118 418

VOUGHT CORP ADVANCED TECHNOLOGY CENTER DALLAS TX F/G 20/4
PROPULSION AUGMENTED CONTROL/LIFT SURFACE VALIDATION FOR MISSILE--ETC(U)
APR 82 R L MASK, J S SPANGLER, C H HAIGHT N60921-80-C-A053
ATC-R-91100/2CR-21 NL

UNCLASSIFIED

1 of 2

A
000008



ATC REPORT NO. R-91100/2CR-21
CONTRACT NO. N60921-80-C-A053

Propulsion Augmented Control/Lift Surface Validation for Missile Maneuver Application

AD A118418
APRIL 1982

R. L. Mask
J. G. Spangler
C. H. Haight

Vought Corporation Advanced Technology Center
P.O. Box 226144
Dallas, Texas 75266

DTIC
AUG 20 1982
H

APPROVED FOR PUBLIC RELEASE: DISTRIBUTION UNLIMITED

Prepared for:
Naval Surface Weapons Center
Dahlgren Laboratory
Dahlgren, Virginia 22448

DTIC FILE COPY



VOUGHT CORPORATION
Advanced Technology Center

82 08 20 043

UNCLASSIFIED

SECURITY CLASSIFICATION OF THIS PAGE (When Data Entered)

REPORT DOCUMENTATION PAGE		READ INSTRUCTIONS BEFORE COMPLETING FORM
1. REPORT NUMBER	2. GOVT ACCESSION NO. AD-A118 418	3. RECIPIENT'S CATALOG NUMBER
4. TITLE (and Subtitle) Propulsion Augmented Control/Lift Surface Validation for Missile Maneuver Application		5. TYPE OF REPORT & PERIOD COVERED Final Report
7. AUTHOR(s) R. L. Mask J. G. Spangler C. H. Haight		6. PERFORMING ORG. REPORT NUMBER R-91100/2CR-21
9. PERFORMING ORGANIZATION NAME AND ADDRESS Vought Corporation Advanced Technology Center P. O. Box 226144 Dallas, Texas 75266		8. CONTRACT OR GRANT NUMBER(s) N60921-80-C-A053
11. CONTROLLING OFFICE NAME AND ADDRESS Naval Surface Weapons Center Dahlgren Laboratory Dahlgren, Virginia 22448		10. PROGRAM ELEMENT, PROJECT, TASK AREA & WORK UNIT NUMBERS
14. MONITORING AGENCY NAME & ADDRESS (if different from Controlling Office)		12. REPORT DATE April 1982
		13. NUMBER OF PAGES 155
		15. SECURITY CLASS. (of this report) UNCLASSIFIED
		15a. DECLASSIFICATION/DOWNGRADING SCHEDULE
16. DISTRIBUTION STATEMENT (of this Report) Approved for Public Release; Distribution Unlimited		
17. DISTRIBUTION STATEMENT (of the abstract entered in Block 20, if different from Report) -		
18. SUPPLEMENTARY NOTES -		
19. KEY WORDS (Continue on reverse side if necessary and identify by block number) Vertical Jet, Propulsive Augmentation, Lift Augmentation, Supersonic Maneuverability, Supersonic Lift Augmentation, Induced Lift, Missile Control Surfaces, Supersonic Jet Flap.		
20. ABSTRACT (Continue on reverse side if necessary and identify by block number) Improved maneuverability and controllability are prime goals in meeting a broad spectrum of tactical missile requirements. Configurations based on the Vought "Propulsion Augmented Control/Lift Surface" (PACS) approach to aeropropulsive integration are candidates for satisfying these requirements. The PACS concept utilizes a jet issuing from a trailing edge nozzle to induce augmented control loadings over fin or wing planforms. The current work provides experimental validation of PACS feasibility for a representative		

DD FORM 1 JAN 73 1473

EDITION OF 1 NOV 65 IS OBSOLETE
S/N 0102- LF- 014- 6601

UNCLASSIFIED

SECURITY CLASSIFICATION OF THIS PAGE (When Data Entered)

UNCLASSIFIED

SECURITY CLASSIFICATION OF THIS PAGE (When Data Entered)

missile fin geometry at typical supersonic/transonic conditions. A test program was carried out for a series of PACS arrangements as well as for a baseline conventional fin/elevon. Significant advantages were quantified for PACS in the context of equivalent baseline elevon/unitary fin deflections, thrust vectoring force augmentation, high mach number force generation, and control surface sizing. The successful feasibility results provide strong motivation for proceeding with coordinated technology and application studies.

Accession	
NTIS	
DTIC	
U	
J	
By	
Distribution	
As	or
Dist	
A	

DSIS
COPY
INSPECTED
2

S/N 0102- LF-014-6601

UNCLASSIFIED

SECURITY CLASSIFICATION OF THIS PAGE (When Data Entered)

FOREWORD

This investigation was performed by Vought Corporation Advanced Technology Center, Dallas, Texas for the Naval Surface Weapons Center (Contract No. N60921-80-C-A053). The NSWC contract monitors were Dr. F. G. Moore and Mr. Richard Solis.

TABLE OF CONTENTS

	<u>PAGE</u>
FOREWORD	ii
LIST OF FIGURES	iv
NOMENCLATURE	v
1.0 INTRODUCTION	1
2.0 PACS CONCEPT	2
3.0 TECHNICAL APPROACH	4
3.1 MODEL INSTALLATION AND INSTRUMENTATION	4
3.2 HIGH SPEED WIND TUNNEL TEST PROGRAM	6
3.2.1 Test Facility	6
3.2.2 Model Descriptions	6
4.0 TEST RESULTS AND DISCUSSIONS	17
4.1 RUN SUMMARY	17
4.2 LIFT AND DRAG PERFORMANCE	17
4.2.1 SIG-D Baseline Performance	17
4.2.2 PACS-1 Performance	17
4.2.3 PACS-2/PACS-4 Performance	22
5.0 CONCLUSIONS	34
6.0 RECOMMENDATIONS	35
7.0 REFERENCES	36
APPENDIX	37

LIST OF FIGURES

<u>FIGURE</u>	<u>DESCRIPTION</u>	<u>PAGE</u>
2-1	PACS Concept - Two-Dimensional Analog	3
3-1	0.1364 Scale SIG-D Model	5
3-2	HSWT Model Support	7
3-3	HSWT Model Support	8
3-4	HSWT End Plate Disc with a Metric SIG-D Fin Installed	9
3-5	Transonic Test Section and Ejector	10
3-6	SIG-D and PACS HSWT Fin Models	12
3-7	PACS Fin Configurations	13
3-8	PACS-1 Fin Installation	14
3-9	PACS-2 Fin Hardware	15
3-10	PACS-4 Fin Installation	16
4-1	Summary of HSWT Test	18
4-2	SIG-D Fin $M_\infty = 1.8$	19
4-3	Lift and Drag Comparisons of the SIG-D and PACS-1 Fins with $\delta_F = 0^\circ$	20
4-4	Lift and Drag Comparisons of the SIG-D and PACS-1 Fins with $\delta_F = 7^\circ$	21
4-5	PACS-2 Fin Lift and Drag Performance - $\delta_j = 135^\circ$	23
4-6	PACS-2 Comparison with Unit Fin	25
4-7	Effect of Jet Angle on Lift and Drag Performance - PACS-2	26
4-8	Comparison of Part and Full-Span Blowing - $\delta_j = 135^\circ$	27
4-9	Lift Generated by Transverse Jet Ejection - $\delta_j = 90^\circ, 135^\circ$	28
4-10	Lift Force Amplification Generated by Transverse Jet Ejection	29
4-11	Lift Amplification vs. M_∞ for $C_\mu = 0.1$	30
4-12	Comparison of Control Effectiveness	32
4-13	Wing Area Reduction Potentials	33

NOMENCLATURE

A	Planform reference area	
c	Chord length	
C_D	Drag coefficient	
C_L	Lift coefficient	
C_{L_0}	Lift coefficient at zero angle of attack	
C_p	Pressure coefficient	
C_μ	Blowing jet momentum coefficient	$\frac{\dot{m}_j \bar{V}_j}{q_\infty A}$
M_∞	Freestream Mach number	
\dot{m}_j	Jet Mass Flow	
q_∞	Freestream dynamic pressure	
Re	Reynolds number	
\bar{V}_j	Jet Velocity obtained by expansion from plenum total pressure to freestream static pressure	
X	Distance	
α	Angle of attack	
δ_F	Flap/elevon deflection angle	
δ_j	Jet deflection angle	

1.0 INTRODUCTION

Improved maneuverability and controllability are prime goals for a broad spectrum of tactical missile requirements. These requirements cover conditions for low dynamic pressure launch, cruise evasive maneuvers, high altitude control responsiveness, and high g terminal targeting maneuvers. Besides the generation of basic maneuver and control forces, lift increments are often required at constrained angles of attack to meet maneuver g requirements without exceeding system limits (e.g., wing/fin effectiveness, inlet stall, adverse plume interactions). Configurations based on the Vought "propulsion augmented control/lift surface (PACS)" approach to aeropropulsive integration are candidates for improving both the controllability and maneuvering lift necessary to satisfy the above requirements. Fin applications provide the potential for increased control effectiveness, reduced actuator force and size (weight) requirements, and improved flexibility in low observable design. A forward wing application can provide maneuvering lift at even low angles of attack in small-size, low-drag geometries.

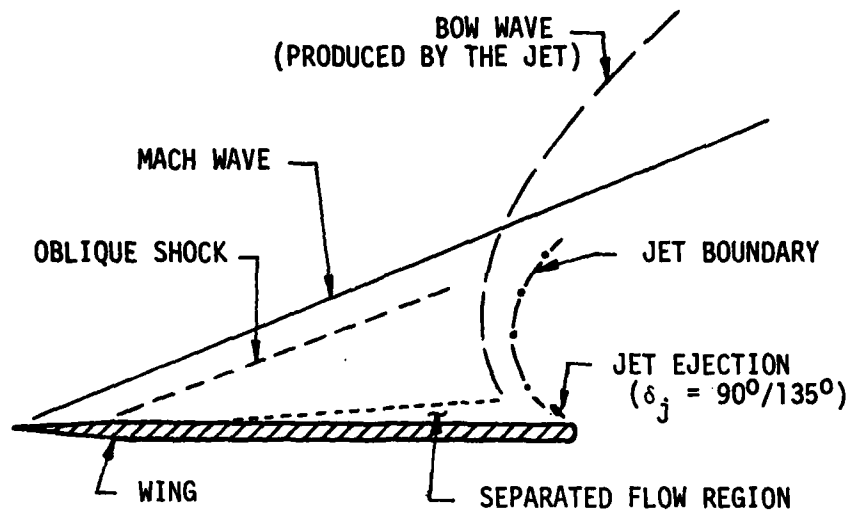
The PACS concept is applicable generically to a wide range of missiles, independent of propulsion system (i.e. rocket, integral rocket/ramjet, supersonic expendable turbine, etc.), and can also be applied specifically to standoff intercept, wide-area defense, or short-range point defense configurations. Missile applications have evolved from extensive IR&D and Navy¹⁻⁴ contract efforts that have utilized propulsive flow injection at the trailing edge of subsonic and transonic airfoil geometries to achieve high lift and tailored moment characteristics while minimizing drag and propulsive bleed requirements. Benefits at subsonic and transonic conditions are realized with rearward near-tangential injection and the associated normal force increments relative to injection momentum are typified experimentally in references 1-4. Benefits in supersonic flight correspond to compatible rotations of the injection jet to normal or upstream angles where jet interaction-induced loadings similar to those exhibited two-dimensionally in reference 5 are realized. The present contract experiments extend the PACS data base to include real missile planform effects from supersonic down to transonic flight conditions and lay the groundwork for specific application studies. The data serve as points of departure for simulations of propulsion integration sources as varied as primary exhaust/combustor bleed, auxiliary high-pressure gas supplies, and small solid fuel thrusters.

2.0 PACS CONCEPT

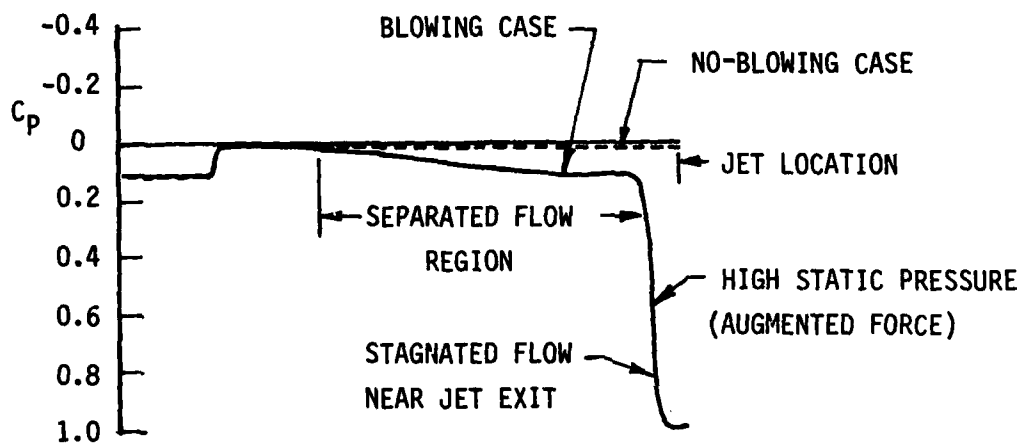
The effective force generated by a control or lifting surface is enhanced if the surface loading can be influenced by auxiliary aeropropulsive flow field perturbations. These flow perturbations can be generated at subsonic and transonic speeds by utilizing active circulation or boundary layer control¹⁻⁴ (e.g., blowing jets) at the trailing edge to alter the upstream surface loading patterns. At supersonic speeds, planform loading can be enhanced by rotatable trailing edge blowing jets, compatible with transonic systems, that utilize the mechanism of forced shock wave-boundary layer interactions. Experiments performed on flat plates⁵⁻⁸ have shown that a jet sheet issuing into a supersonic flow region influences the upstream pressure distributions by establishing a standing shock structure and associated boundary layer separation. The jet sheet forces the external flow to stagnate and separate near the jet exit creating a bow shock wave, as illustrated in Figure 2-1. A high local static pressure region is established ahead of the jet location which adds a force on the control surface in the same direction as the reaction force of the jet, thus augmenting the overall control effect.

When properly integrated into a missile configuration this type of control augmentation has the potential for enhancing performance and reducing or eliminating the requirements for movable control surfaces and their associated actuators. The PACS concept offers significant control augmentation benefits with relatively small bleed-off of propulsion energy. Applications for selected missions/configurations also show trade benefits in weight and packaging by replacing conventional fin actuators with compressed gas or small solid fuel impulse thrusters to supply the control jet without bleeding the main propulsion. This approach also provides control augmentation after engine burn-out for terminal maneuver requirements.

The purpose of this study has been to generate PACS lift/control augmentation data for a representative supersonic/transonic missile planform and to compare the results with the forces achieved through conventional unitary or deflected control surface configurations. Although the scope of the present program precluded optimization of the benefits of a PACS system, it successfully demonstrated the potential benefits that are inherent with this approach.



A. REPRESENTATIVE SUPERSONIC FLOW FIELD WITH JET EJECTION



B. PRESSURE DISTRIBUTION

FIGURE 2-1 PACS CONCEPT - TWO-DIMENSIONAL ANALOG

3.0 TECHNICAL APPROACH

The existing data base for supersonic missile maneuverability/control-ability is limited. There is a continual need to establish a foundation from which generic configurations can be evaluated. Requirements for performance seem to consistently exceed proven technology validations. The specialized nature of most missile systems and missions has forced experimental and analytical efforts to consider point designs without the opportunity to assess basic technology improvements. This program has been structured to investigate a basic category of phenomena related to control/maneuver force effectiveness. While some analytical background does exist, it is readily obvious that new experimental data is critical to provide guidelines to future technology advances. In keeping with this argument, the approach to preliminary evaluation of the PACS concept has centered on a basic high speed wind tunnel test program, as described in the following section.

Performance estimates for the several PACS configurations and the SIG-D baseline (c.f. Section 3.2.2) were generated using a superposition calculation approach. The isolated wing/fin geometry performance was estimated with a linearized aerodynamic wing-body code utilizing a supersonic panel method. The PACS supersonic performance estimates were determined from correlations given in references 1, 5, 9, and 10.

3.1 MODEL INSTALLATION AND INSTRUMENTATION

In order to fairly evaluate the potential benefits expected with the PACS concept it was decided to focus the feasibility testing on three-dimensional configurations. As an attempt at simplification and to avoid interaction effects with the basic vehicle configuration, so as to test the performance of just the planform surfaces, an existing end-plated test installation was utilized. This allowed testing of three-dimensional control surface models in a manner that provided direct comparisons between a baseline and the various PACS configurations. The fin from the Vought SIG-D missile wind tunnel model, shown in Figure 3-1, was chosen as the test baseline because of its representative control requirements for a state-of-the-art supersonic missile. A large, thin, round disk was selected for the mounting base to provide clean supersonic flow to the test models, independent of angle of attack.

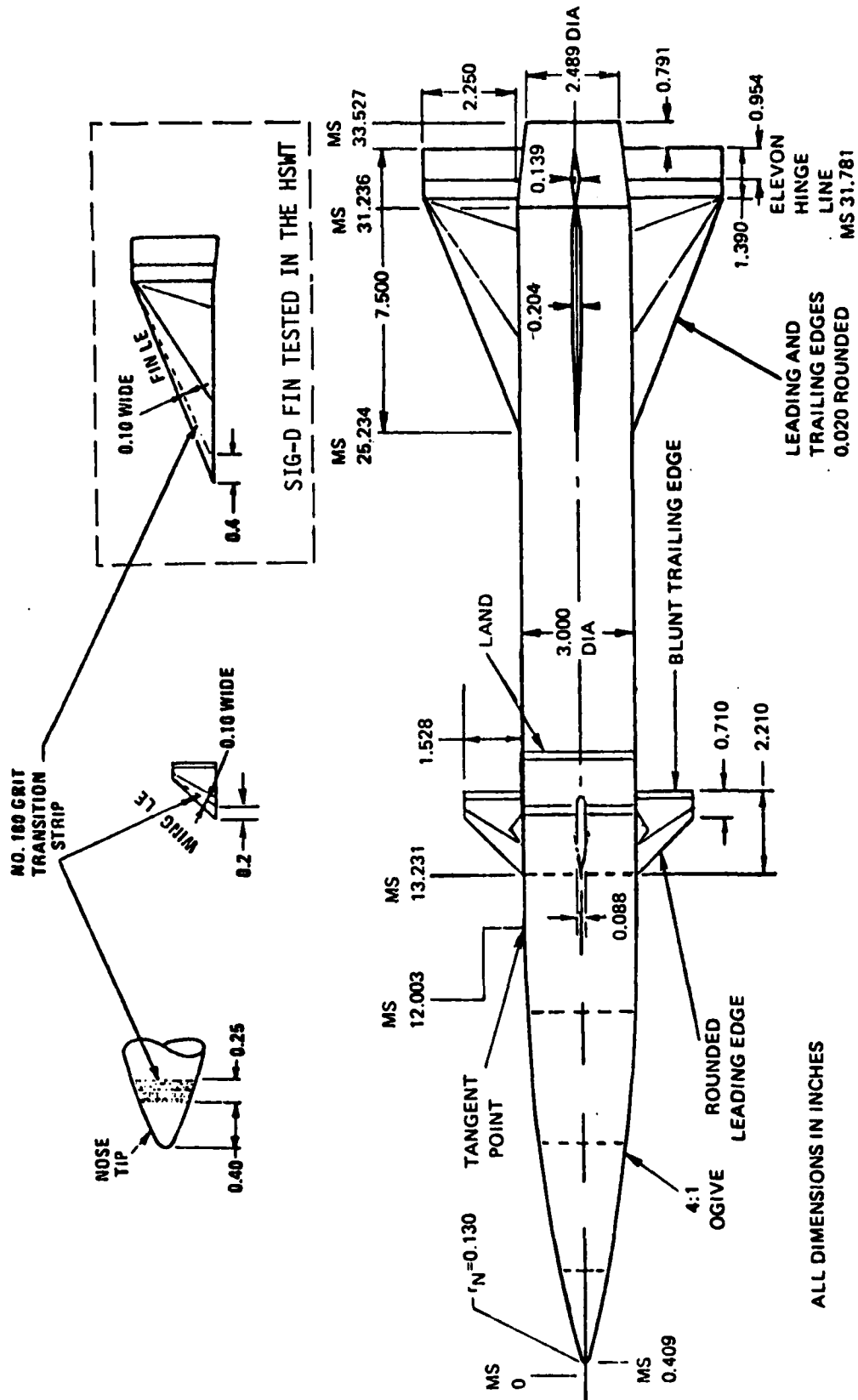


FIGURE 3-1 0.1364 SCALE SIG-D WIND TUNNEL MODEL

A sketch of the model support assembly is shown in Figure 3-2. Photographs of the model support installation in the tunnel are shown in Figures 3-3 and 3-4. The metric models were attached to a force balance at the center of the end-plate disc. The radius of the disc used with the models was 15 inches (38.1 cm). This radius was twice as large as the model root chord and approximately 6.5 times the model span thus insuring unperturbed three-dimensional flow over the fin models at both transonic and supersonic speeds. The fin and balance were fixed to the disc reference axis and rotated as a unit on the sting support. The high-pressure air source was connected through the hollow balance to the model plenum, as shown in Figure 3-2.

The balance output measurements supplied lift, drag, pitching moment and root bending moment information. The fin models and balance were dynamically isolated from the disc. The end-plate disc had six static pressure taps located in the surface to allow determination of local Mach numbers. Two static pressure orifices located ahead of the model were used to identify local freestream Mach numbers. Four orifices positioned near the upper and lower surfaces identified root leading edge wedge Mach numbers and mid-wing section Mach numbers. Discussion of the experimental results is presented in Section 4.0.

3.2 HIGH SPEED WIND TUNNEL TEST PROGRAM

3.2.1 Test Facility

The supersonic/transonic wind tunnel experiments were conducted in the Vought Corporation High Speed Wind Tunnel (HSWT). This facility is a variable pressure blow-down wind tunnel with a test section of 1.22 m by 1.22 m (4 ft by 4 ft) capable of Mach numbers from 0.5 to 5.0 and unit Reynolds numbers from 6 to 125 million per meter (2 to 38 million per foot). The HSWT has two test chambers, one for transonic tests and another for supersonic tests. A sketch of the HSWT transonic test section is shown in Figure 3-5. The PACS concept validation tests covered both transonic and supersonic Mach numbers from 0.9 to 3.0, at Reynolds numbers ranging from $7-8 \times 10^6$ per foot.

3.2.2 Model Descriptions

The HSWT metric fin models include the baseline SIG-D missile fin configuration and several PACS fin configurations. The SIG-D metric fin, shown in Figures

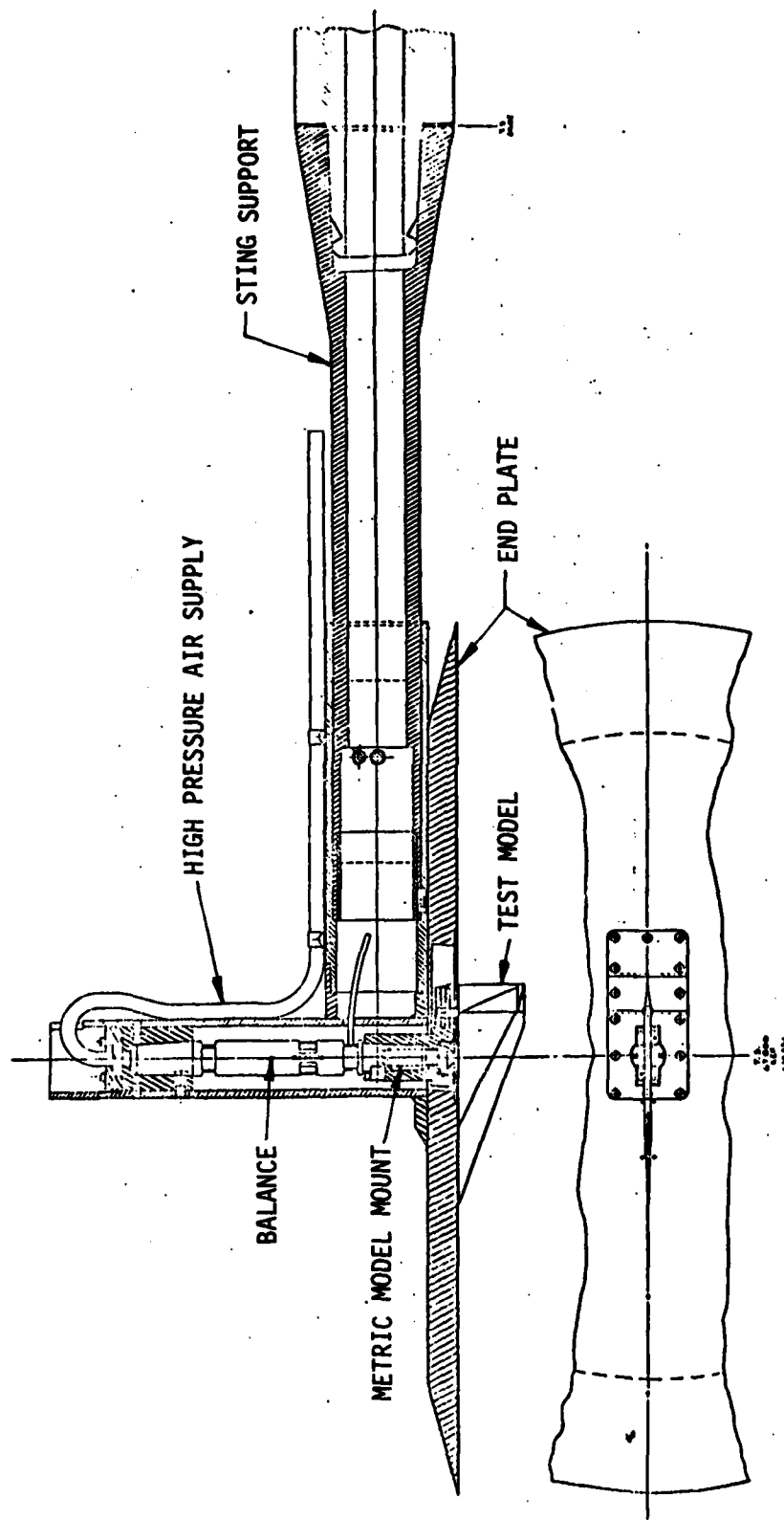


FIGURE 3-2 HSWT MODEL SUPPORT



FIGURE 3-3 HSWT MODEL SUPPORT



FIGURE 3-4 HSWT END PLATE DISC WITH A METRIC SIG-D FIN INSTALLED

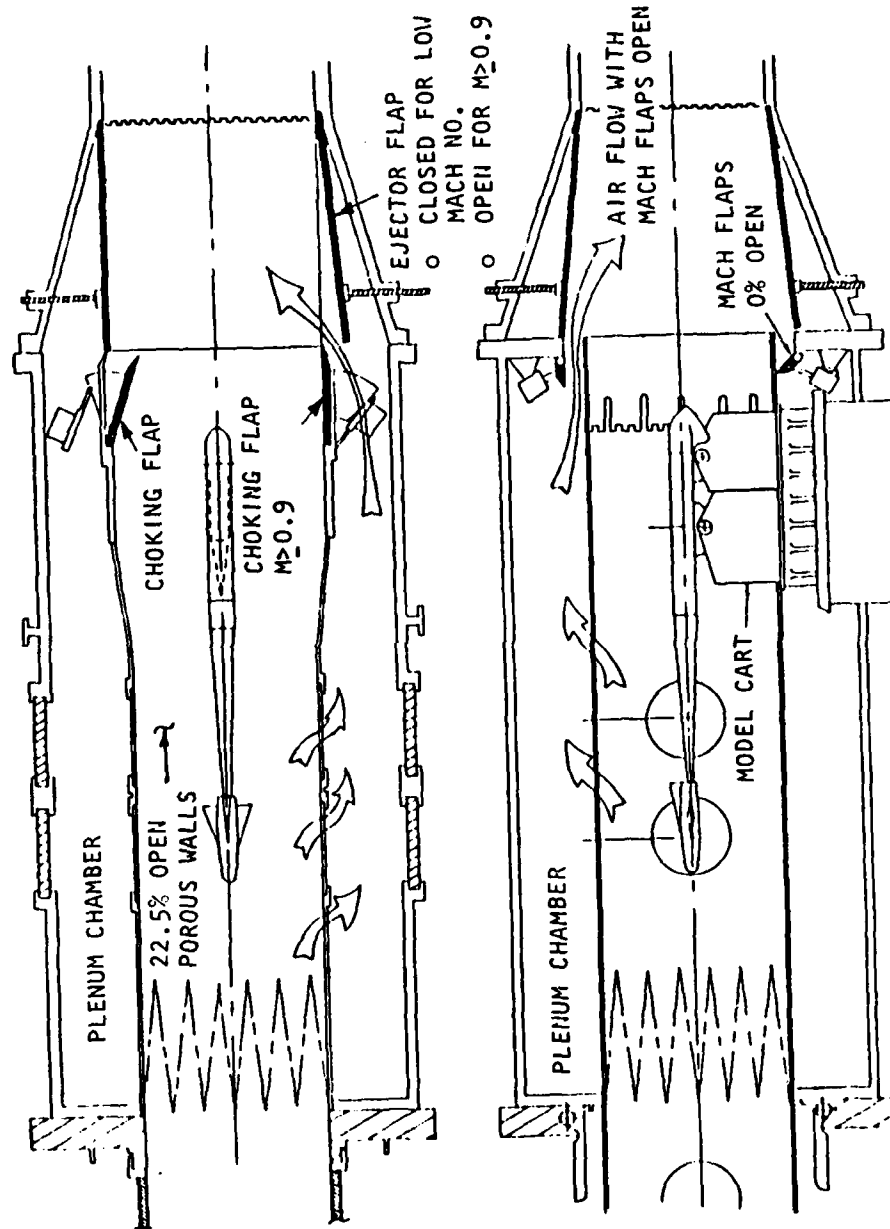


FIGURE 3-5 TRANSONIC TEST SECTION AND EJECTOR

3-4 and 3-6, is a 45-82 hex wing section, with a maximum thickness of 0.038C, coupled with a double-wedge full-span metric flap/elevon. The elevon test model was designed with a 0° and 7° deflection capability.

Several metric PACS configurations were sized to the envelope of the SIG-D fin geometry. The HSWT PACS models consist of a main wing design with an internal ducting plenum supplying high-pressure air (controlling C_{μ} conditions) to the various blowing jet arrangements attached to the fin trailing edge. These model variations are identified in Figures 3-6 and 3-7.

The PACS-1 geometry (see photograph in Figure 3-8) was designed for tangential blowing over a flap/elevon arrangement to provide an improved integrated cruise performance. The PACS -2 and 4 configurations (Figures 3-9, 10) are full and part-span vectored thrust (90°/135°) geometries designed for high maneuvering lift augmentations at supersonic speeds. The PACS-3 and 5 configurations were designed and fabricated for cruise drag improvements but were not tested. A discussion on the performance of each of these test configurations is presented in Section 4.

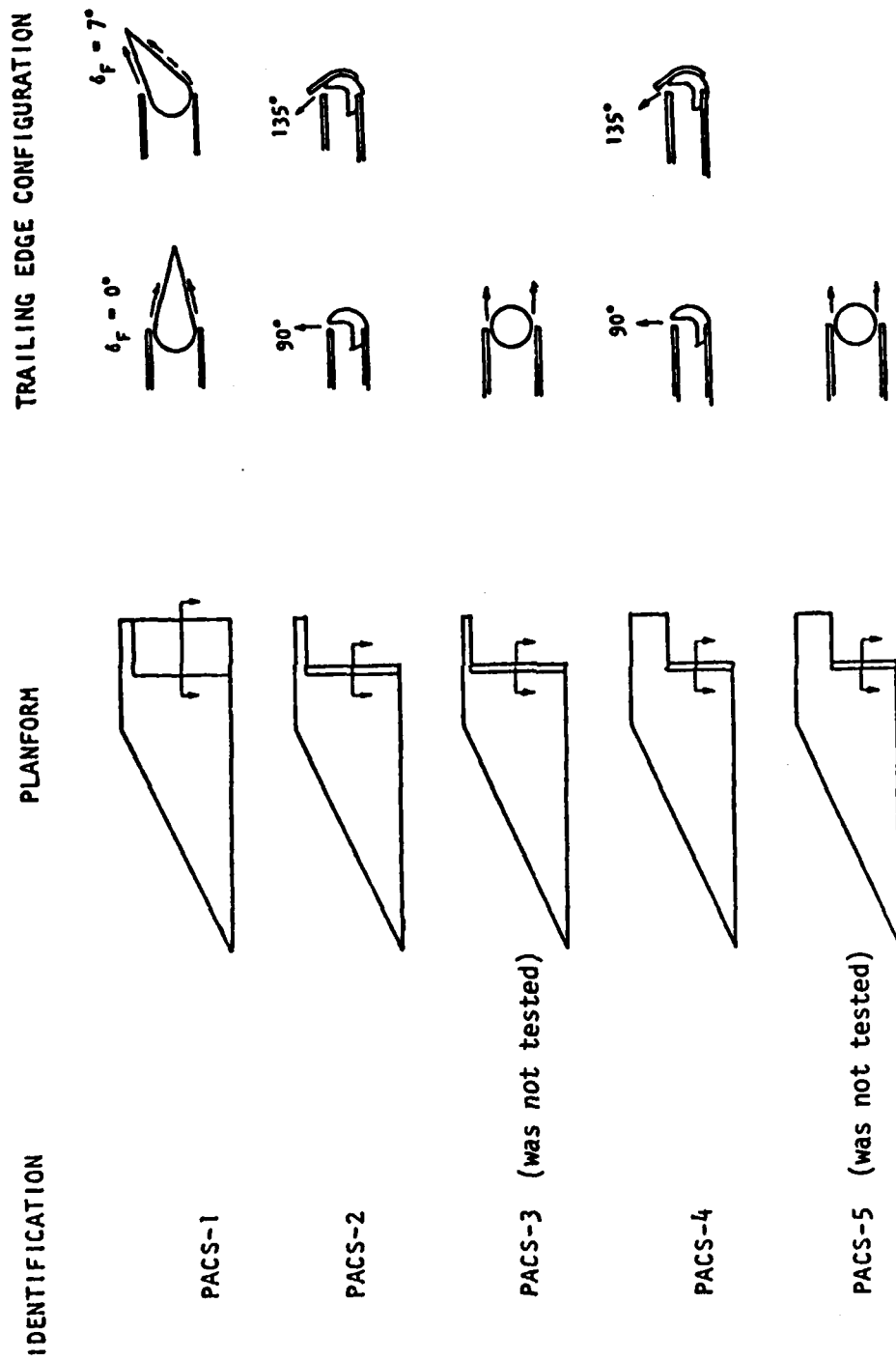


FIGURE 3-7 PACS FIN CONFIGURATIONS



FIGURE 3-8 PACS-1 FIN INSTALLATION

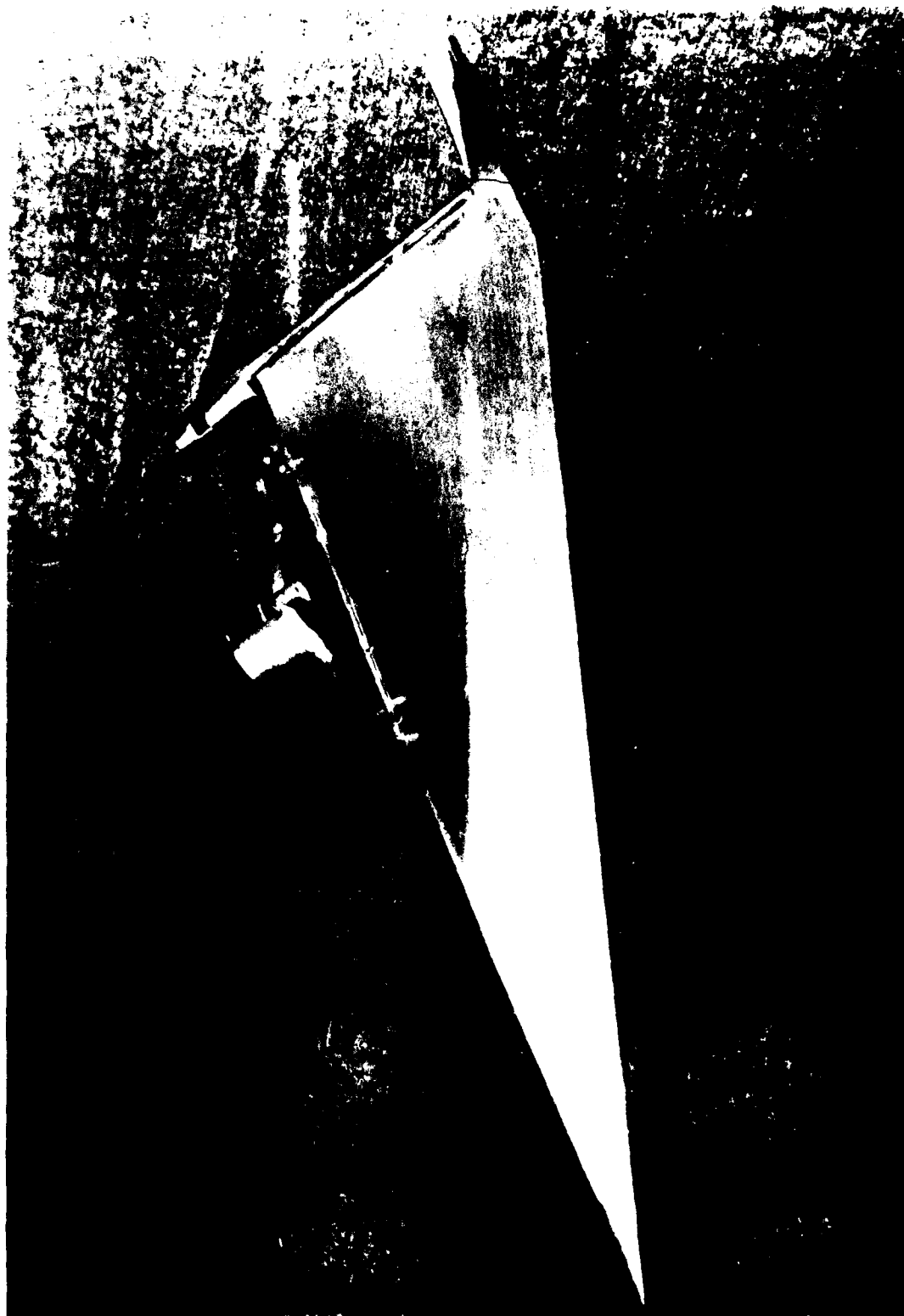


FIGURE 3-9 PACS-2 FIN HARDWARE

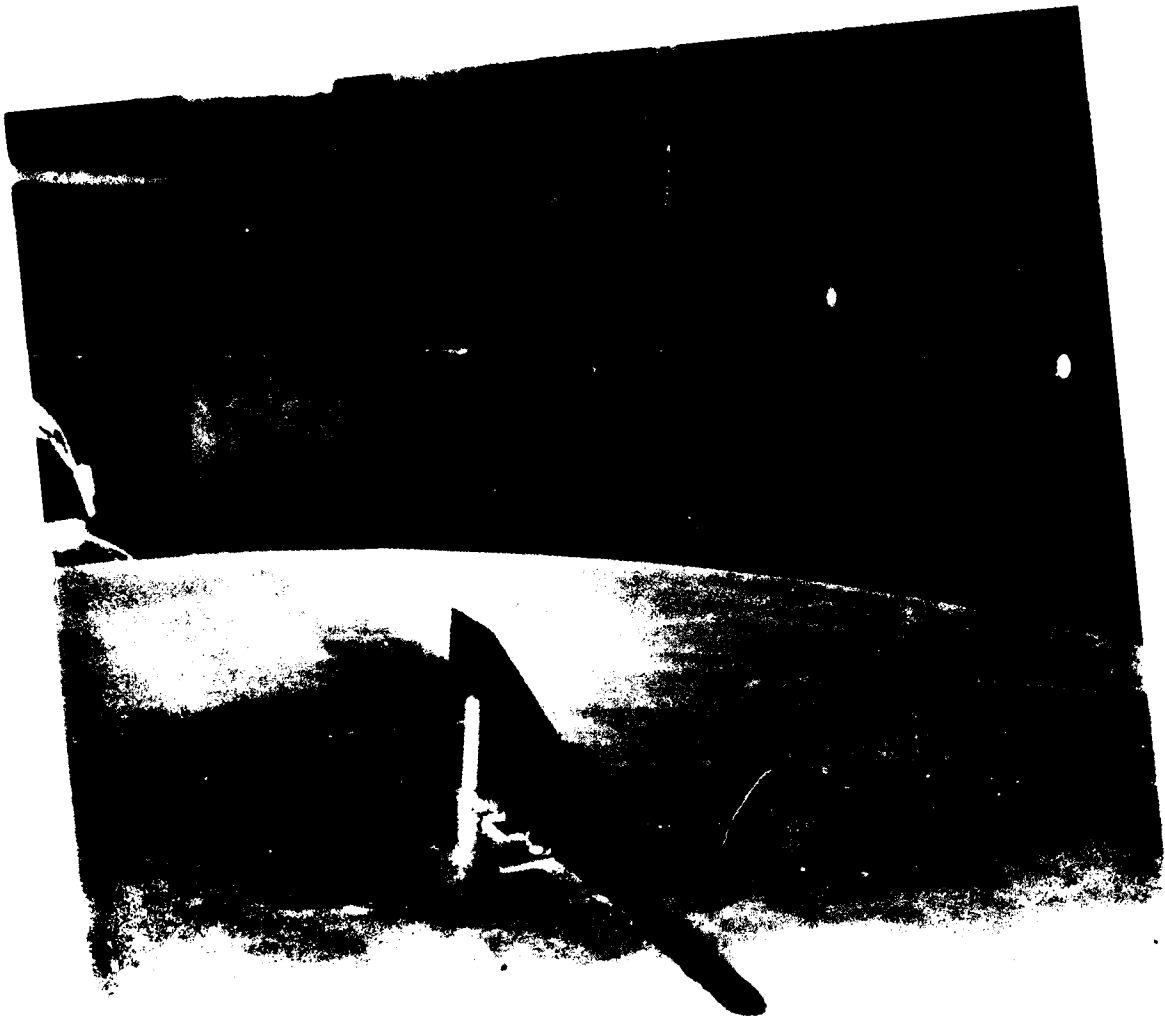


FIGURE 3-10 PACS-4 FIN INSTALLATION

4.0 TEST RESULTS AND DISCUSSION

4.1 RUN SUMMARY

A brief overview of the tests performed in the Vought HSWT is given in Figure 4-1. A detailed summary of the specific runs is listed in the Appendix including plotted data (C_L vs α and C_L vs C_D) for each individual test case. The initial test quantified the baseline SIG-D performance with/without flap deflection at supersonic and transonic speeds. After establishing the baseline performance, tests were then performed on the PACS configurations for the same range of flow conditions. The first tests established the influence of tangential blowing coupled with flap/elevon deflection (PACS-1). The following tests examined PACS transverse jet ejection (90° and 135° , PACS-2 and 4) for full and part-span blowing. These tests covered the Mach number range from 0.9 to 3.0. The angle of attack ranged from 0° to 12° , limited by the sting support maximum pitch angle and tunnel run/pump-up time constraints.

4.2 LIFT AND DRAG PERFORMANCE

A limited discussion on the lift and drag performance of each individual configuration is presented in the following sections. The performance of each configuration is shown for $M_\infty = 1.8$, followed by a detailed examination of the PACS-2 and 4 configurations overall performances. Detailed information on each individual test case is given in the Appendix.

4.2.1 SIG-D Baseline Performance

The SIG-D baseline fin performance at $M_\infty = 1.8$ is shown in Figure 4-2. The SIG-D baseline performance is defined for two elevon deflections, $\delta_F = 0^\circ$ and 7° . At $\alpha = 0^\circ$ the SIG-D fin C_{L_0} and C_D for $\delta_F = 0^\circ$ are 0.00 and 0.01, respectively. For $\delta_F = 7^\circ$, a $C_{L_0} = 0.06$ is generated providing a nominal lift increment of $\Delta C_L = 0.06$ with angle of attack. The baseline SIG-D performance, typical of conventional missile control systems, provides reference information for the following discussions. The SIG-D fin performance at other Mach numbers is summarized in the Appendix.

4.2.2 PACS-1 Performance

The PACS-1 tangential jet configuration performance at $M_\infty = 1.8$ is shown in Figures 4-3 and 4-4 for a flap/elevon deflection of 0° and 7° , respectively.

CONFIGURATION	M_∞	C_H
SIG-D $\delta_F = 0^\circ$	1.4, 1.8, 3.0	--
$\delta_F = 7^\circ$	0.9, 1.4, 1.8, 3.0	--
PACS-1 $\delta_F = 0^\circ$	0.9, 1.8, 3.0	0.0 - 0.0997
$\delta_F = 7^\circ$	0.9, 1.8, 3.0	0.0 - 0.0925
$\delta_F = 20^\circ$	0.9	0.0 - 0.0233
PACS-2 $\delta_J = 135^\circ$	1.4, 1.8, 3.0	0.0 - 0.111
PACS-4 $\delta_J = 90^\circ$	0.9, 1.4, 1.8, 3.0	0.0 - 0.0997
$\delta_J = 135^\circ$	1.4, 1.8, 3.0	0.0 - 0.1308

FIGURE 4-1 SUMMARY OF HSMT TEST

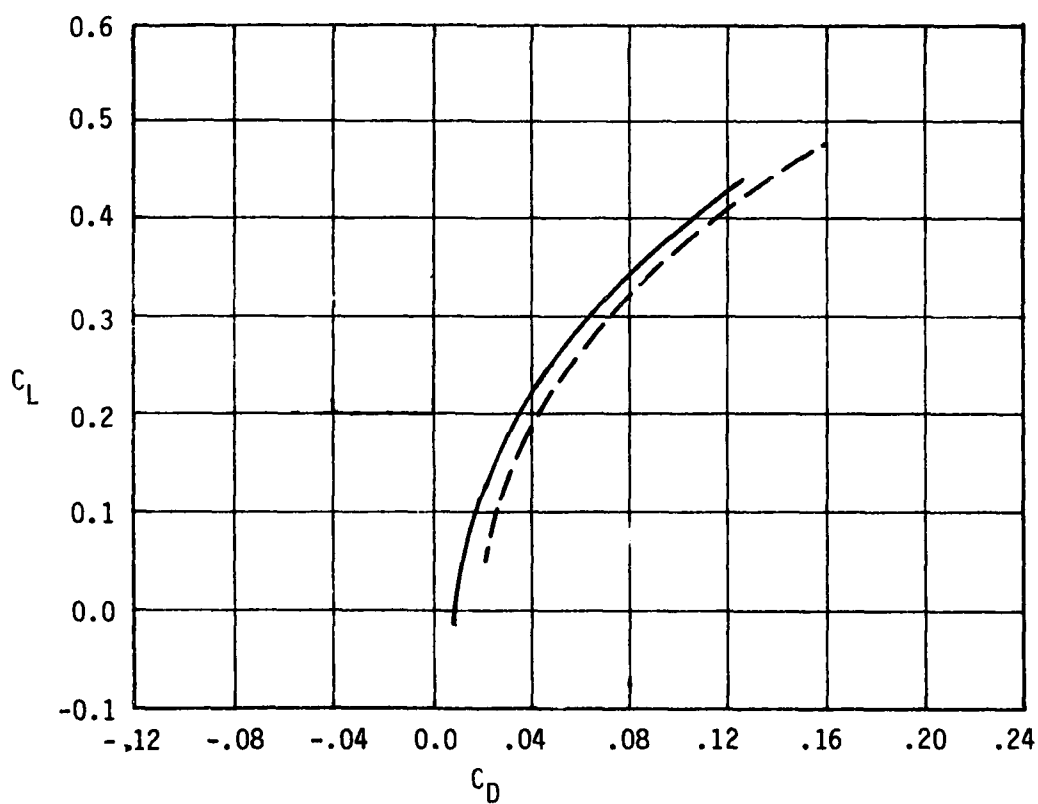
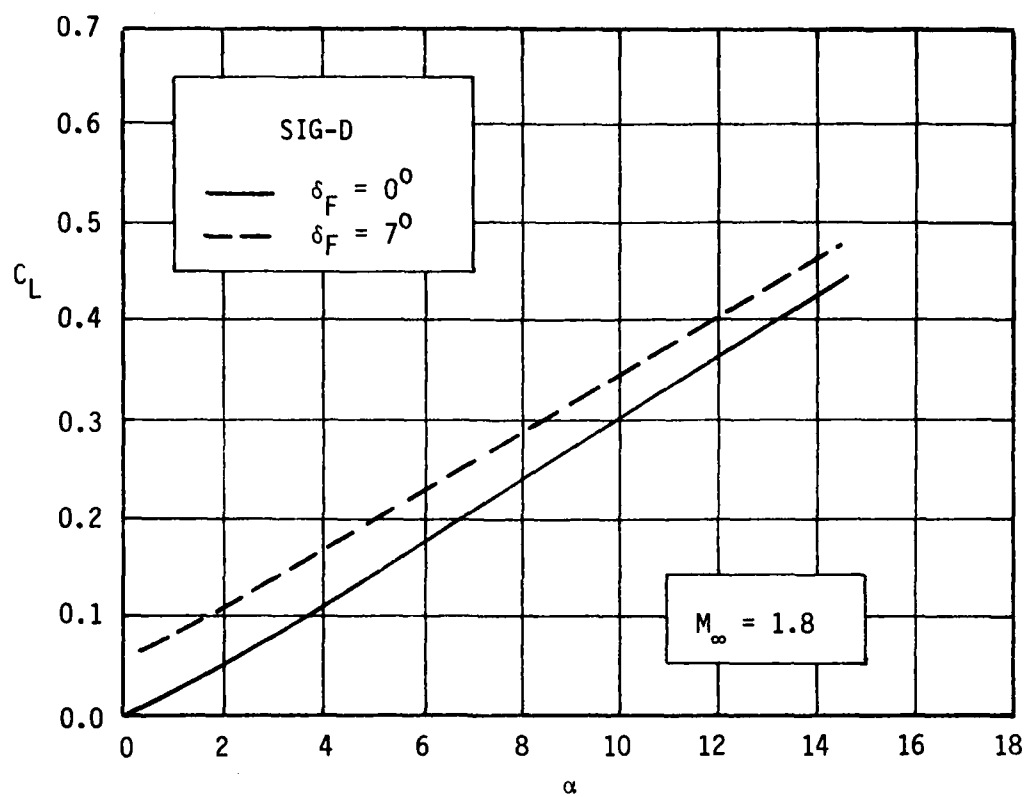


FIGURE 4-2 SIG-D FIN, $M_\infty = 1.8$

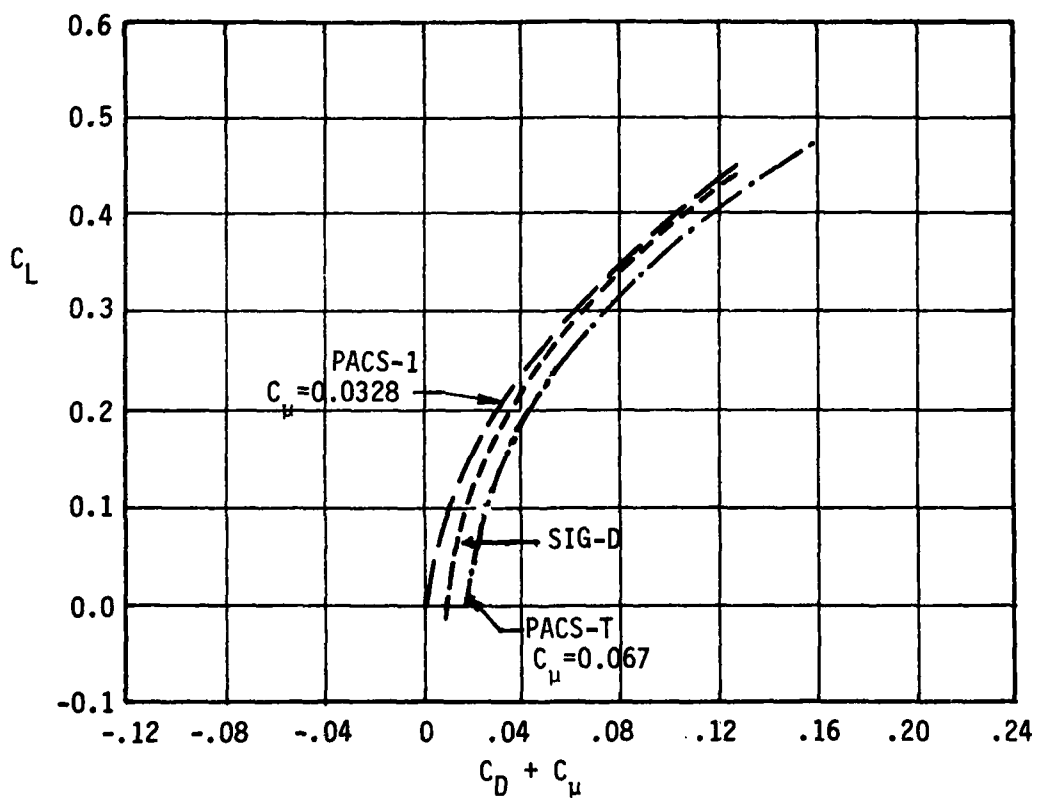
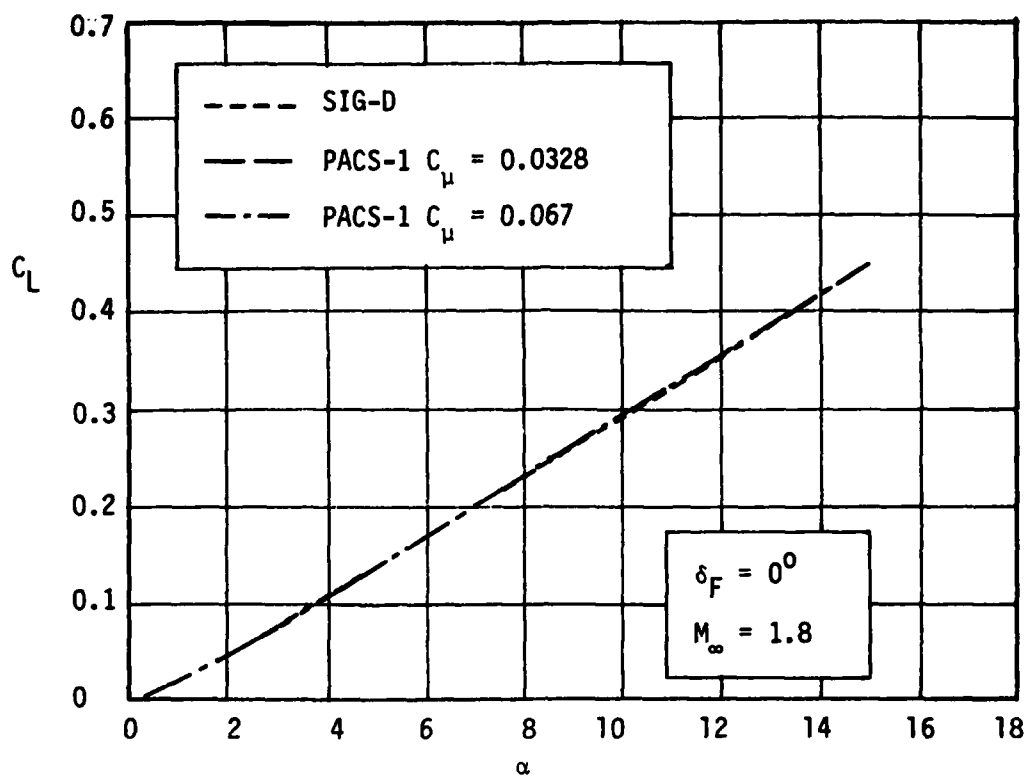


FIGURE 4-3 LIFT AND DRAG COMPARISONS OF THE SIG-D AND PACS-1 FINS WITH $\delta_F = 0^\circ$

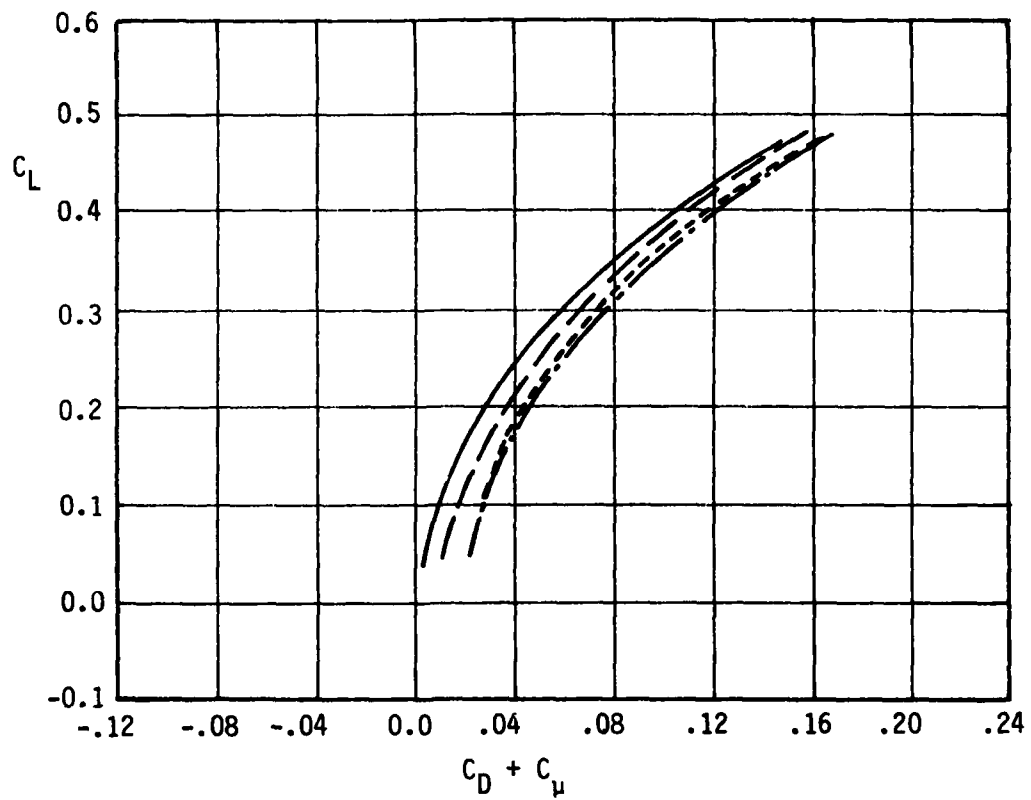
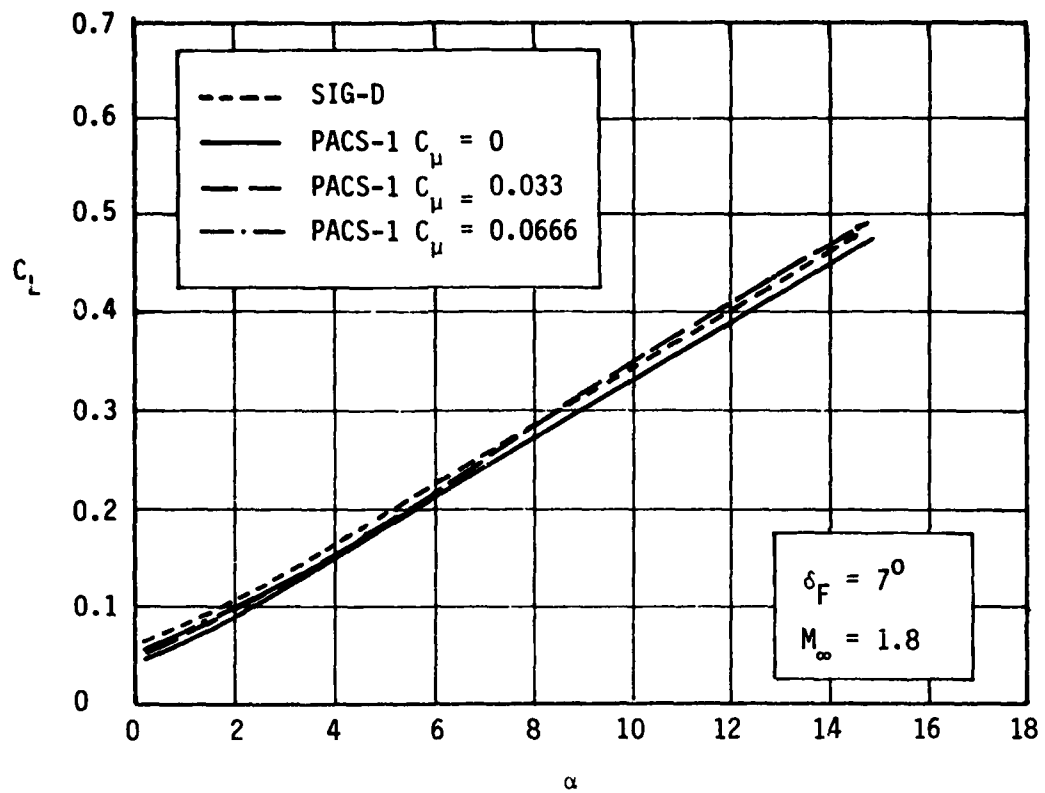


FIGURE 4-4 LIFT AND DRAG COMPARISONS OF THE SIG-D AND PACS-1 FIN WITH $\delta_F = 7^\circ$

No noticeable lift augmentation is seen over the baseline configuration. This is because in supersonic flow, upstream flow perturbations can only be generated by strong boundary layer perturbations and forced changes in the external shock structure. At subsonic and transonic flow conditions, favorable perturbations can be generated with a tangential jet near the trailing edge.¹⁻⁴ The prime benefit of tangential blowing at supersonic speeds is the ability to reduce the total drag $(C_D + C_\mu)^*$, as shown by the drag polars in Figures 4-3 and 4-4. This drag reduction is a result of the increase in boundary layer displacement thickness associated with the jet mass addition, which reduces the wave drag. However, with over blowing (i.e., $C_\mu = 0.067$) the total drag increased. This is a result of increased skin friction, associated with higher jet velocities, and adverse shock structure set up by the larger jet plume. Thus an optimum blowing condition can be achieved, providing a minimum total drag. The optimum drag condition for this fin arrangement is very close to the $C_\mu = 0.0328$ test case. ($\delta_F = 0^\circ$).

4.2.3 PACS-2/PACS-4 Performance

The PACS-2 and 4 concepts utilize transverse jet injection ($\delta_j = 90^\circ, 135^\circ$) to generate high maneuvering forces at supersonic speeds. (The concept was discussed in Section 2.0.) The model hardware discussed in Section 3.2, identifies the PACS-2 and PACS-4 geometries (c.f. Figure 3-6) as full and part span slotted jet configurations, respectively. The initial discussion of these configurations will address a limited number of test cases identifying the general performance trends at $M_\infty = 1.8$, followed with a detailed summary of the overall performance from $M_\infty = 0.9$ to 3.0. Additional lift and drag information on the individual test cases can be found in the Appendix.

The PACS-2 ($\delta_j = 135^\circ$) lift and drag performance at $M_\infty = 1.8$ is shown in Figure 4-5. This figure identifies the typical performance of the PACS-2 ($\delta_j = 135^\circ$) at different blowing conditions with reference to the baseline SIG-D ($\delta_F = 0^\circ$) performance. The data show that with increased blowing, large increments in lift can be generated. The data also show that these lift increments remain constant with angle of attack. Accompanying the lift increments,

* C_D corresponds to the measured balance force in the drag direction. Since this includes the blowing thrust force, adding C_μ to C_D provides an upper bound for equivalent profile/planform drag. (Assumes total C_μ recovery.)

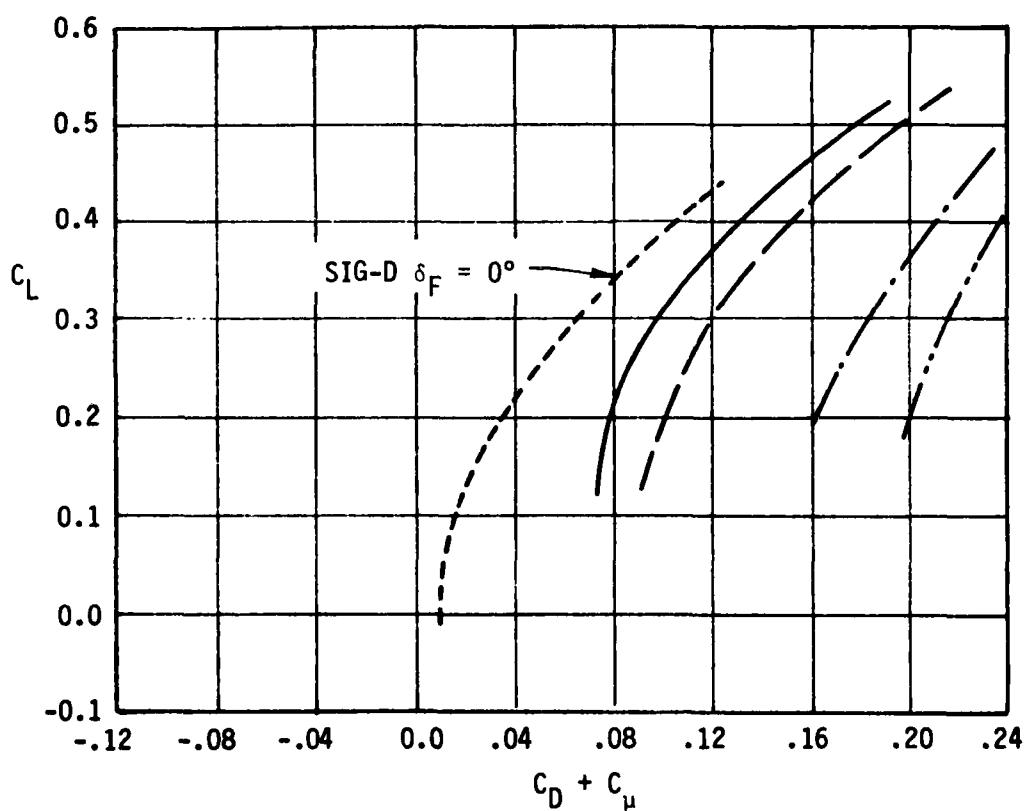
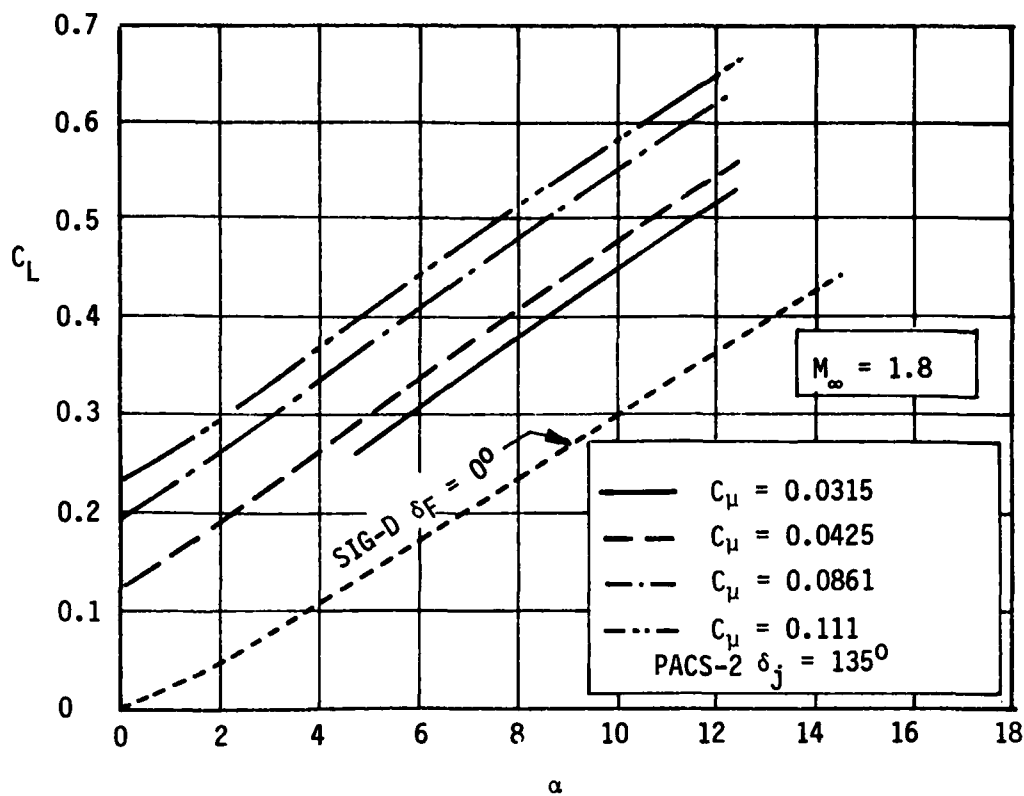


FIGURE 4-5 PACS-2 FIN LIFT AND DRAG PERFORMANCE, $\delta_j = 135^\circ$

generated by a new external shock structure, are related increases in drag. However, for typical missile maneuver applications these drag increases are small compared to the total vehicle drag. To clearly illustrate the potential control effectiveness of the PACS-2 concept, selected curves are replotted in Figure 4-6. This example illustrates that the PACS-2 fin at $\alpha = 0^\circ$ with $C_\mu = 0.111$ generates the equivalent lift of the baseline SIG-D fin at an $\alpha = 7.7^\circ$. This increase in control effectiveness offers new potentials for missile fin/wing designs.

Tests were also conducted to examine the sensitivity of jet incidence angle on performance. The results of these tests are shown in Figure 4-7 for the PACS-2 configuration with jet incidence at 90° and 135° . The jet incidence angle of 135° had the strongest influence on the upstream external shock structure and generated the higher lift forces, thus showing jet orientation is very important in the PACS design.

Tests were also performed to identify the effects of the jet slot length on the lift augmentation. A performance comparison of full and part-span blowing, PACS-2 and PACS-4, tested at the same C_μ (0.042) is shown in Figure 4-8. For the same blowing condition the full-span slot (PACS-2) produces a much higher lift value than the part-span geometry (PACS-4). These results indicate that long narrow slots are more effective than the shorter slot lengths, and furthermore show that effects from the inboard slot location do not noticeably feed out onto the outer trailing panel of the PACS-4 fin.

A summary of the overall lift improvements (increased C_{L_0} at $\alpha = 0^\circ$) generated by the transverse jet injection is presented in Figure 4-9. The data for the full and part-span blowing configurations are presented for $\delta_j = 90^\circ$ and 135° over the tested M_∞ range from 0.9 to 3.0. Lines of constant amplification ratio (C_{L_0}/C_μ) identify zones where high lift augmentation of the jet reaction force is generated. A replot of these data, Figure 4-10, shows the lift amplification of each configuration as a function of blowing conditions. At very low C_μ values, high augmentation ratios are generated. For the higher C_μ values the lift augmentation is reduced, resulting from diminishing returns on the jet influence on the upstream flow conditions. The M_∞ influence on the full and part-span blowing configurations is shown in Figure 4-11 for a selected $C_\mu = 0.1$. This figure illustrates the typical impact of M_∞ on the PACS concept. For a constant blowing case, the augmentation, in general, decreases with increasing M_∞ .

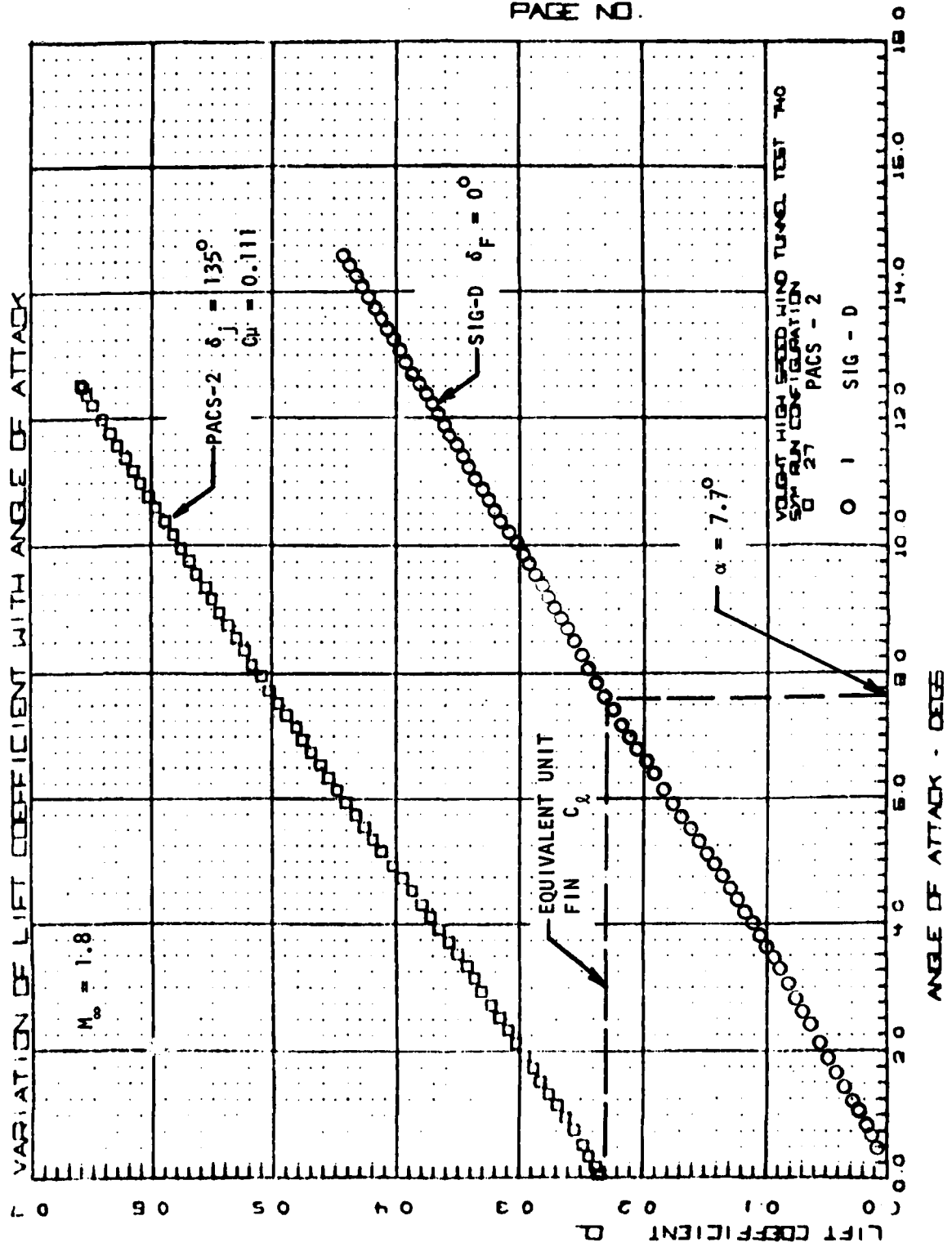


FIGURE 4-6 PACS-2 COMPARISON WITH UNIT FIN

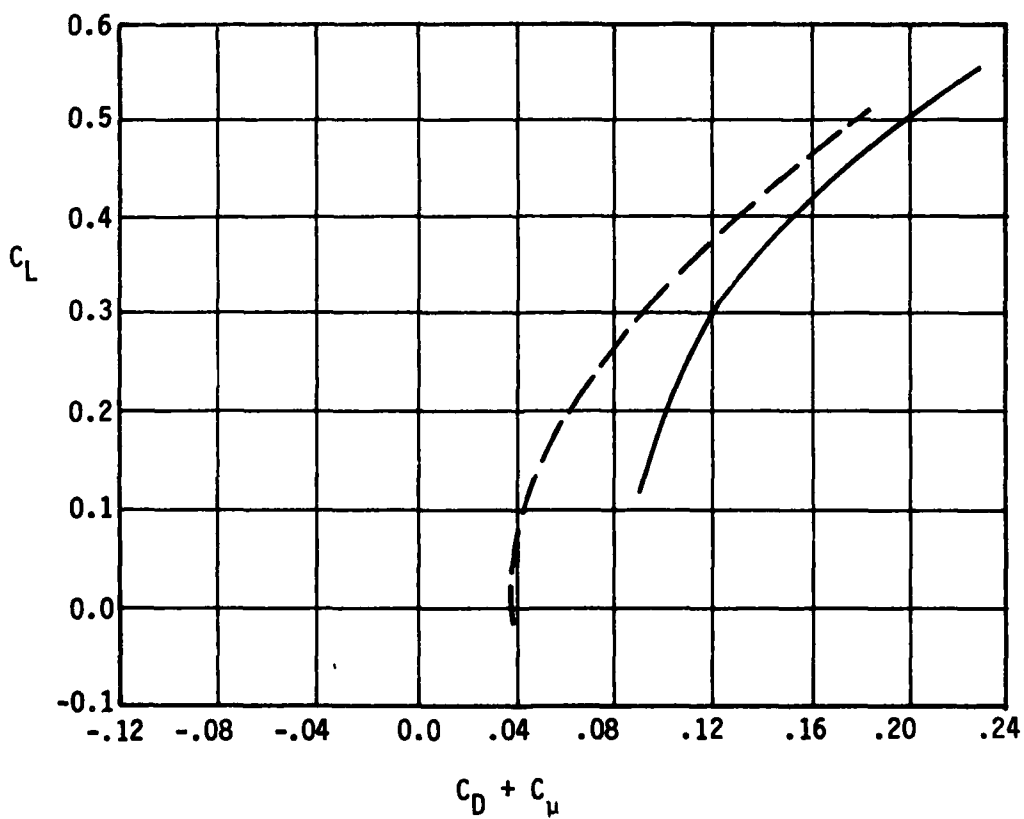
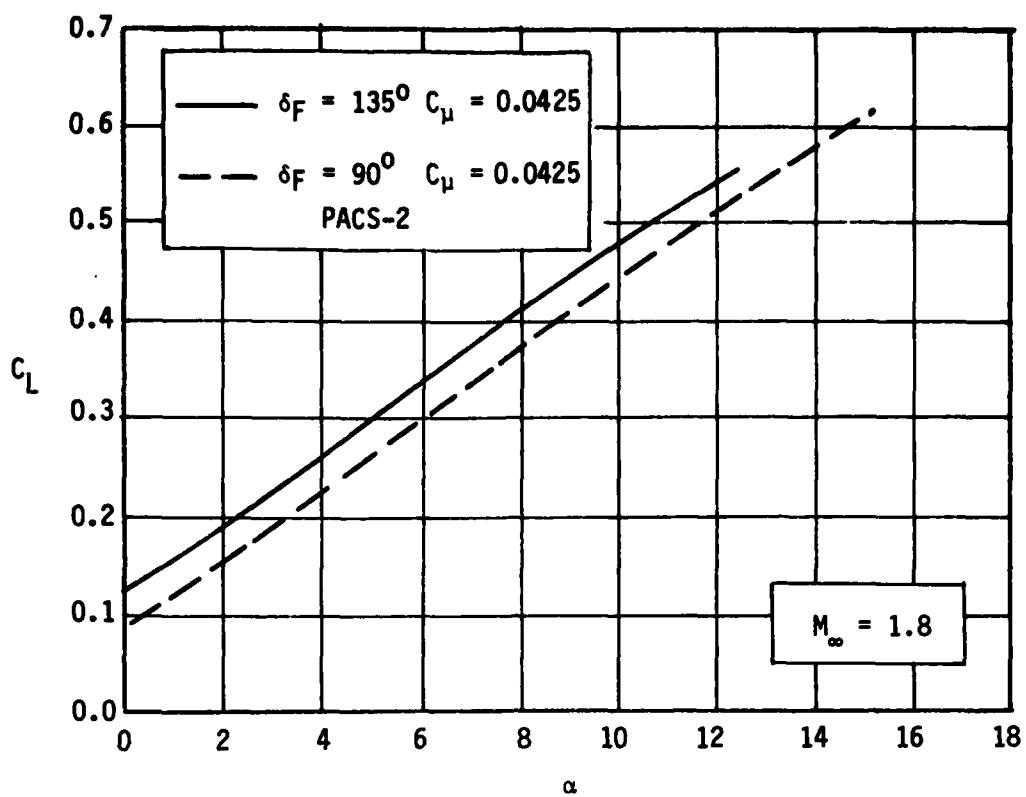


FIGURE 4-7 EFFECT OF JET ANGLE ON LIFT AND DRAG PERFORMANCE - PACS-2

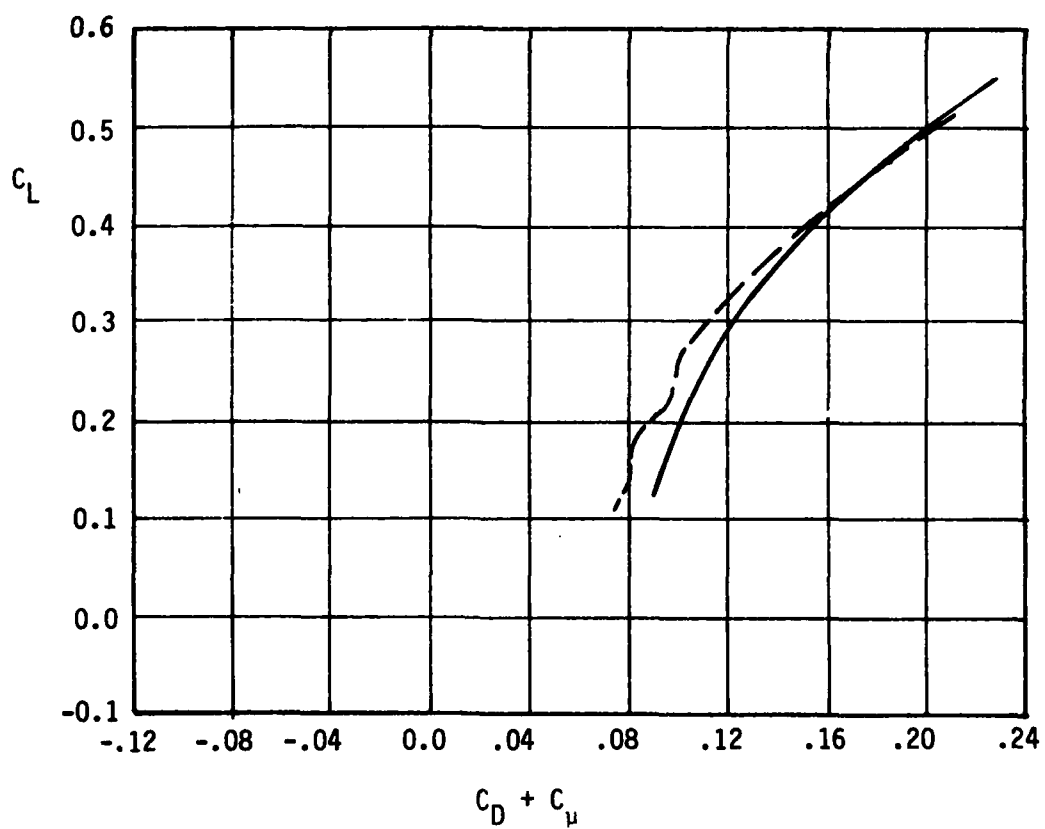
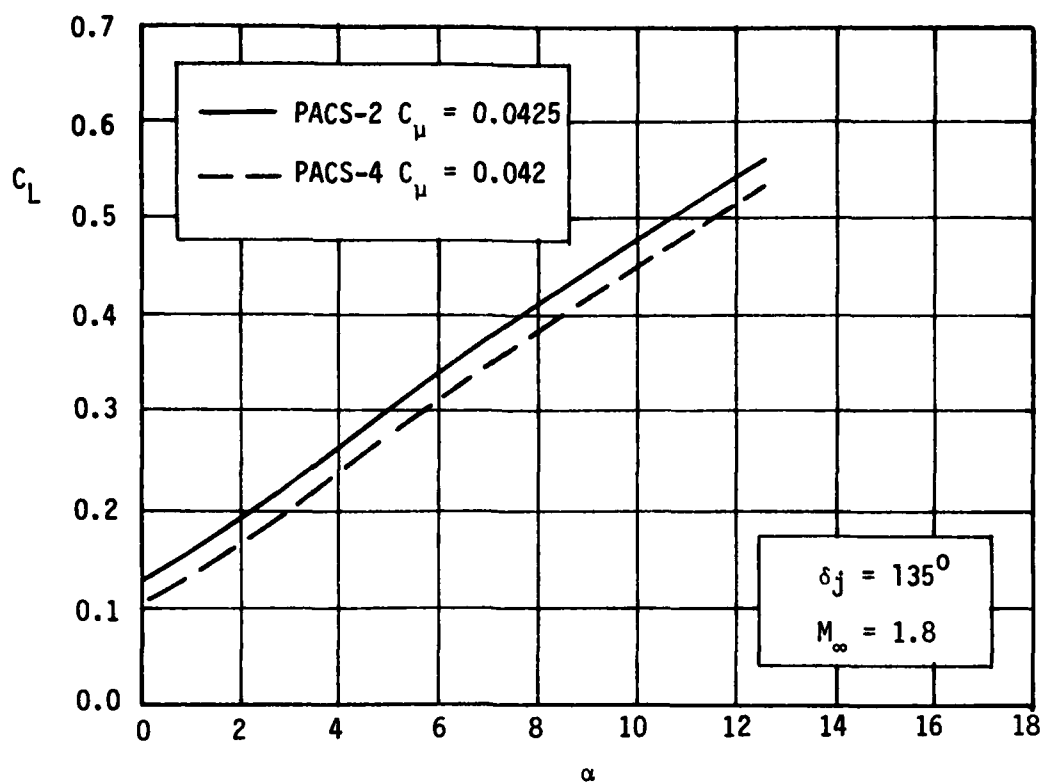


FIGURE 4-8 COMPARISON OF PART AND FULL SPAN BLOWING, $\delta_j = 135^\circ$

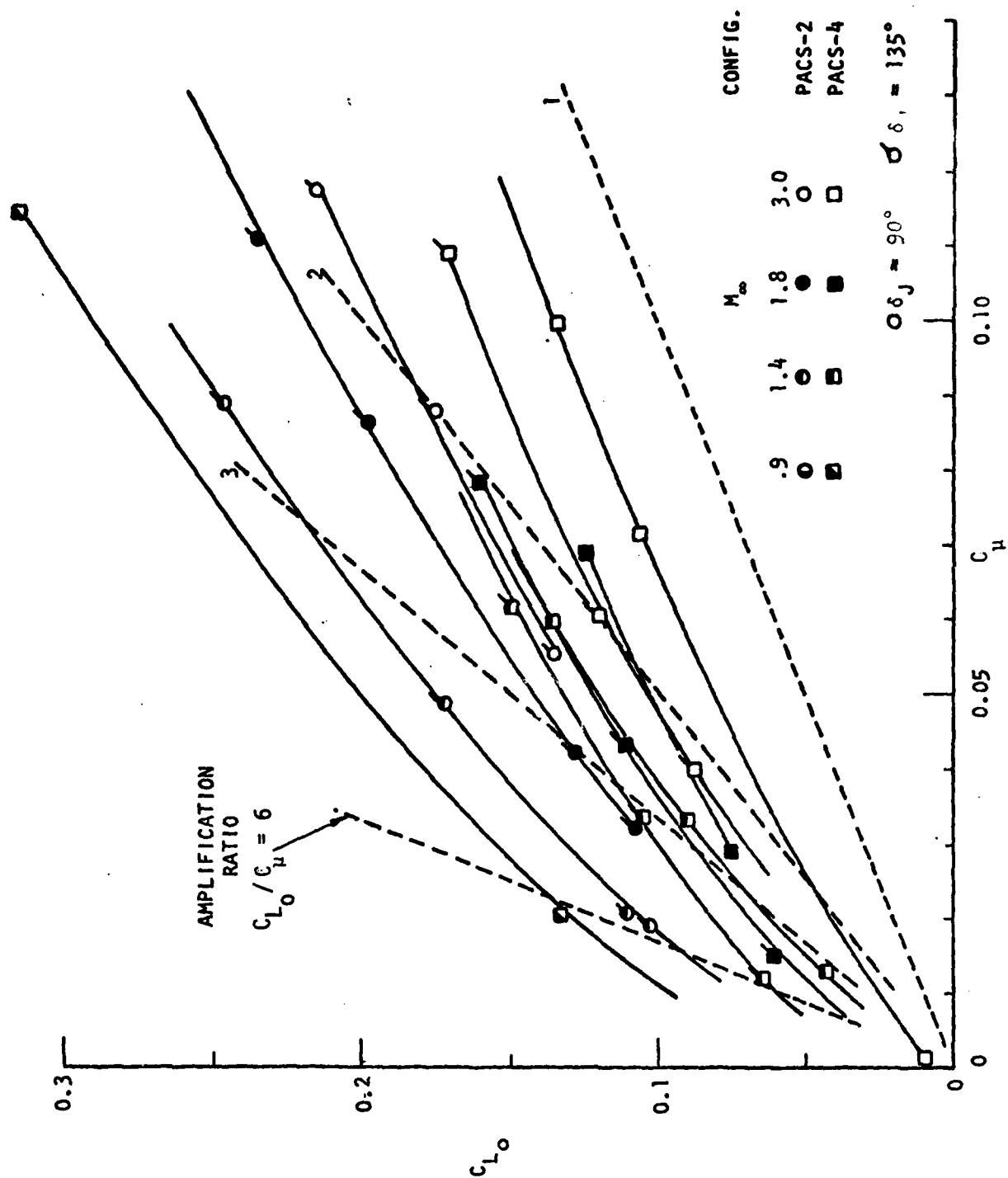


FIGURE 4-9 LIFT GENERATED BY TRANSVERSE JET EJECTION — $\delta_j = 90^\circ, 135^\circ$

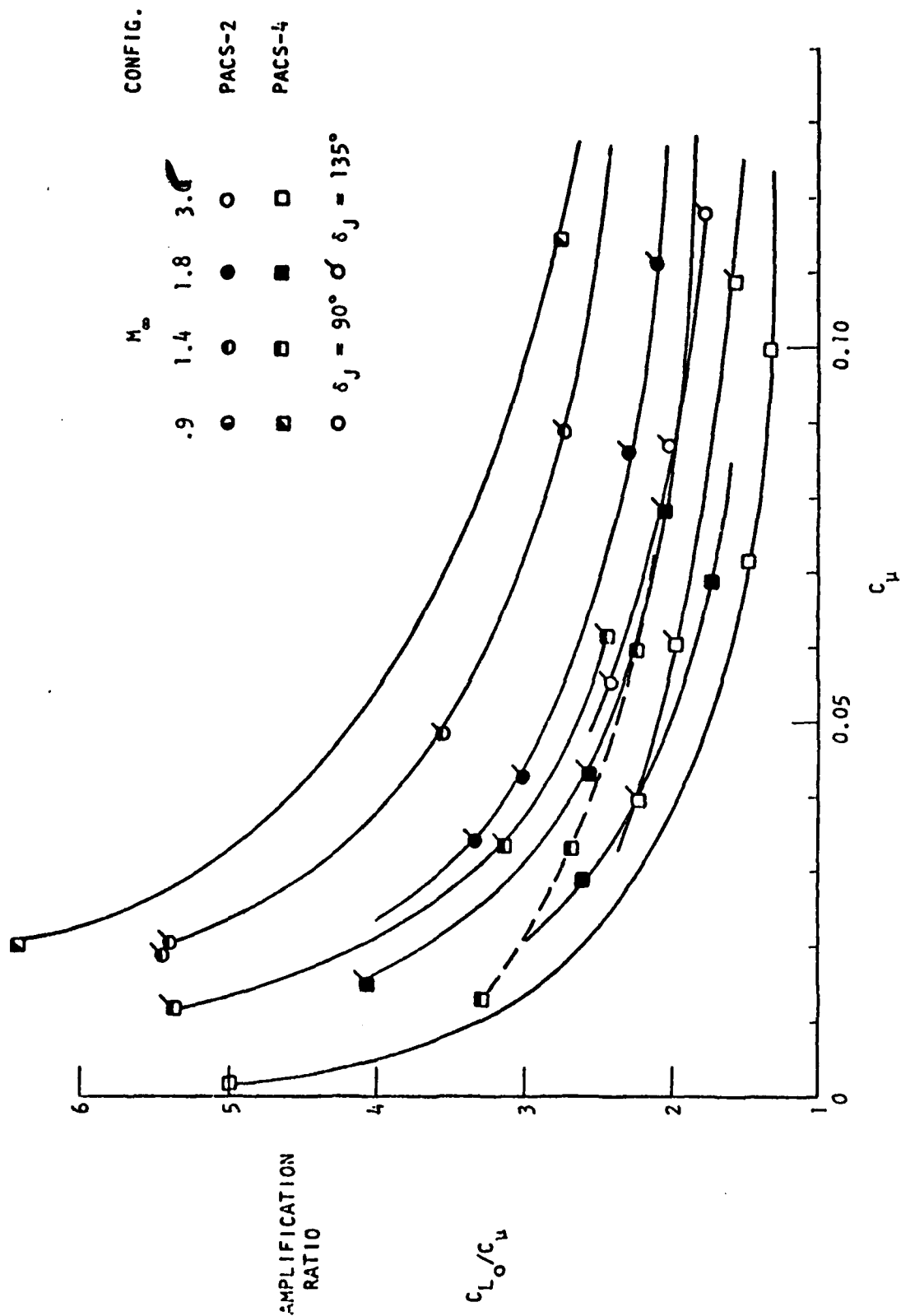


FIGURE 4-10 LIFT FORCE AMPLIFICATION GENERATED BY VERTICAL JET EJECTION

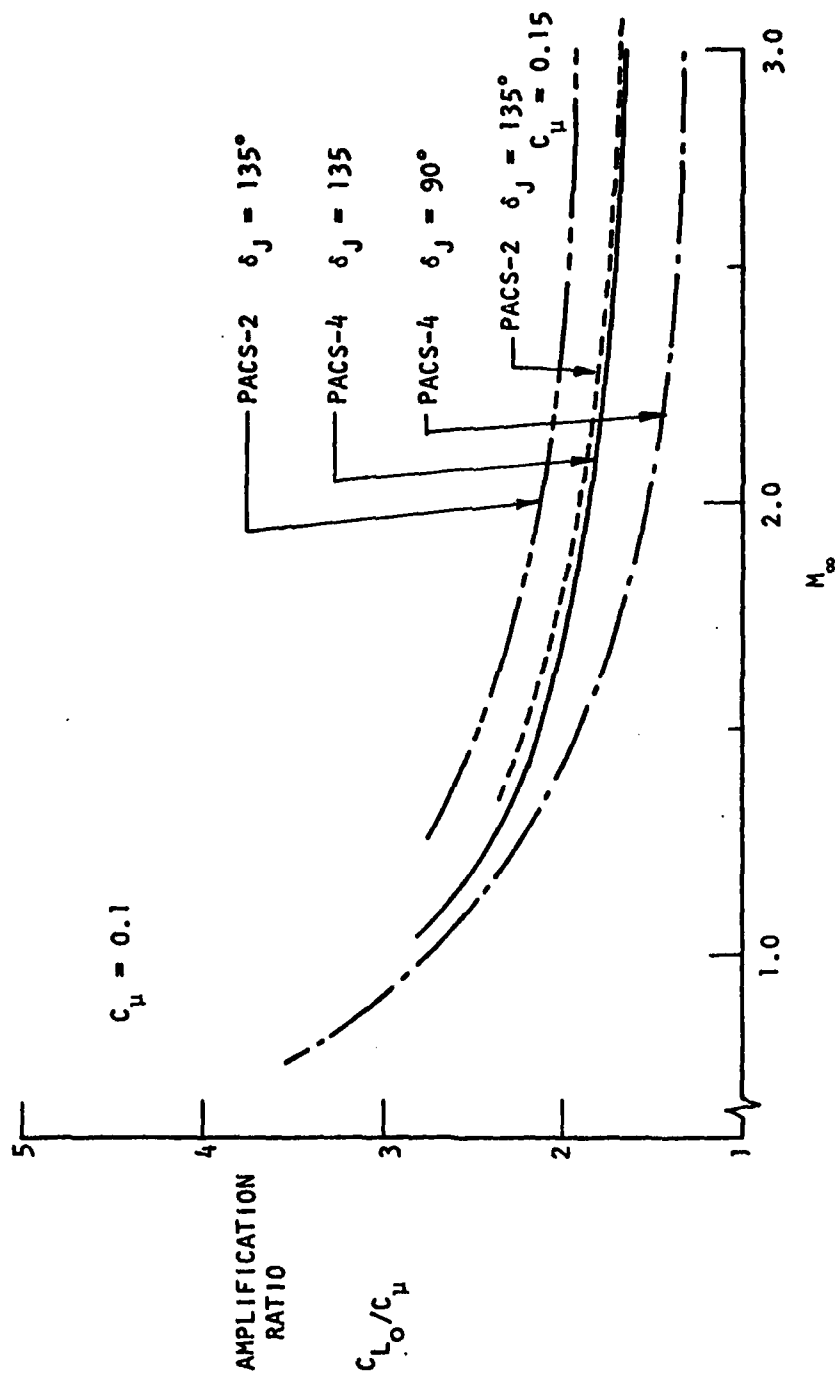


FIGURE 4-11 LIFT AMPLIFICATION VS. M_∞ FOR $C_\mu = 0.1$

Over the full range of M_∞ and C_μ , the PACS-2 ($\delta_j = 135^\circ$) provided the best overall performance. A summary of the control effectiveness of this configuration over the tested M_∞ range from 0.9 to 3.0 is shown in Figure 4-12. This figure compares the PACS-2 blowing effectiveness against the SIG-D control surface (elevon) effectiveness. The SIG-D ($\delta_F = 17.5^\circ$) extrapolated curve was predicted analytically using the $\delta_F = 7^\circ$ experimental data as verification of the analytical method. The experimental data show that the lift increment generated by a SIG-D elevon deflection of 17.5° can be generated by the PACS-2 configuration with a $C_\mu = 0.05$. It is important to note that the PACS-2 effectiveness does not drop off as fast as that of the baseline control surface with M_∞ . This indicates that the PACS-2 concept is more effective than conventional control methods at increased M_∞ .

An important benefit of the PACS concept is its potential for reducing the control surface size. Subject to vehicle angle of attack constraints, the ratio of fin areas producing equivalent forces can be defined, Figure 4-13. For a vehicle α orientation of 7.5° and 15° , an area reduction of 30% can be realized for the higher blowing case, $C_\mu = 0.15$. The capability of reducing the fin/wing size offers an additional option to the missile fin/wing design.

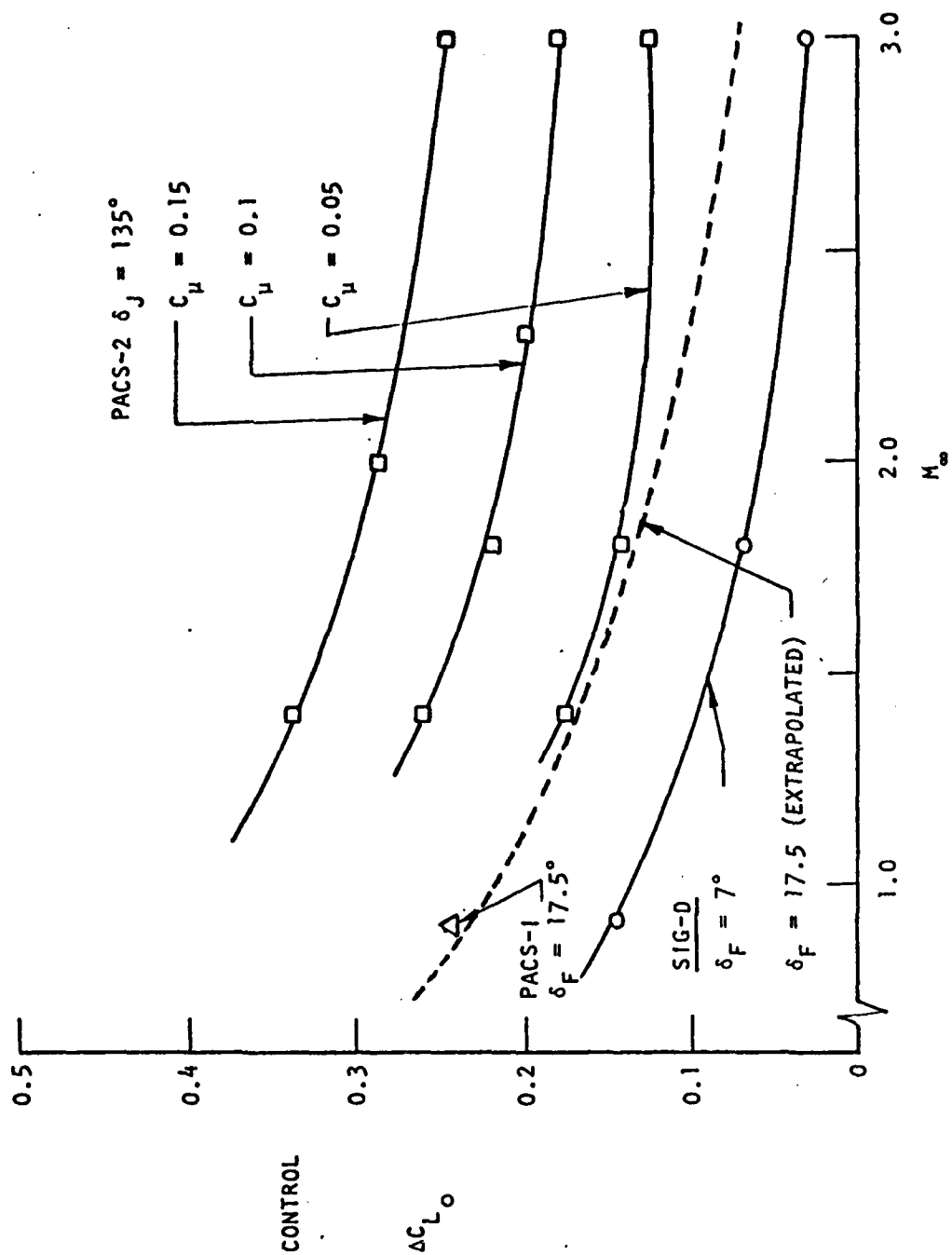


FIGURE 4-12 COMPARISON OF CONTROL EFFECTIVENESS

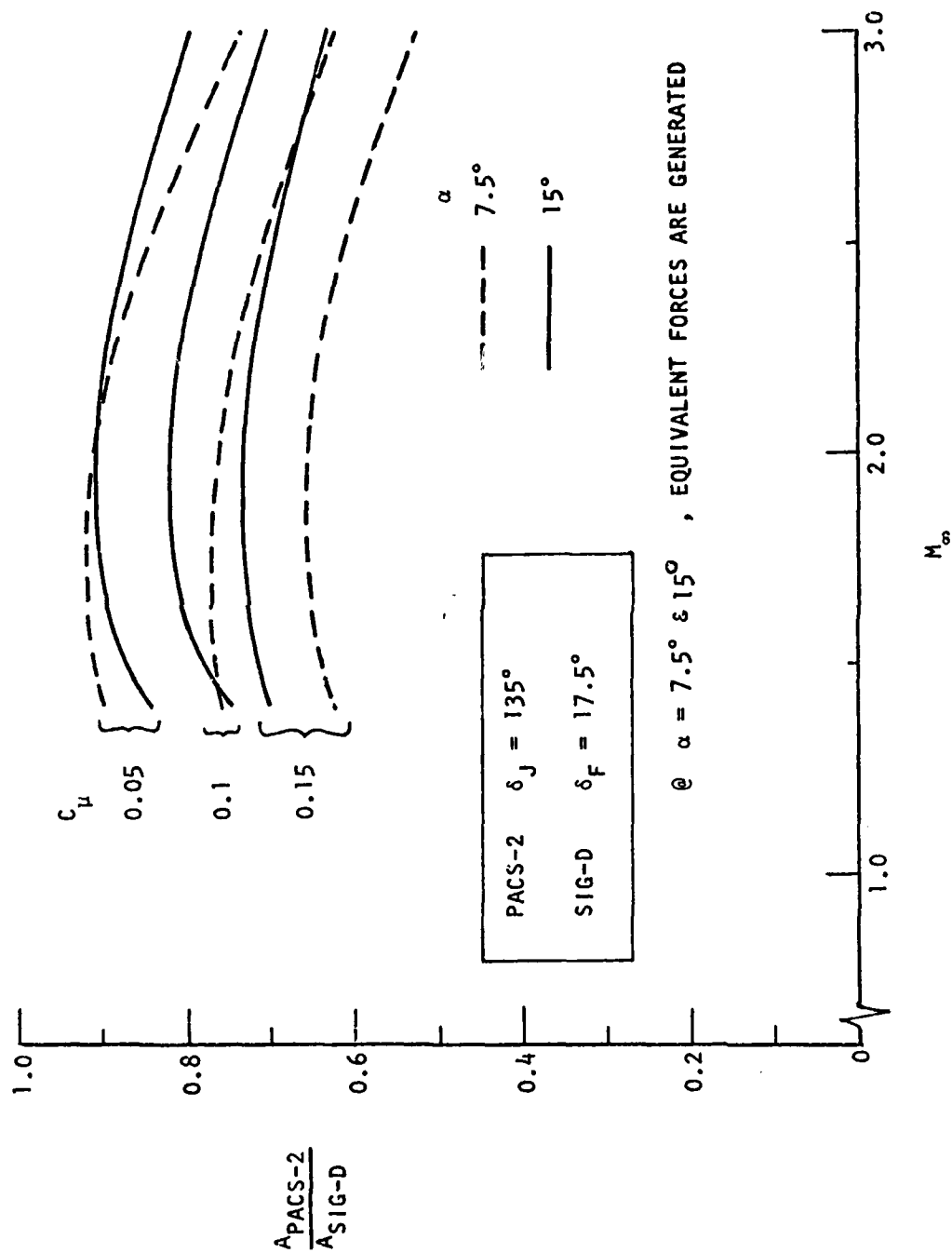


FIGURE 4-13 WING AREA REDUCTION POTENTIALS

5.0 CONCLUSIONS

The HSWT tests on missile fin configurations validated the feasibility of the PACS concept for transonic and supersonic applications ($M_\infty = 0.9-3.0$)

- o PACS-1, tangential jet configuration, tests validated drag ($C_D + C_\mu$) reduction with non-optimized blowing conditions. Drag reductions over the baseline SIG-D fin of $\Delta C_D = 0.007$ were achieved with a $C_\mu = 0.032$.
- o PACS-2, transverse jet injection ($\delta_j = 135^\circ$), with $C_\mu = 0.111$ induced lift coefficient increments at $\alpha = 0^\circ$ over 0.3, equivalent to a unitary SIG-D fin at a deflection angle of 7.7° . This value was predicted to be as high as 10° for an extrapolated C_μ of 0.15.
- o The HSWT test illustrated that lift increments equivalent to those generated by a SIG-D elevon deflection of 17.5° could be generated by the PACS-2 ($\delta_j = 135^\circ$) configuration with a $C_\mu \leq 0.05$.
- o The PACS-2 and PACS-4, full and part-span transverse jet blowing tests, showed the high aspect ratio blowing slot (full-span blowing) as being the more effective in generating high lift augmentations for equivalent blowing conditions.
- o The orientation of the transverse jet is very important to the PACS performance. The upstream blowing case, $\delta_j = 135^\circ$, was most effective in generating higher lift augmentations.
- o For PACS at a $C_\mu = 0.15$, control force increments 70% and 250% greater than the baseline are projected at $M_\infty = 1.8$ and 3.0, respectively.
- o Reductions in fin size of 25-40% are indicated, relative to the baseline SIG-D operating at the same force levels.
- o The limited testing of non-optimized PACS geometries provides guidelines for optimization/application recommendations.

6.0 RECOMMENDATIONS

The success of the PACS feasibility tests provides strong motivation for proceeding with coordinated technology and application studies. Technology requirements include extended wind tunnel tests to produce an empirical data base for a range of wing/fin candidates, concentrating on both the high efficiency-low C_u and the high force-high C_u ends of the spectrum. Analysis/optimization of planform effects and missile aeropropulsion integration is also required. Application tasks must begin focusing on propulsion/bleed candidates, structural/thermal requirements, and cost-effective design and fabrication techniques. The latter area would include methodology in superplastic metal forming, reinforced carbon/carbon materials, diffusion bonding, and new steel alloys. Inherent modularism in the PACS concept permits early entry into component validation testing and technology demonstration flight tests.

7.0 REFERENCES

1. Mask, R. L., and Krall, K. M., "Low Speed Wind Tunnel Test of an ATC Optimized High Lift Wing," ATC Report No. B-94300/4TR-34, August 1974.
2. Haight, C. H., and Spangler, J. G., "Test Verification of a Transonic Airfoil Design Employing Active Diffusion Control," ATC Report No. B-94300/5CR-34, June 13, 1975, NADC Contract No. N62269-74-C-0517.
3. Mask, R. L., and Haight, C. H., "Transonic Maneuver/Cruise Airfoil Design Employing Active Diffusion Control", Published in Viscous Flow Drag Reduction, AIAA Progress in Astronautics and Aeronautics, Volume 72, 1980.
4. Mask, R. L., "Low Drag Airfoil Design Utilizing Passive Laminar Flow and Coupled Diffusion Control Techniques," ATC Report No. R-91100/9CR-71, September 1980, published in Viscous Flow Drag Reduction, AIAA Progress in Astronautics and Aeronautics, Volume 72, 1980.
5. Amick, James L., "Circular-Arc Jet Flaps at Hypersonic Speeds," AIAA Paper No. 70-553, May 13-15, 1970.
6. Cubbison, R. W., Anderson, B. H., and Ward, J. J., "Surface Pressure Distributions with a Sonic Jet Normal to Adjacent Flat Surface at Mach 2.92 to 6.4," NASA TN-D-580, 1960.
7. Romeo, D. J. and Sterrett, J. R., "Aerodynamic Interaction Effects Ahead of a Sonic Jet Exhausting Perpendicularly from a Flat Plate into a Mach Number 6 Free Stream," NASA TN-D-743, 1961.
8. Werle, M. J., Driftmeyer, R. T., and Shaffer, D. G., "Two-Dimensional Jet Interaction with a Mach 4 Mainstream," NOLTR 70-50 May 1970.
9. Carmichael, Ralph L., "A Computer Program for the Estimation of the Aerodynamics of Wing-Body Combinations," NASA Ames Research Center, 1970.
10. Werle, M. J., "a Critical Review of Analytical Methods for Estimating Control Forces Produced by Secondary Injection," NOLTR-68-5, January 1968.

APPENDIX

The following figures identify the lift and drag performance of each configuration tested. Table 1 identifies, by run number, the test conditions; M_∞ , M_∞ (M_∞ at the end plate), α , P_o (freestream total pressure), P_{oj} (jet total pressure), and C_μ for each test case. The first set of figures identifies C_L vs α for each run. The second set of figures plots C_L vs C_D for each run. To account for the blowing influence on total drag, the addition of C_μ (identified in Table 1) to the C_D is required to identify $C_D + C_\mu$ effects on measured performance.

TABLE 1
HSWT - TEST NO. 740

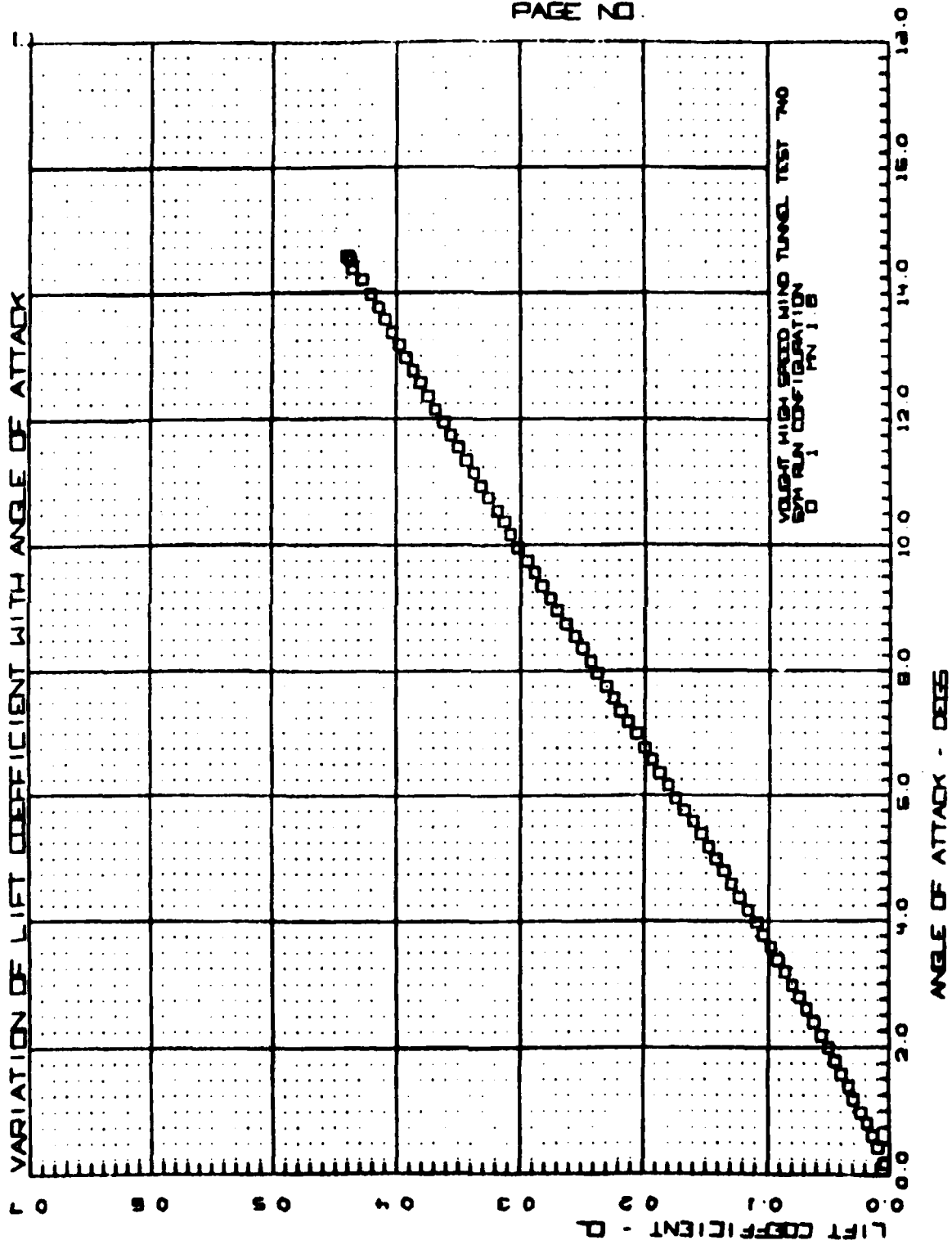
RUN	CONF.	M_∞	$M_{\infty p}$	α	P_o	$\delta_{F/J}$	P_{oj}	C_μ
1	SIG-D	1.8	1.845	0/15	32.5	0	-	-
2	↓	3.0	3.02	0/20	60	0	-	-
3	↓	3.0	3.02	0/20	60	-7°	-	-
4	↓	1.8	1.845	0/15	32.5	7°	-	-
5	↓	3.0	3.02	0/20	60	7°	-	-
6	PACS-1	↓	↓	0/15	60	0	0	0
7	↓	↓	↓	↓	↓	0	90	0.0678
8	↓	↓	↓	↓	↓	0	120	0.093
9	↓	↓	↓	↓	↓	7	90	0.068
10	↓	↓	↓	↓	↓	7	120	0.0925
11	↓	1.8	1.845	↓	32.5	7	65	0.033
12	↓	↓	↓	↓	↓	7	120	0.0666
13	↓	↓	↓	↓	↓	7	0	0
14	↓	↓	↓	↓	↓	0	120	0.0670
15	↓	↓	↓	↓	↓	0	65	0.0328
16	PACS-2	↓	↓	↓	↓	90	0	0
17	↓	↓	↓	↓	↓	↓	65	0.0475
18	PACS-4	↓	↓	0/12.5	↓	↓	120	0.0697
19	↓	3.0	3.02	↓	60	↓	120	0.0997
20	↓	↓	↓	↓	↓	↓	0	0
21	↓	↓	↓	↓	↓	↓	90	0.0715
22	PACS-2	↓	↓	↓	↓	135°	90	0.0866
23	↓	↓	↓	↓	↓	↓	120	0.1176
24	↓	1.8	1.845	↓	32.5	↓	65	0.0425
25	↓	↓	↓	↓	↓	↓	120	0.0861
26	↓	↓	↓	↓	↓	↓	50	0.0315
27	↓	↓	↓	↓	↓	↓	150	0.1110
28	↓	3.0	3.02	↓	60	↓	60	0.0555
29	↓	1.3	1.46	↓	28.7	↓	0	0
30	↓	1.4	1.54	↓	30	↓	40	0.0189

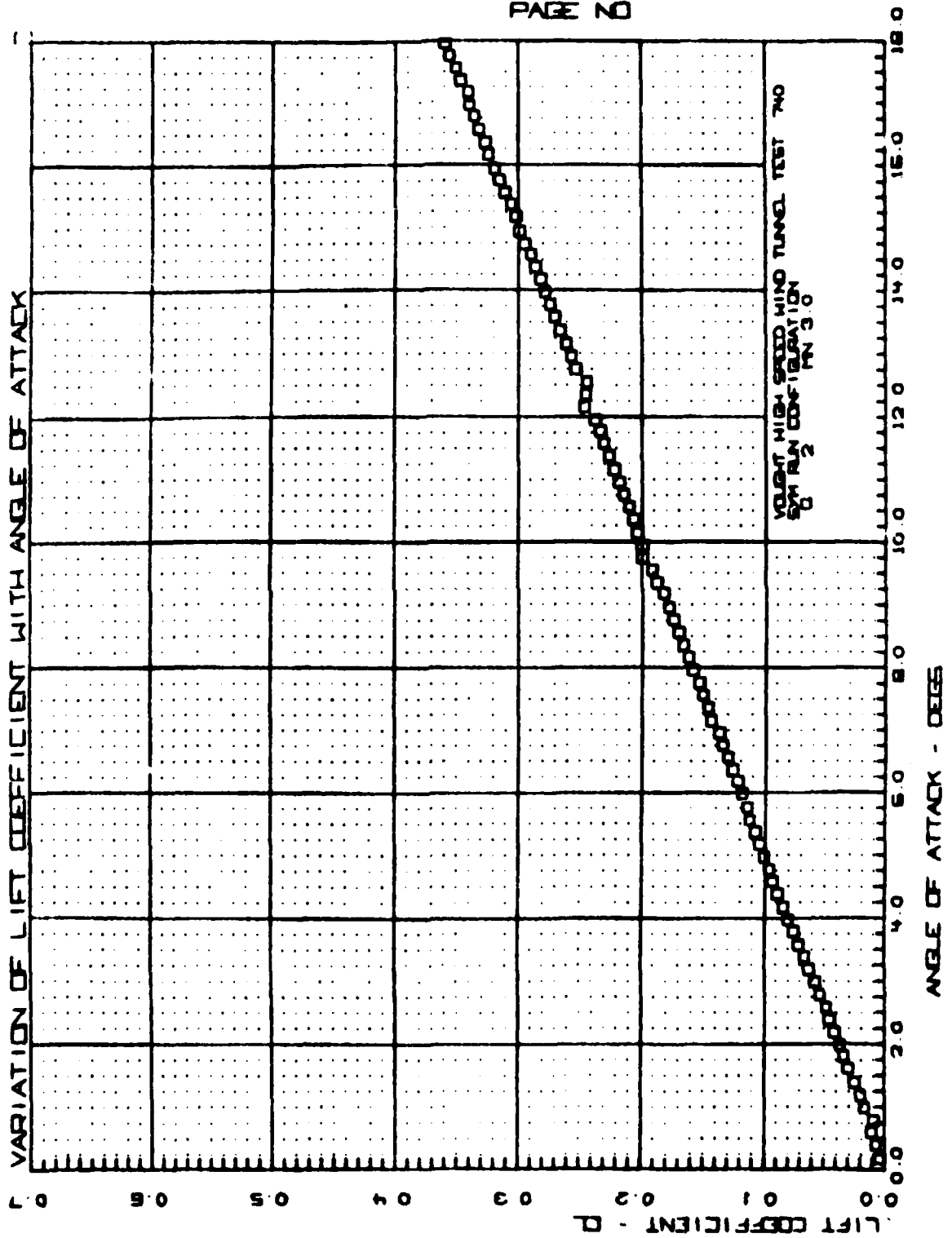
TABLE 1

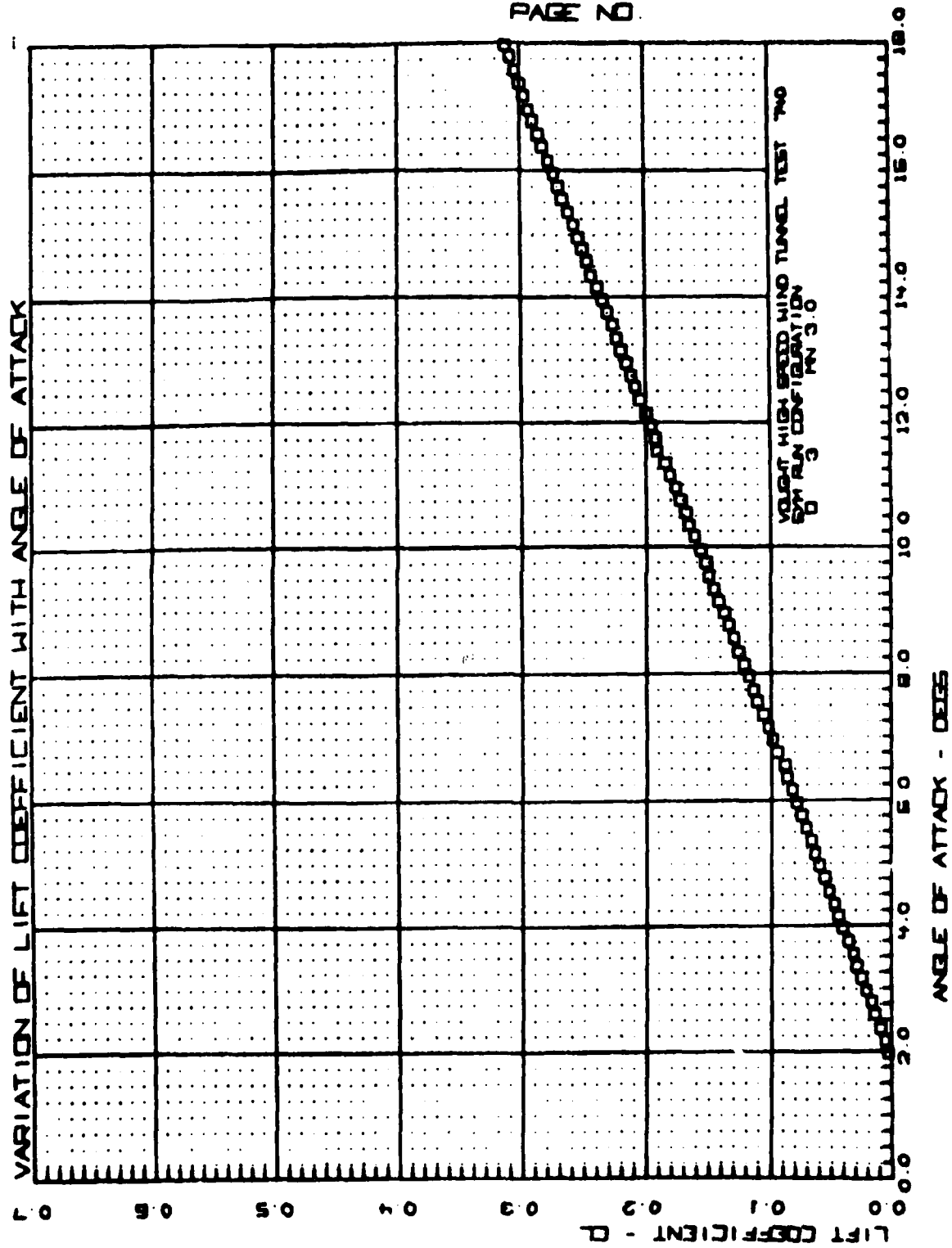
HSWT - TEST NO. 740 (Cont'd)

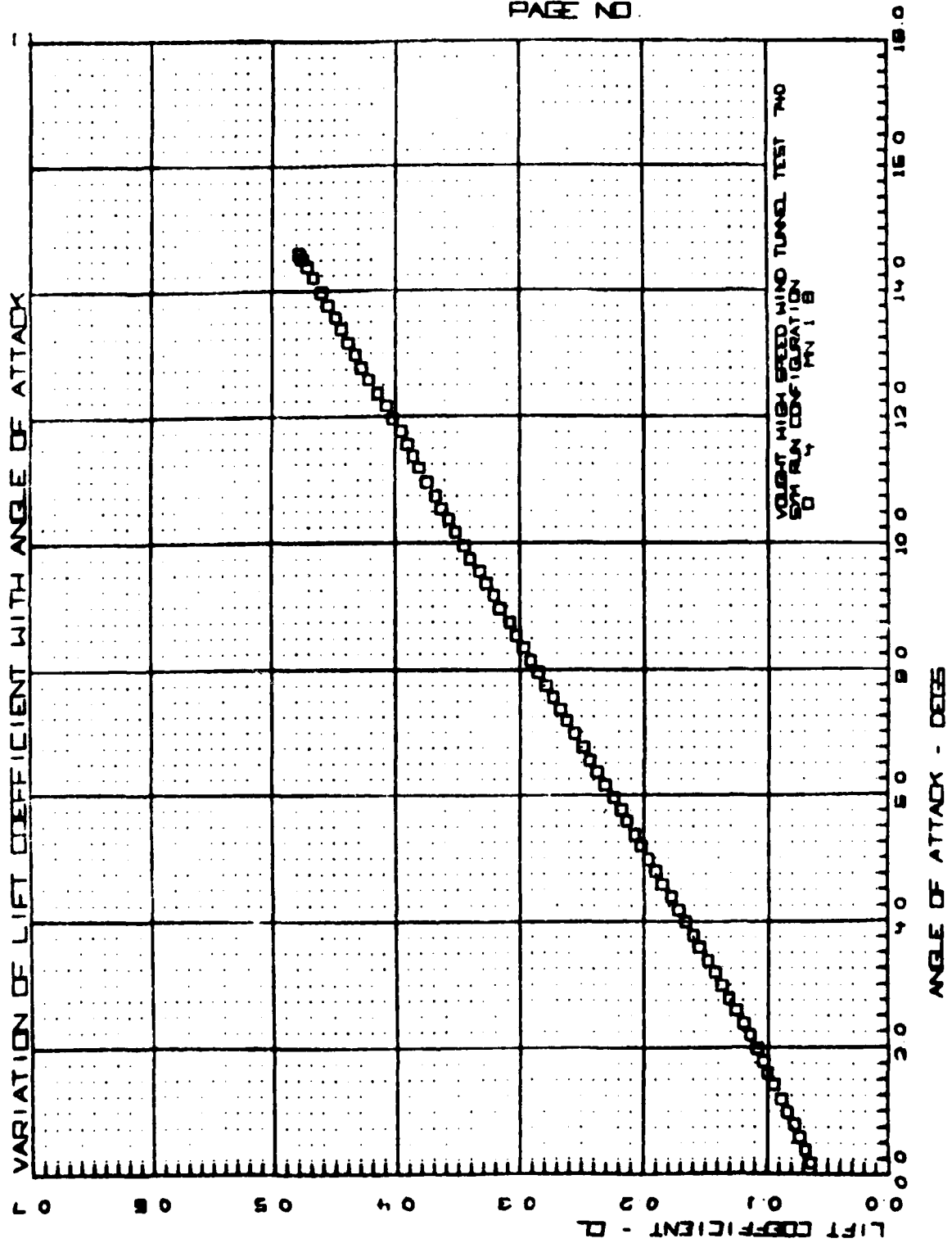
RUN	CONF.	M_∞	$M_{\infty p}$	α	P_o	δ_F/J	P_{oj}	C_μ
31	PACS-2	1.4	1.54	0/12.5°	30	135°	40	0.020
32	↓	↓	↓	↓	35	↓	90	0.0488
33	↓	↓	↓	↓	↓	↓	150	0.0892
34	PACS-4	↓	↓	↓	↓	↓	40	0.0120
35	↓	↓	↓	↓	↓	↓	90	0.0336
36	↓	↓	↓	0/6°	↓	↓	150	0.0616
37	↓	1.8	1.84	0/12.5°	32.5	↓	40	0.0163
38	↓	↓	↓	↓	↓	↓	90	0.042
39	↓	↓	↓	↓	↓	↓	150	0.076
40	↓	3.0	3.02	↓	60	↓	60	0.0390
41	↓	↓	↓	↓	↓	↓	90	0.0748
42	↓	↓	↓	↓	↓	↓	150	0.1308
43	↓	1.8	1.84	↓	32.5	90	65	0.0284
44	↓	1.4	1.54	0/6°	35	↓	40	0.0123
45	↓	↓	↓	↓	↓	↓	90	0.0325
46	↓	↓	↓	↓	↓	↓	150	0.060
47	SIG-D	↓	↓	↓	↓	0°	--	--
48	↓	↓	↓	↓	↓	7°	--	--
49	↓	↓	↓	↓	↓	↓	--	--
50	PACS-4	0.9	0.9	0/12.5°	22	90°	40	0.0205
51	↓	↓	↓	↓	↓	↓	150	0.114
52	PACS-1	0.9	↓	↓	↓	7°	40	0.0248
53	↓	↓	↓	↓	↓	20°	40	0.0233
54	↓	↓	↓	↓	↓	↓	--	--
55	↓	↓	↓	↓	↓	0°	--	--

VARIATION OF LIFT COEFFICIENT WITH
ANGLE OF ATTACK

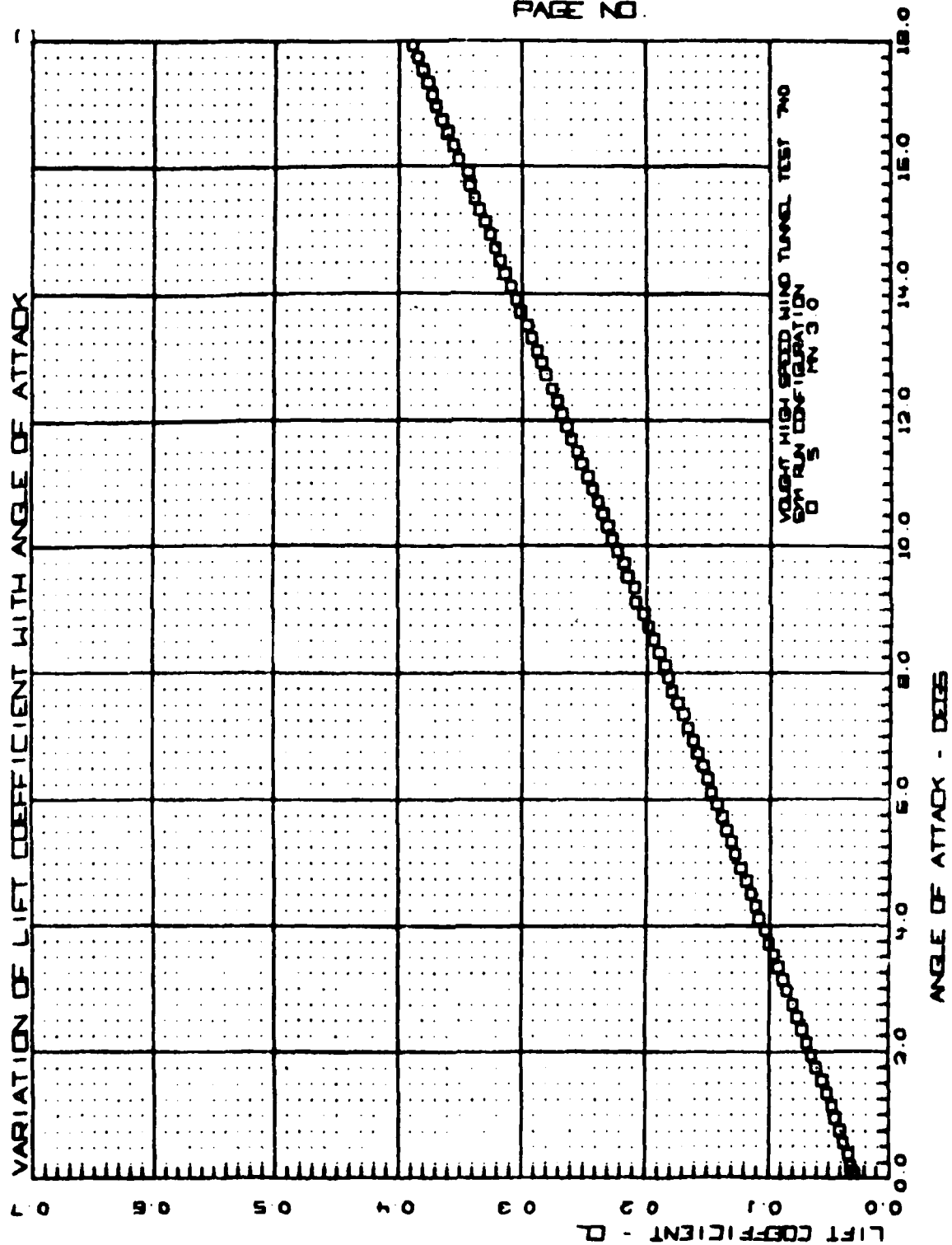


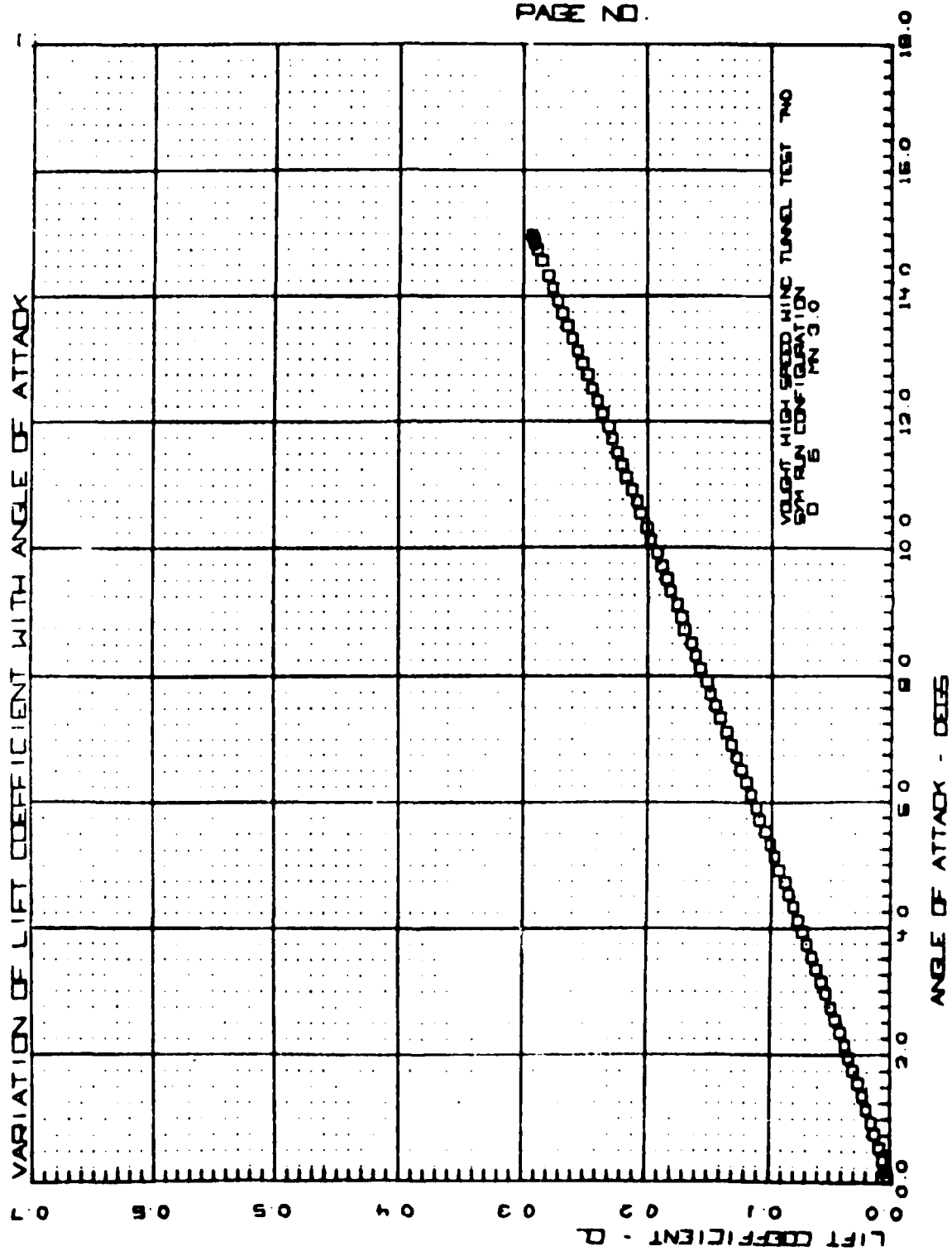


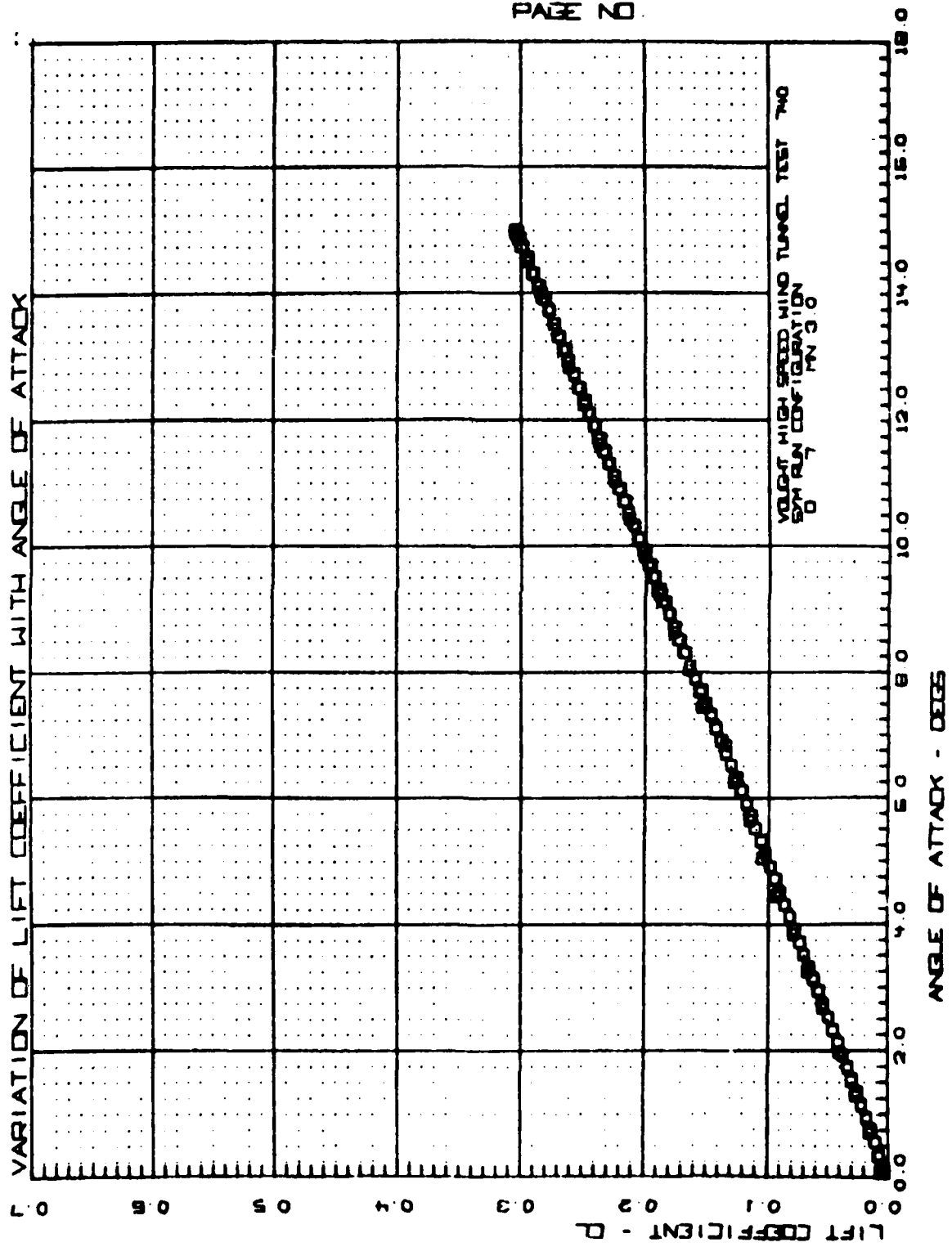


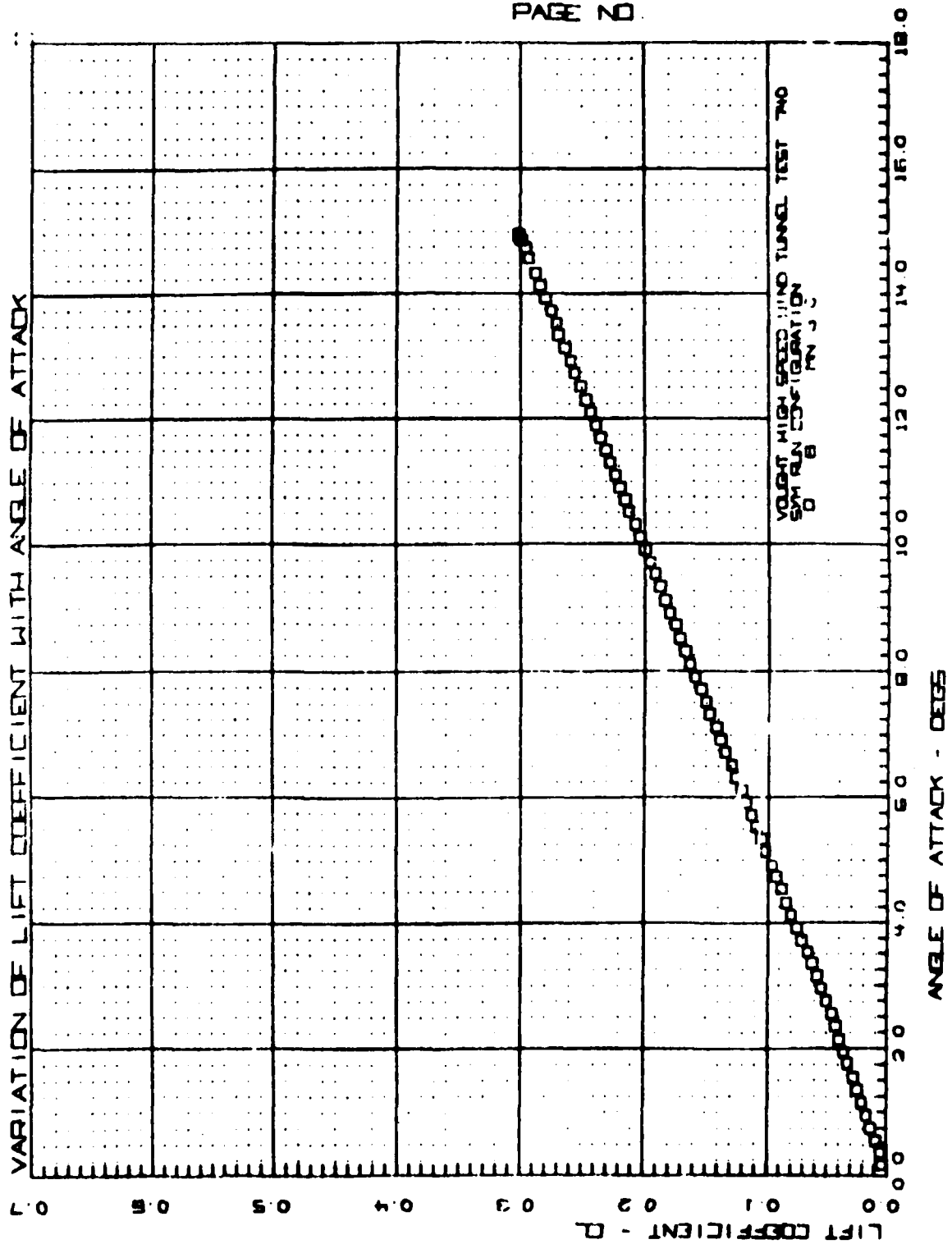


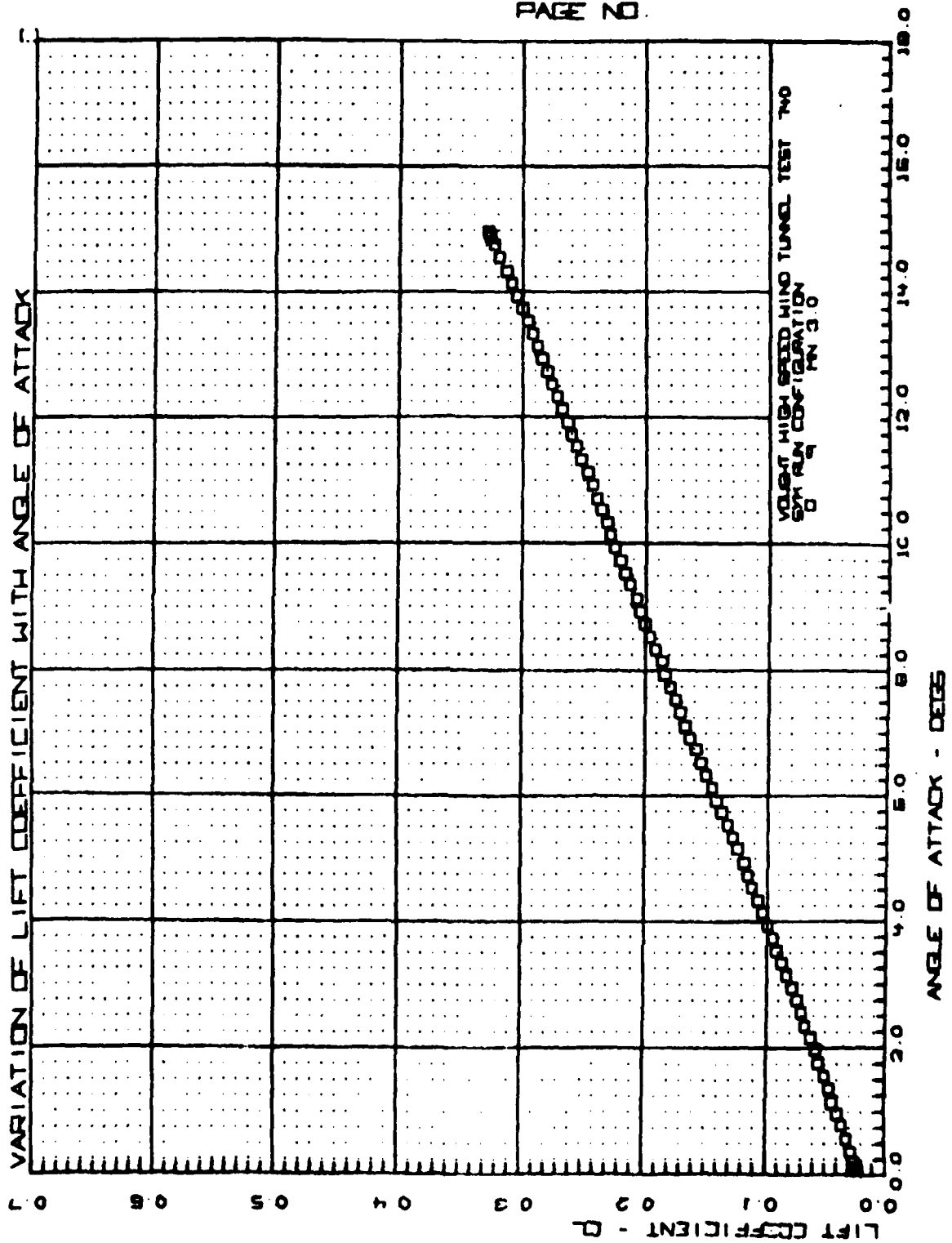
VOUGHT HUNT TEST 740
PAGE NO.

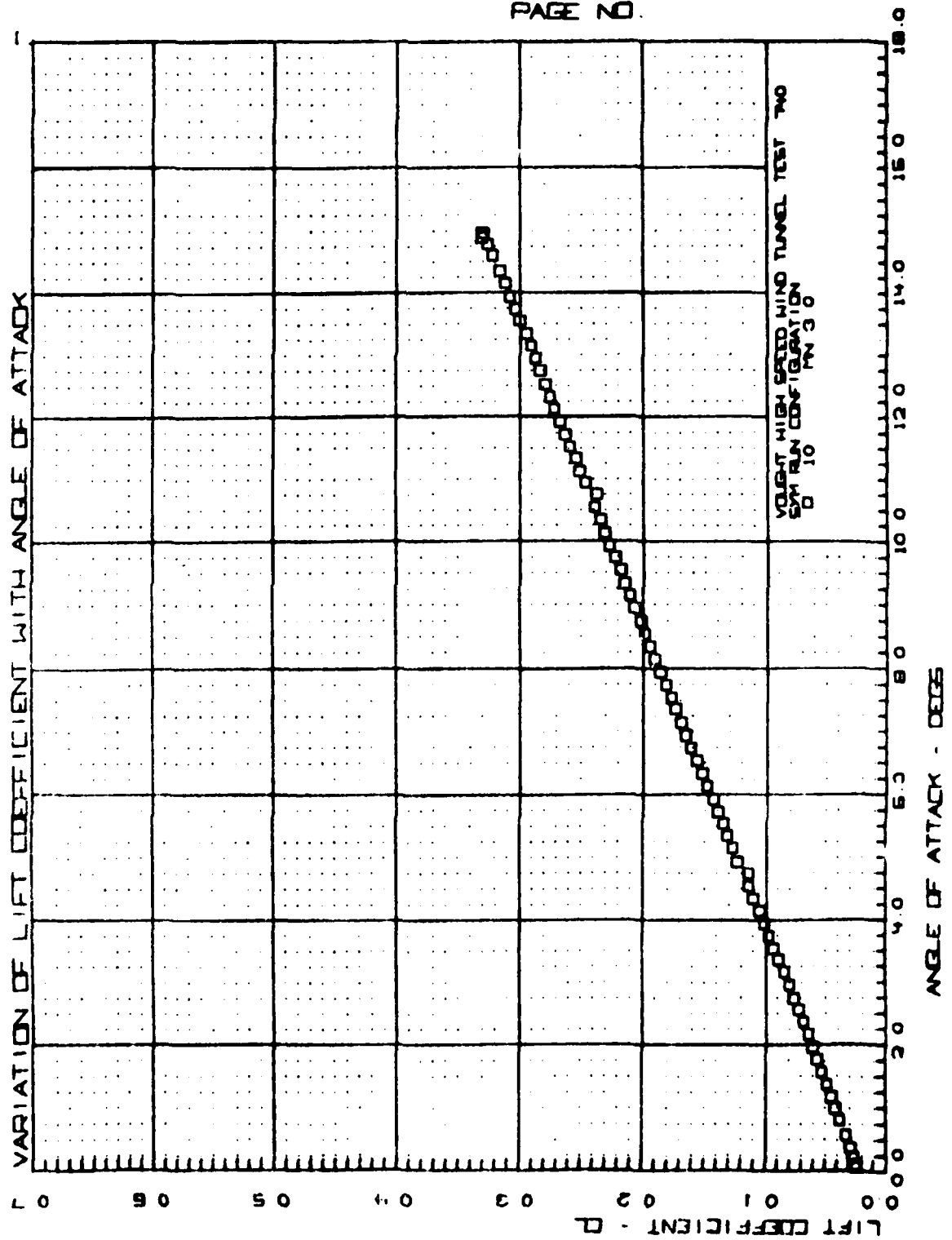




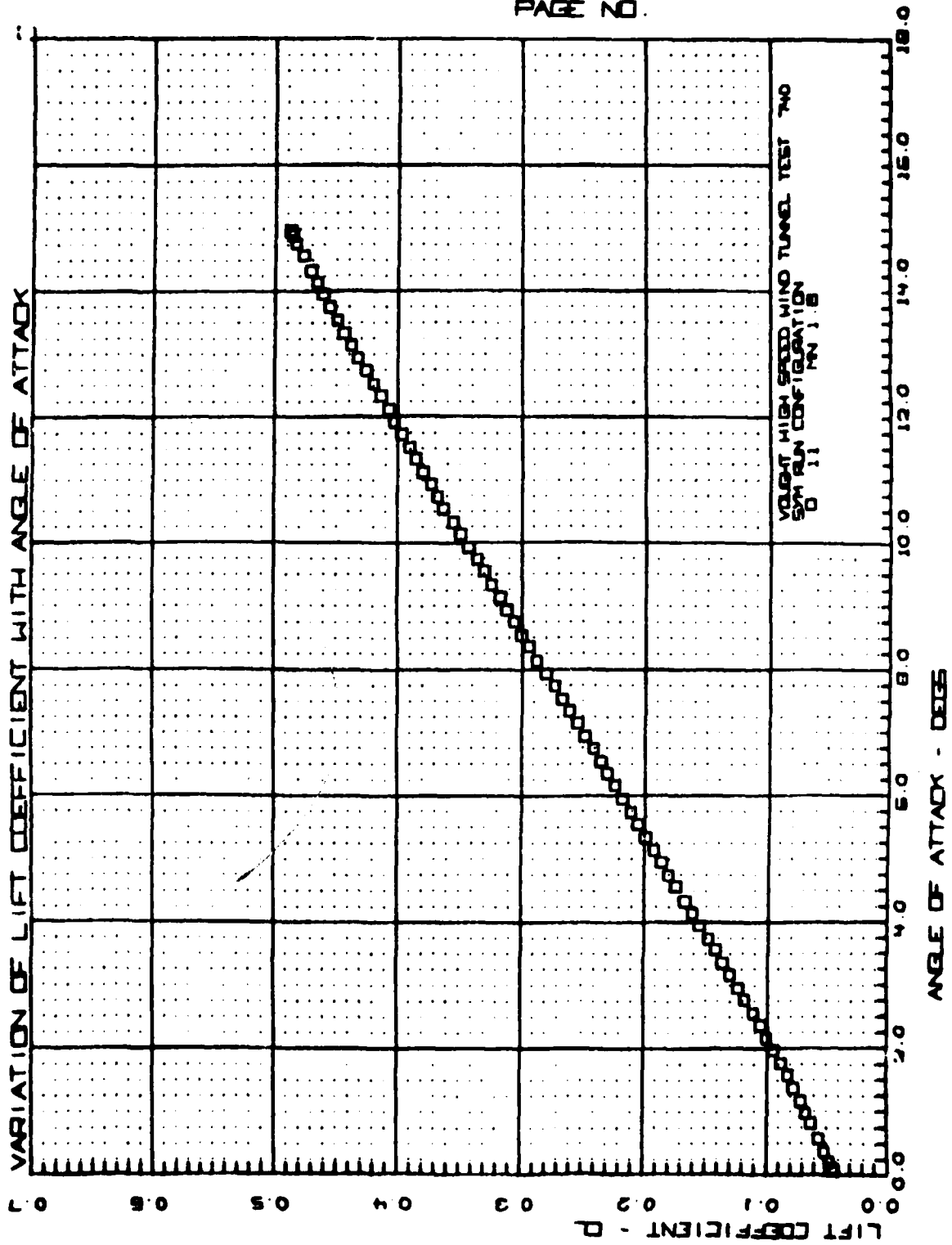


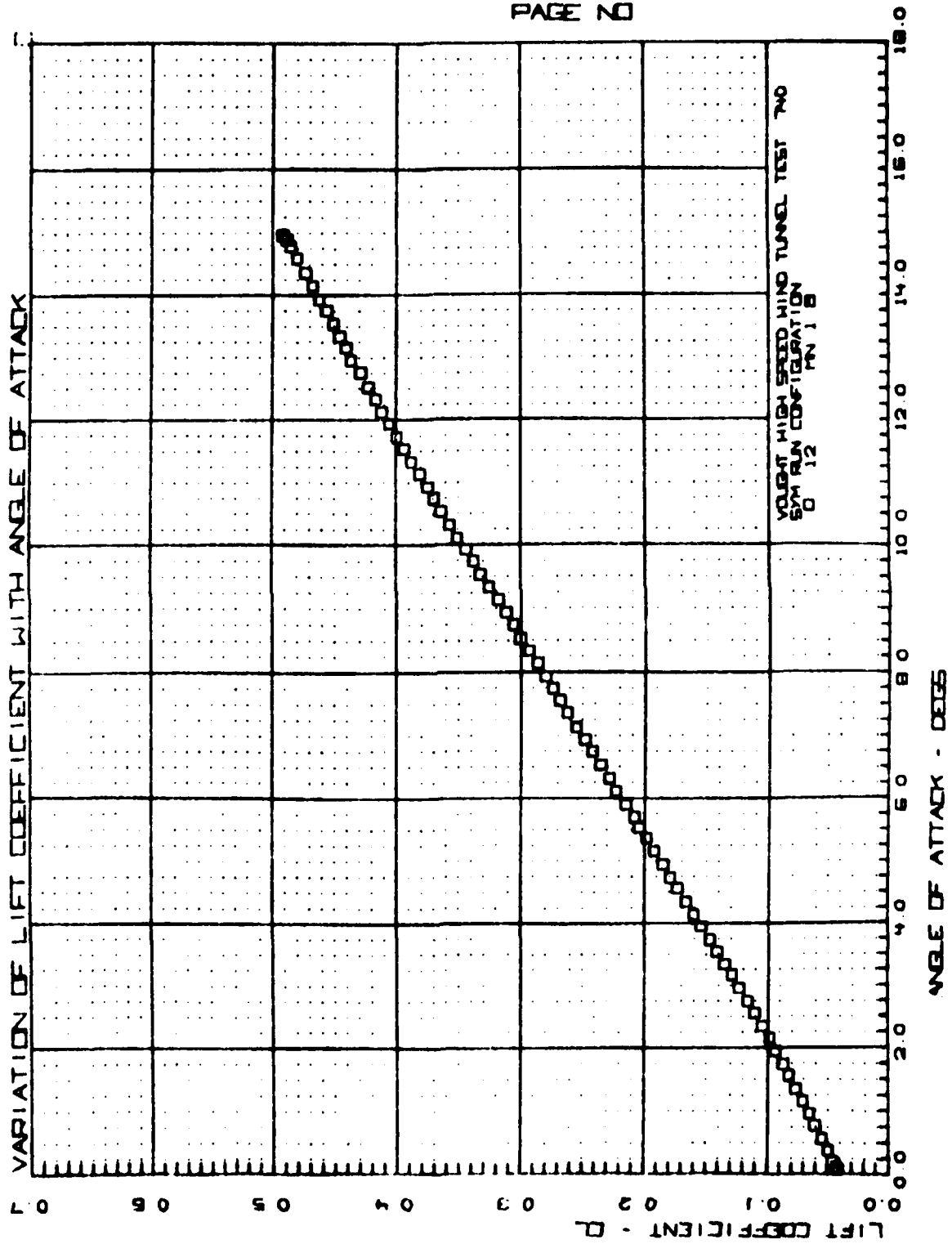


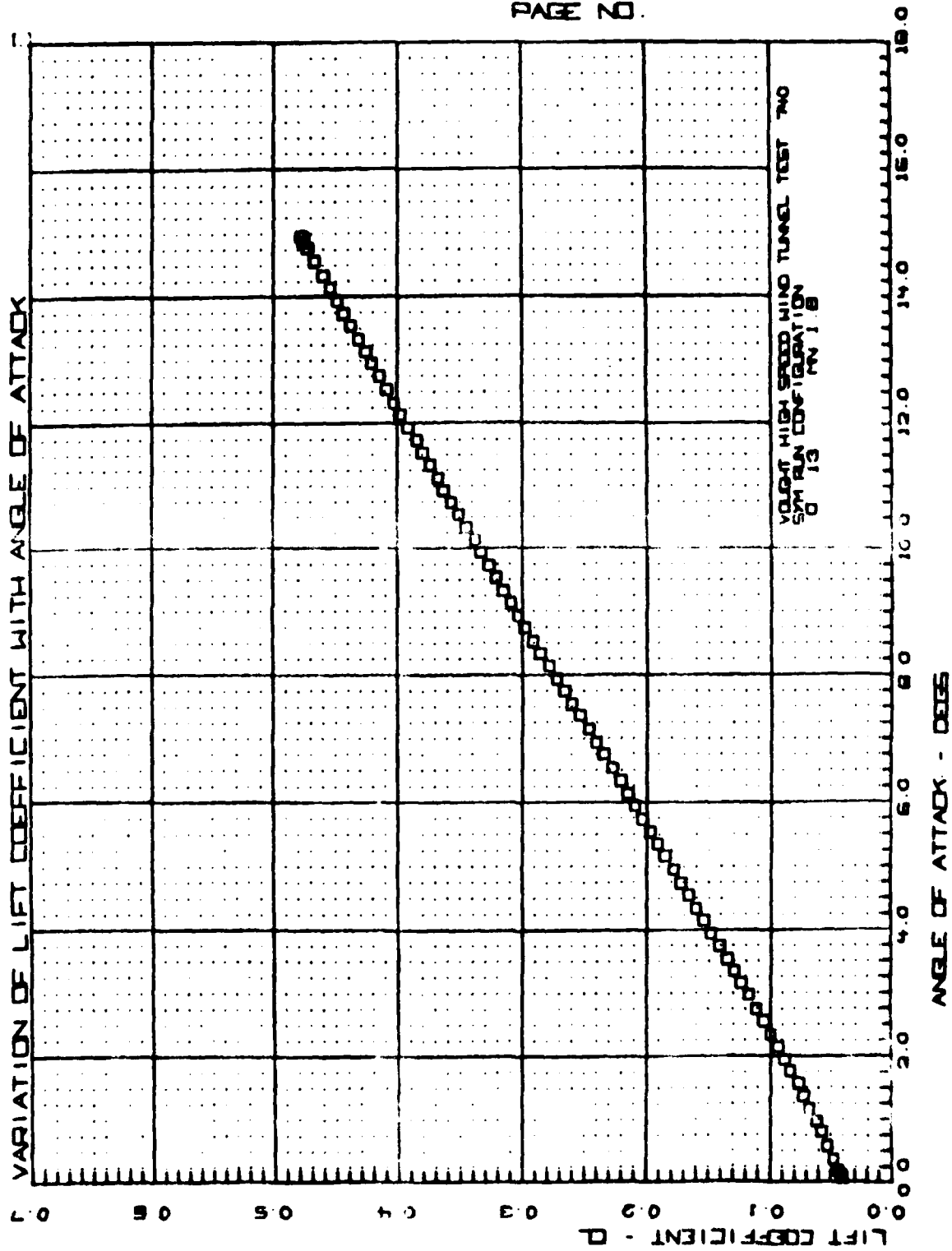


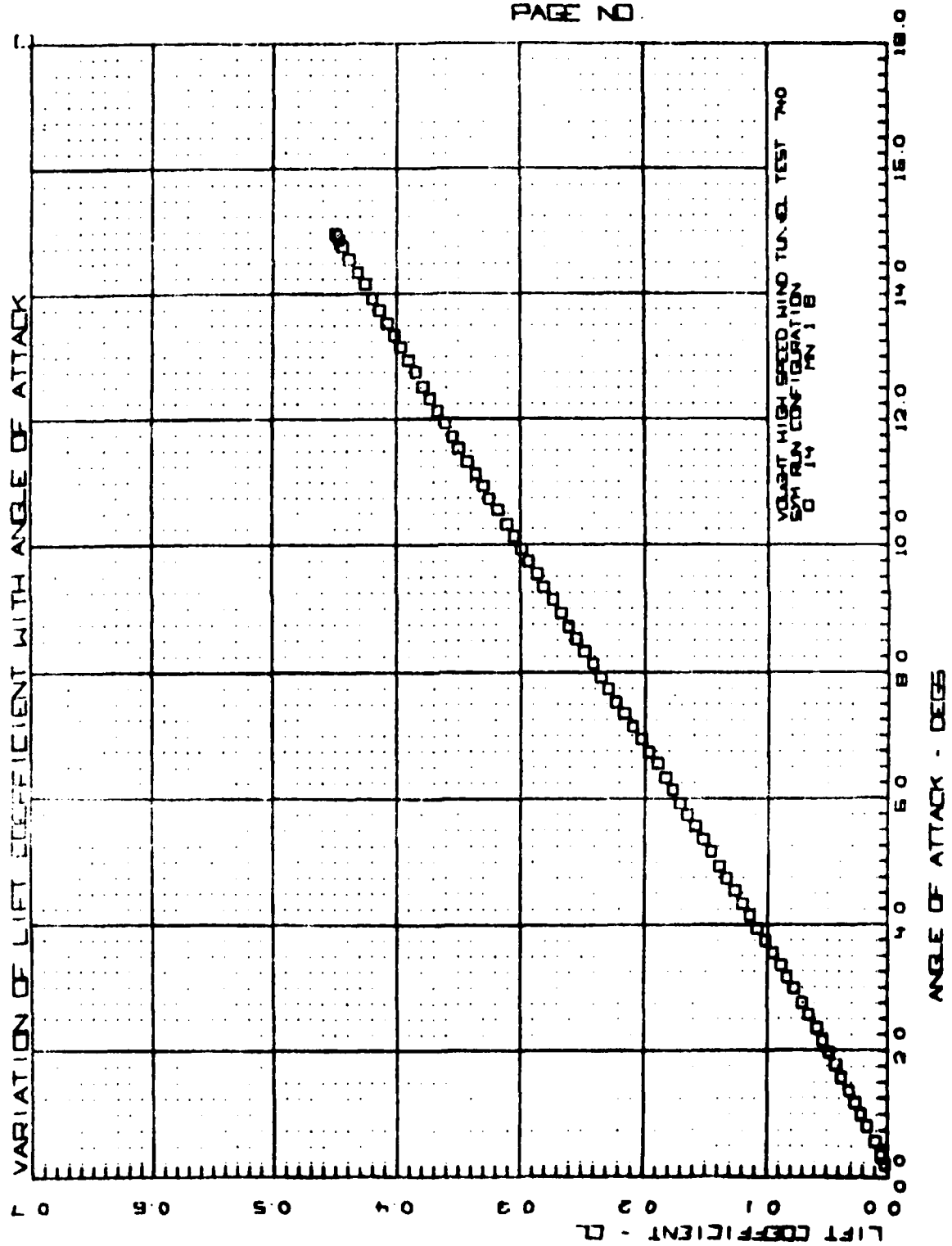


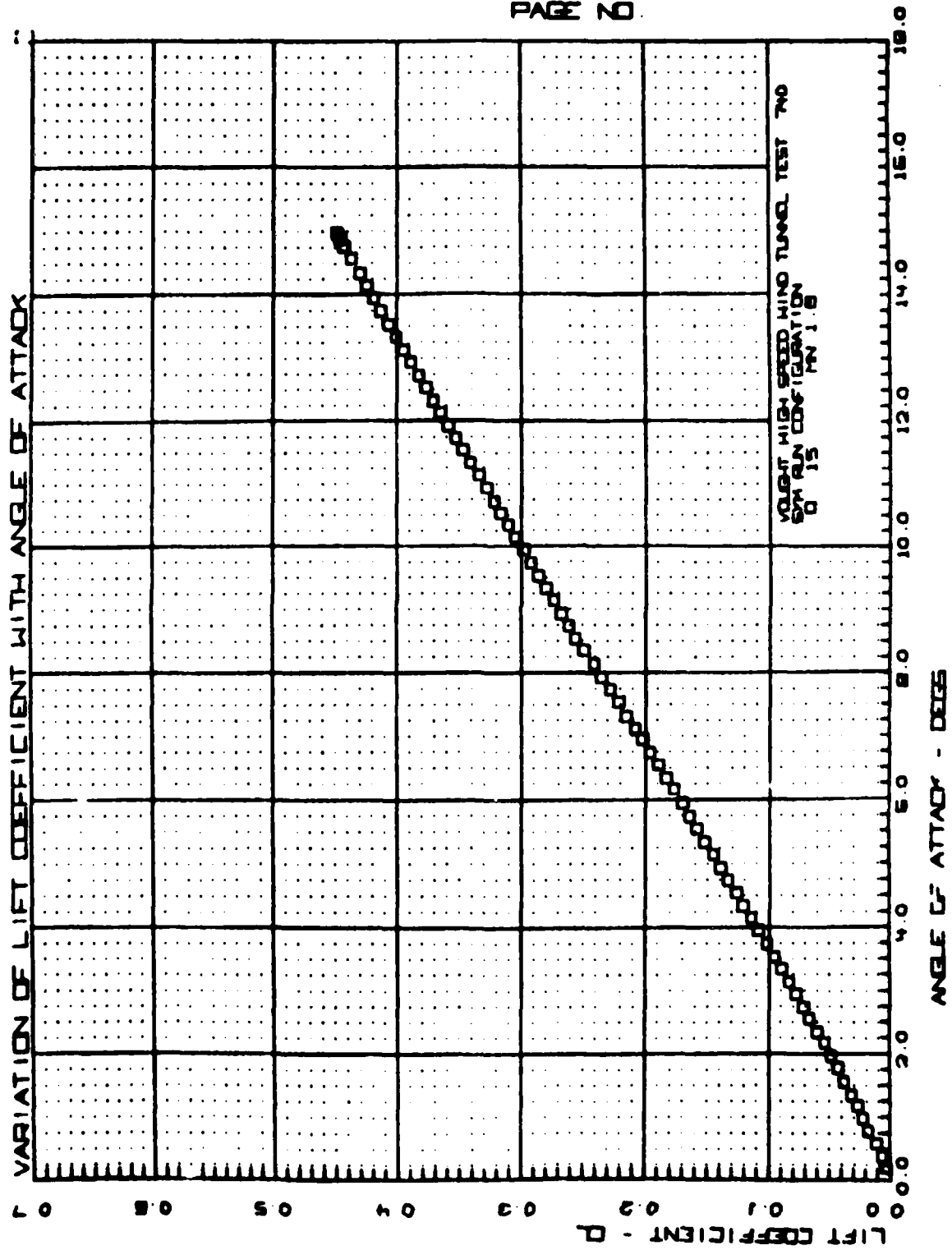
VOLIGHT HEAT TEST 740
PAGE NO.

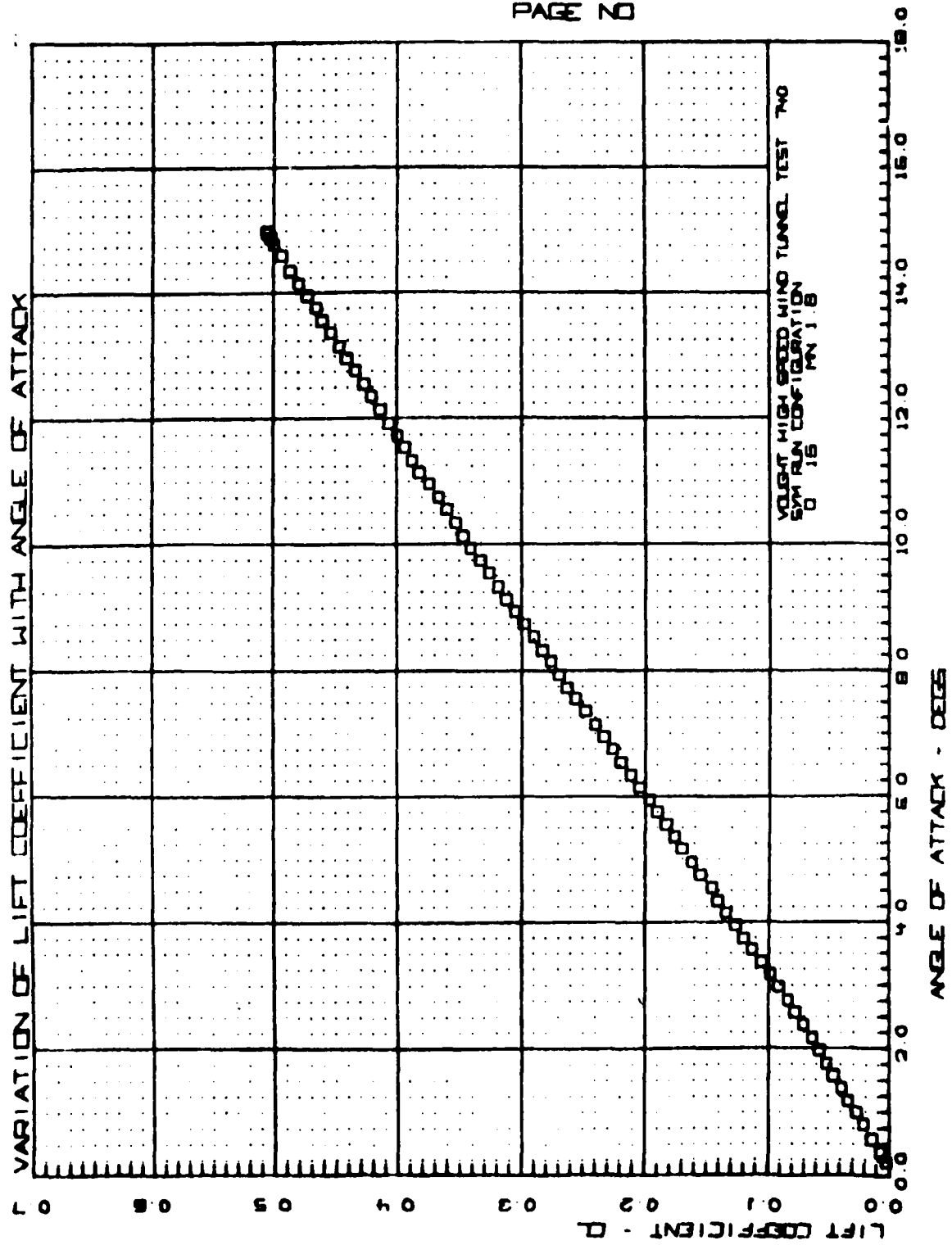


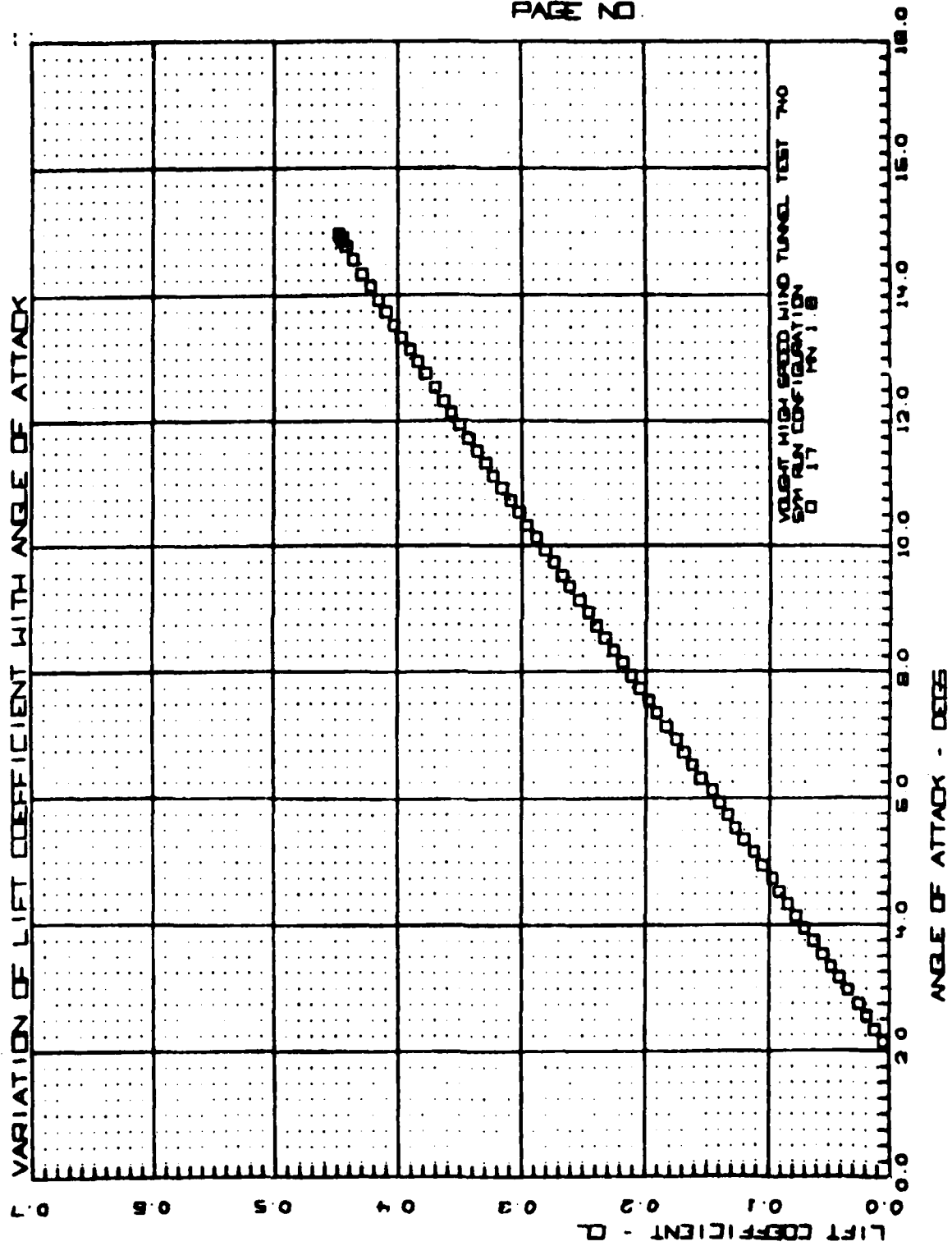


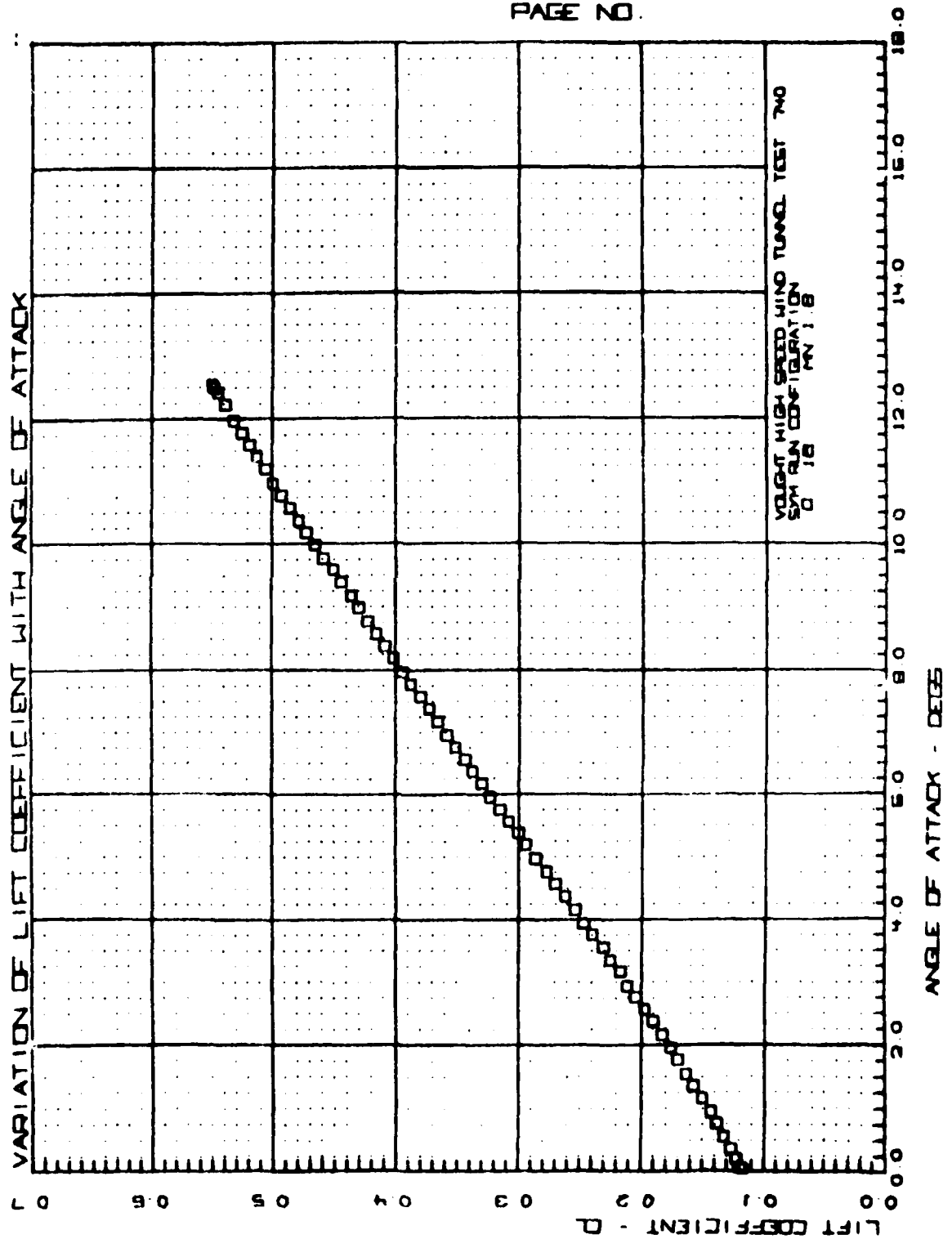


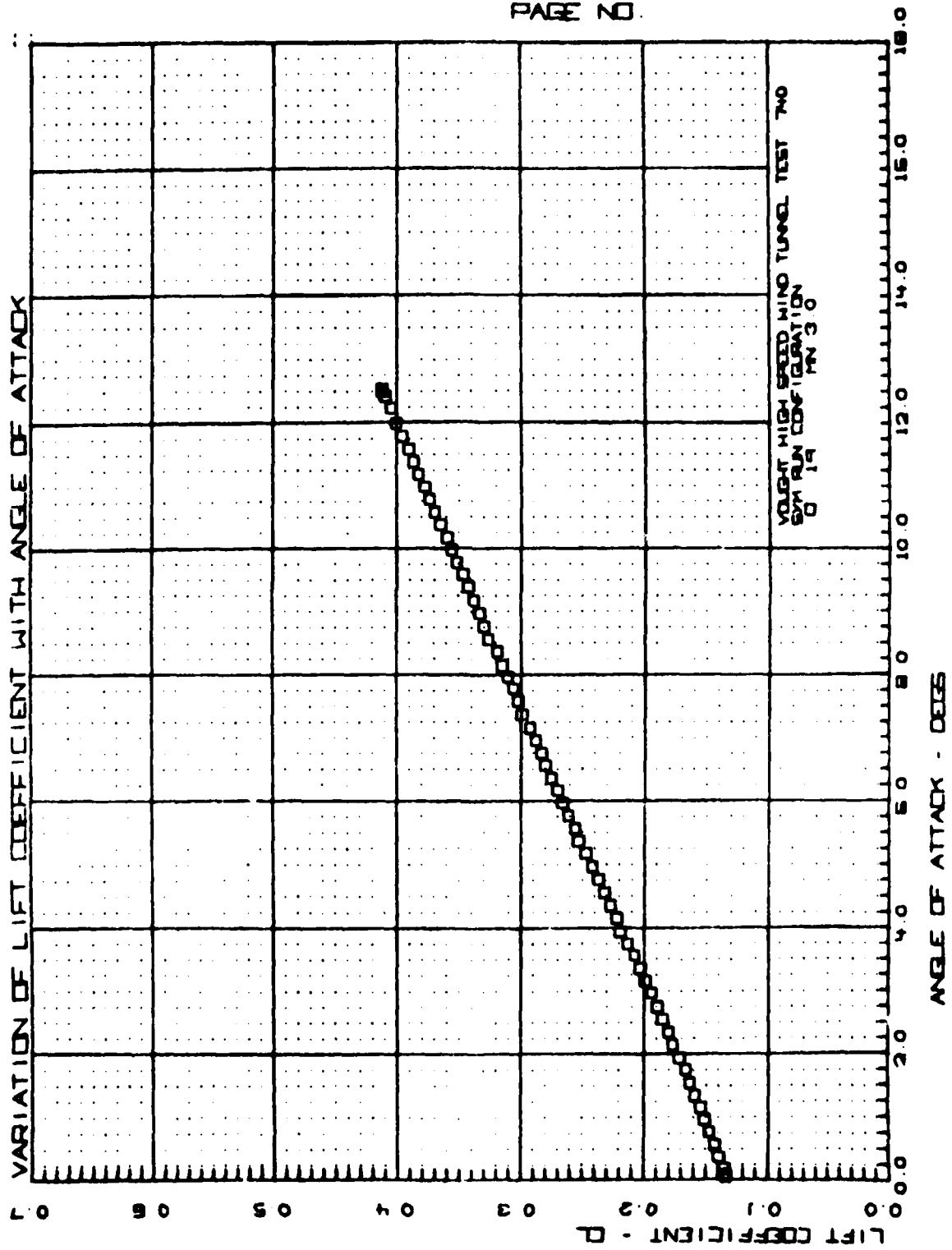


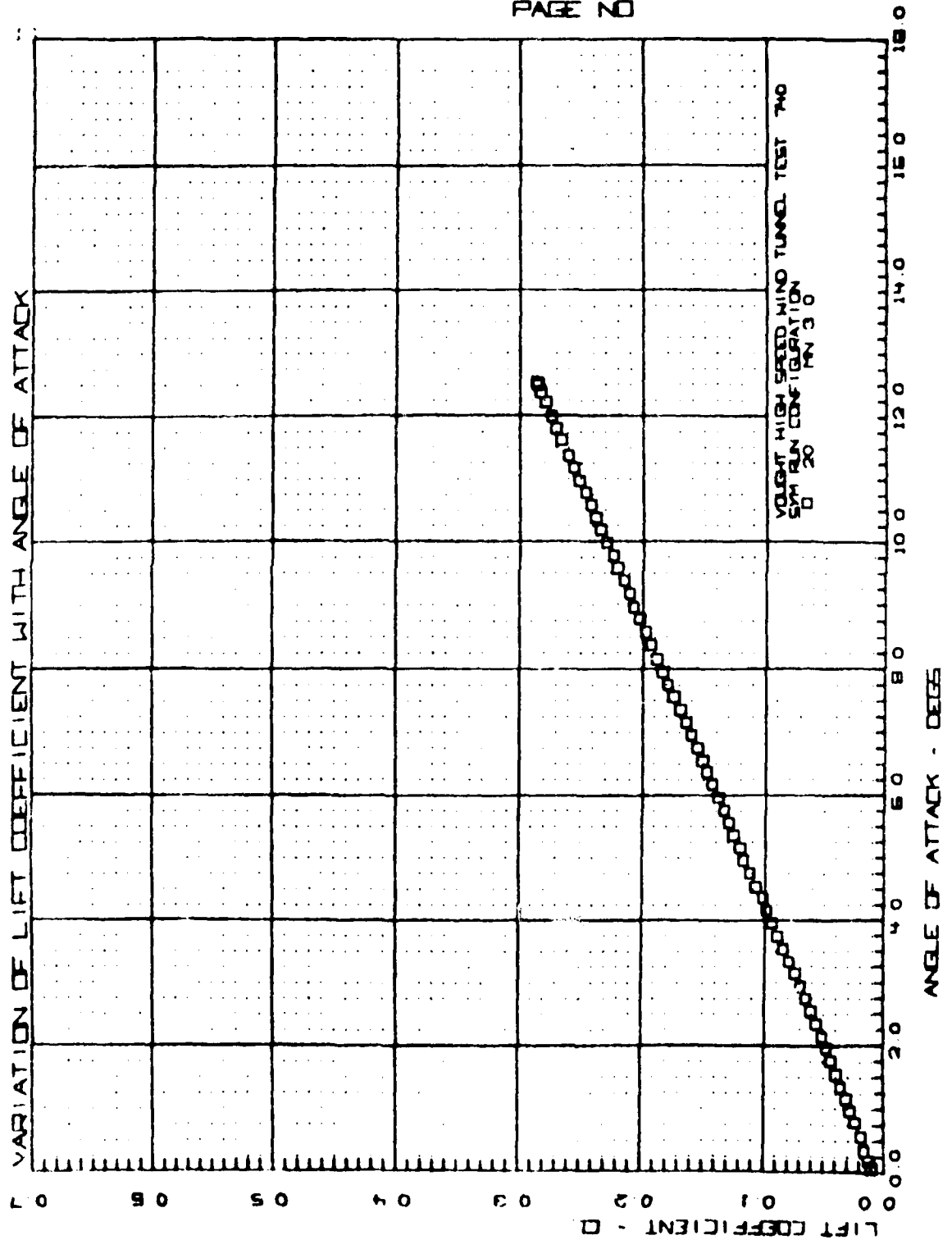


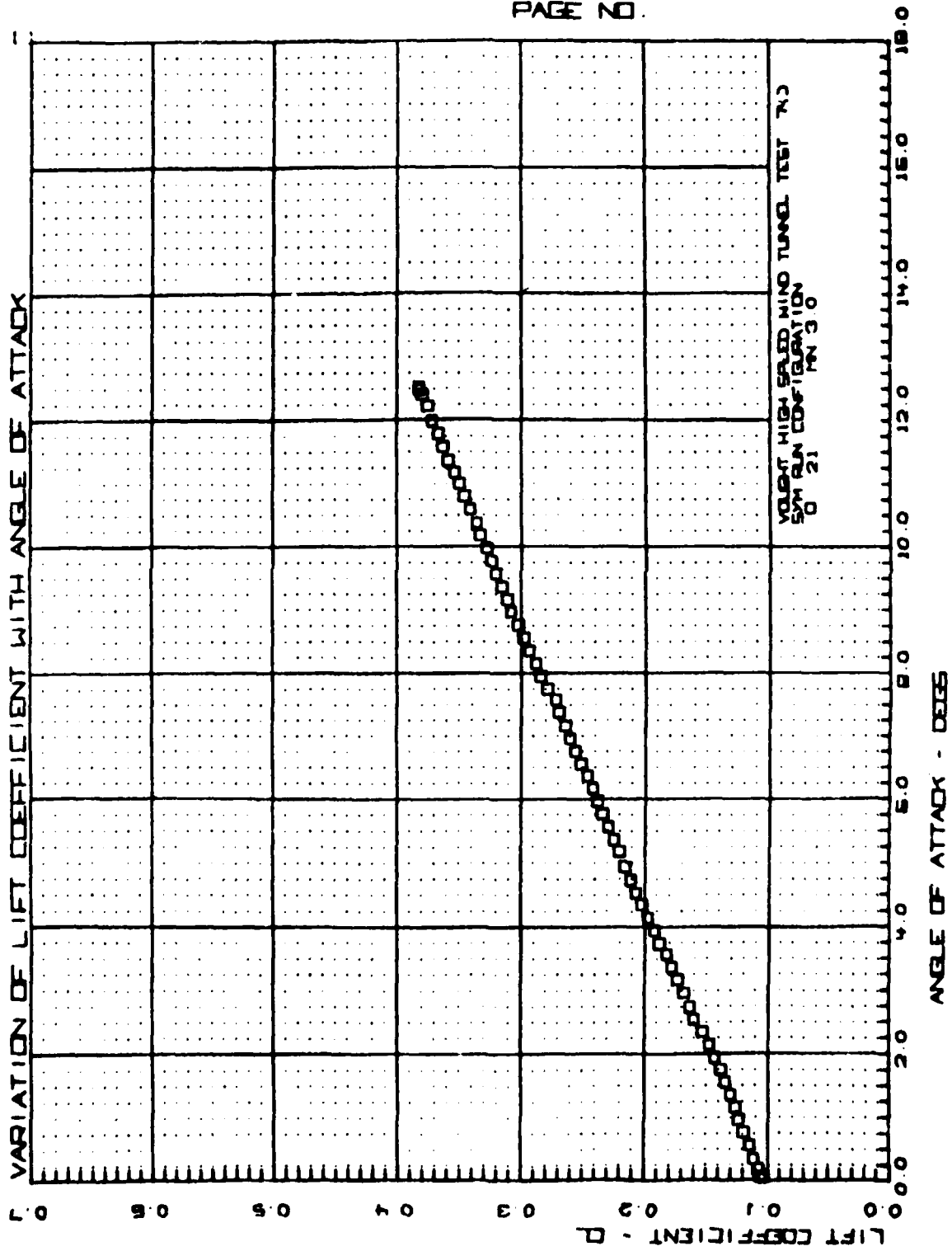


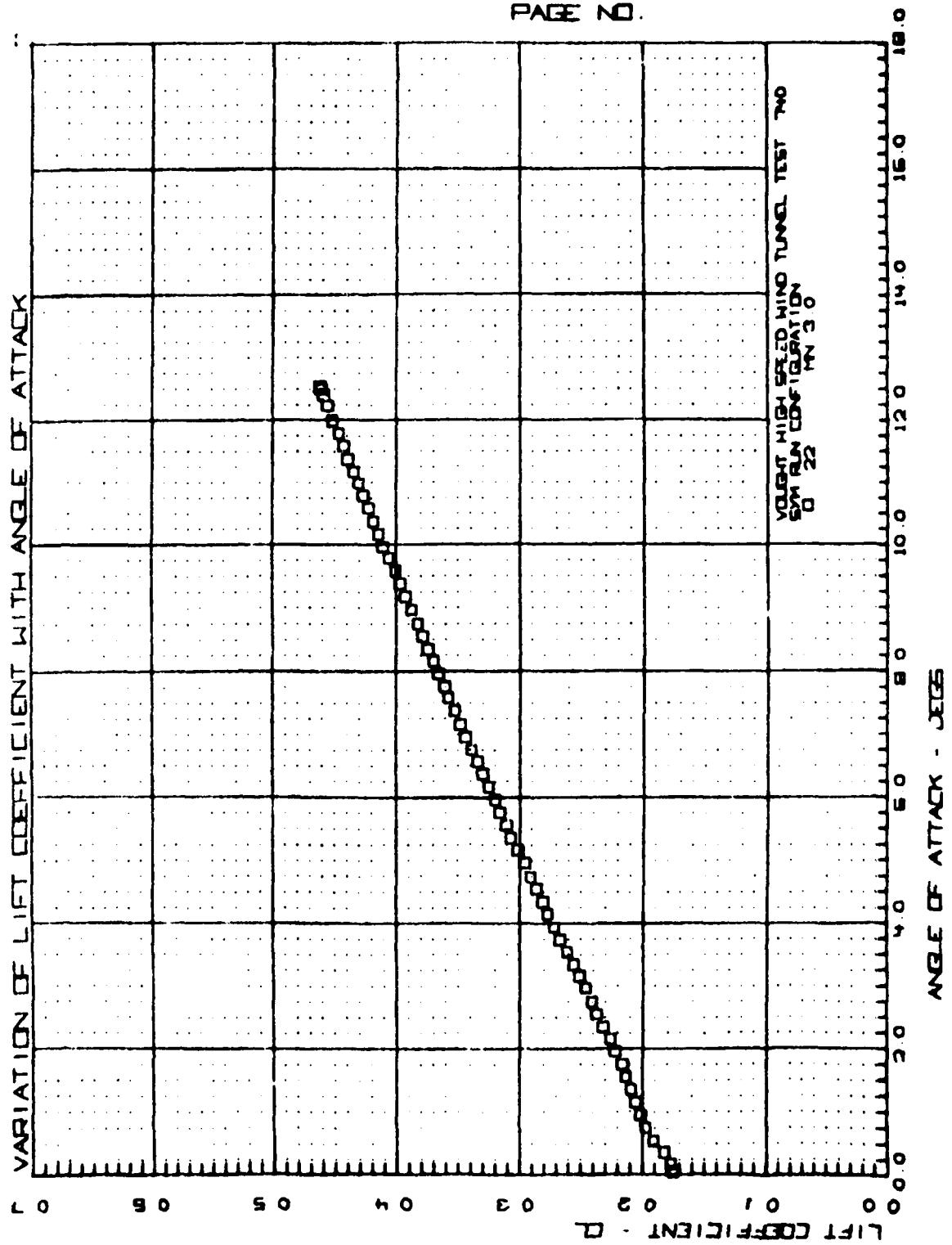


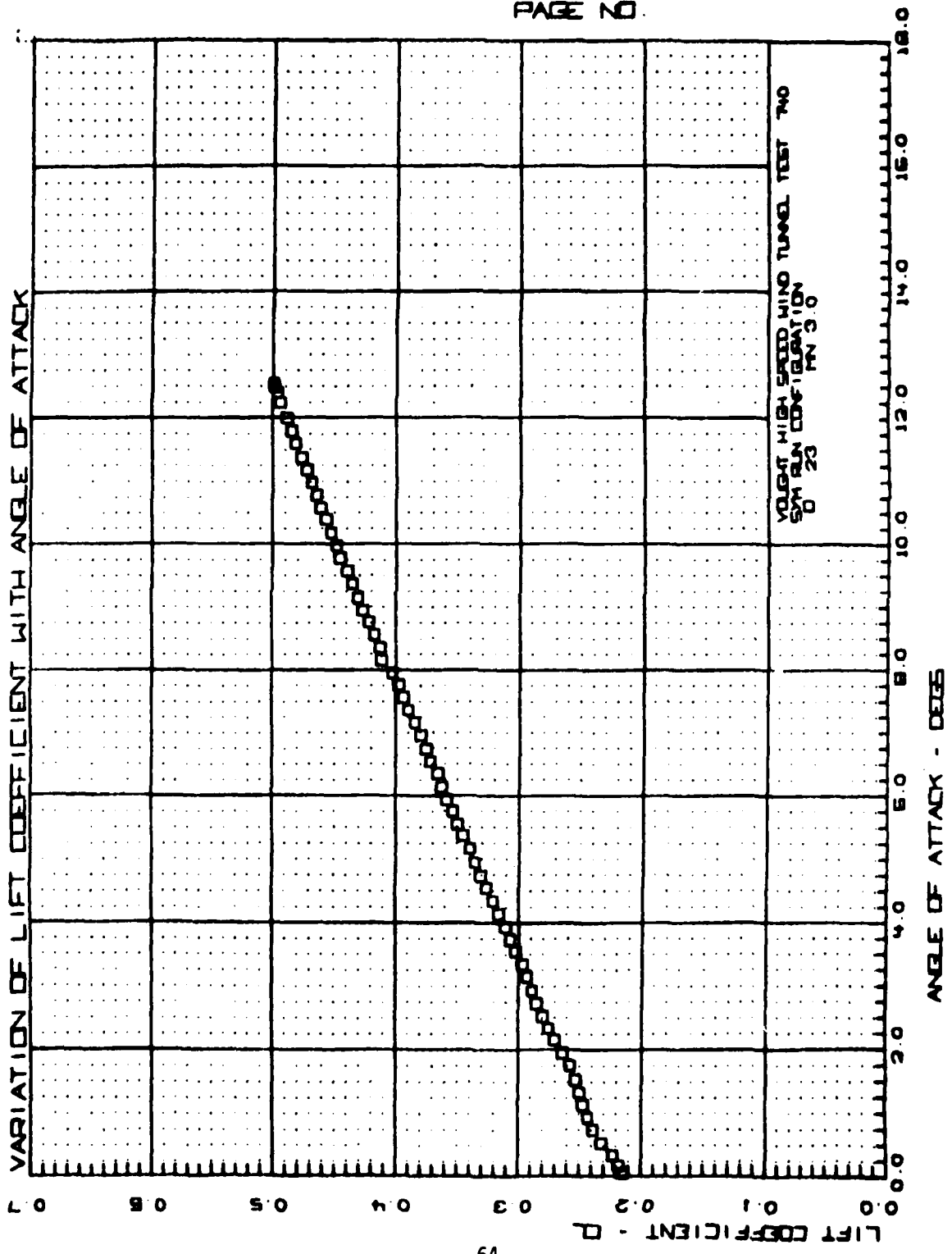


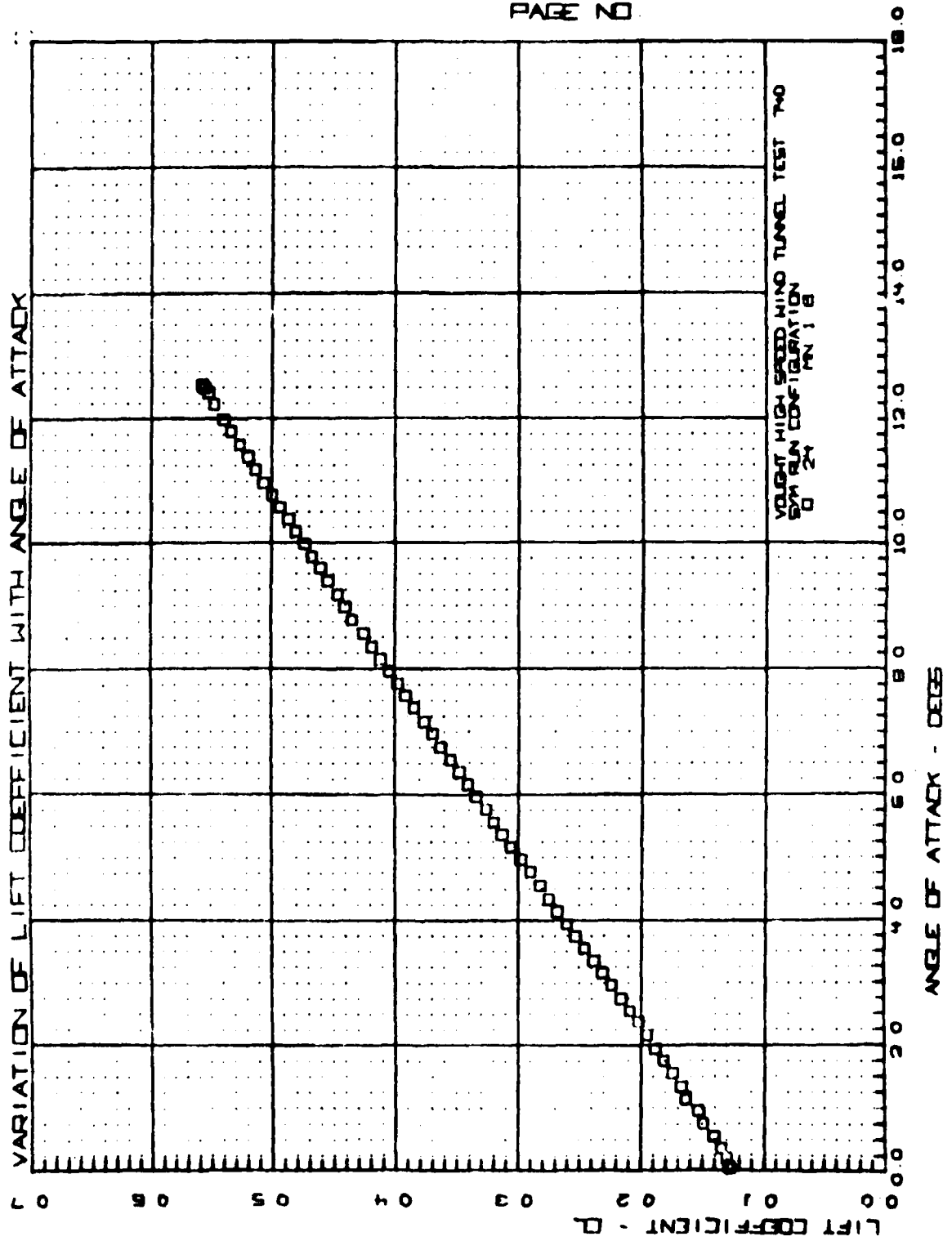


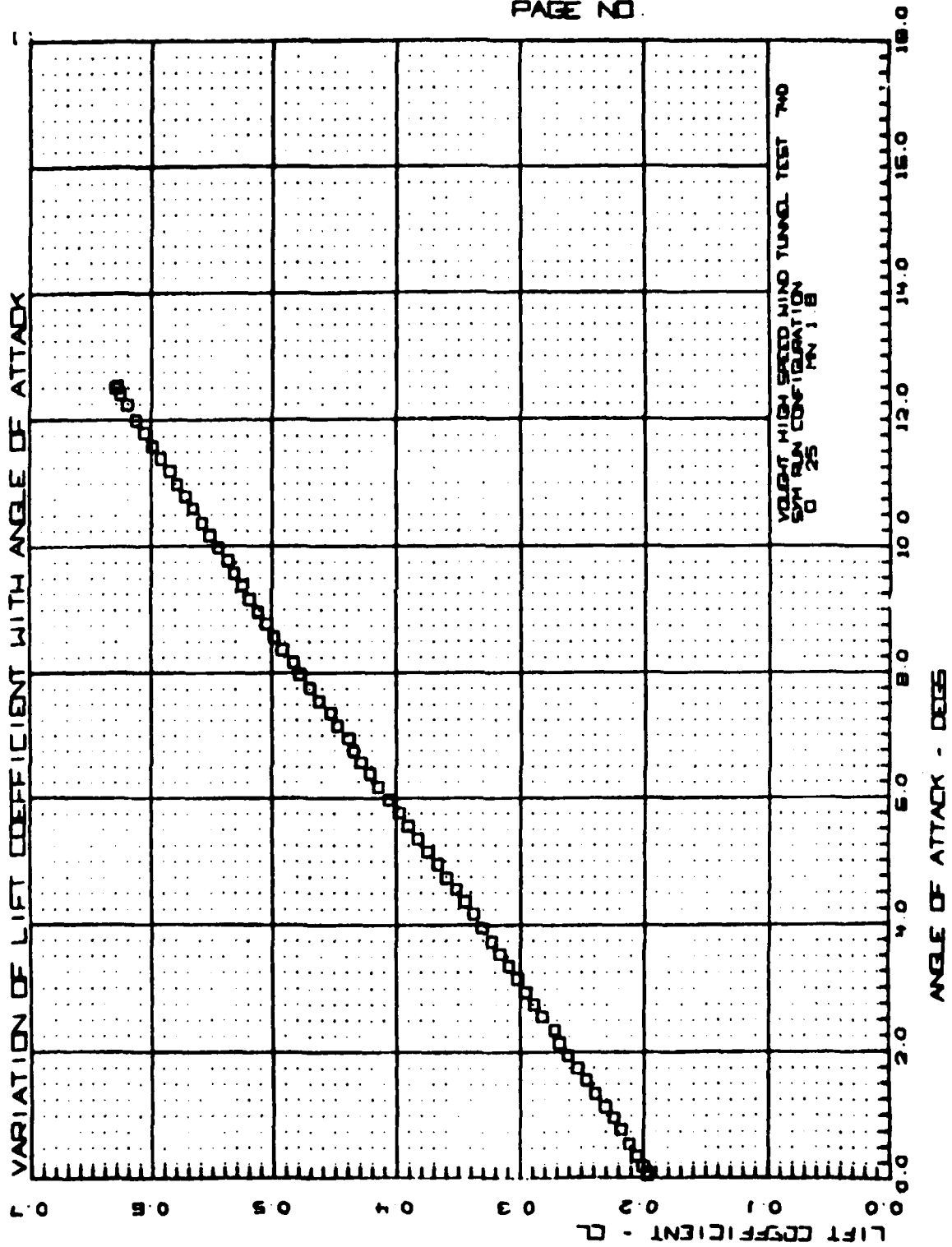


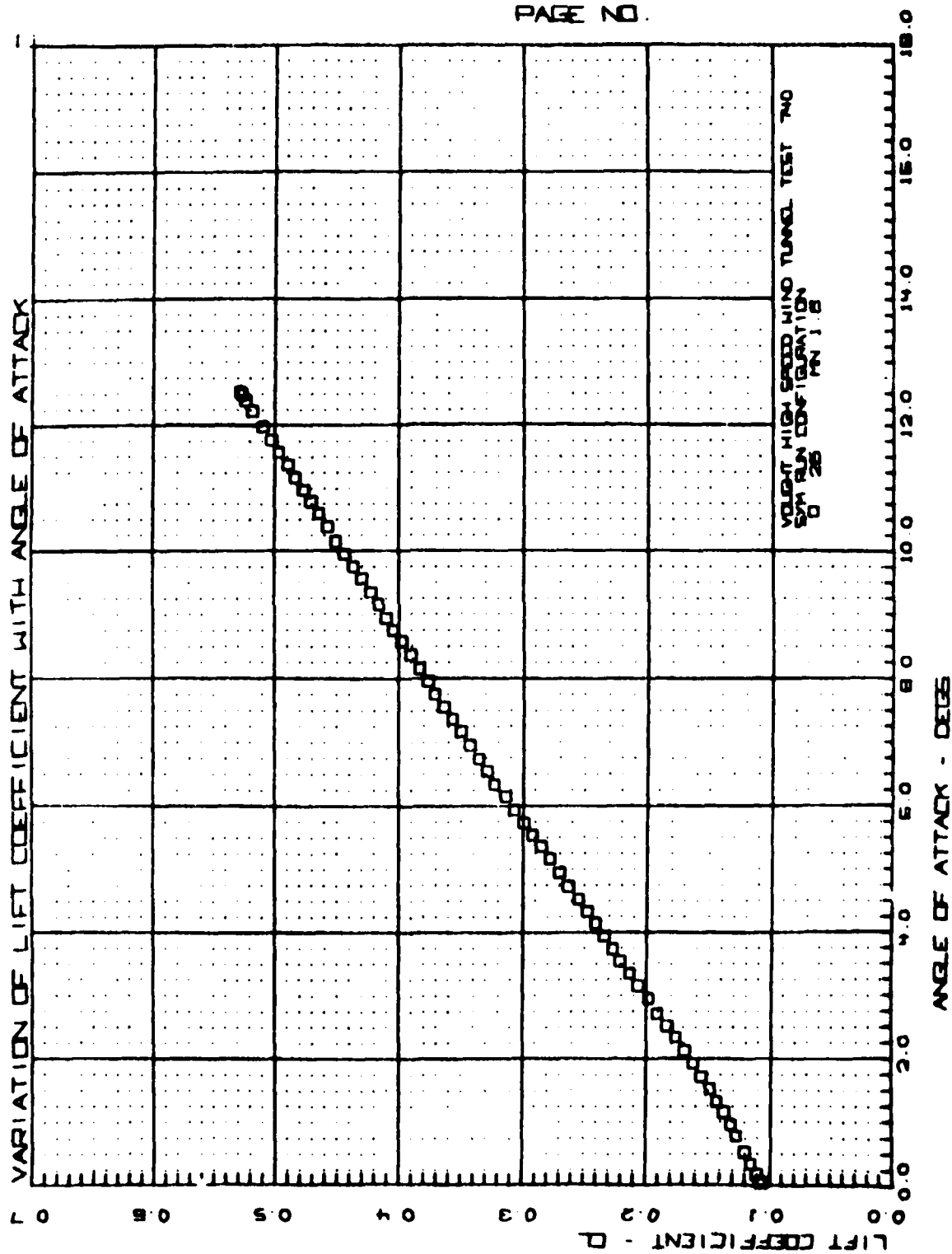




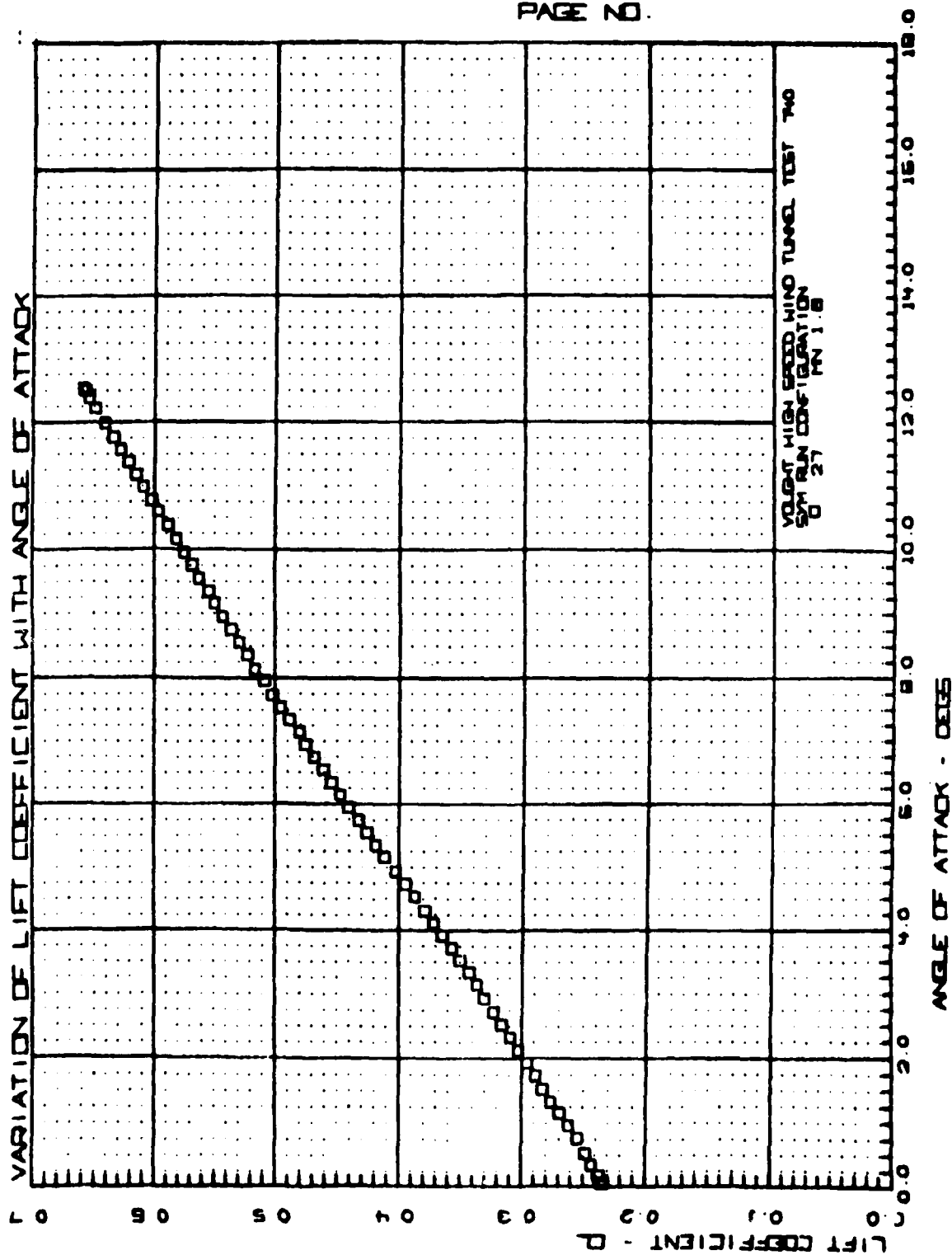


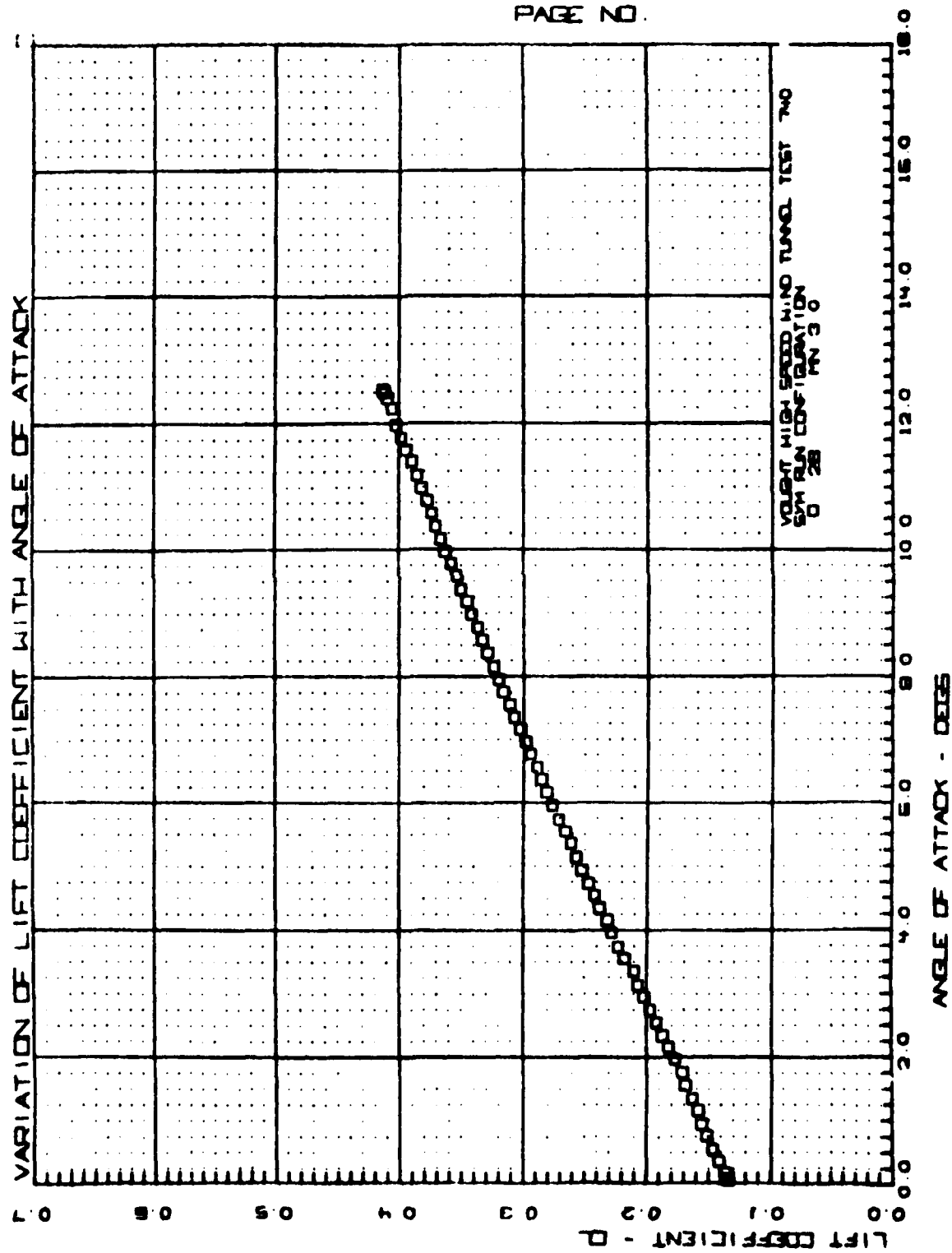


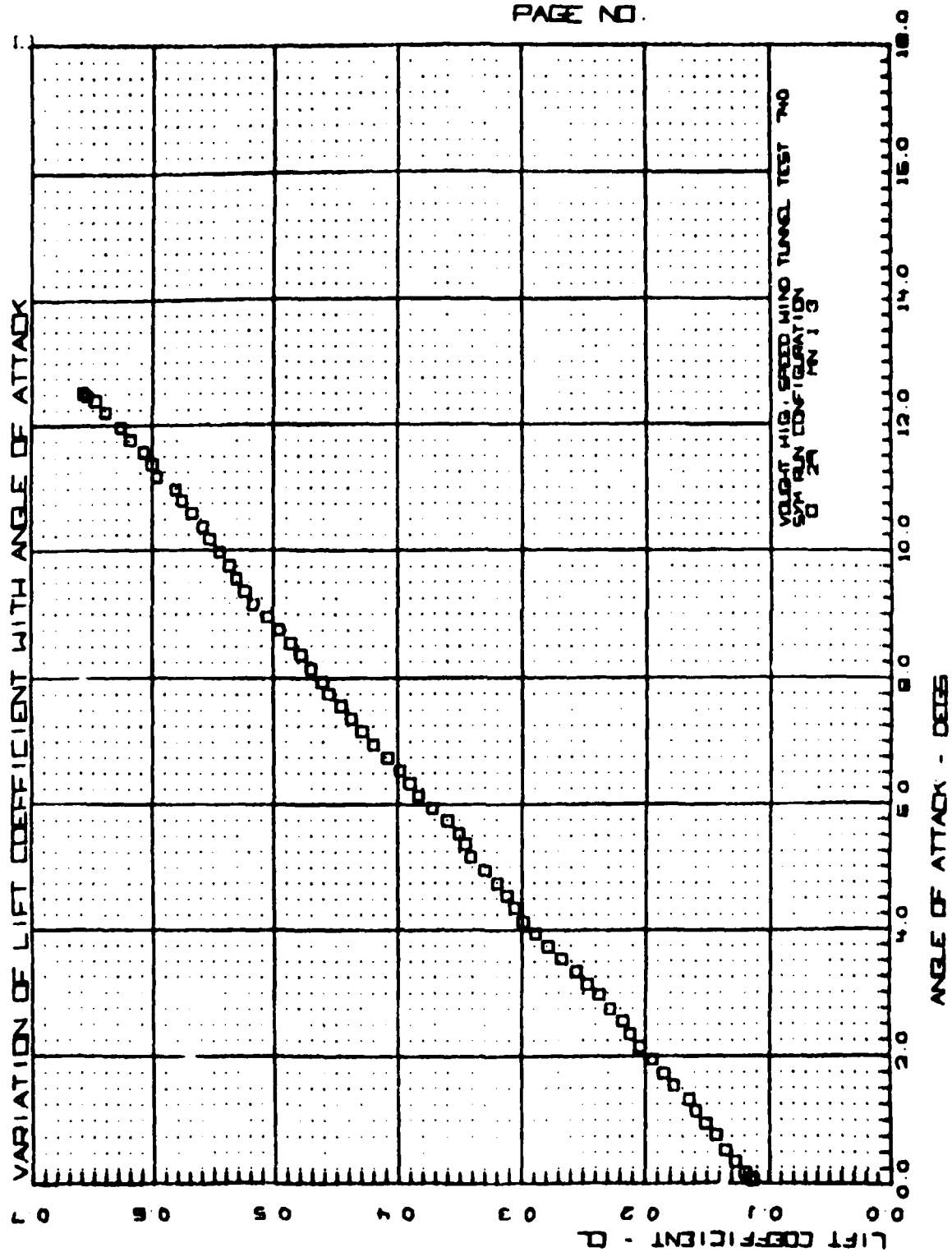


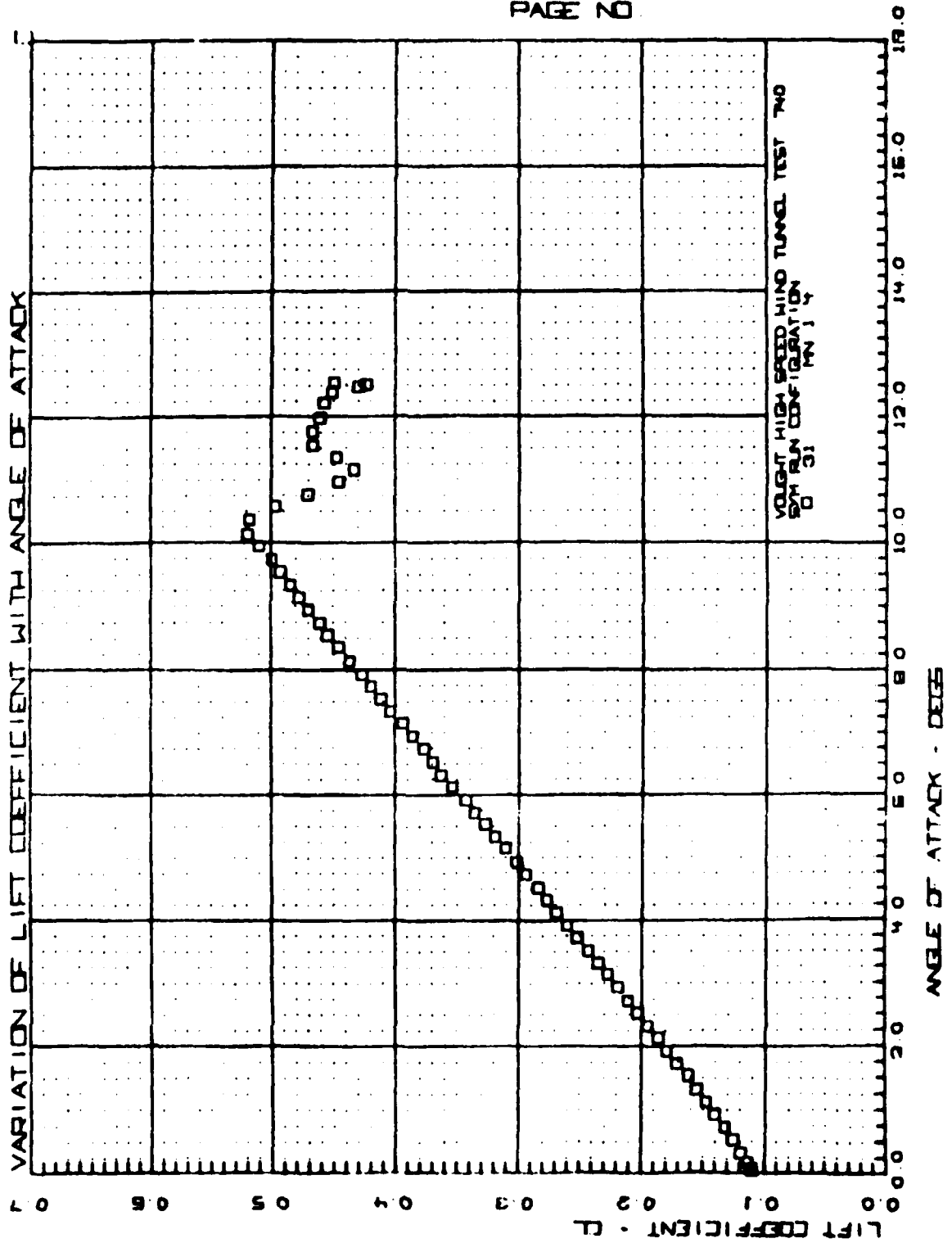


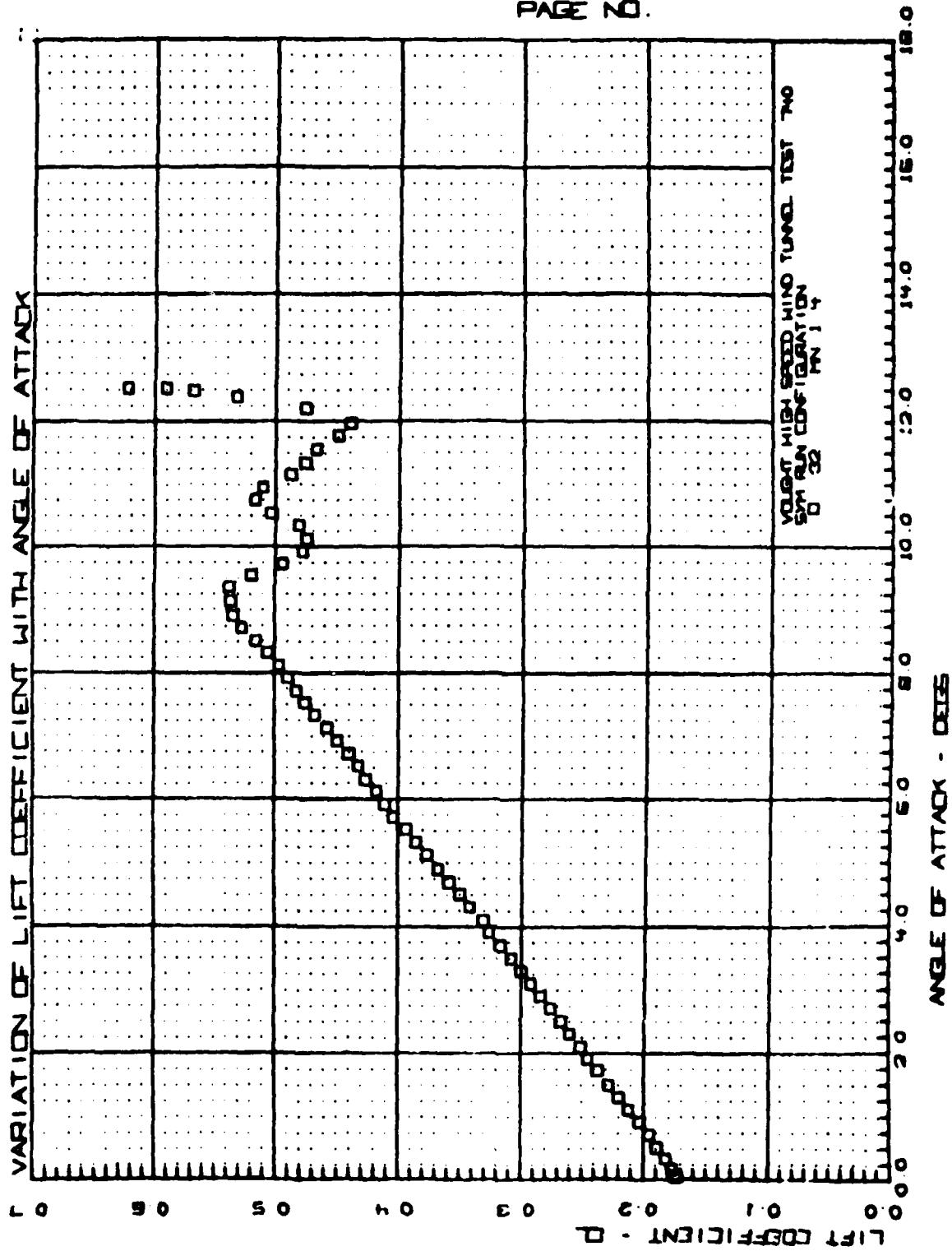
VOUGHT HEAT TEST TWO
PAGE NO.

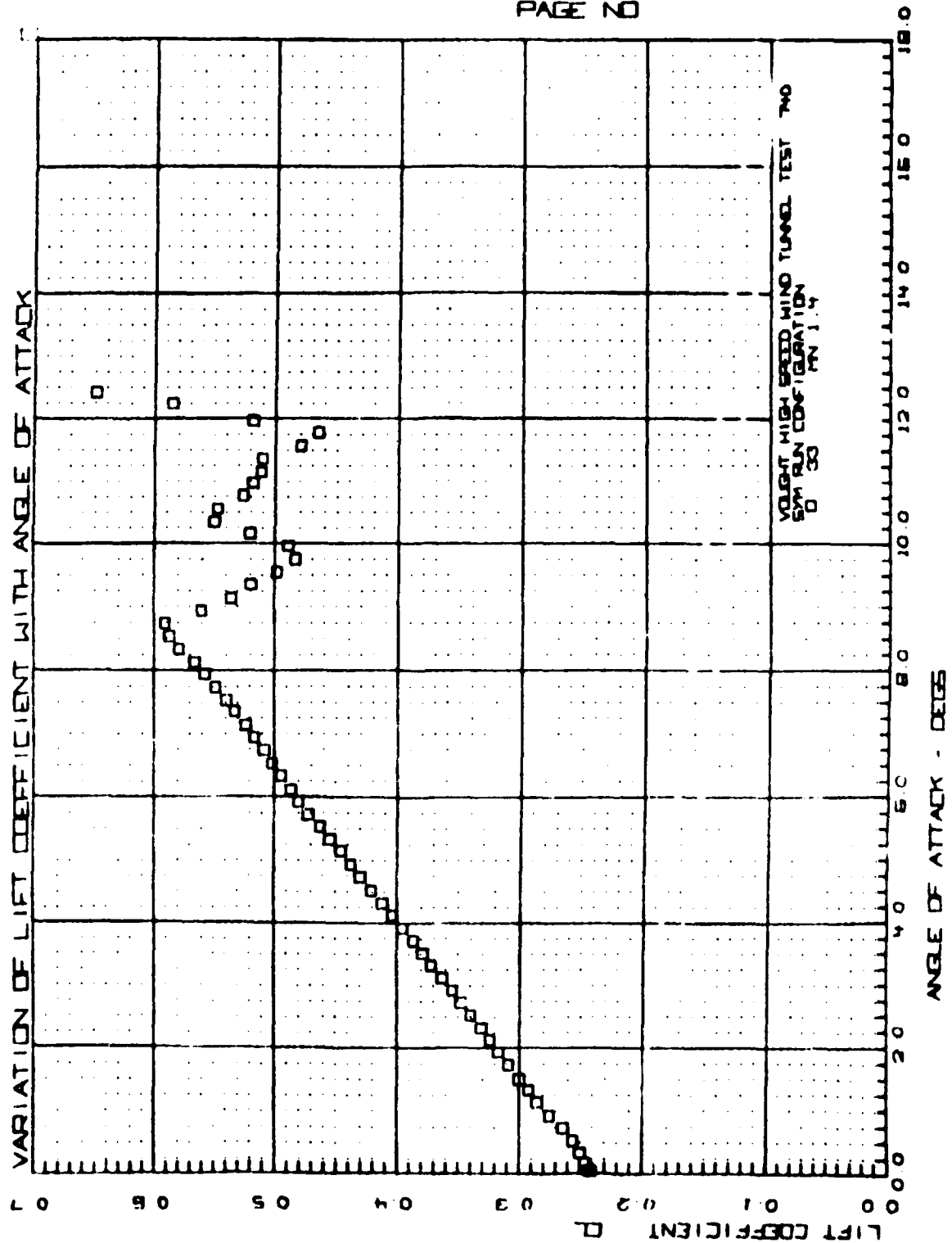


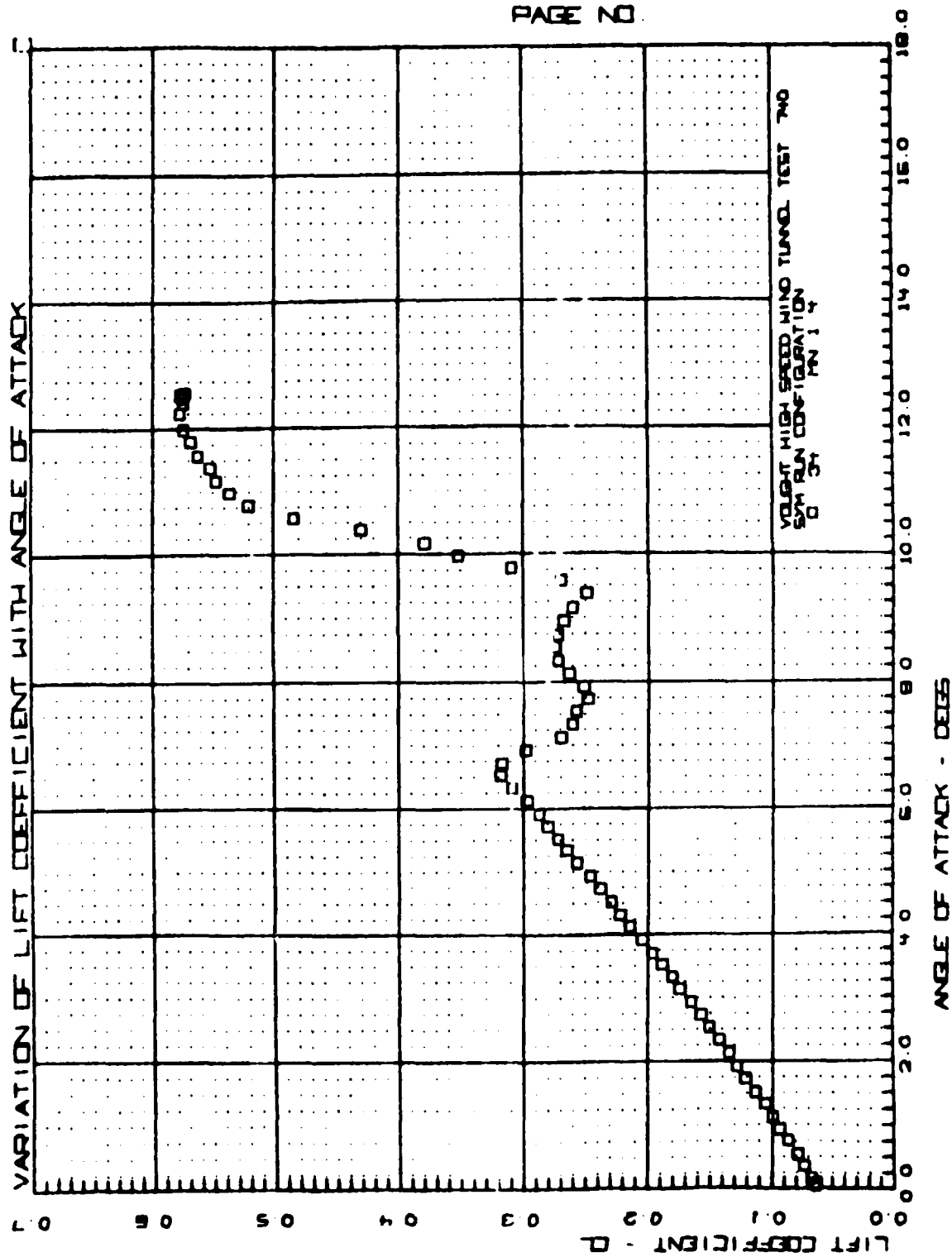




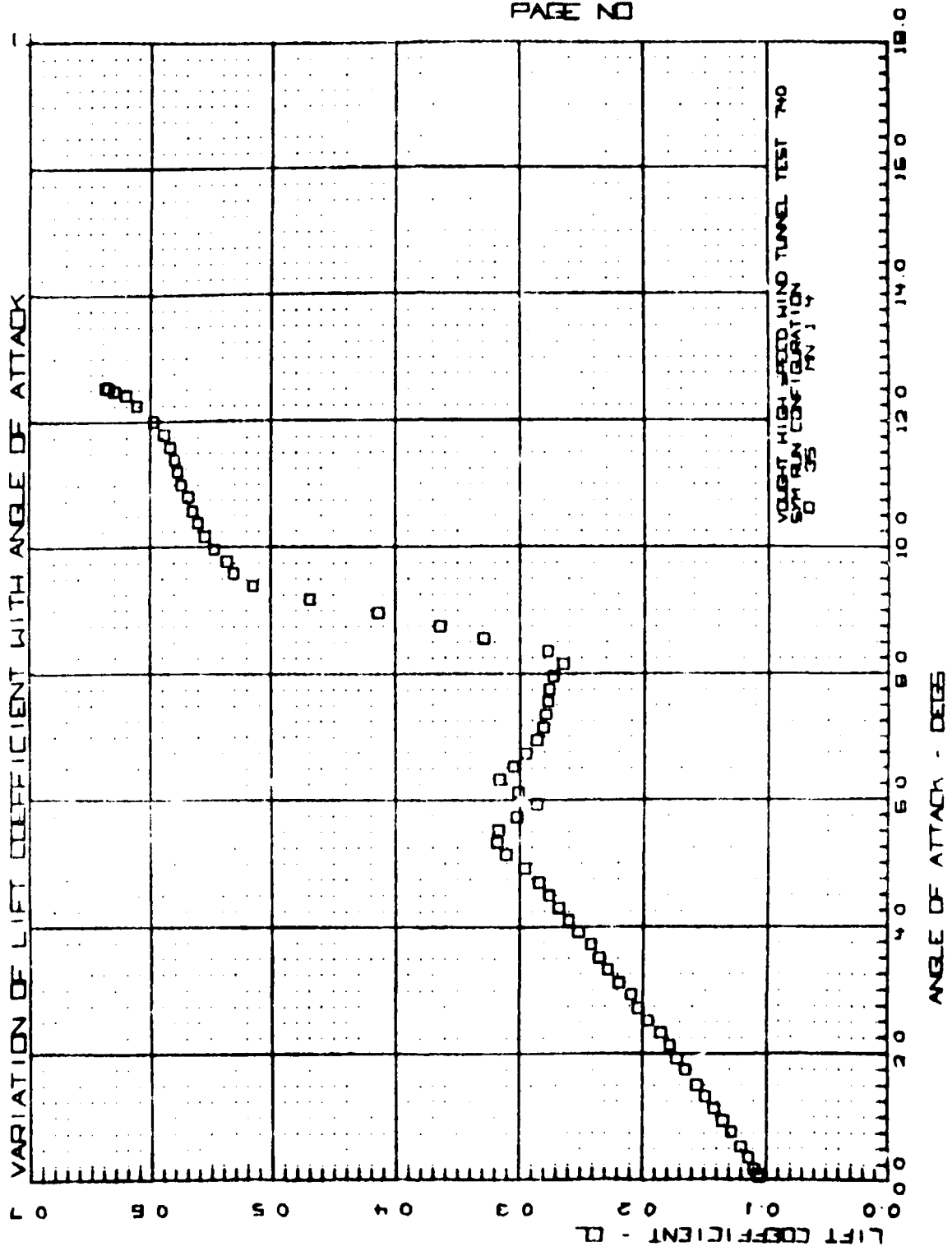


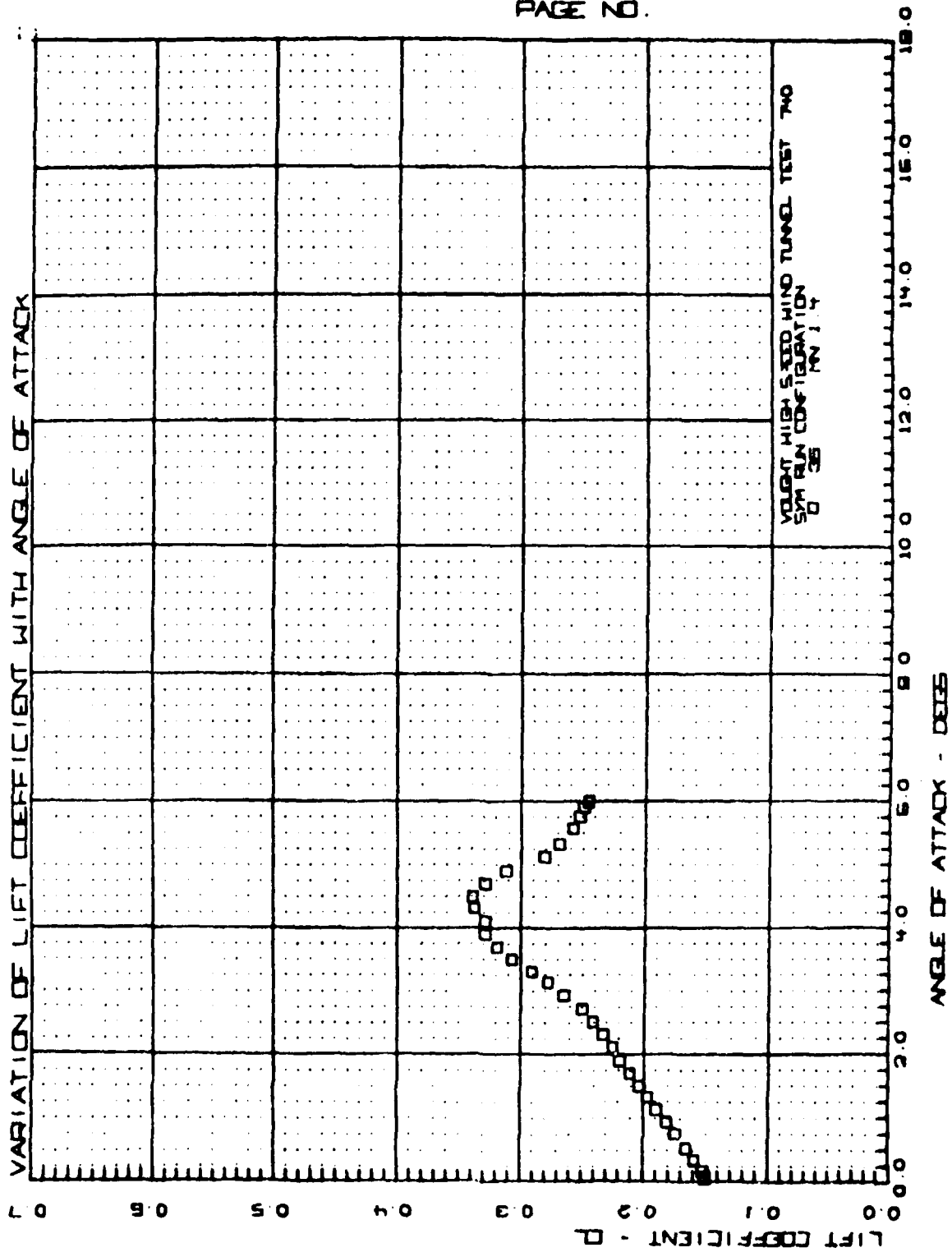


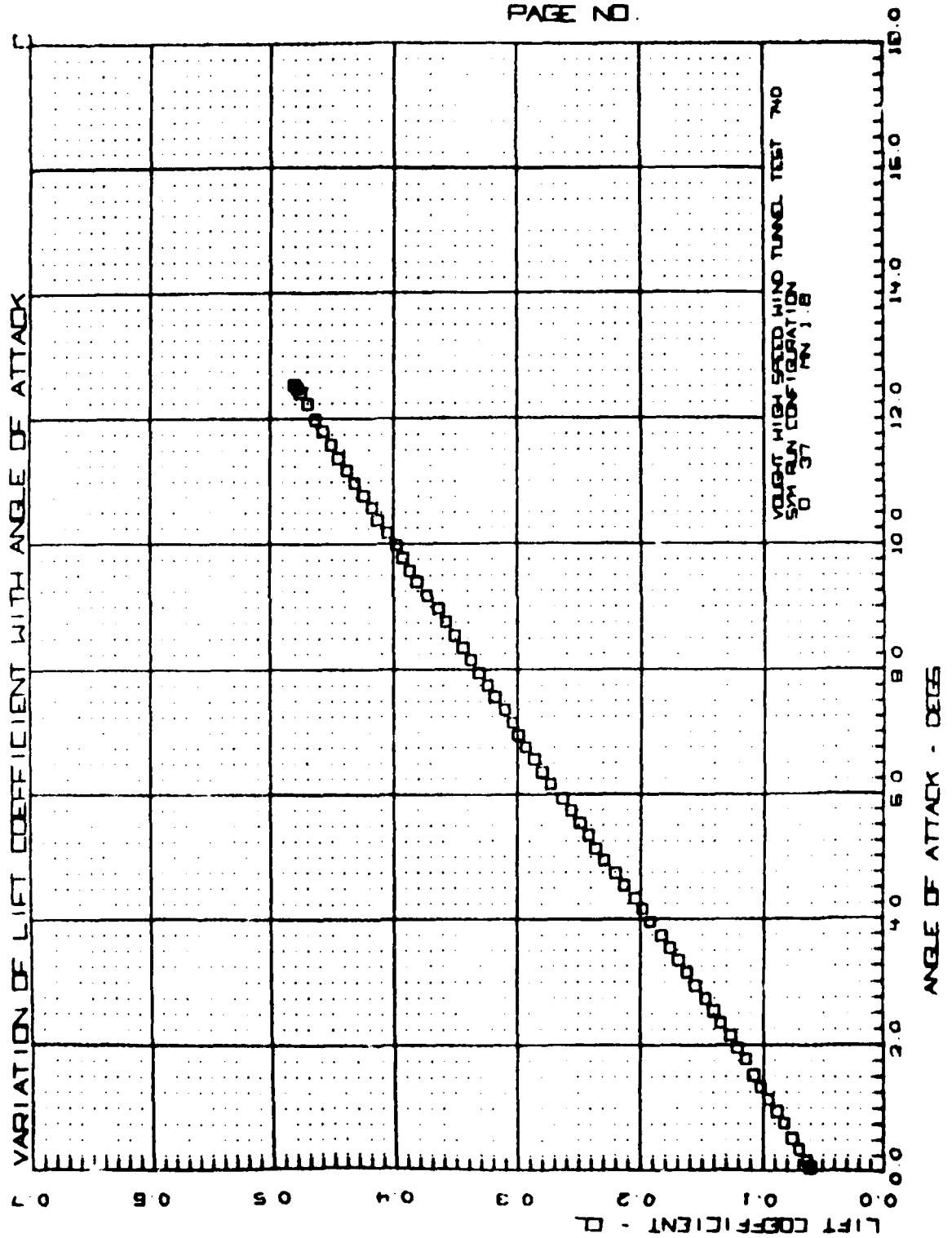


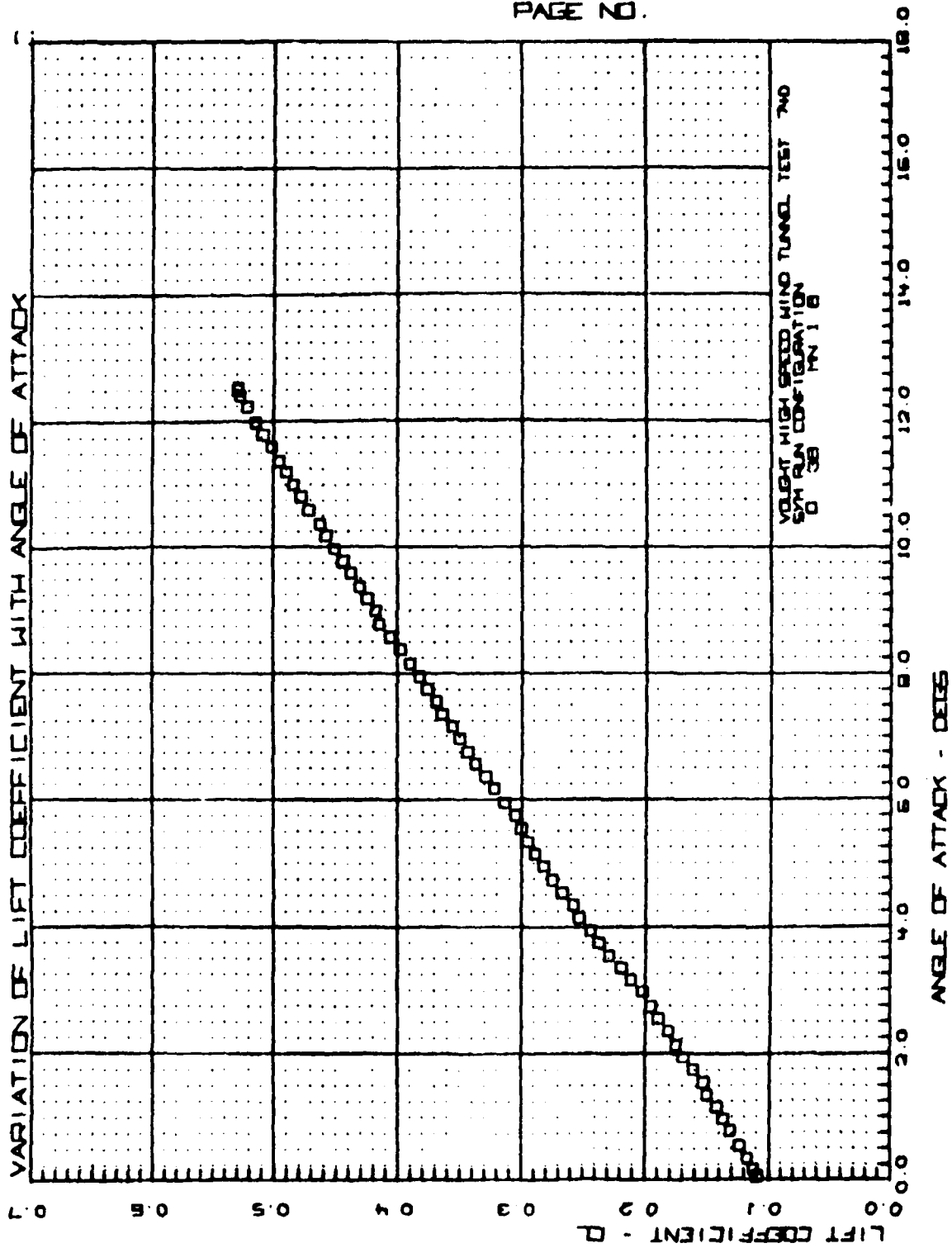


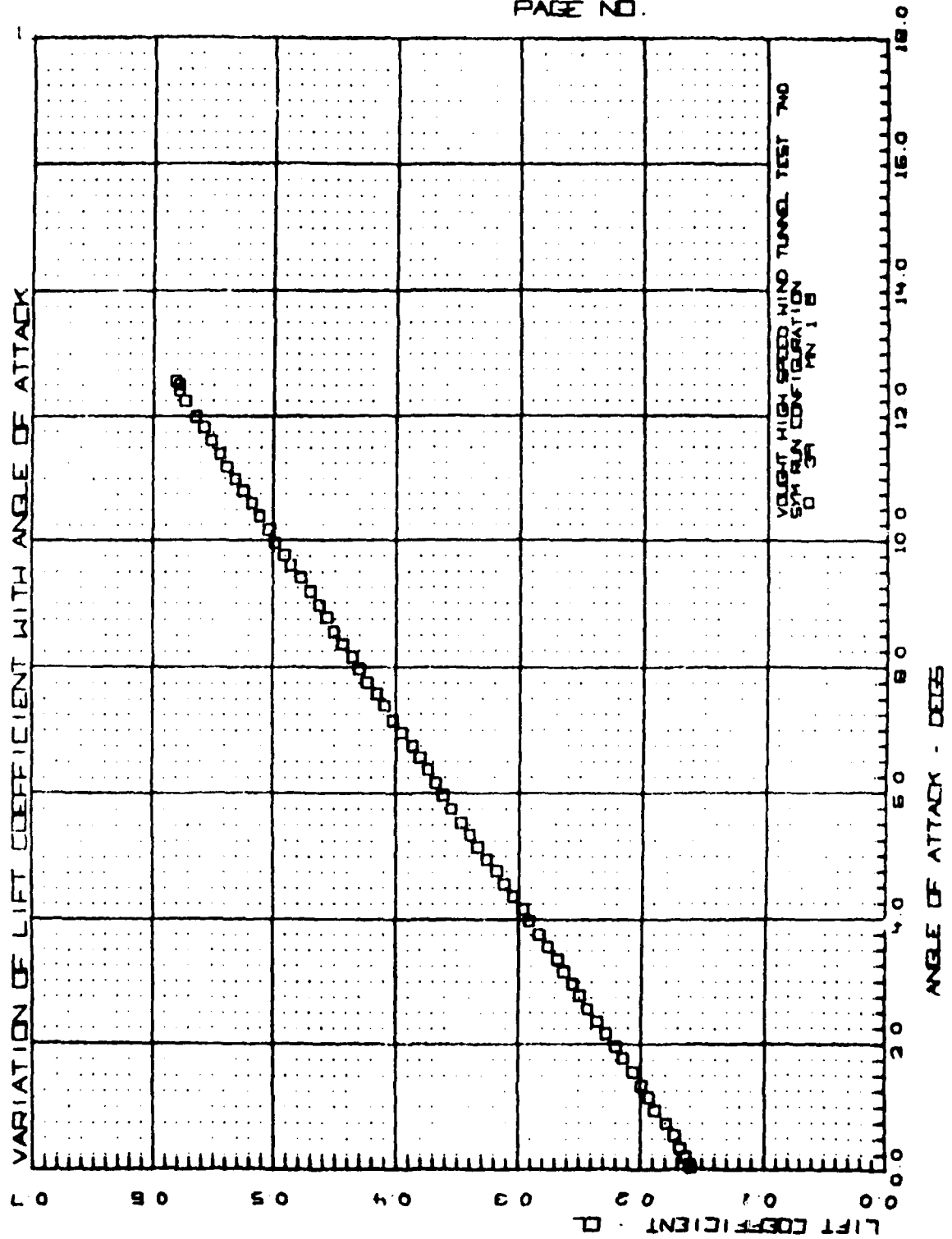
VOUGHT HEAT TEST TWO
PAGE NO

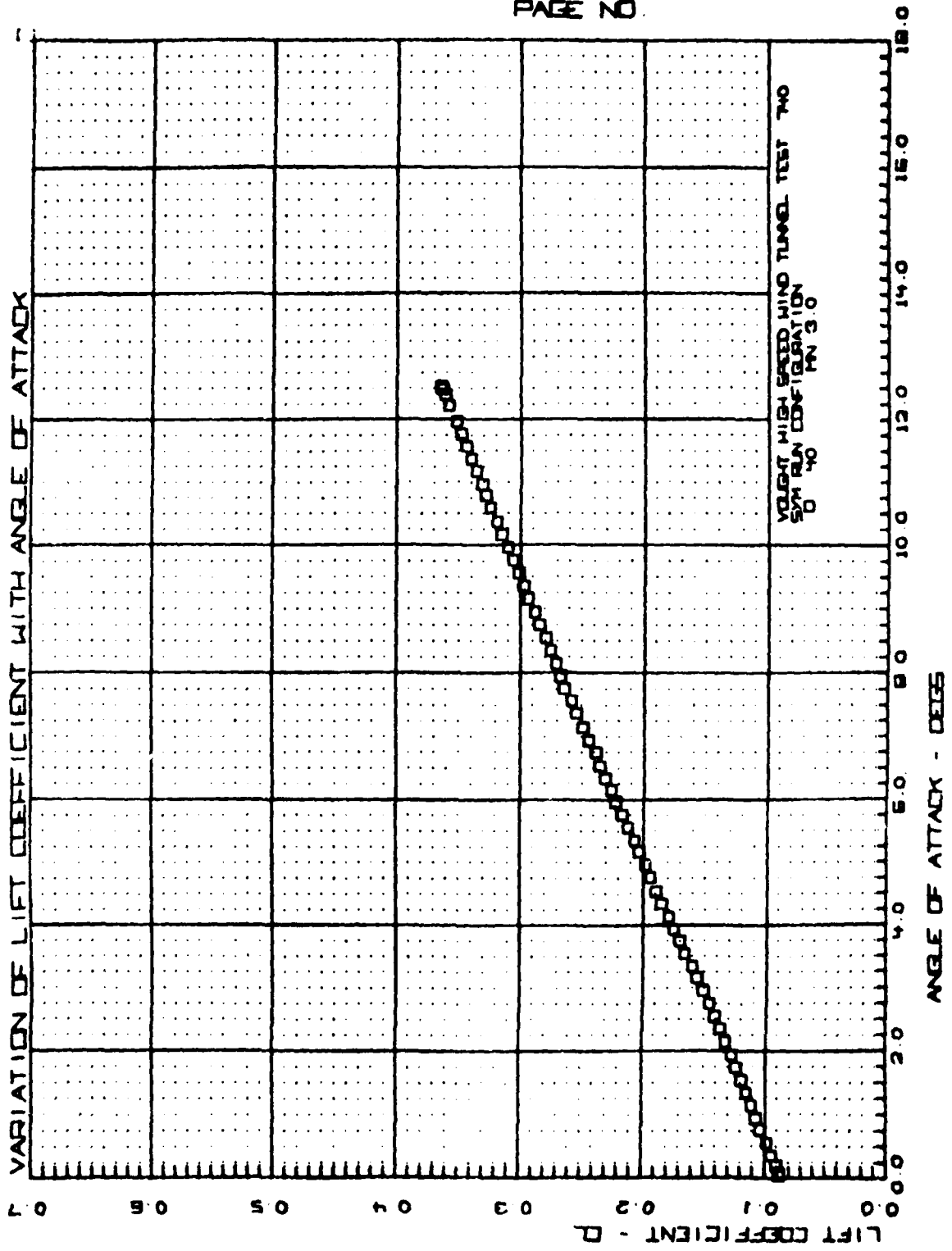


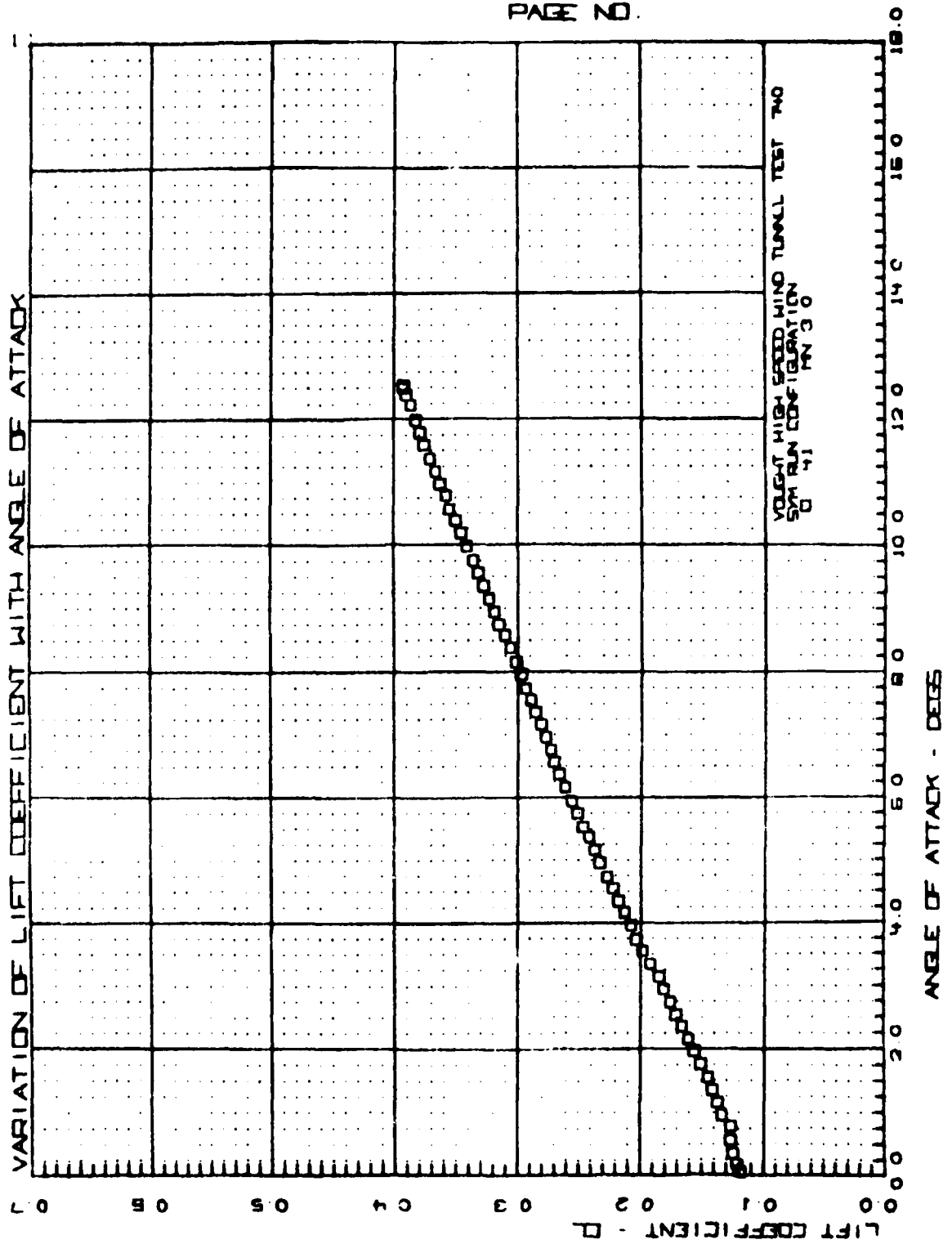


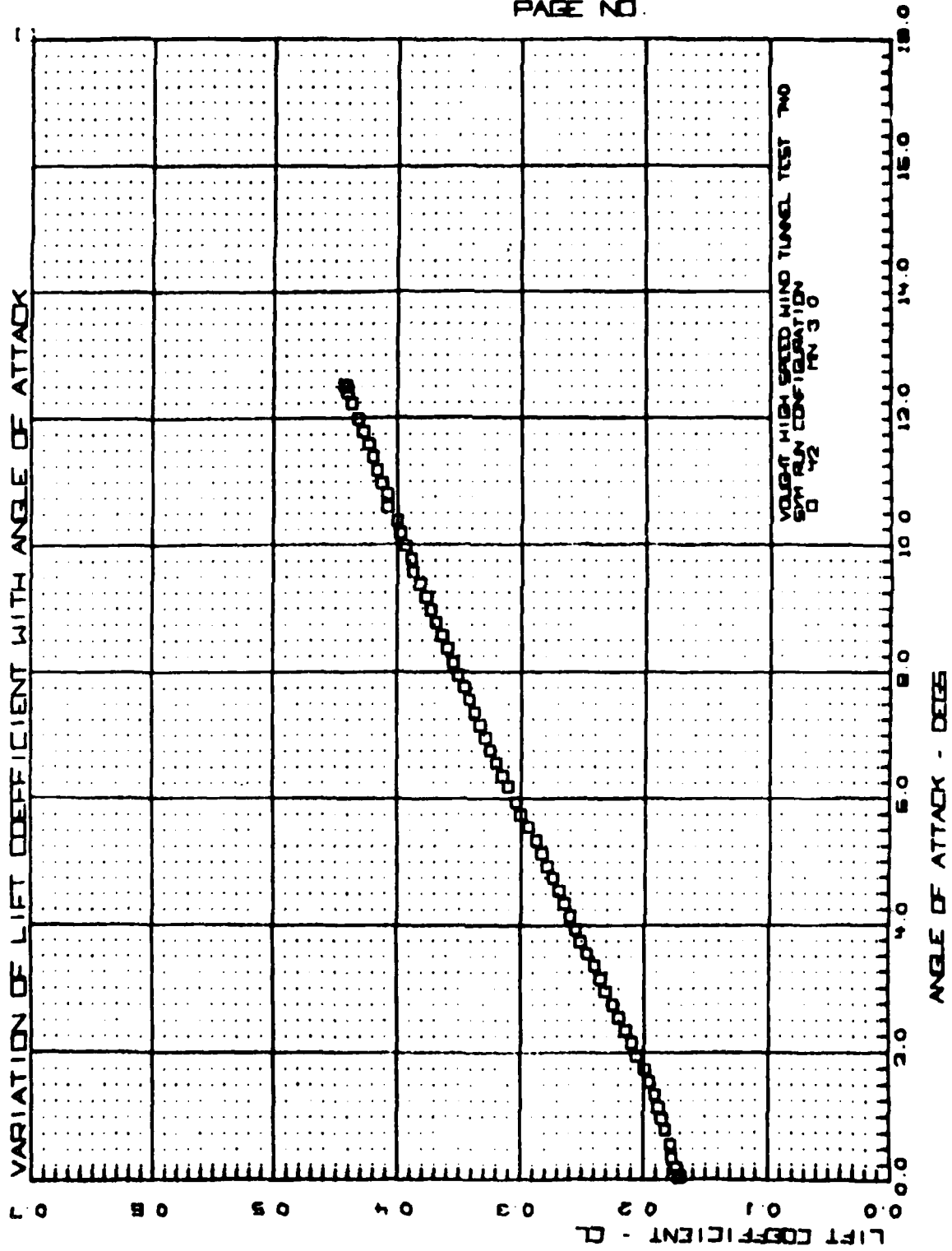


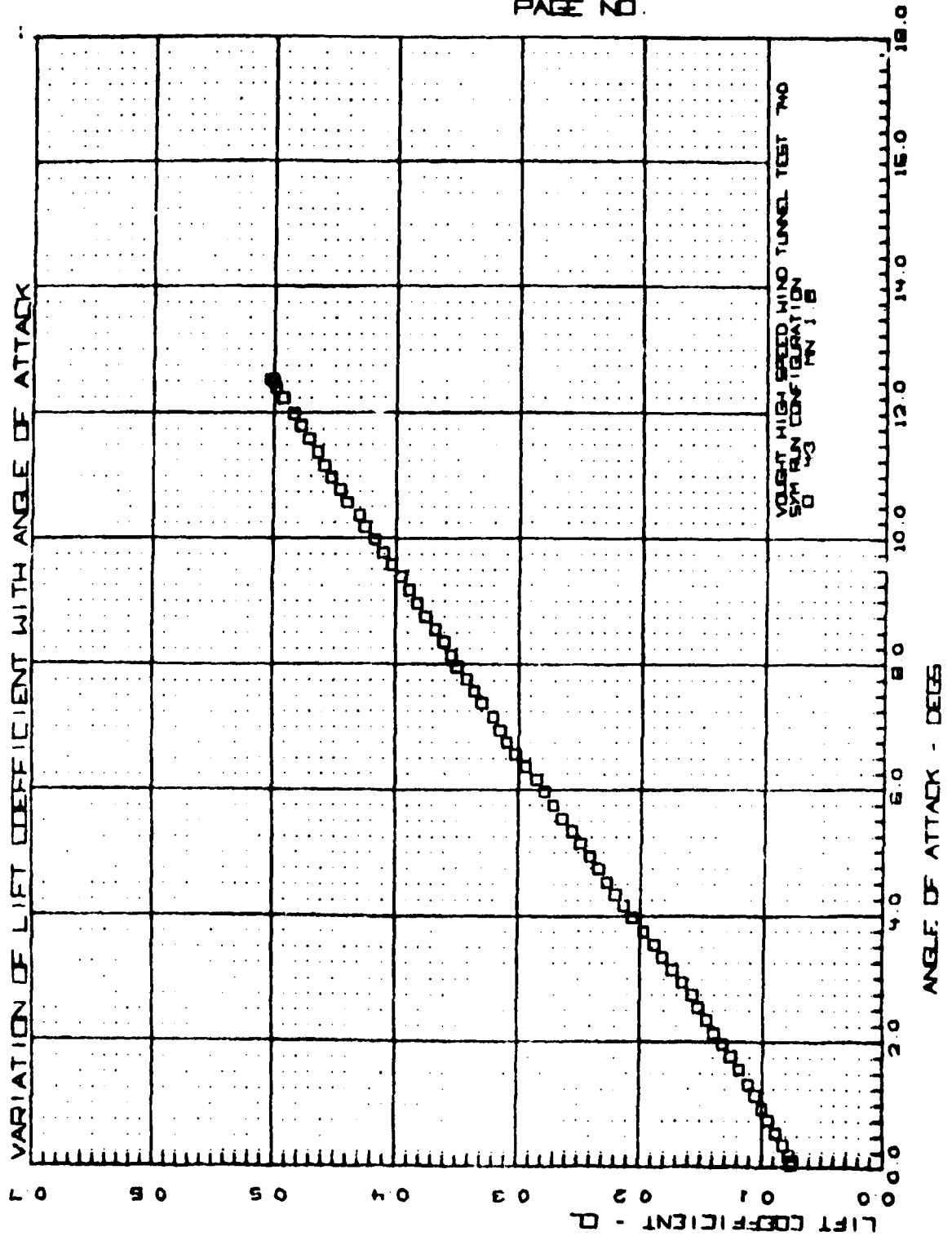




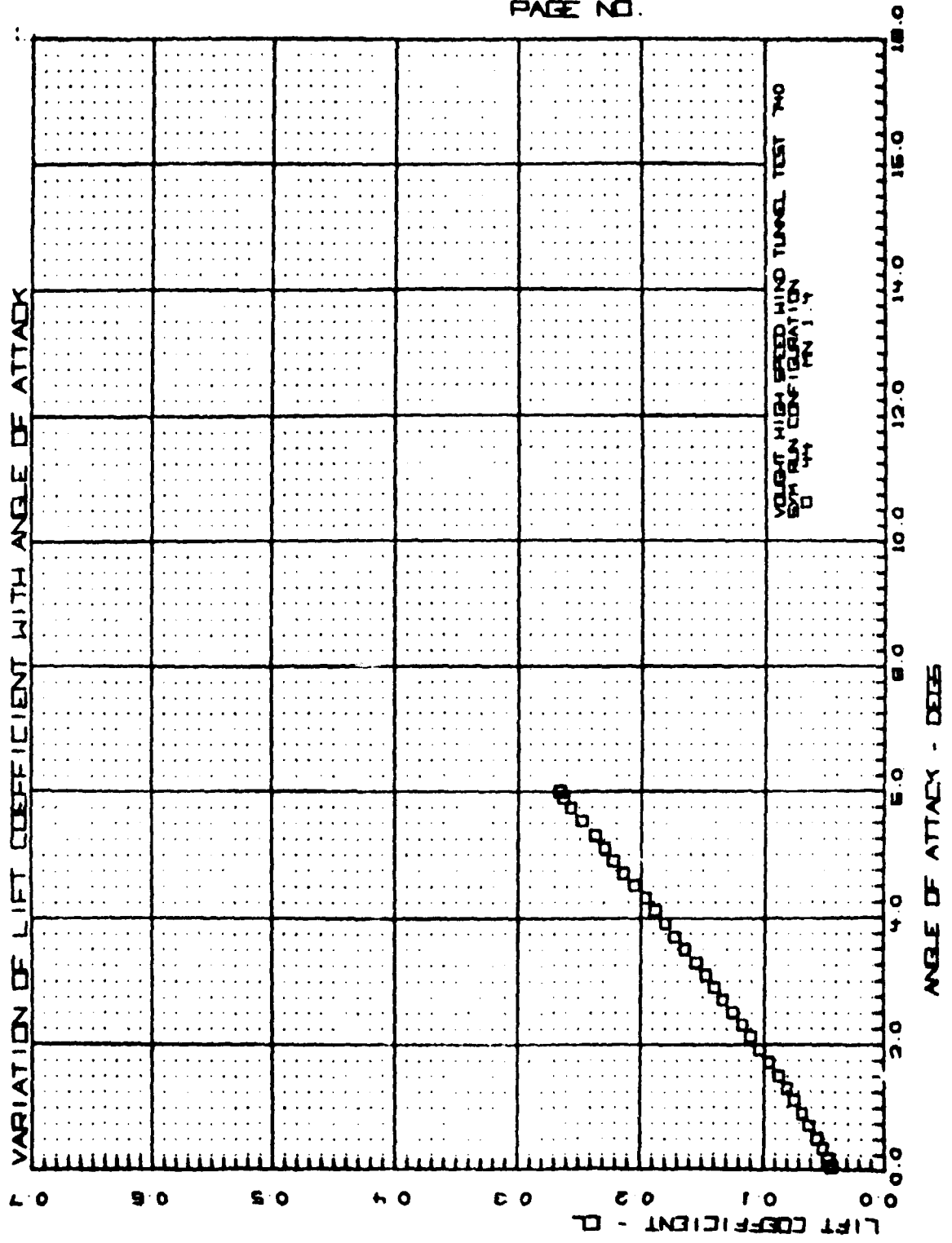


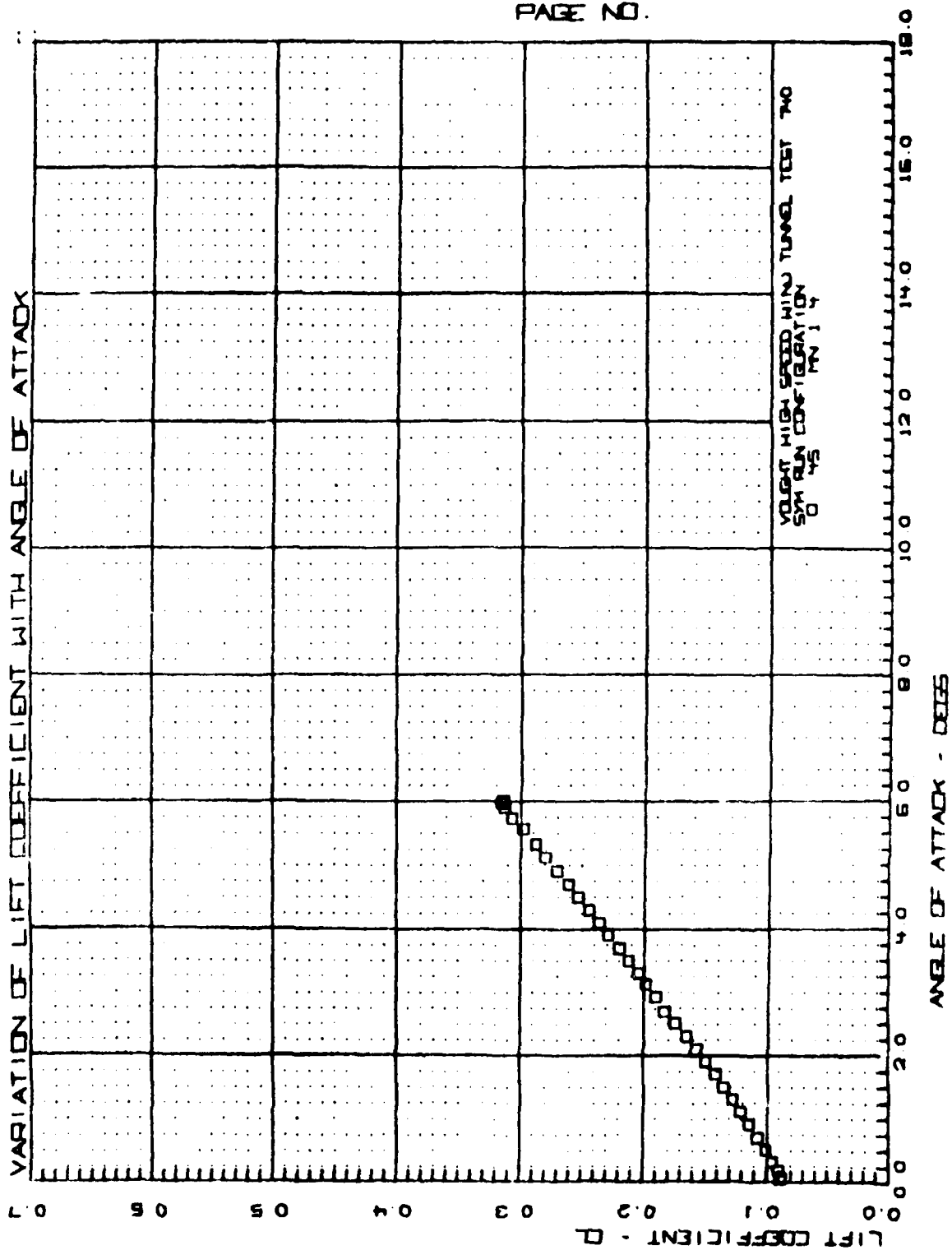


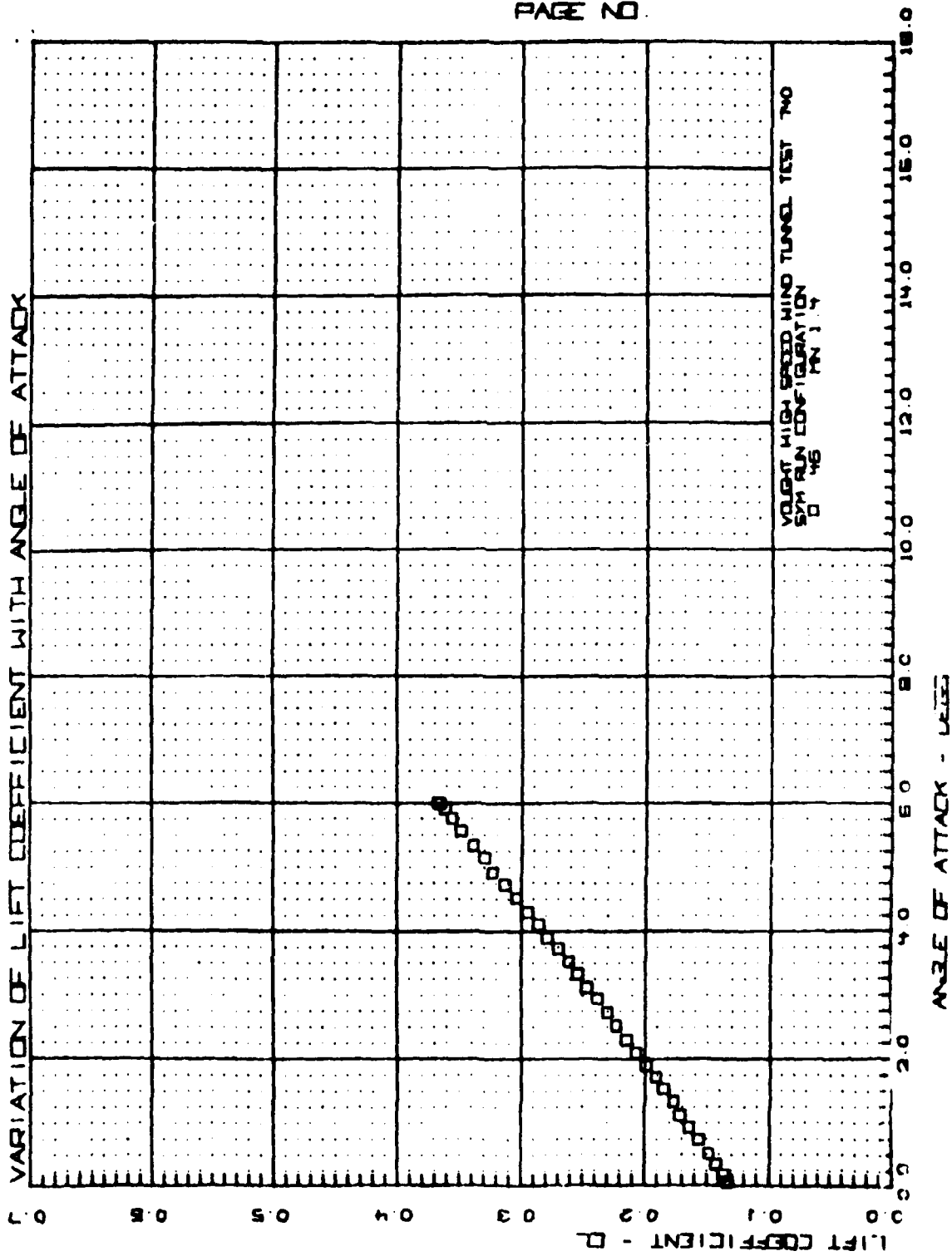




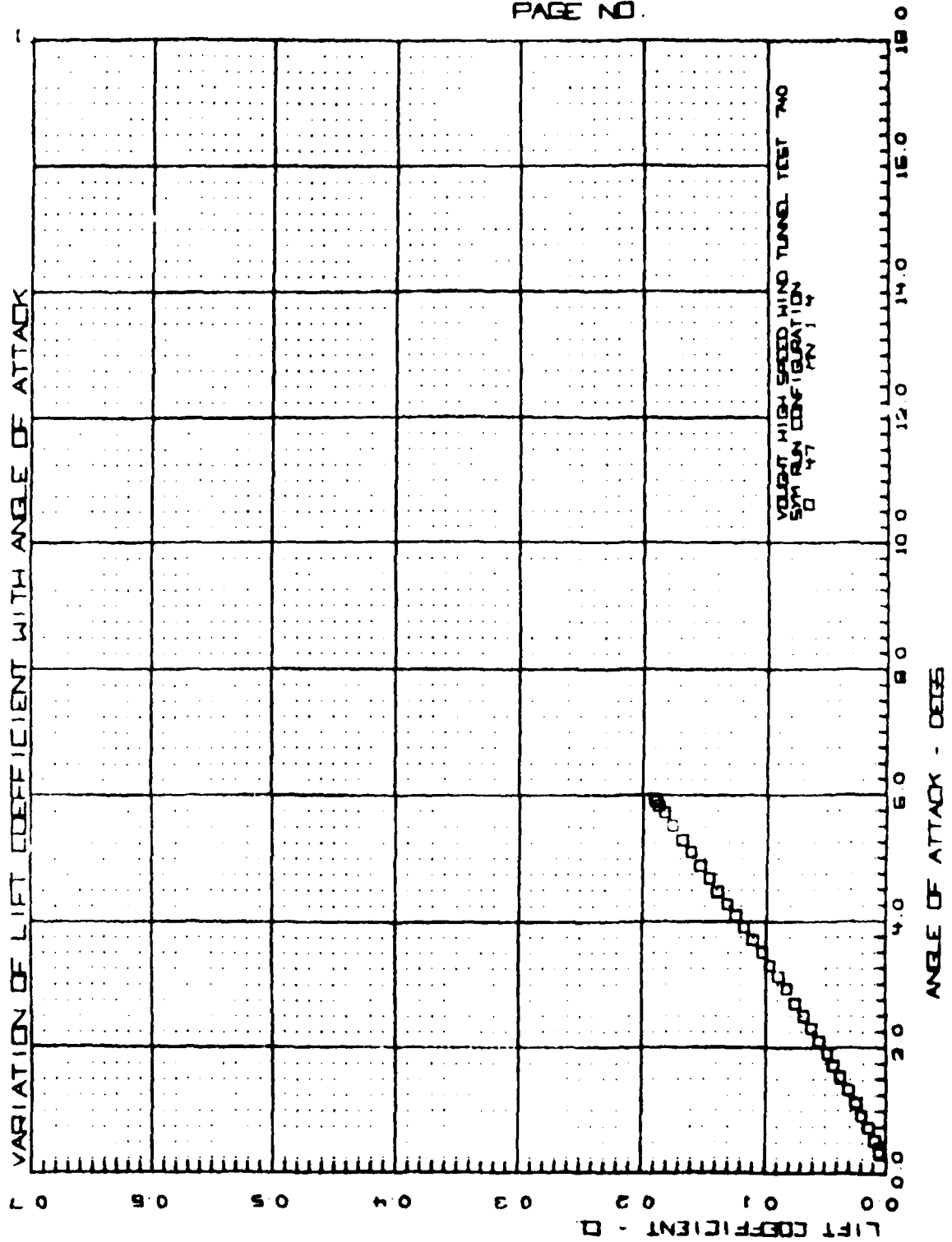
VOUGHT HUNT TEST 740
PAGE NO.

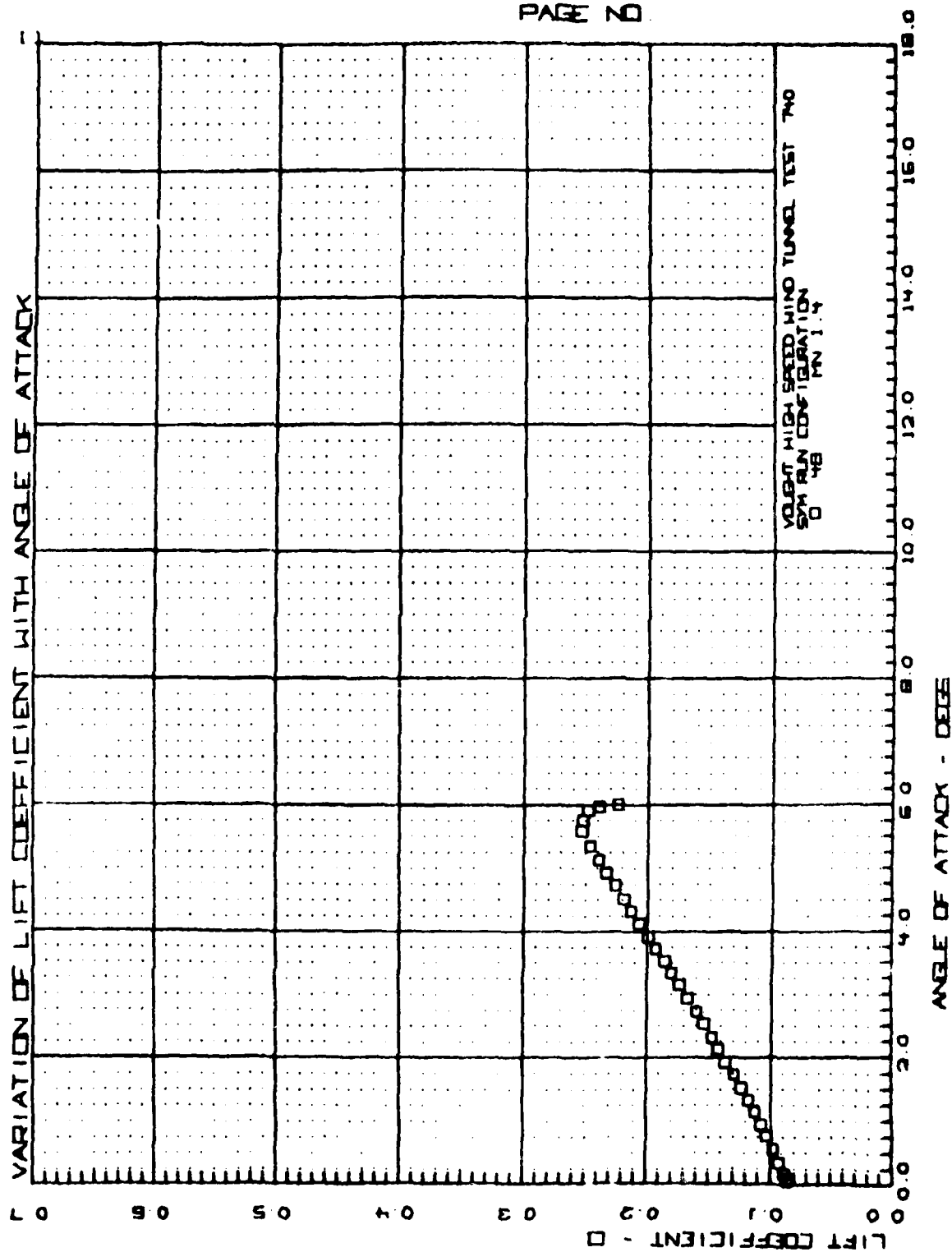




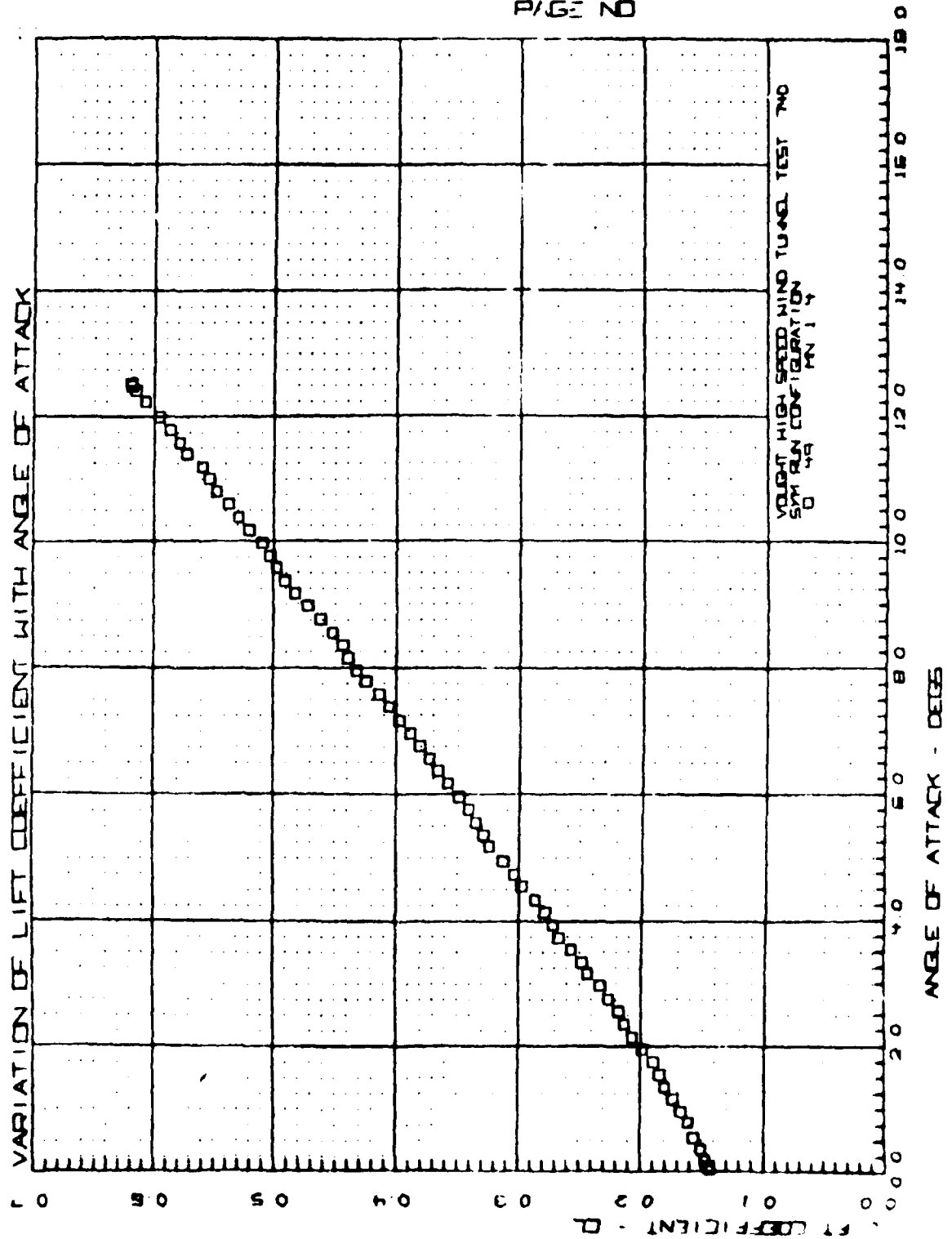


VOUGHT HBAT TEST 740
PAGE NO.





VOUGHT HEAT TEST TWO
PAGE NO



AD-A118 418

VOUGHT CORP ADVANCED TECHNOLOGY CENTER DALLAS TX F/G 20/4
PROPULSION AUGMENTED CONTROL/LIFT SURFACE VALIDATION FOR MISSIL--ETC(U)
APR 82 R L WASK, J G SPANGLER, C H HAIGHT N60921-80-C-A053
ATC-R-91100/2CR-21 ML

UNCLASSIFIED

2-2

2-2

2-2

2-2

2-2

2-2

2-2

2-2

2-2

2-2

2-2

2-2

2-2

2-2

2-2

2-2

2-2

2-2

2-2

2-2

2-2

2-2

2-2

2-2

2-2

2-2

2-2

2-2

2-2

2-2

2-2

2-2

2-2

2-2

2-2

2-2

2-2

2-2

2-2

2-2

2-2

2-2

2-2

2-2

2-2

2-2

2-2

2-2

2-2

2-2

2-2

2-2

2-2

2-2

2-2

2-2

2-2

2-2

2-2

2-2

2-2

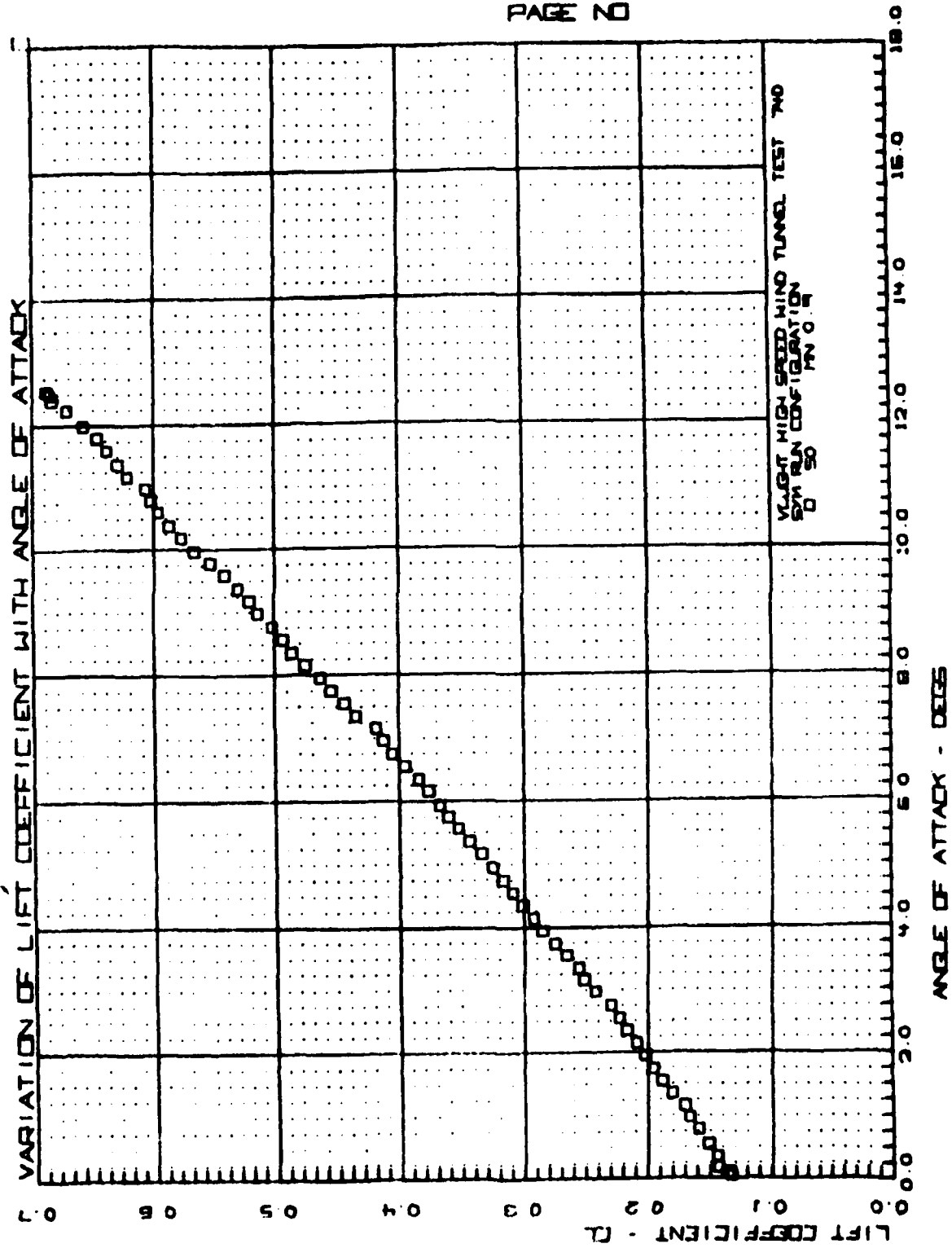
2-2

END

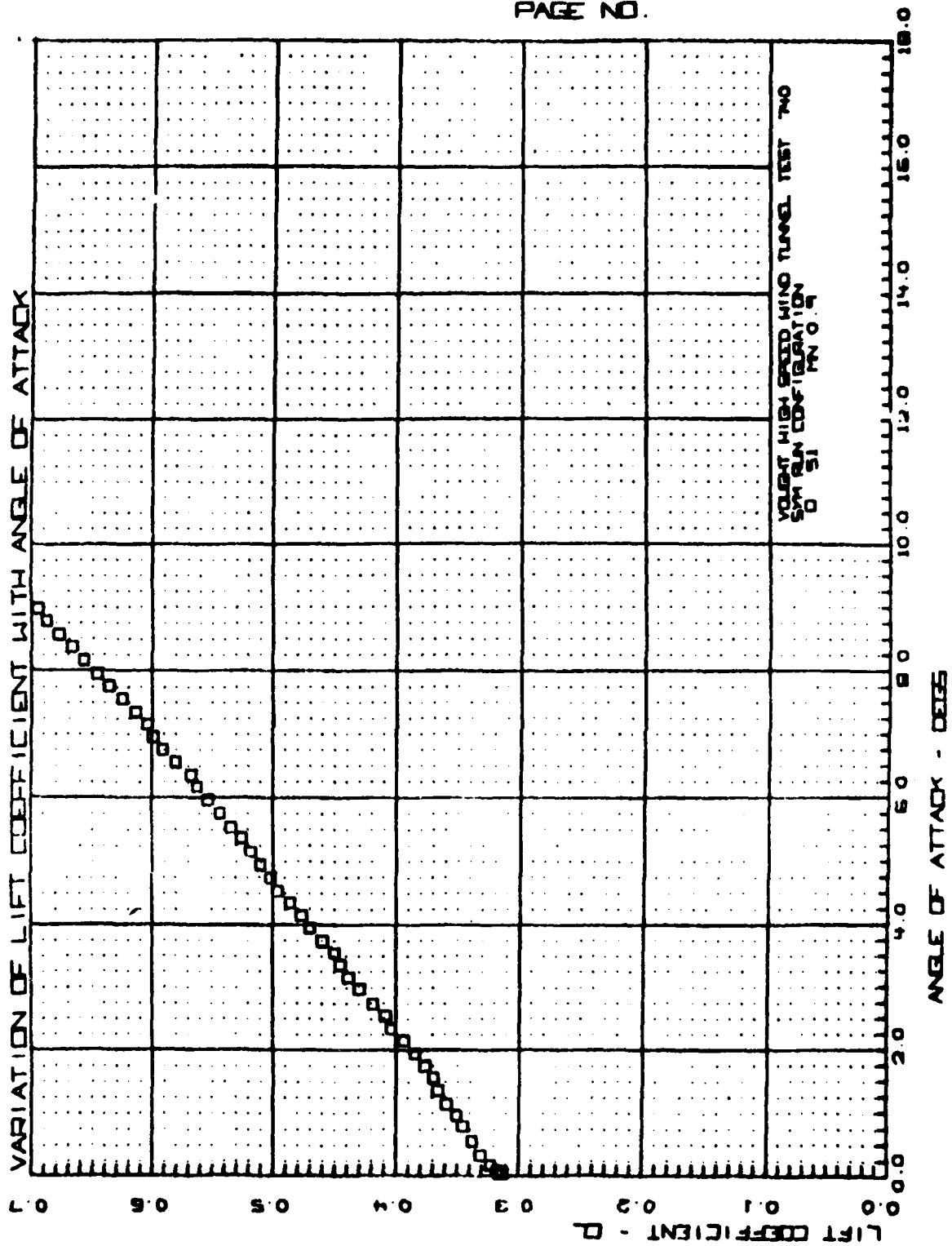
DATE

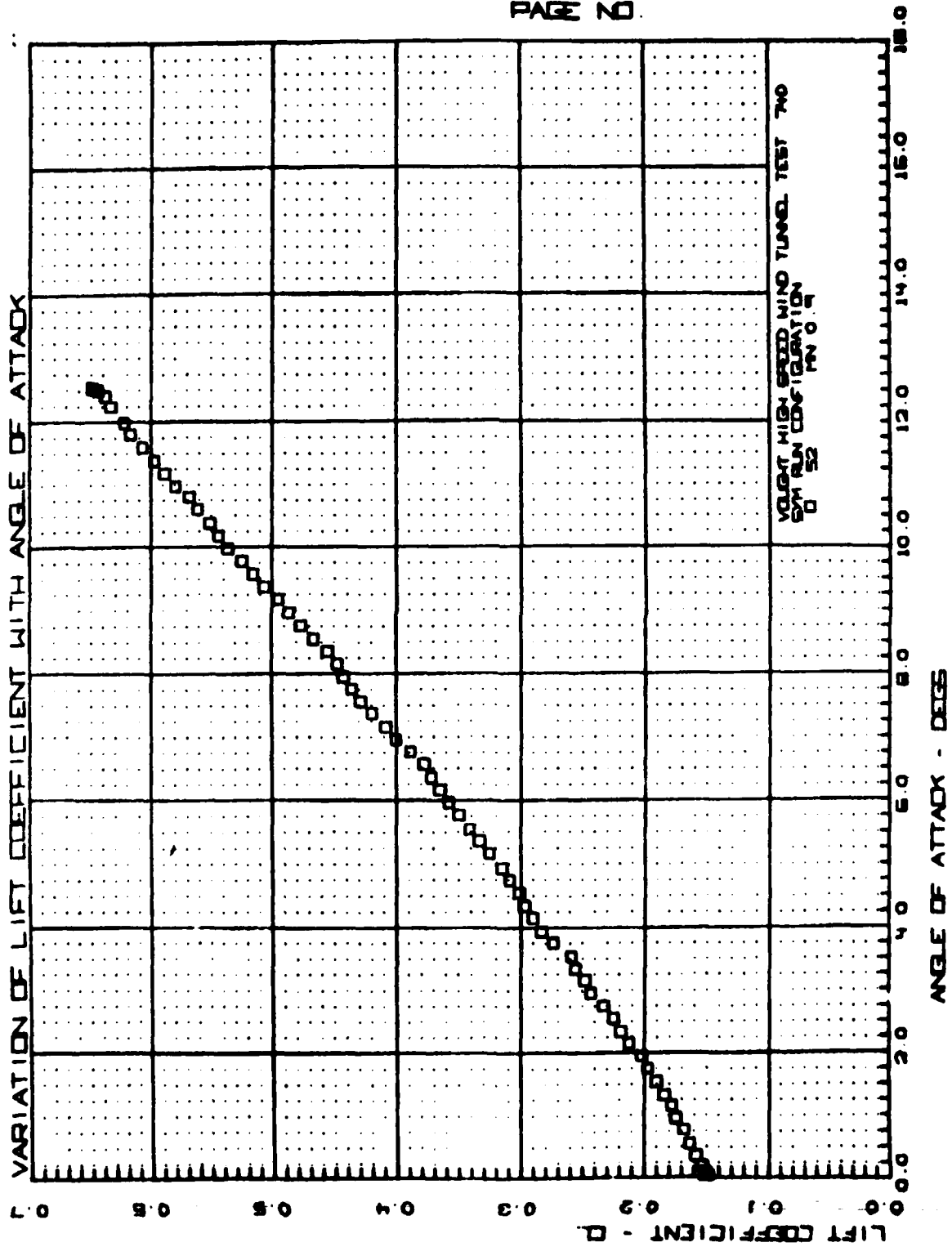
FILED

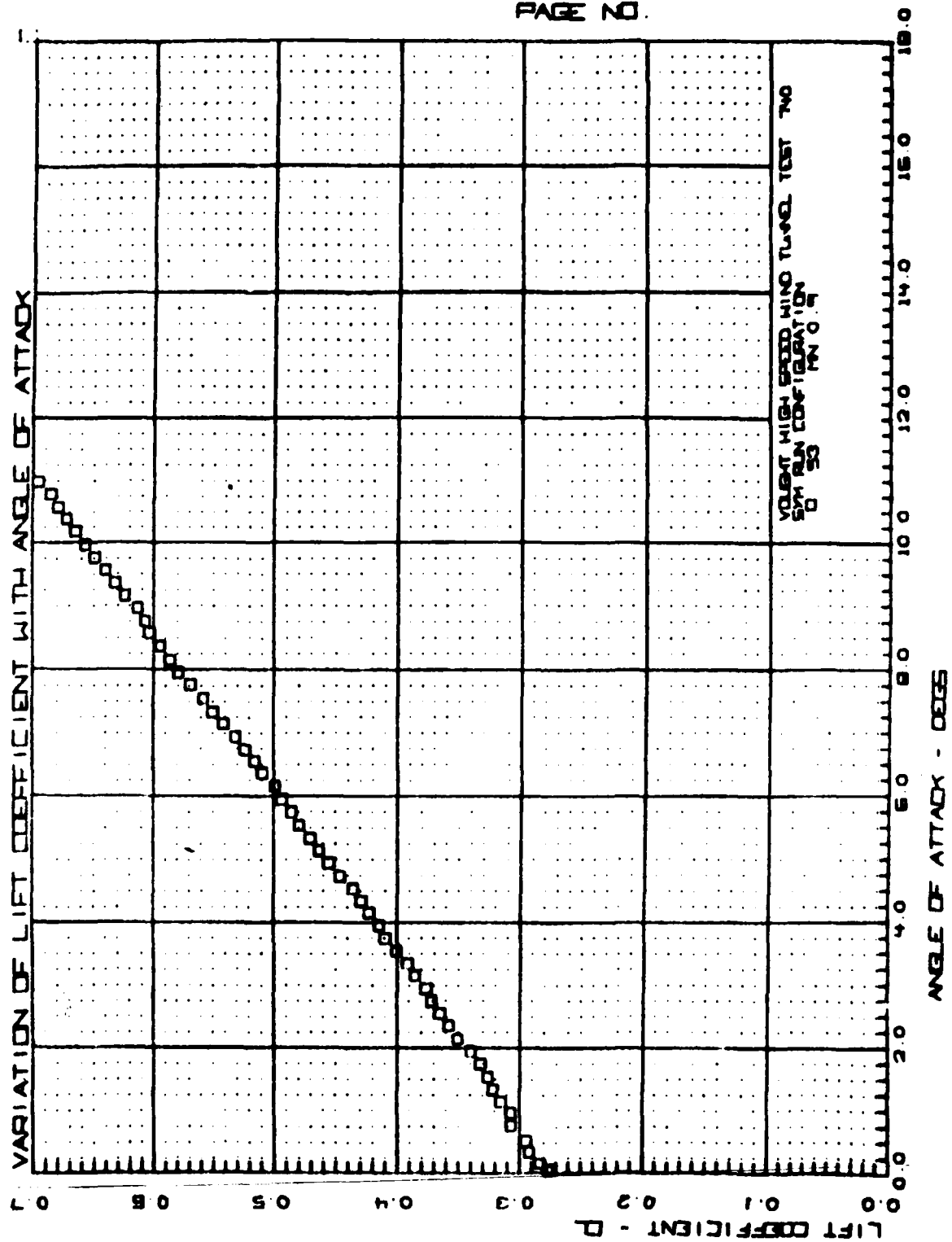
DTIC

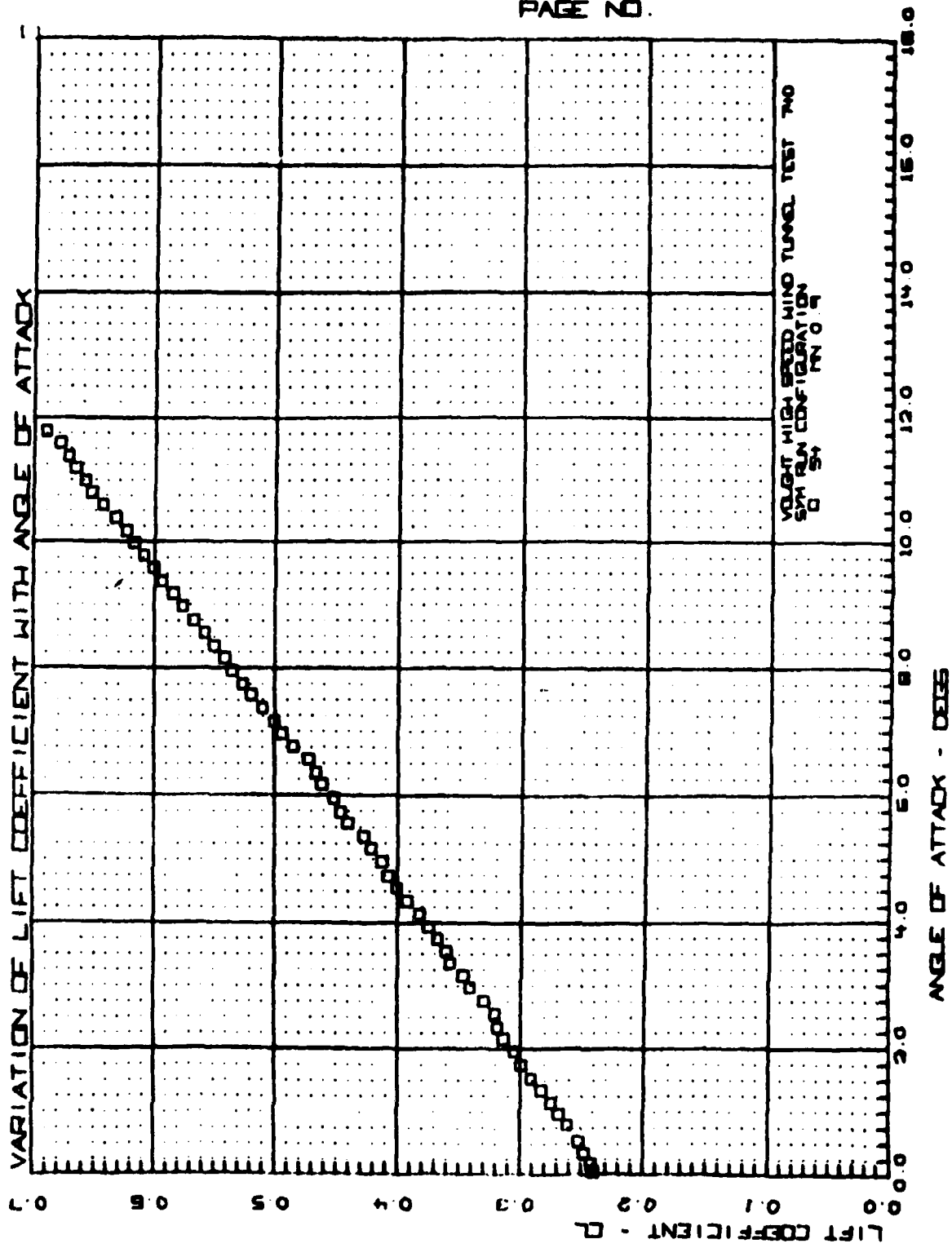


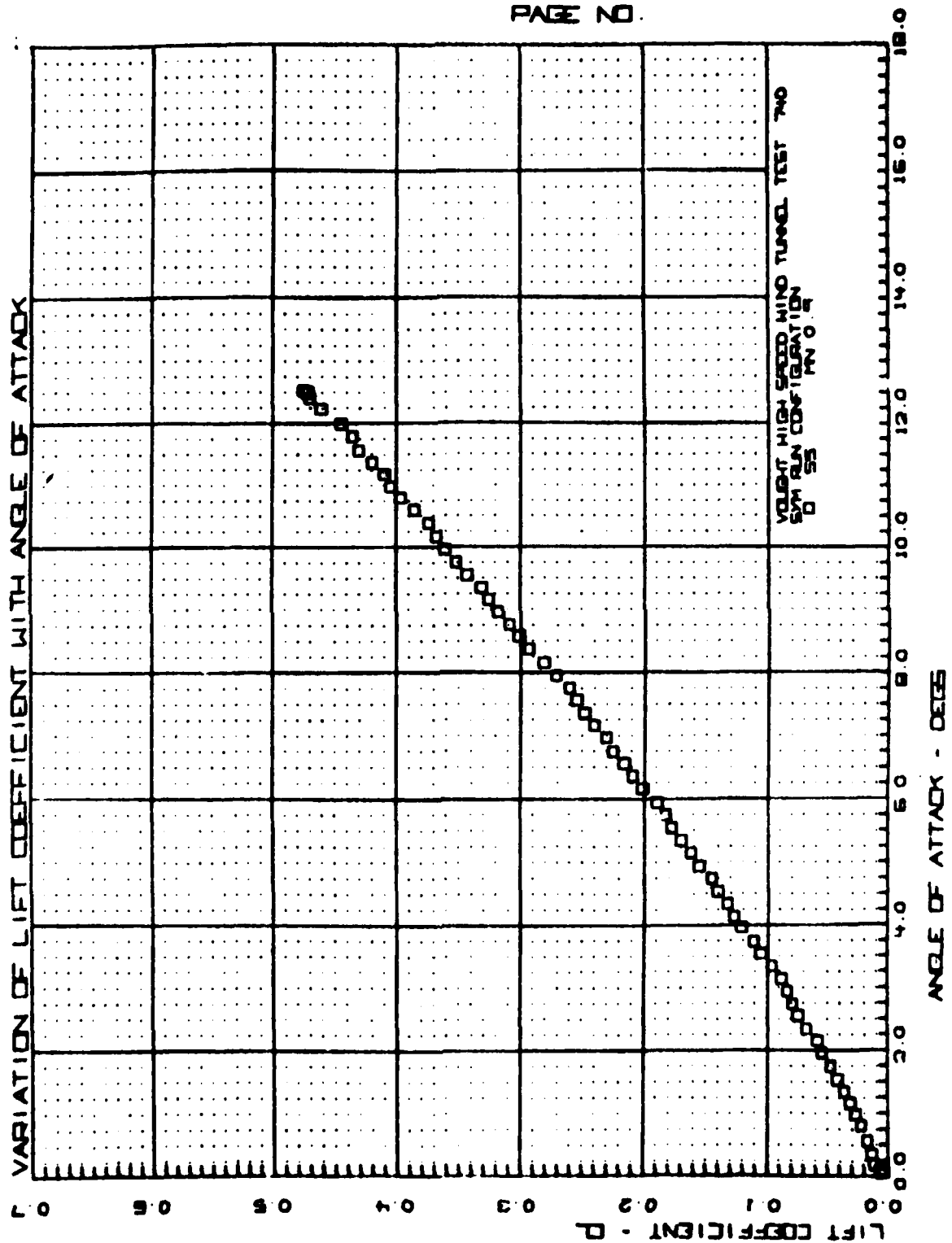
VOLUNT HUNT TEST TWO
PAGE NO.



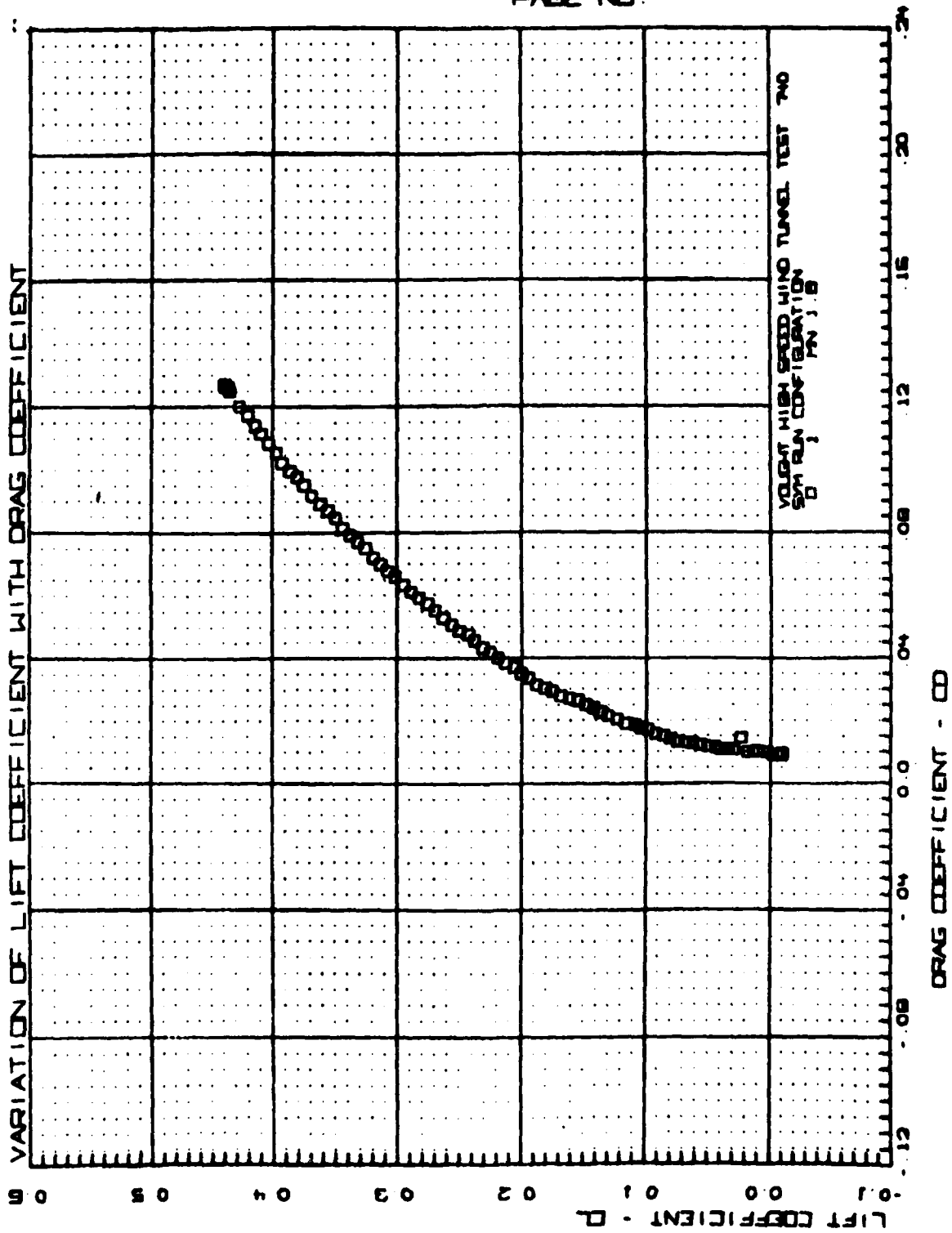


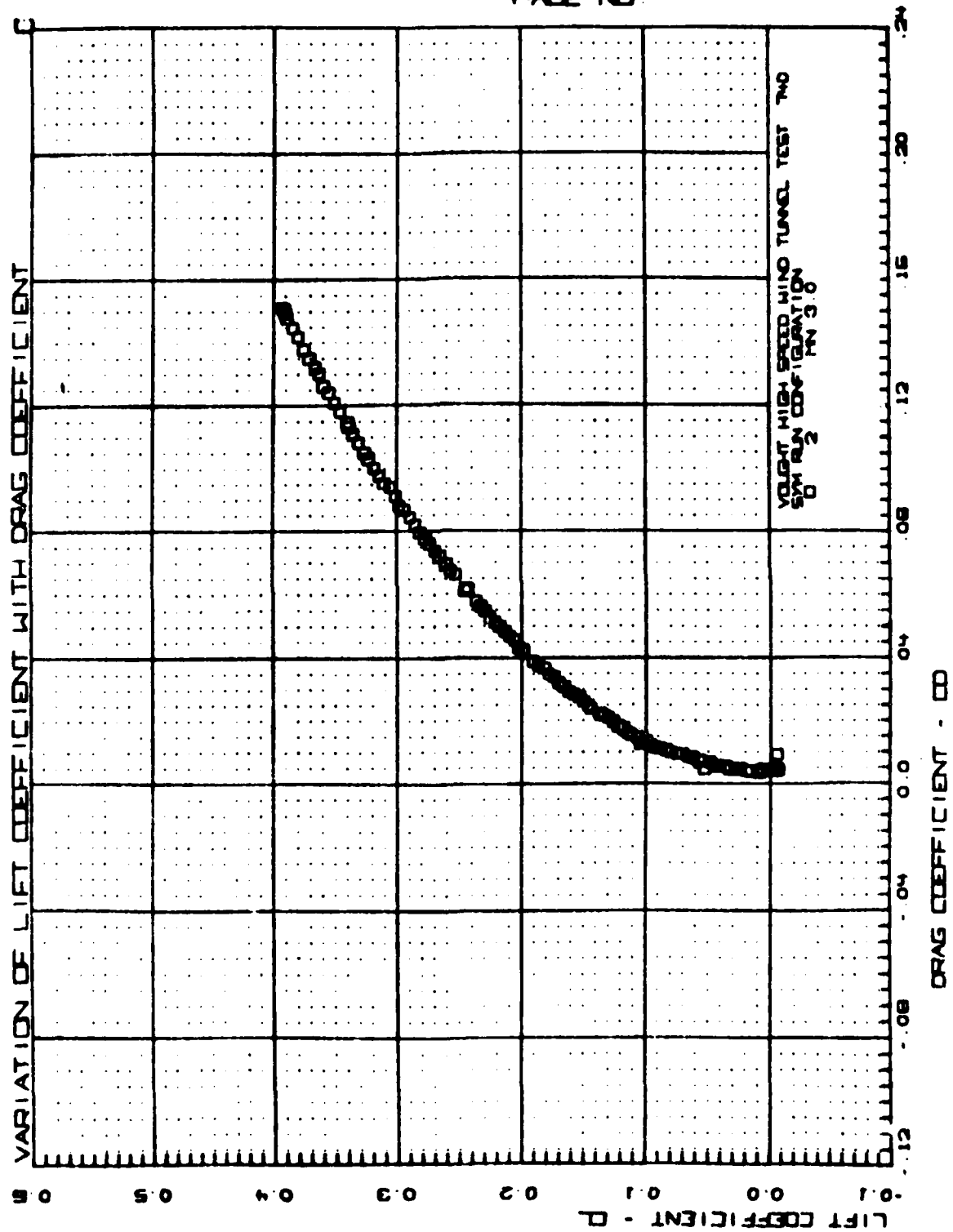


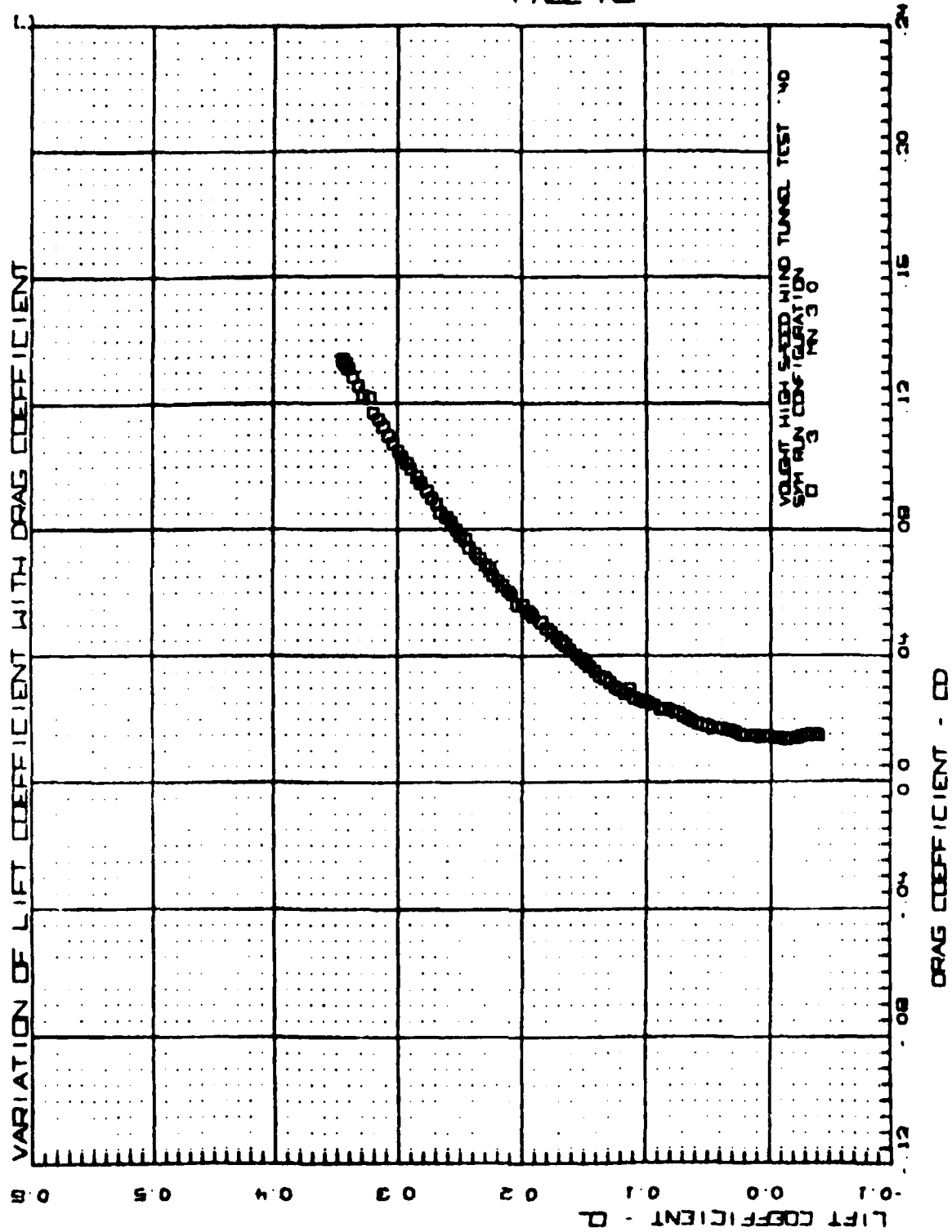


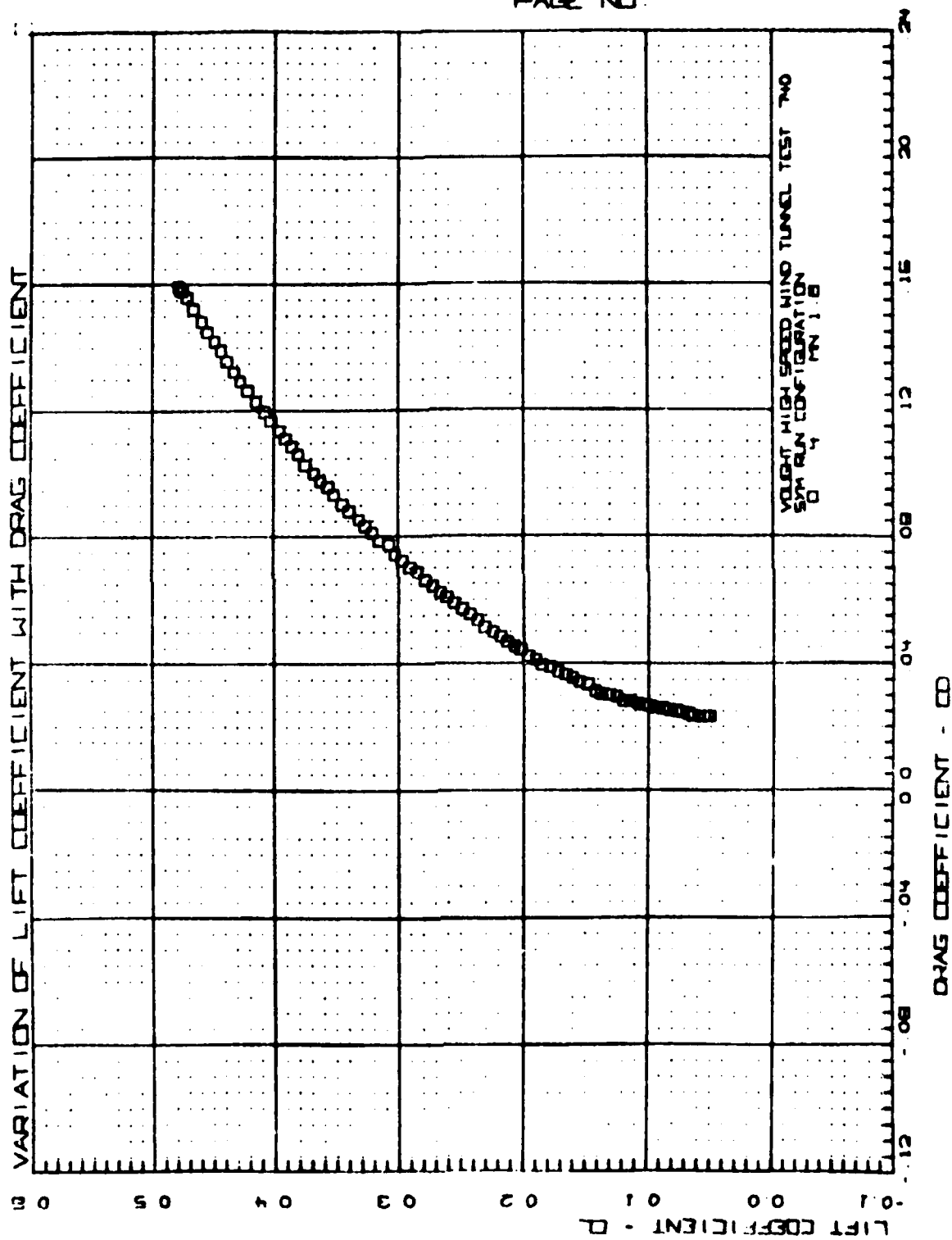


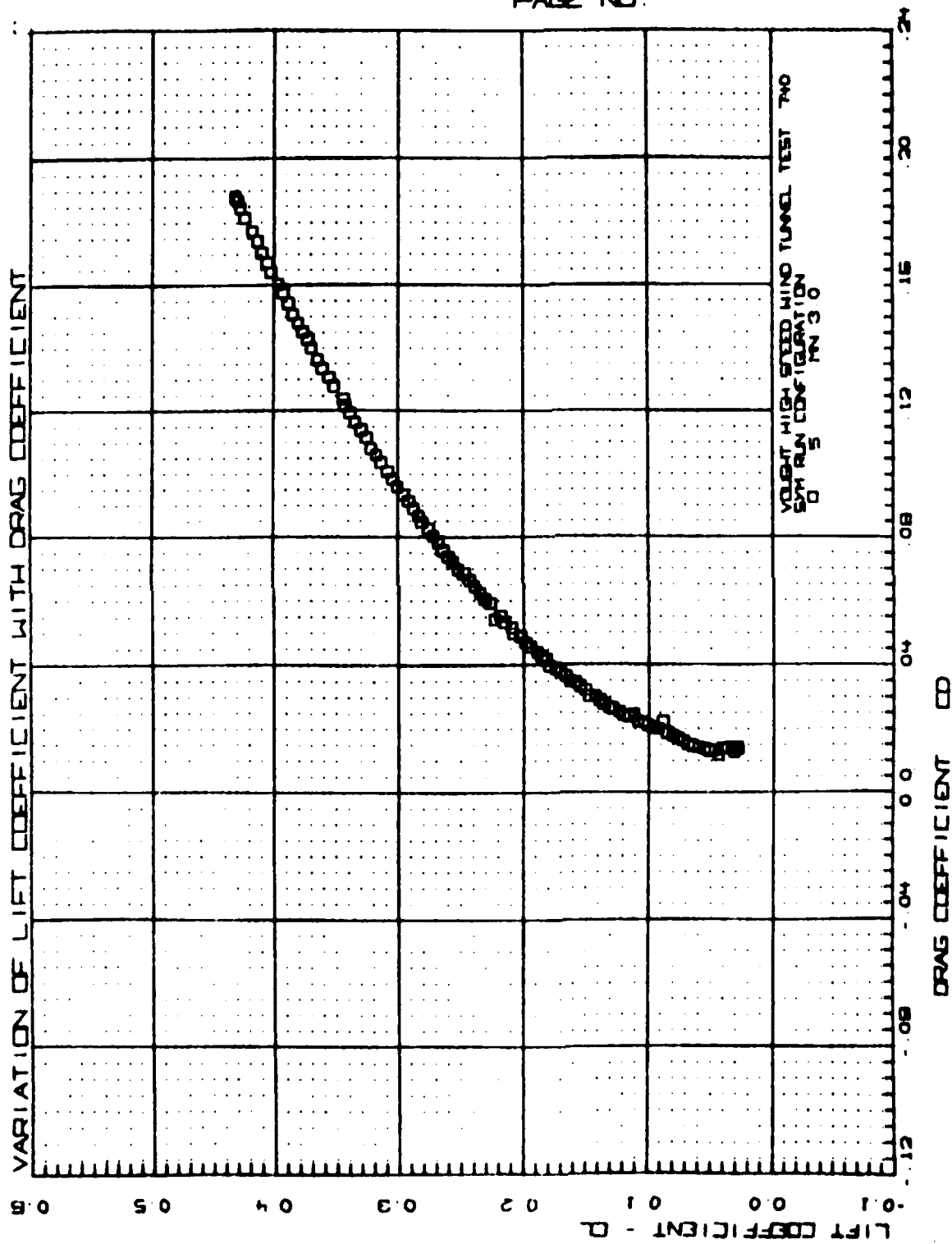
VARIATION OF LIFT COEFFICIENT WITH
DRAG COEFFICIENT

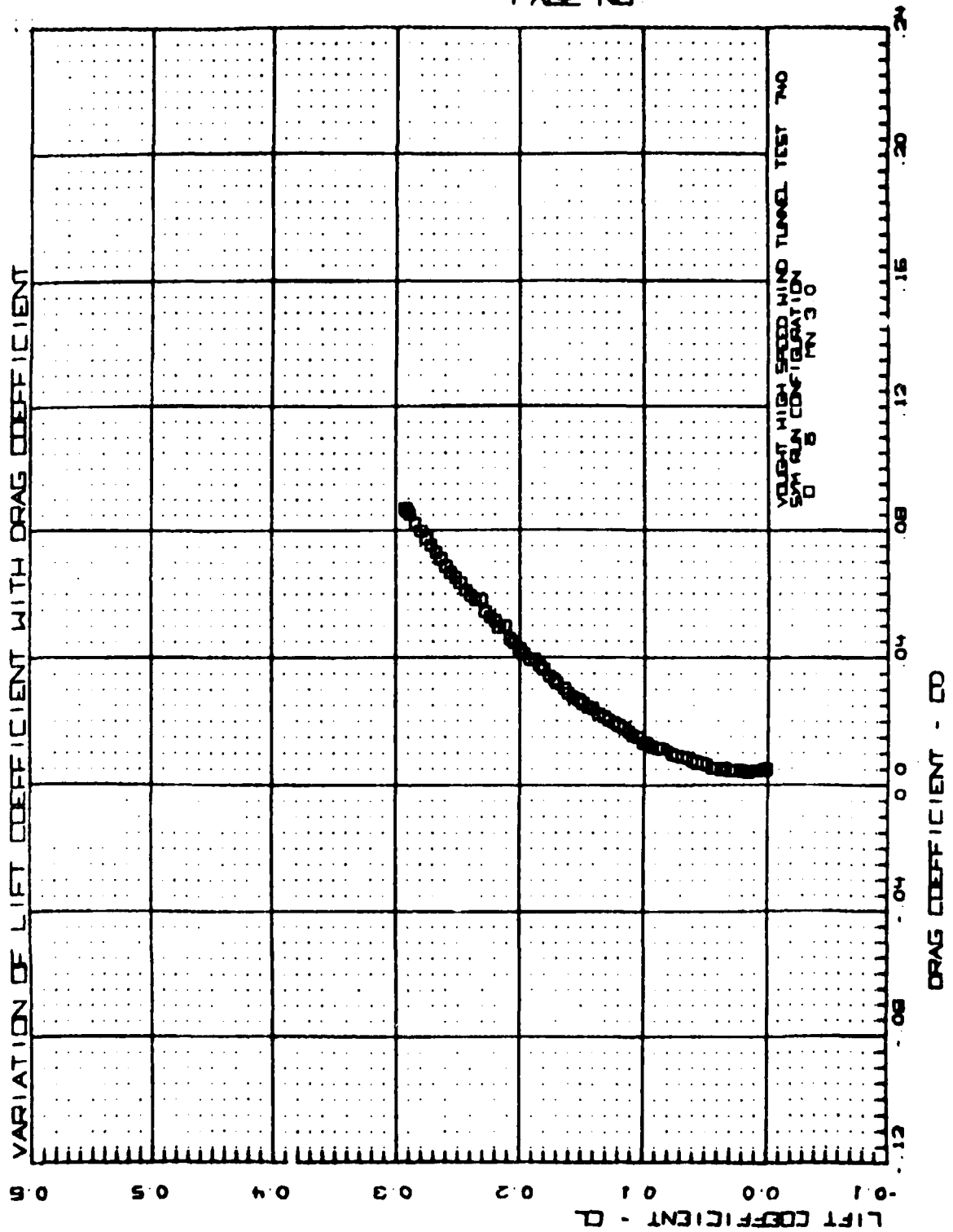


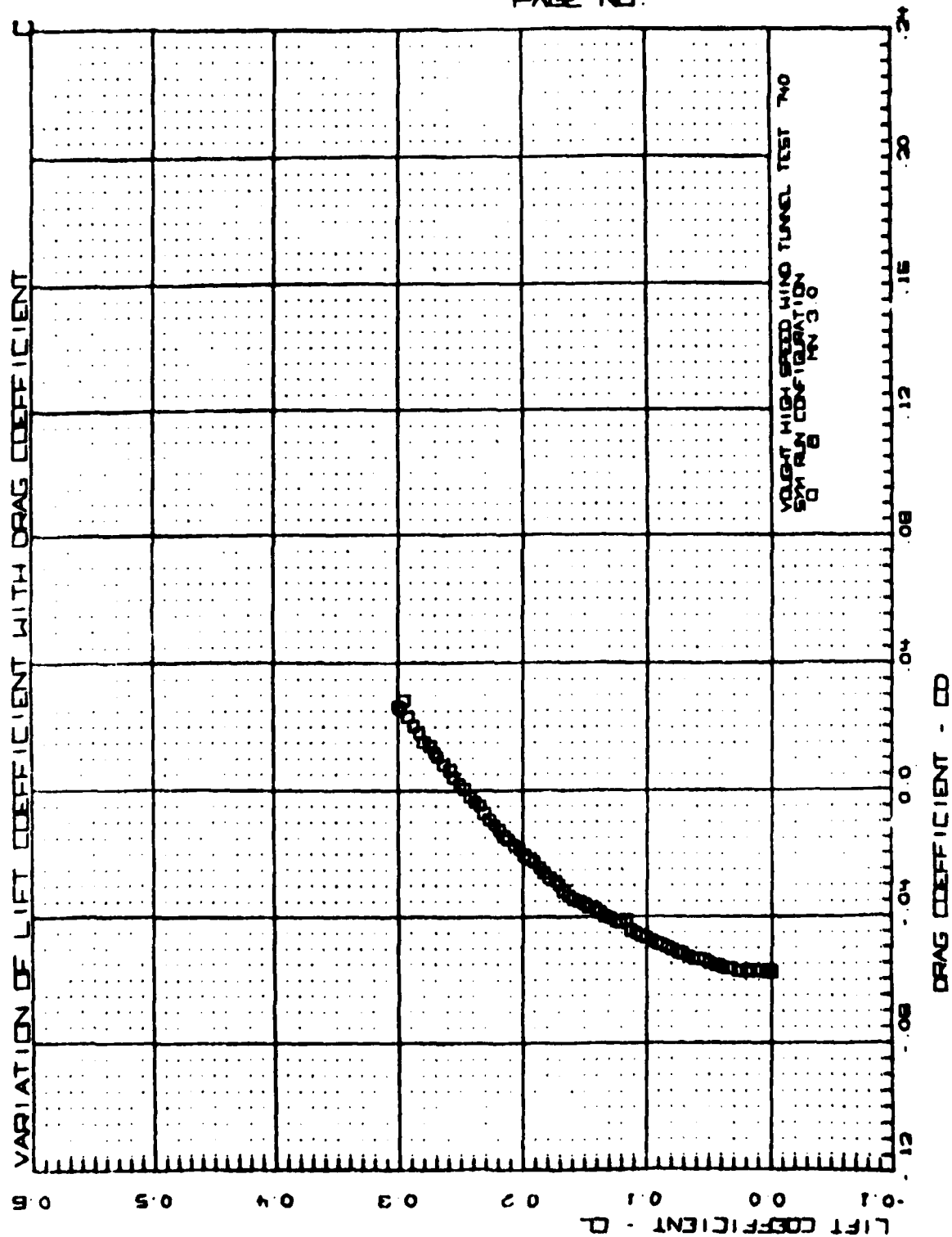


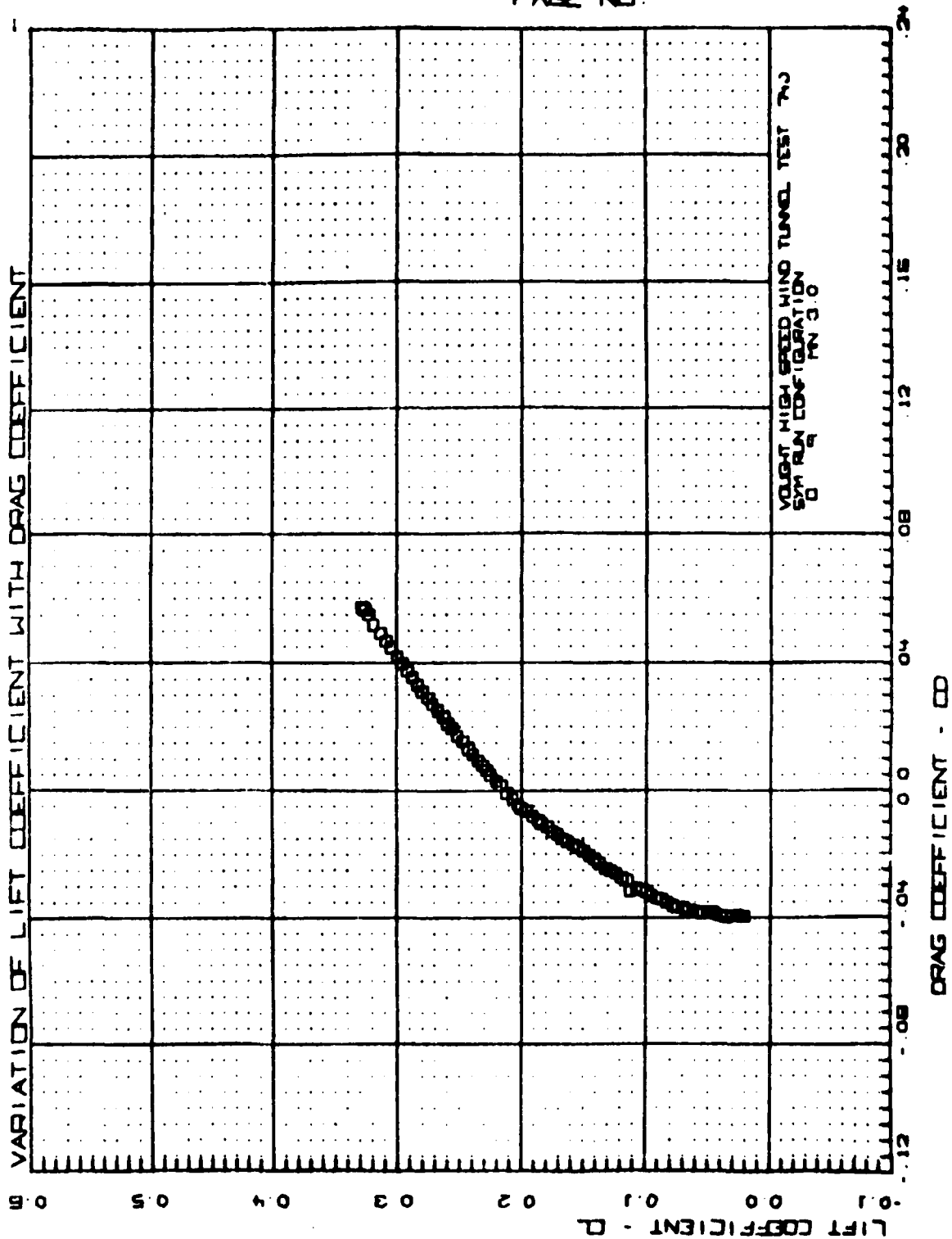


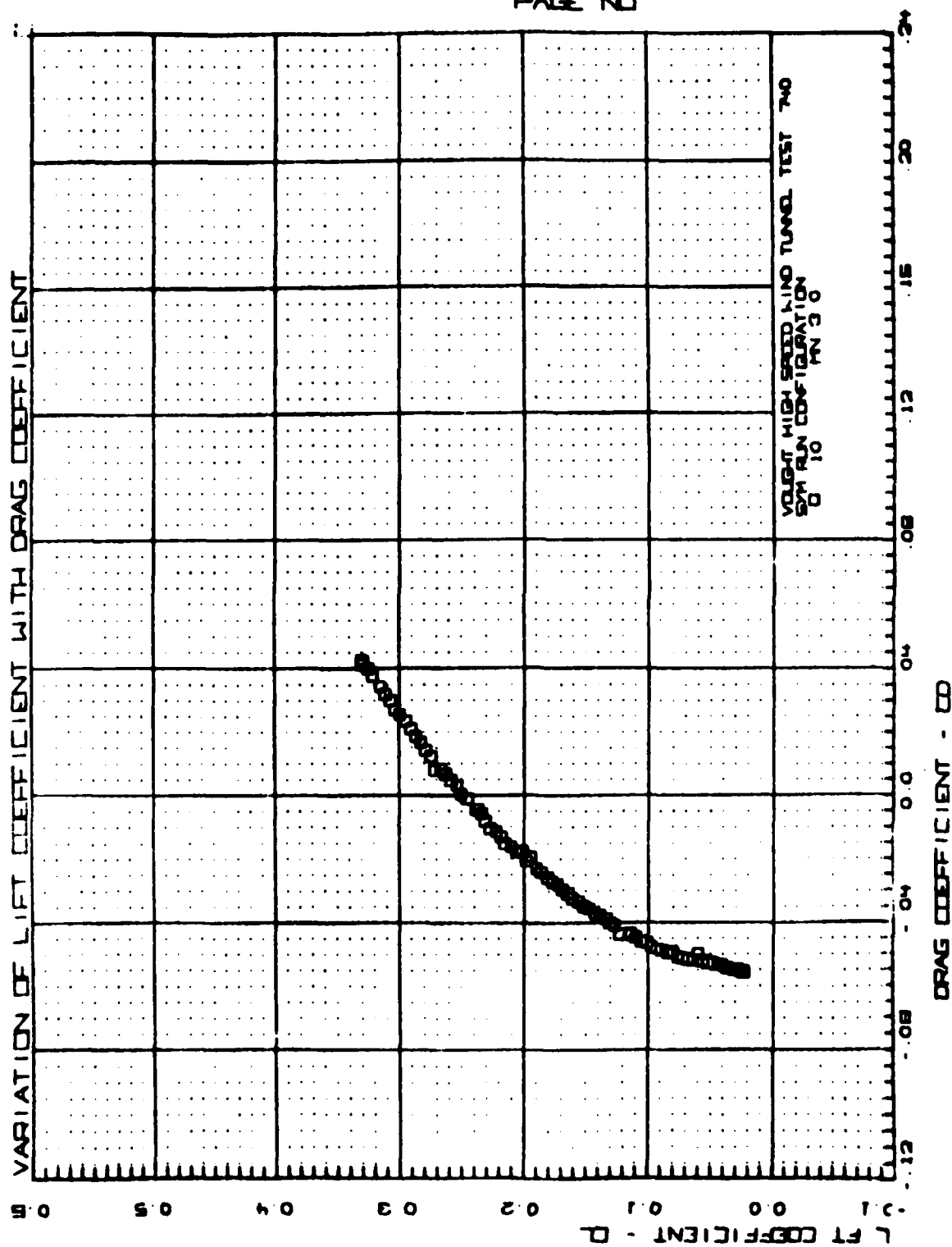


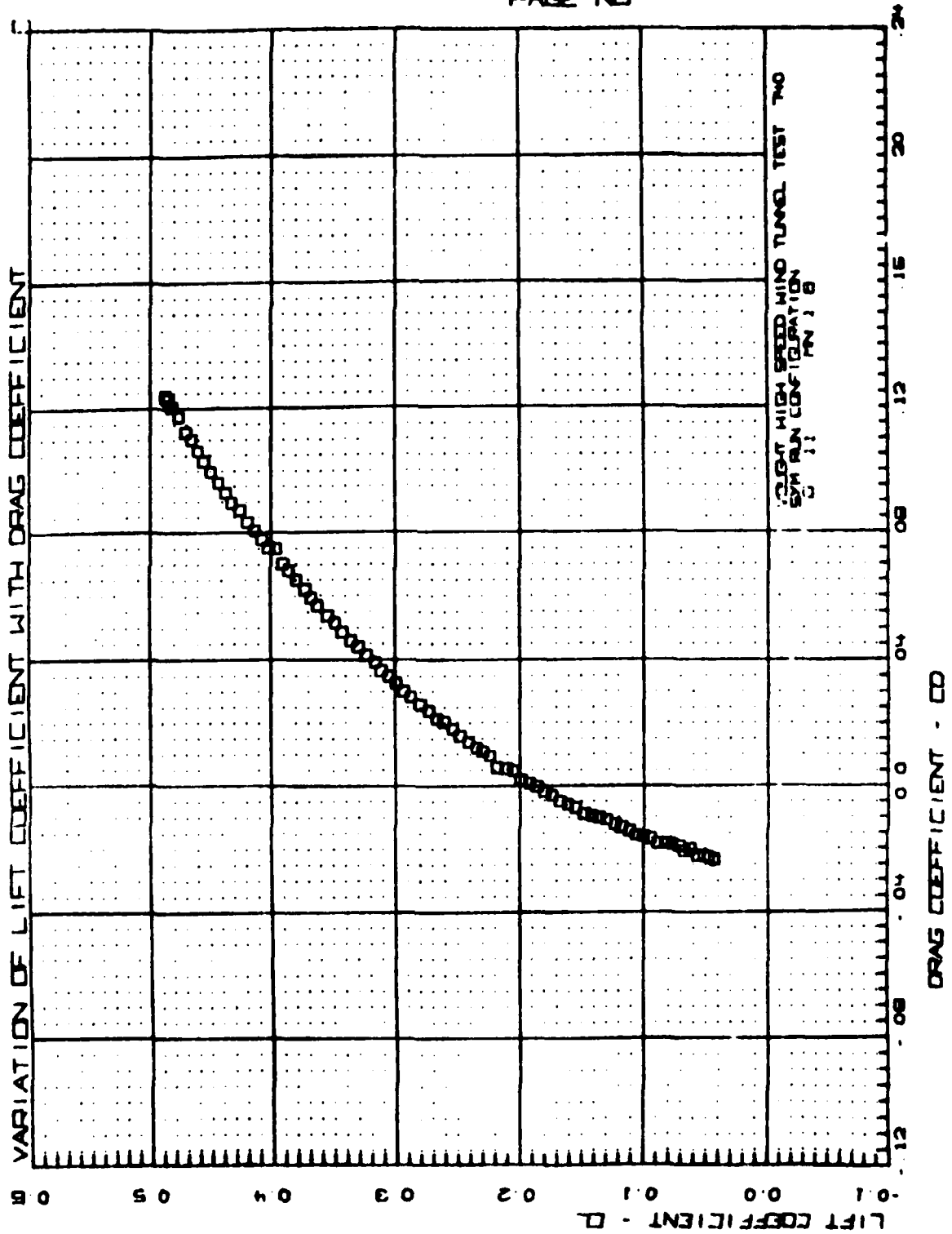




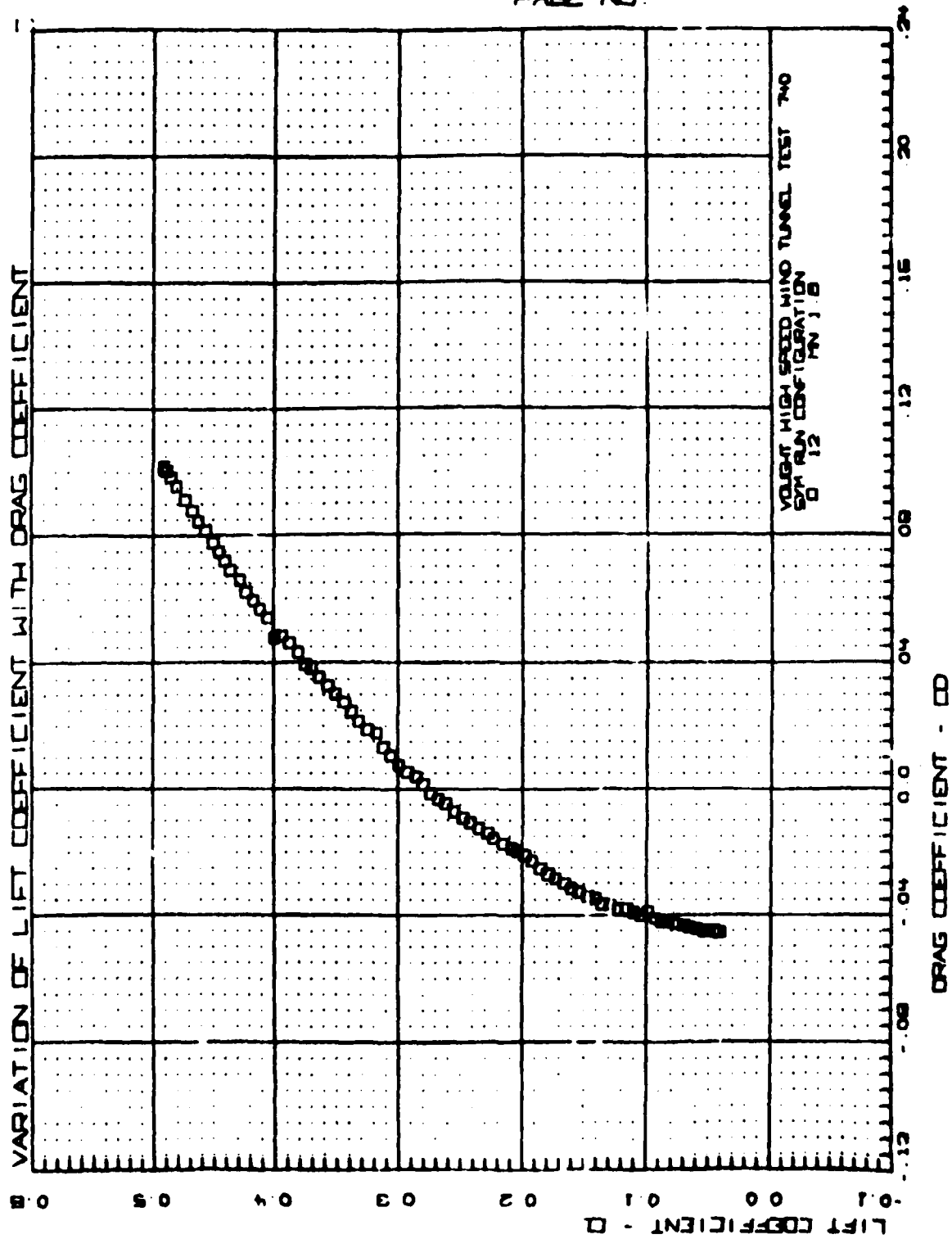




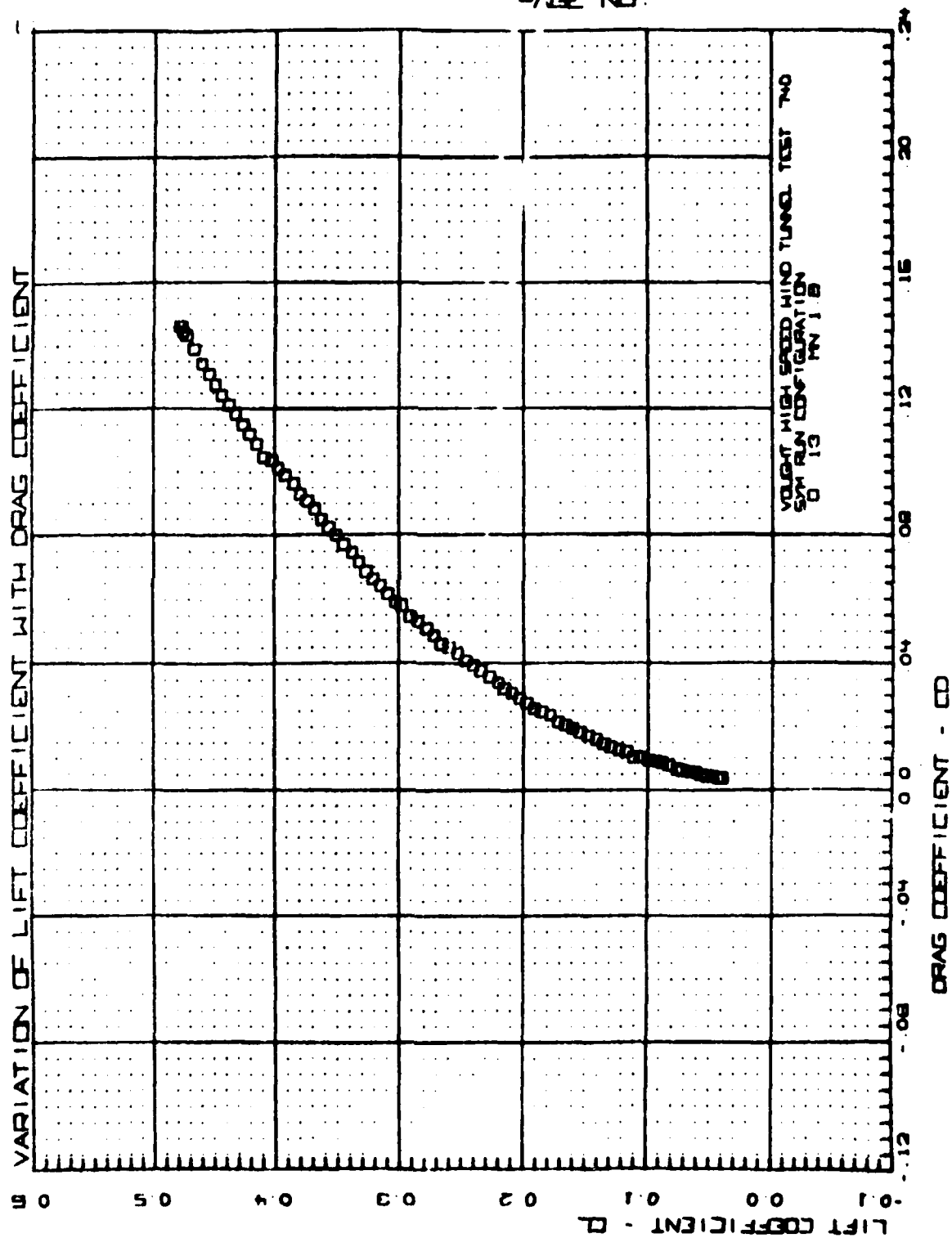


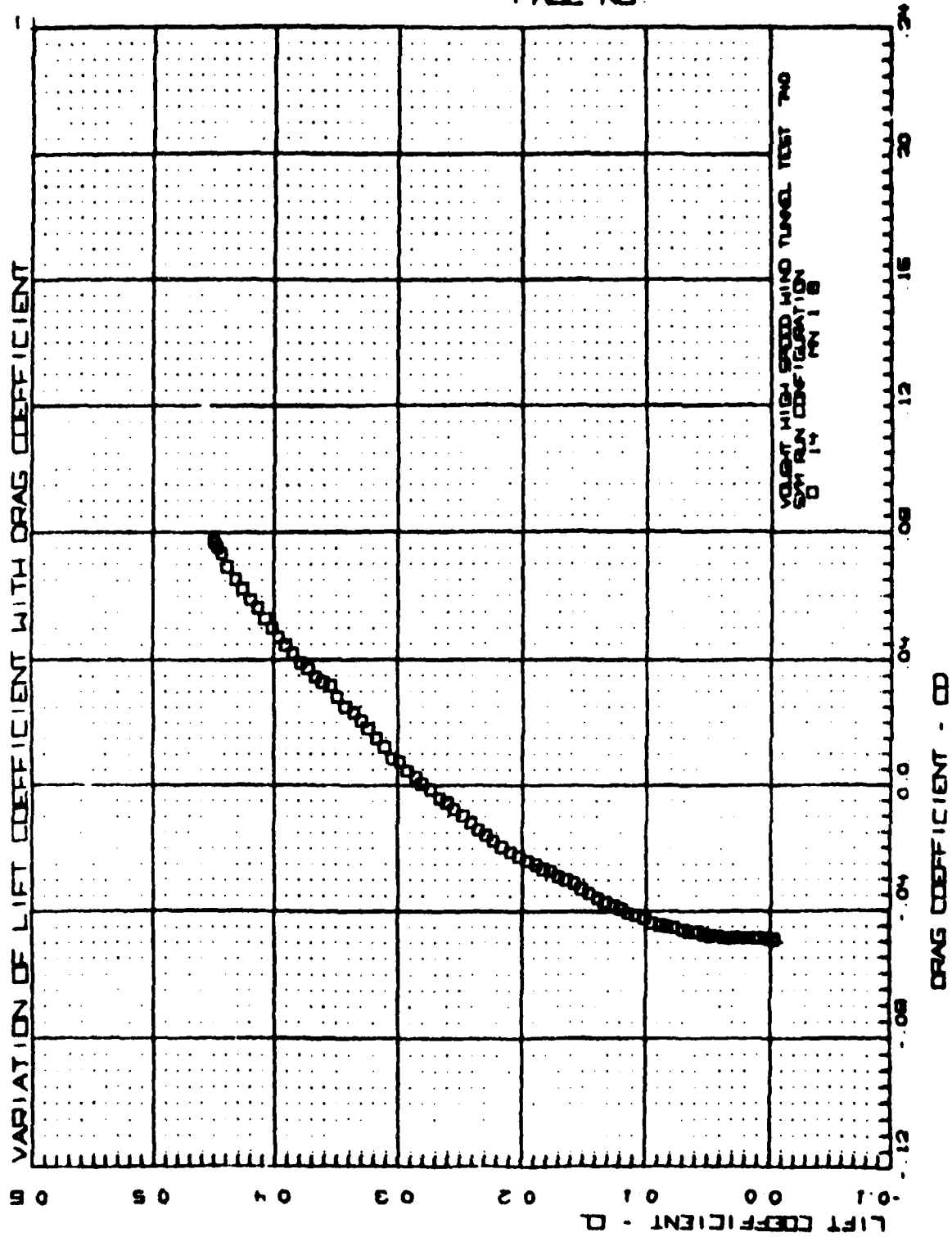


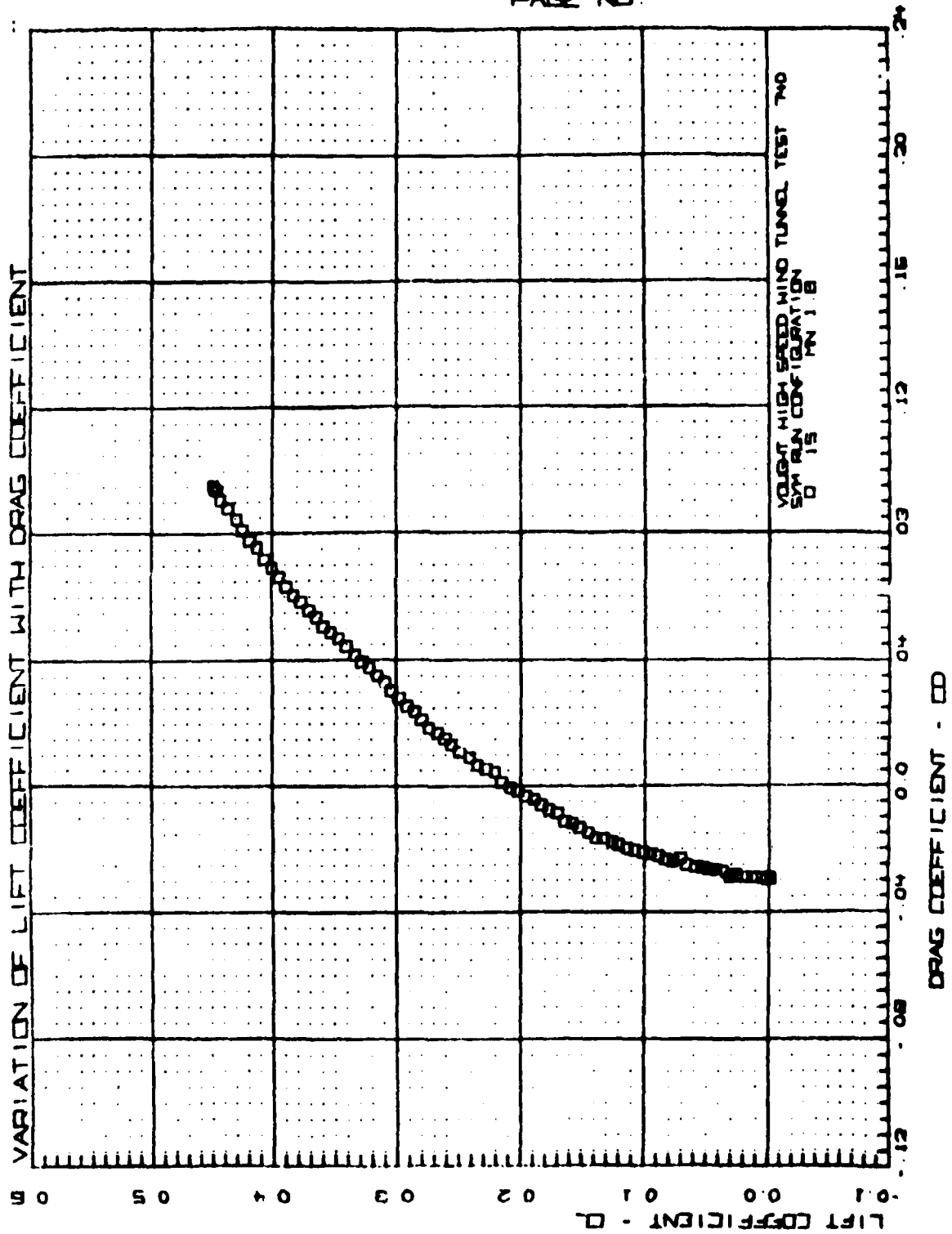
VOUGHT HEAT TEST TWO
PAGE NO.

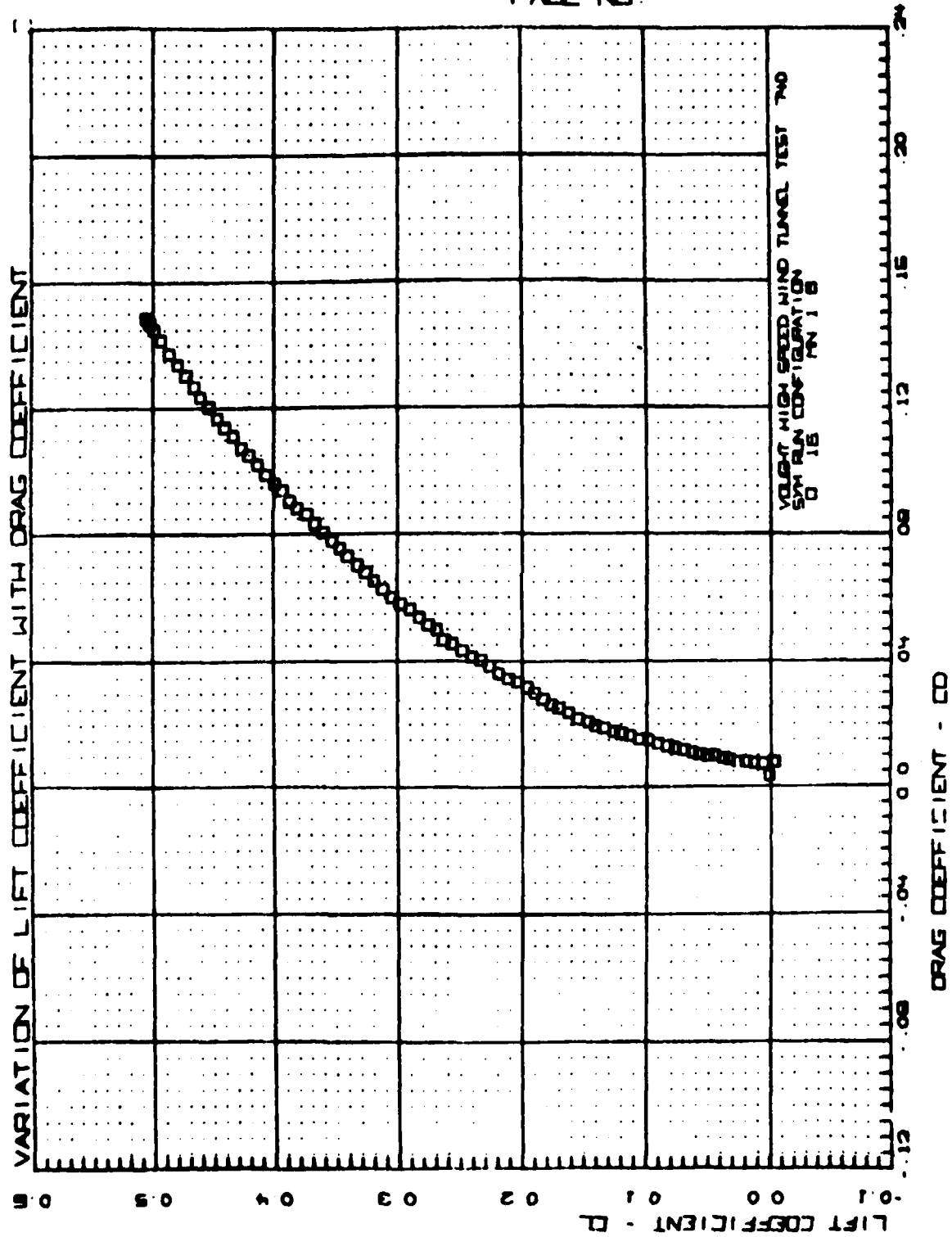


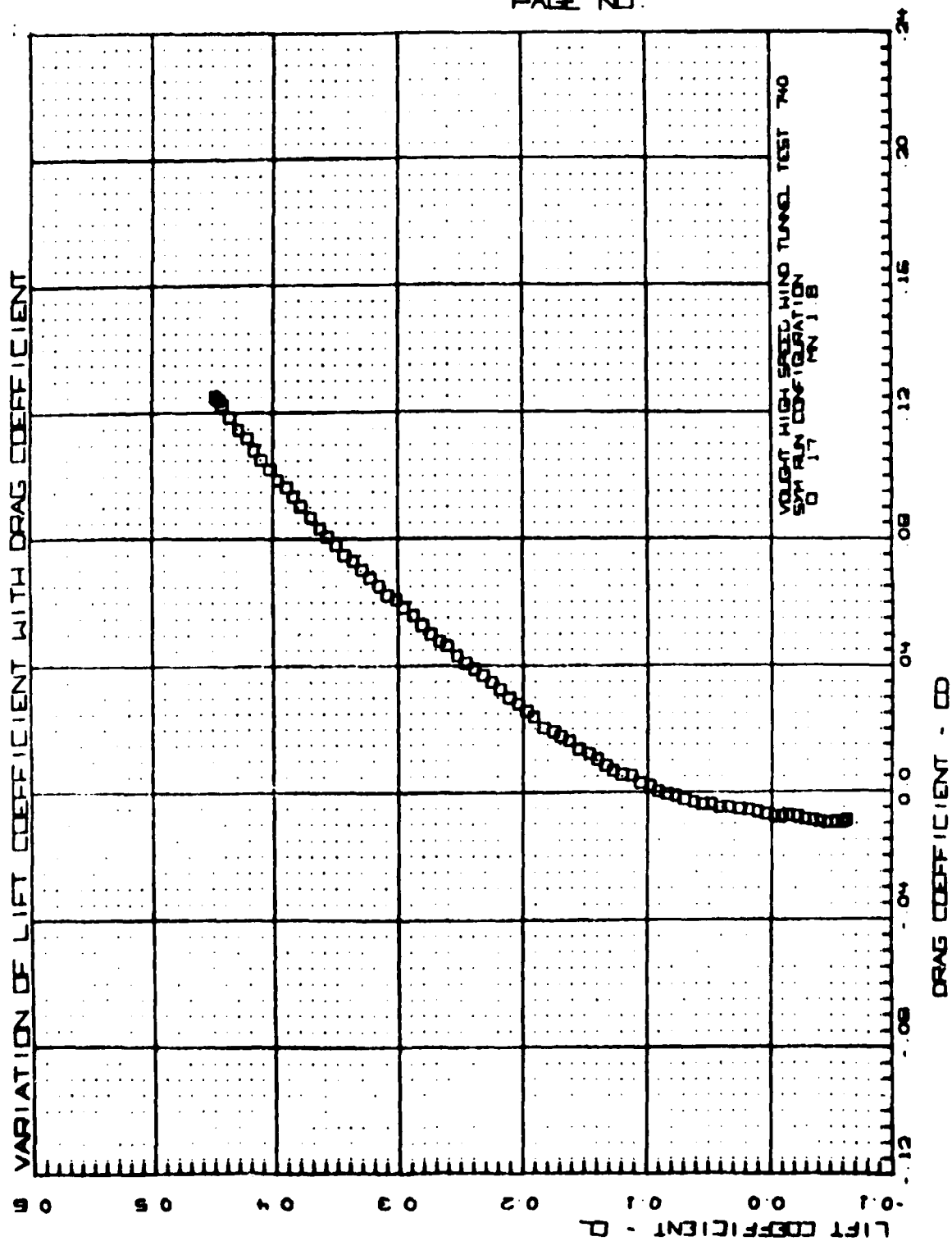
WRIGHT HEAT TEST TWO
PAGE NO.

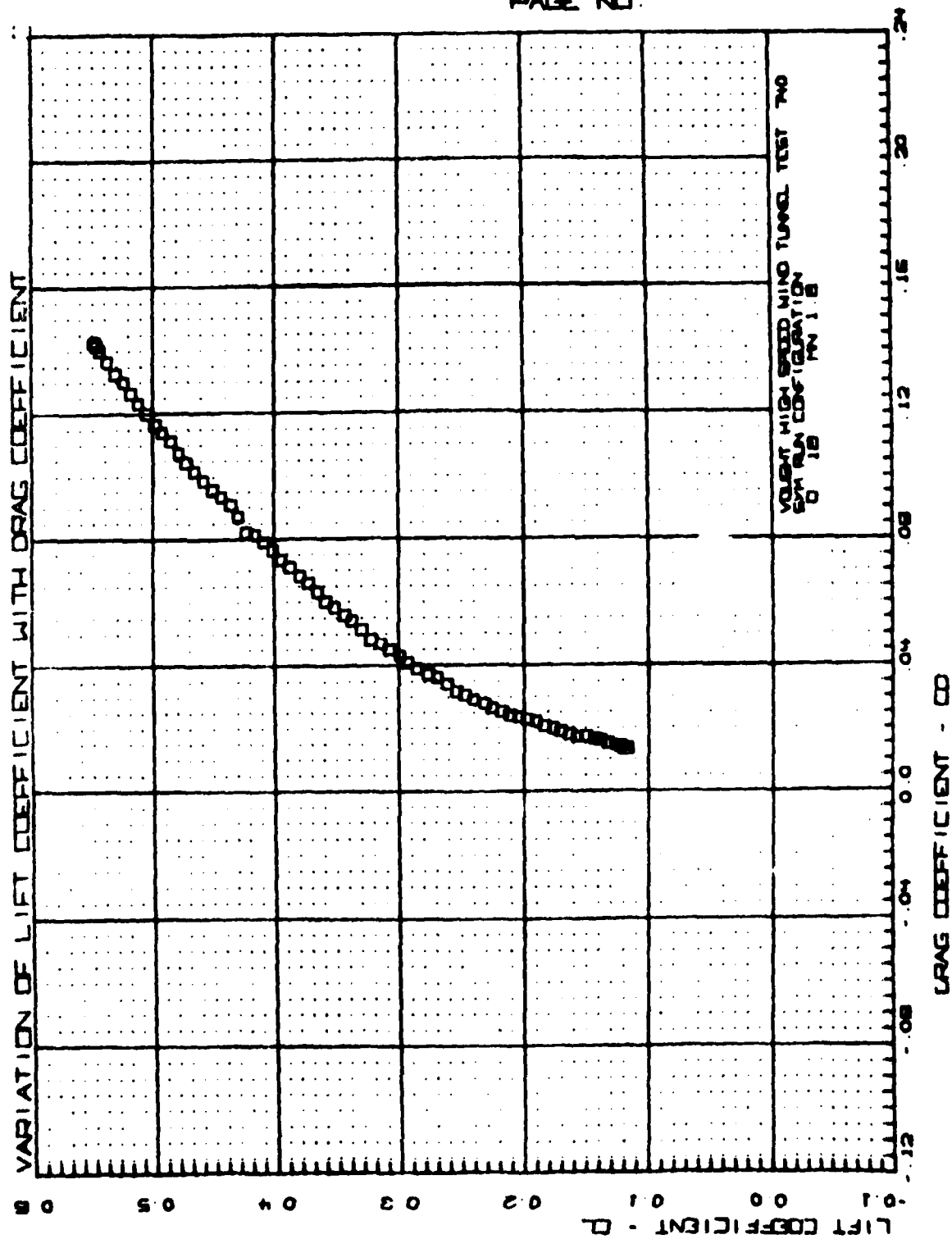


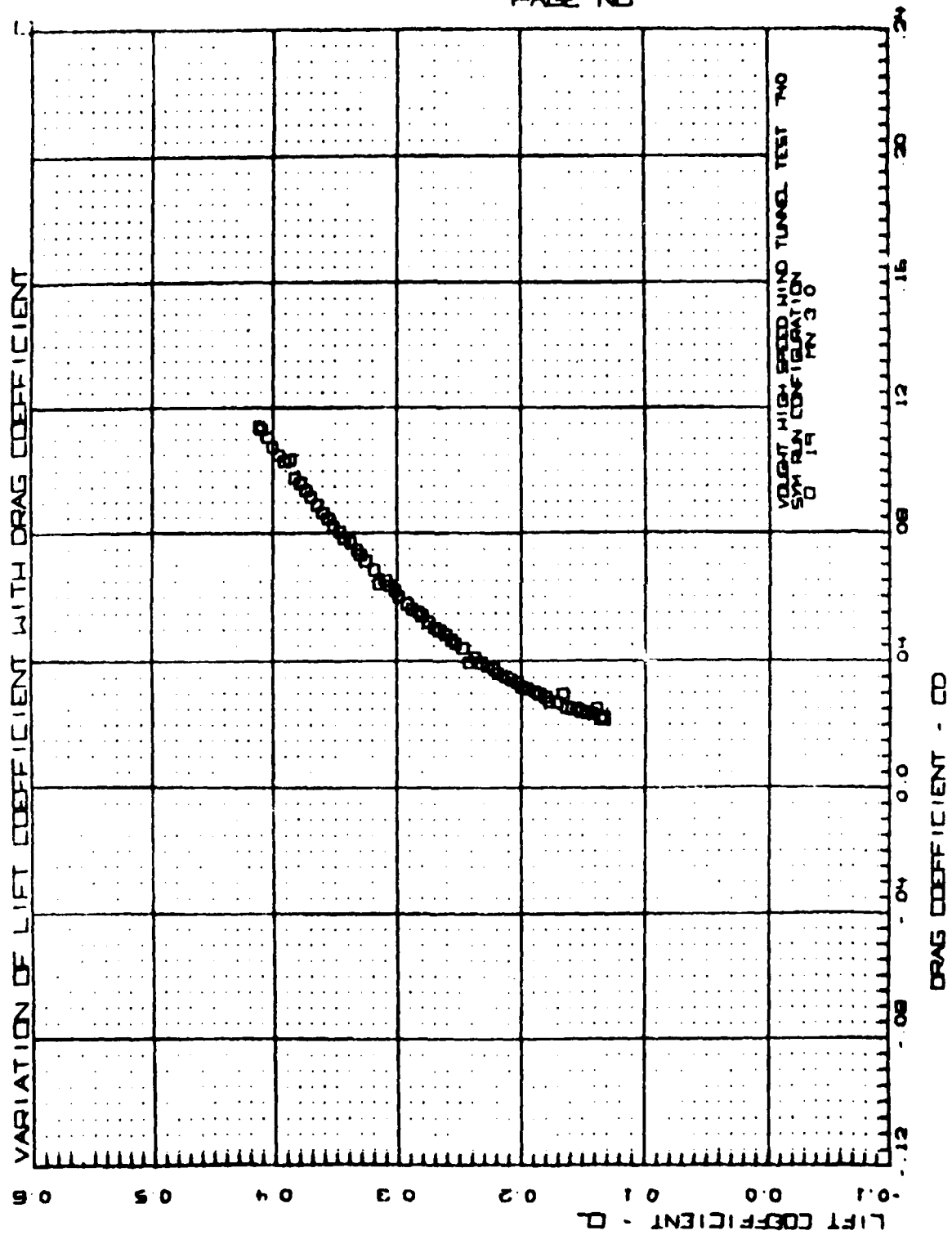


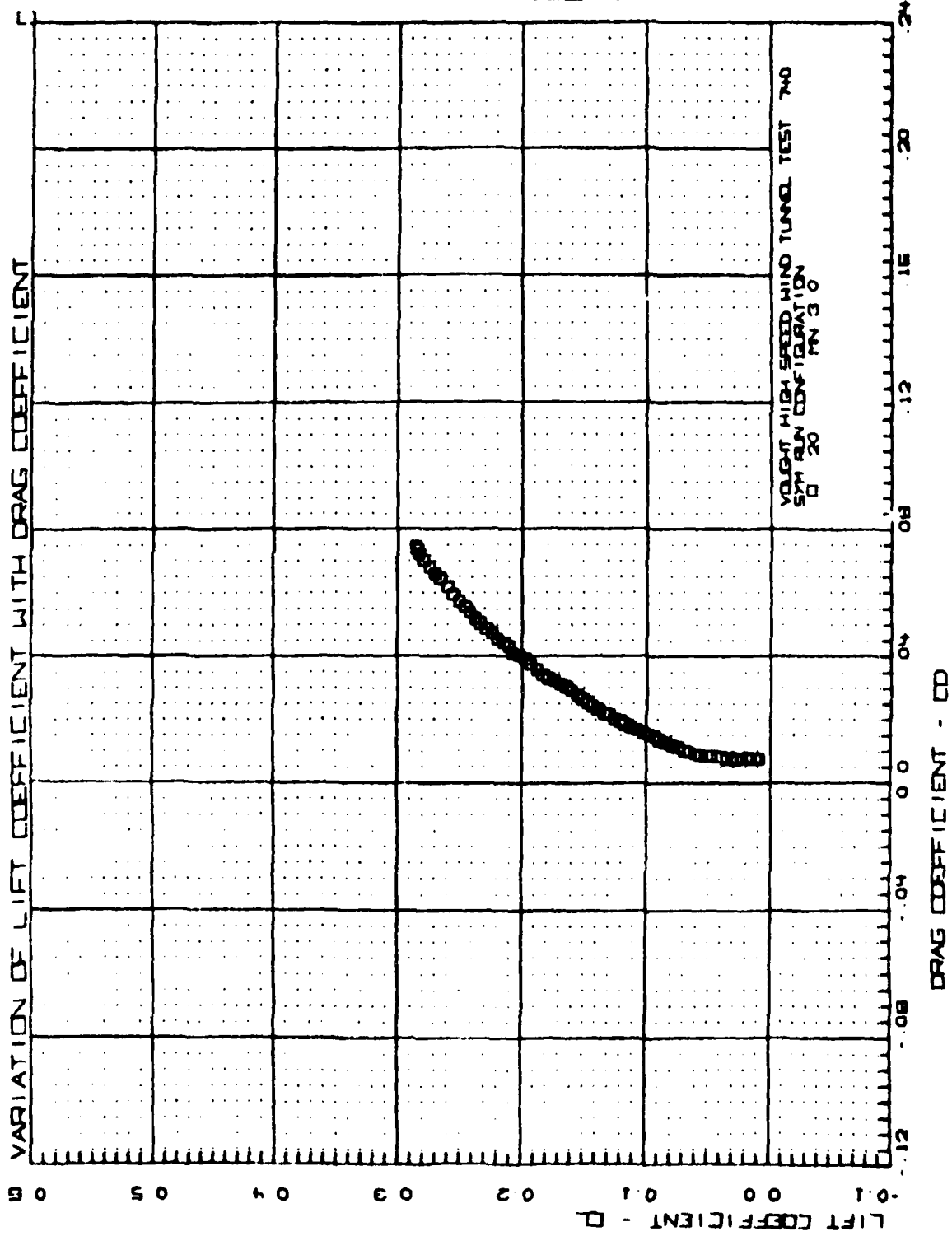


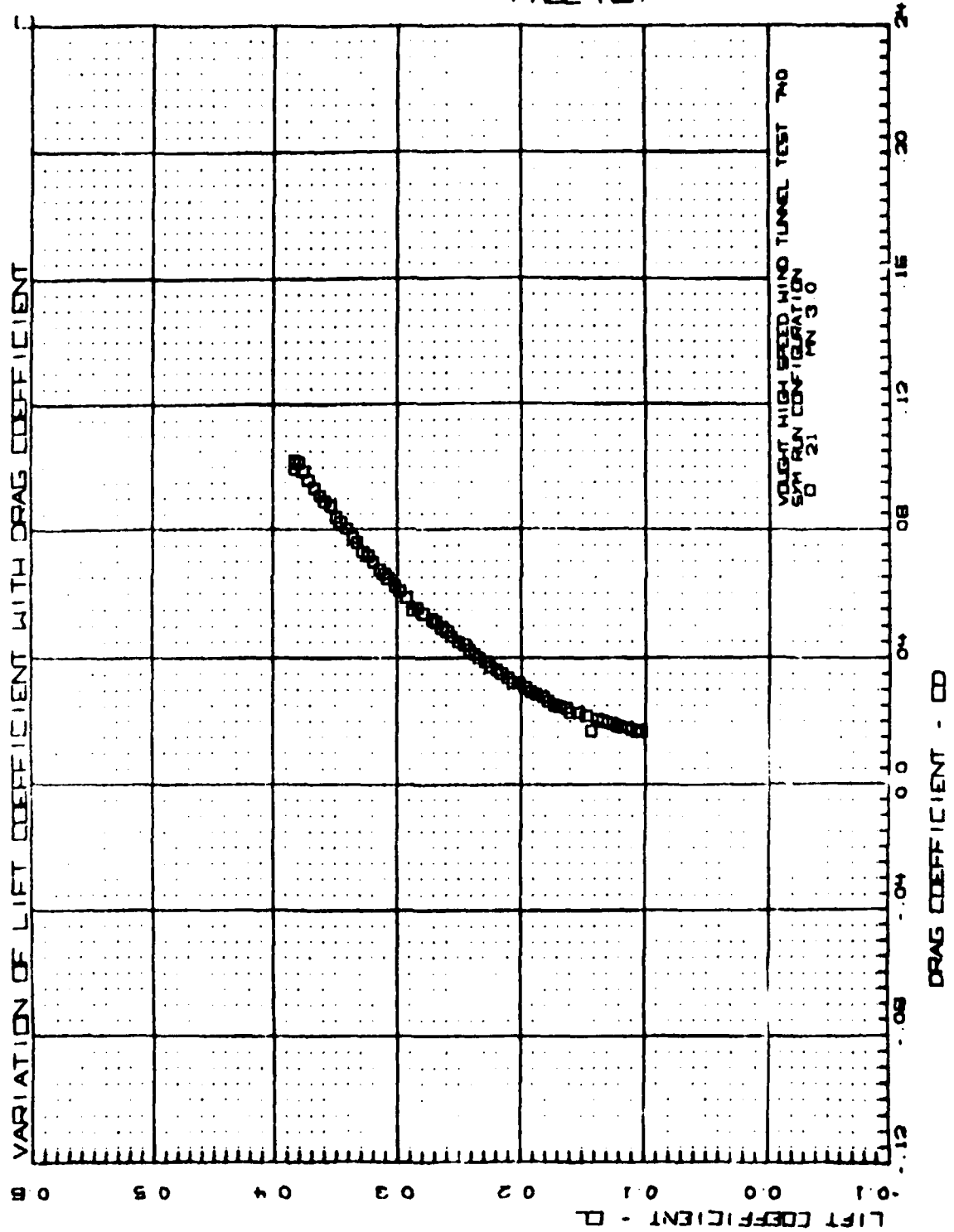




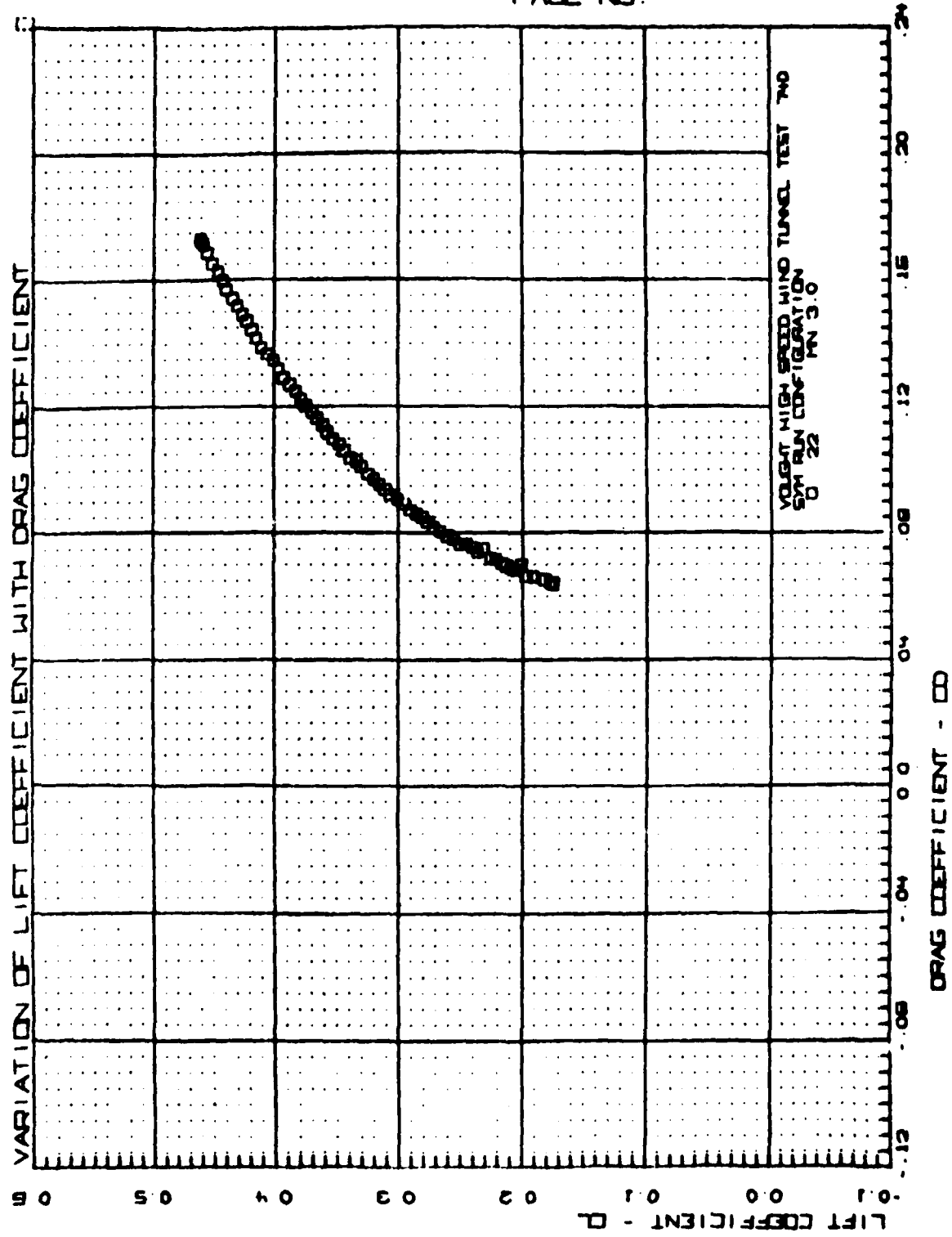


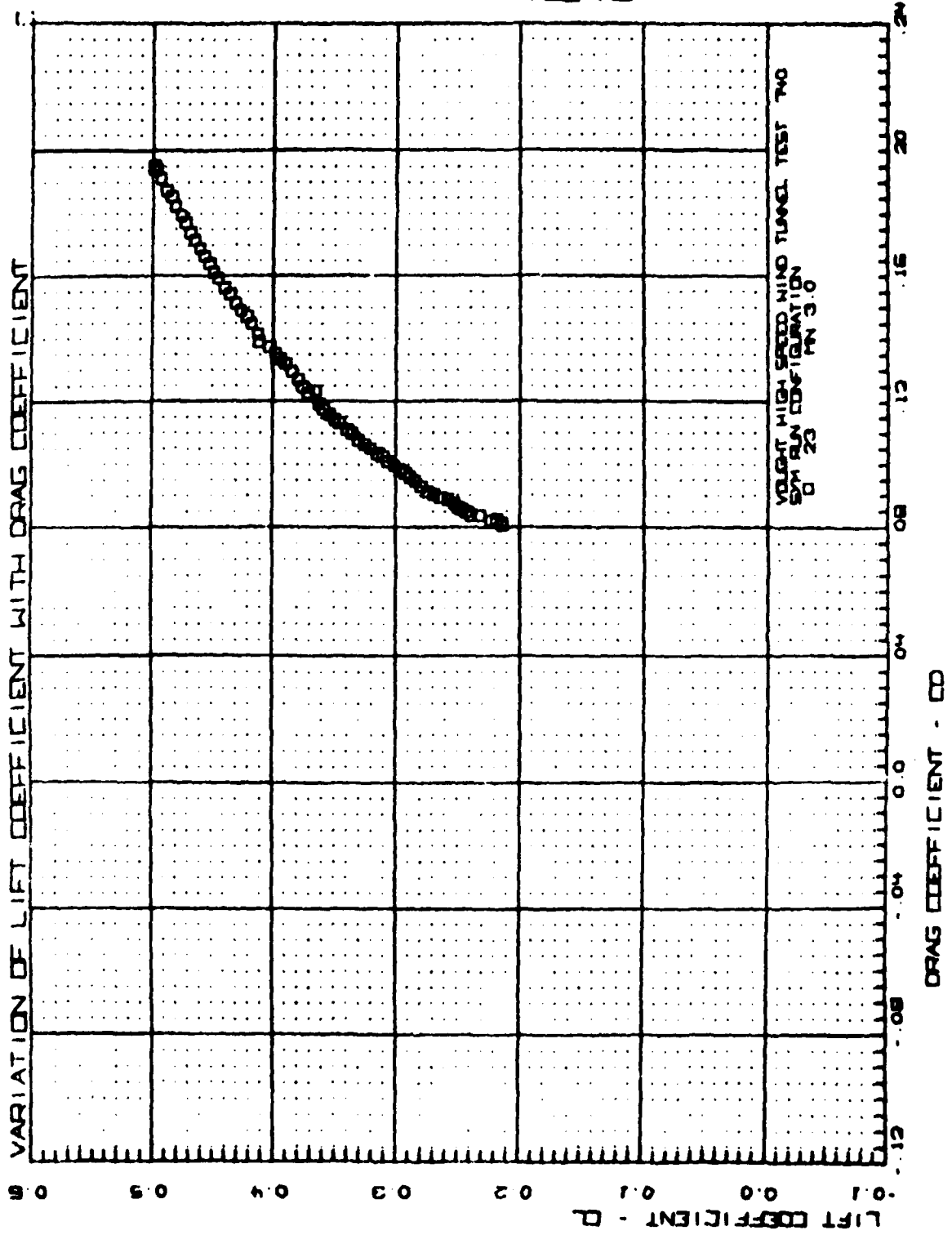


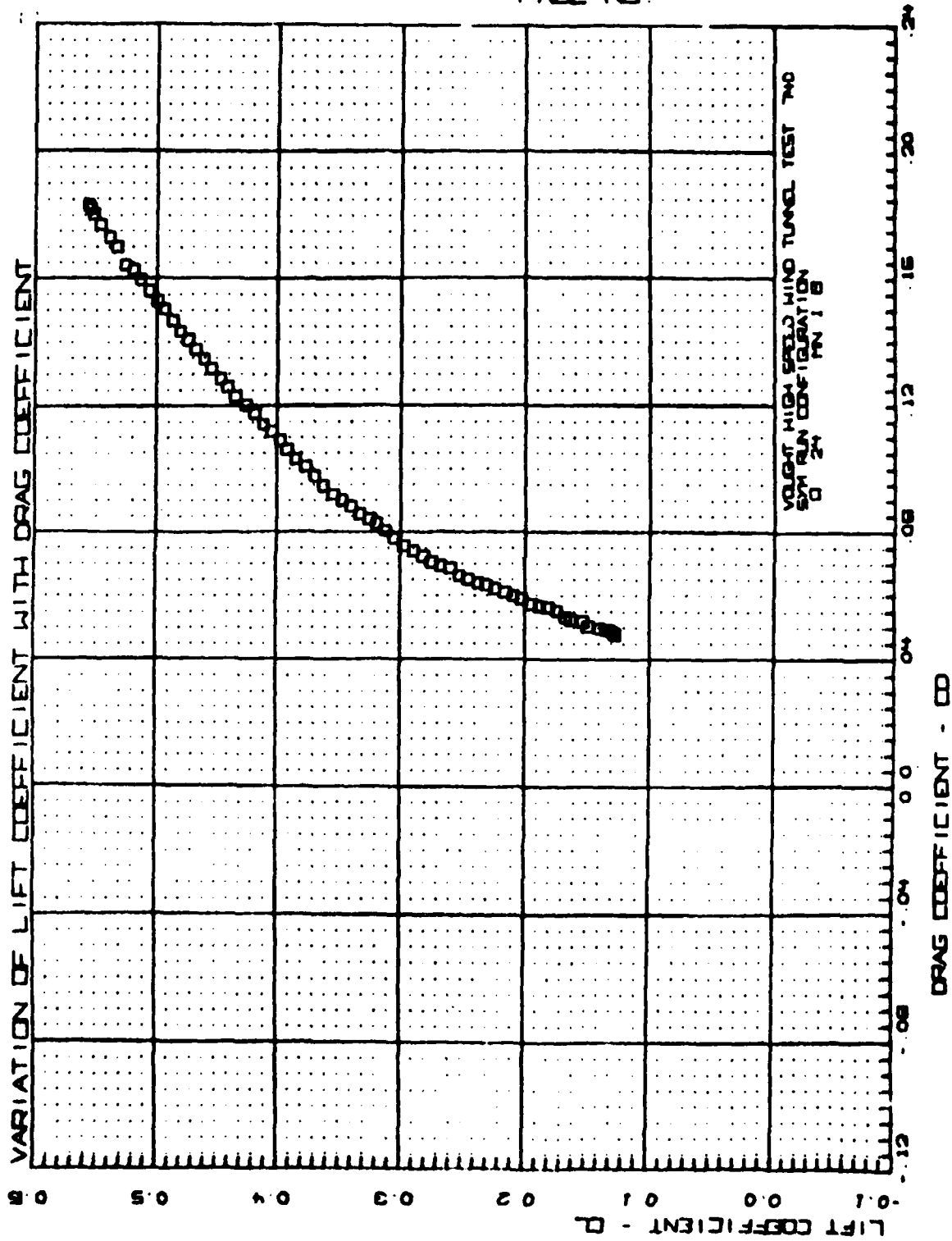


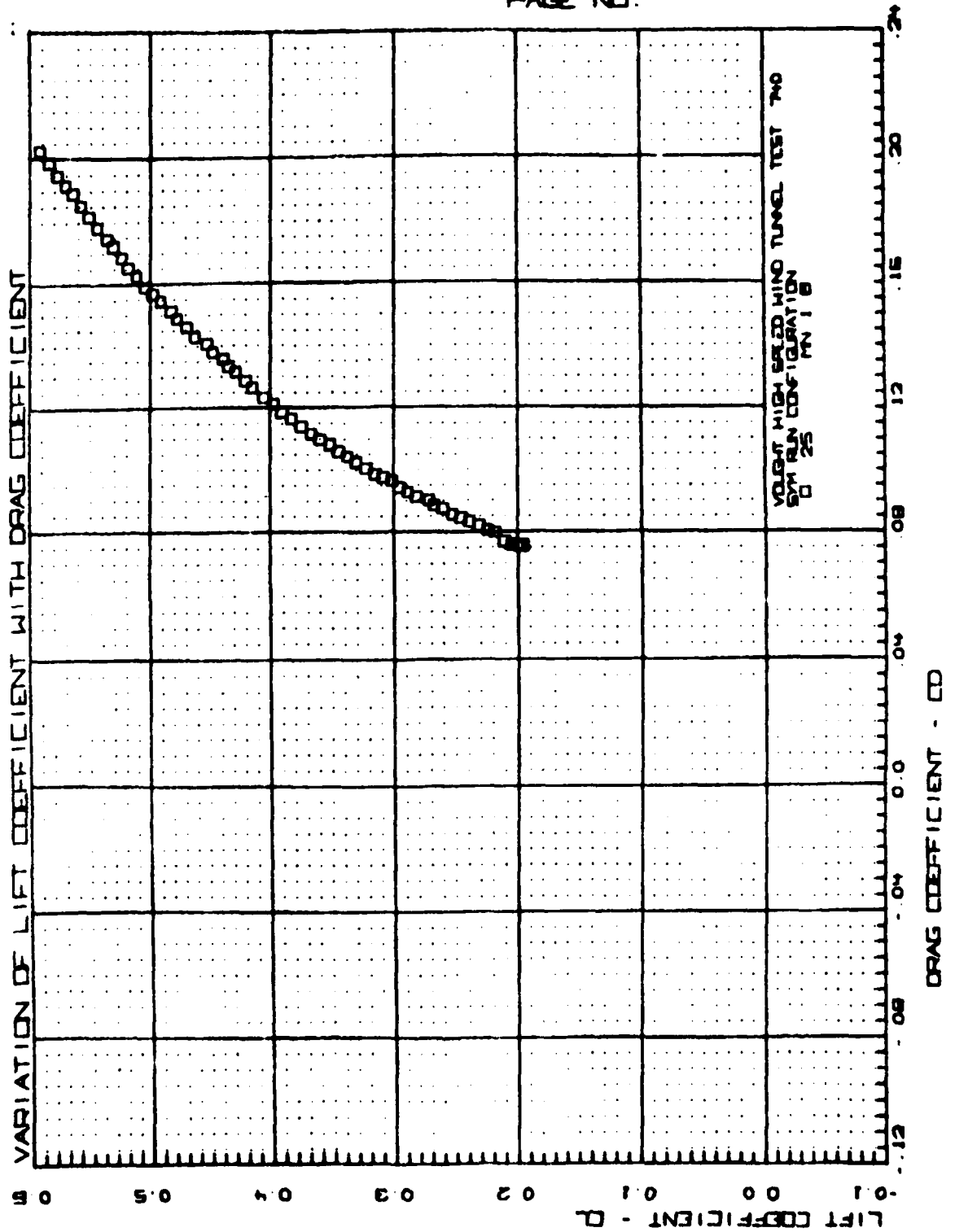


VOUGHT HEAT TEST TWO
PAGE NO.

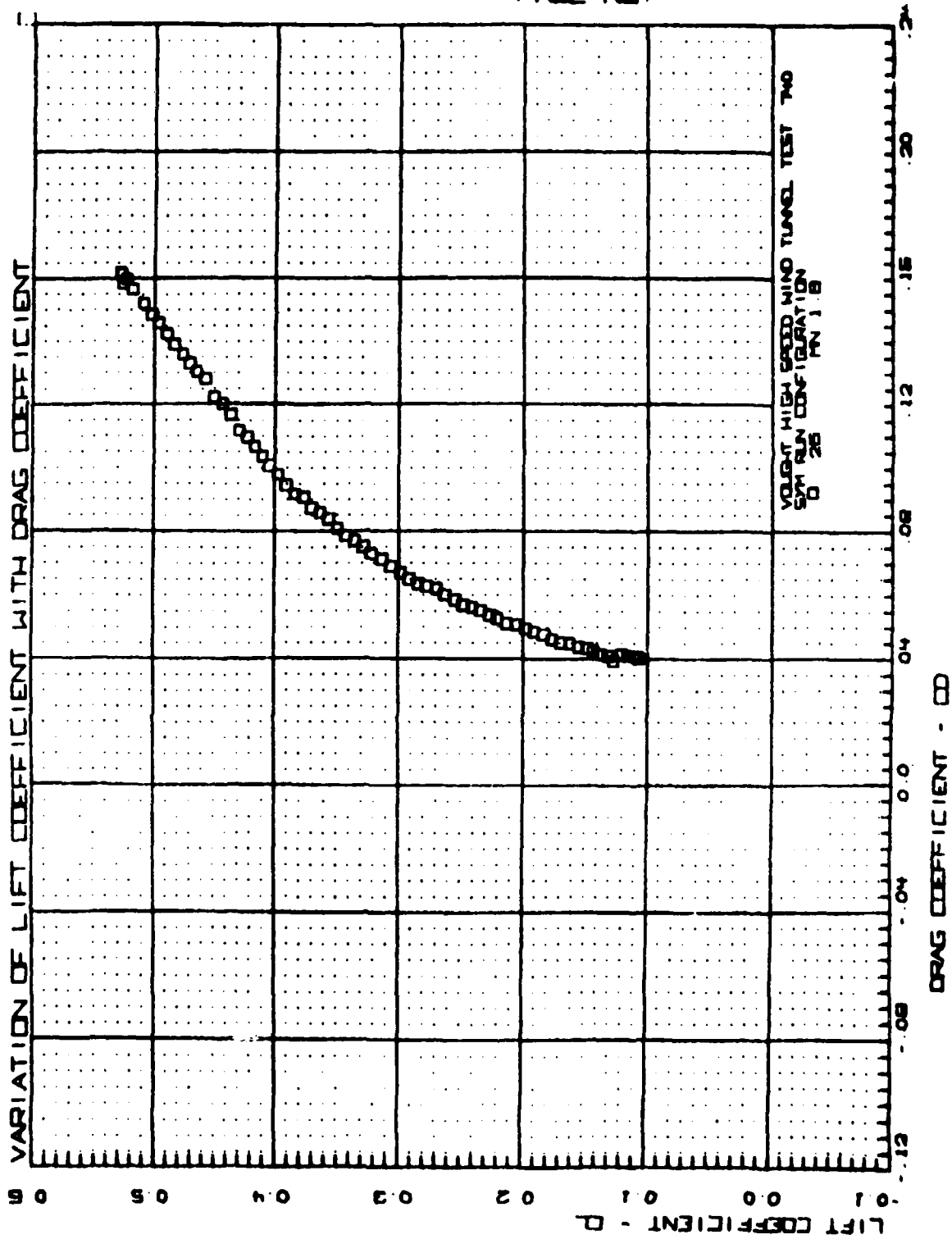


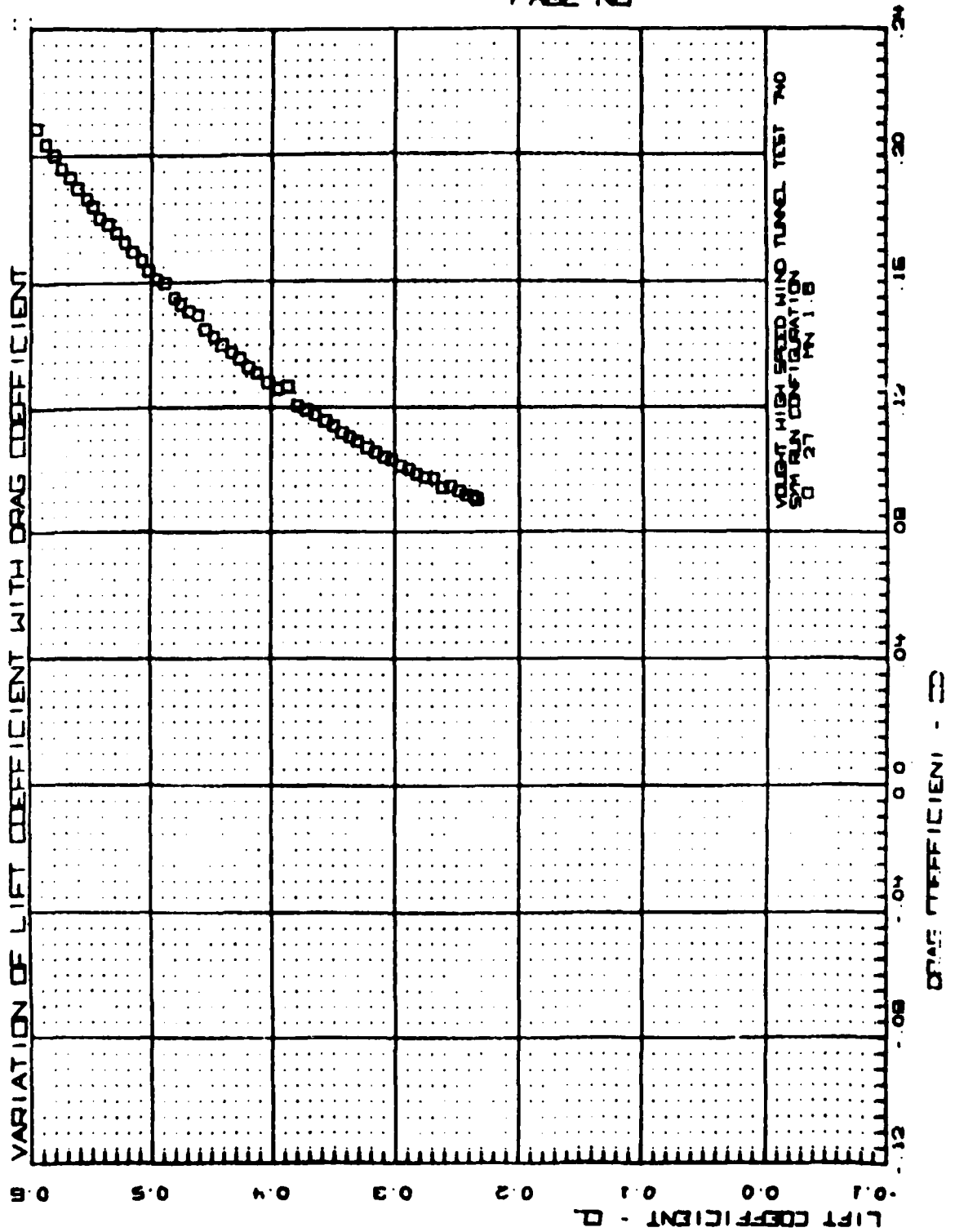




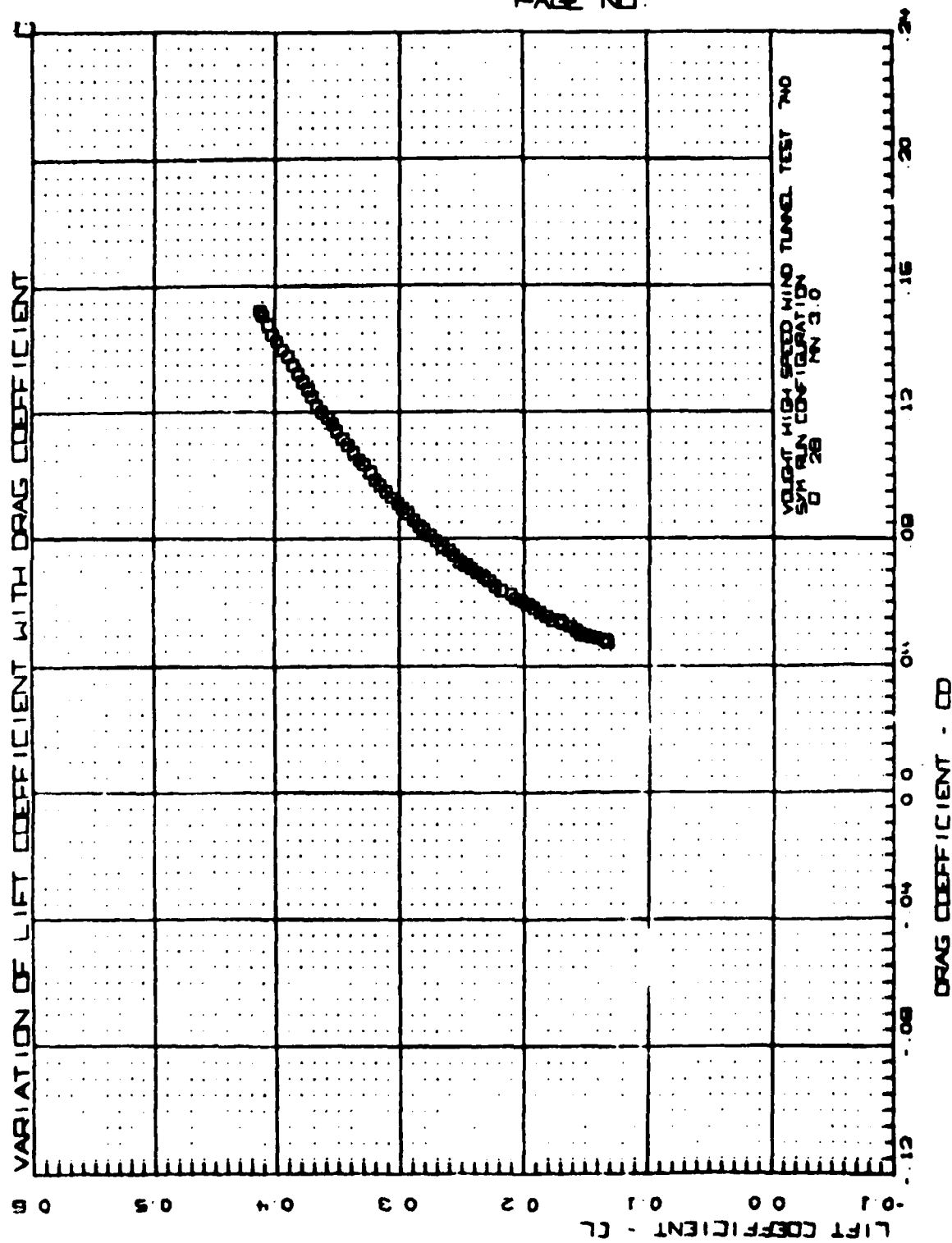


VOUGHT HEAT TEST 740
PAGE NO.

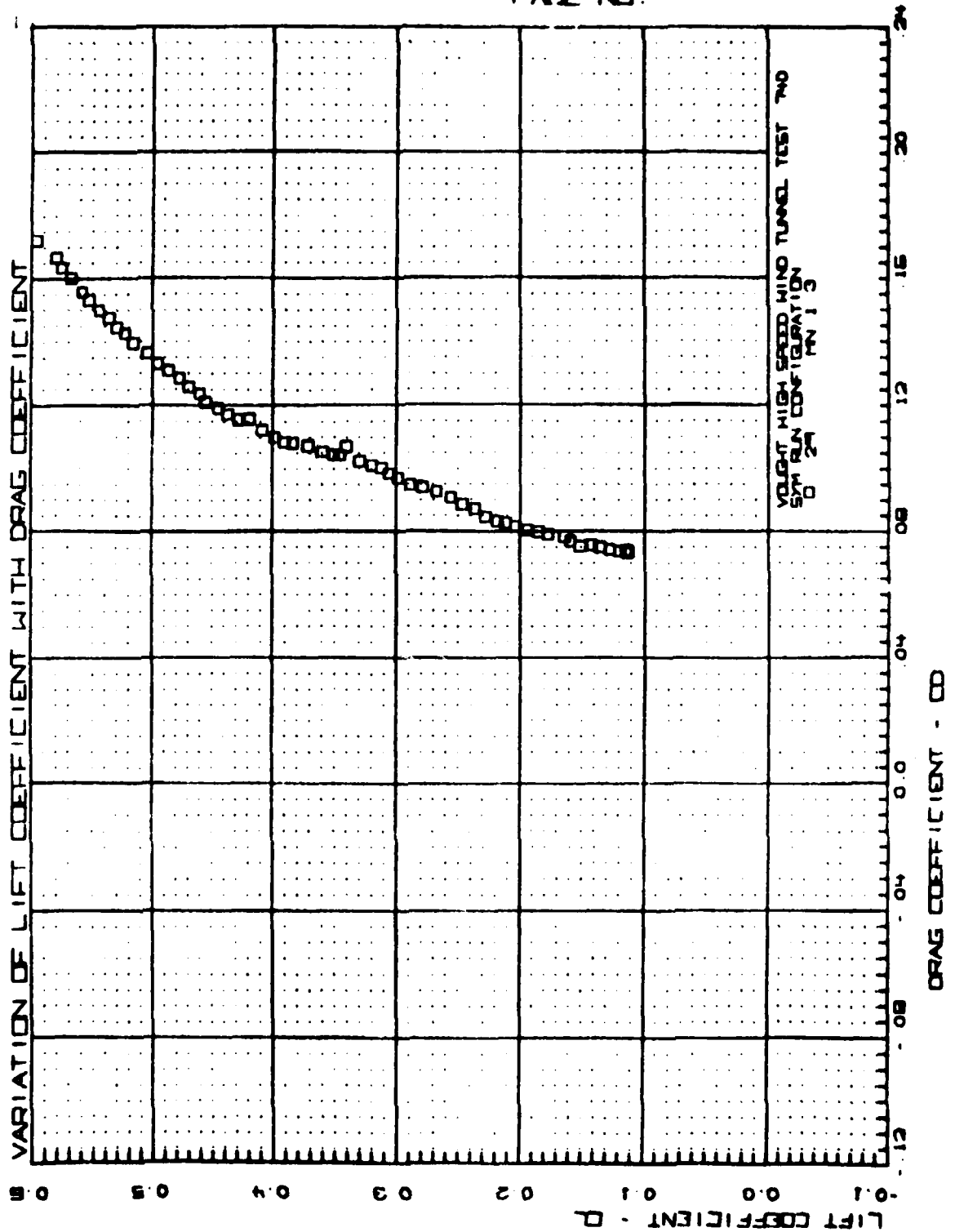


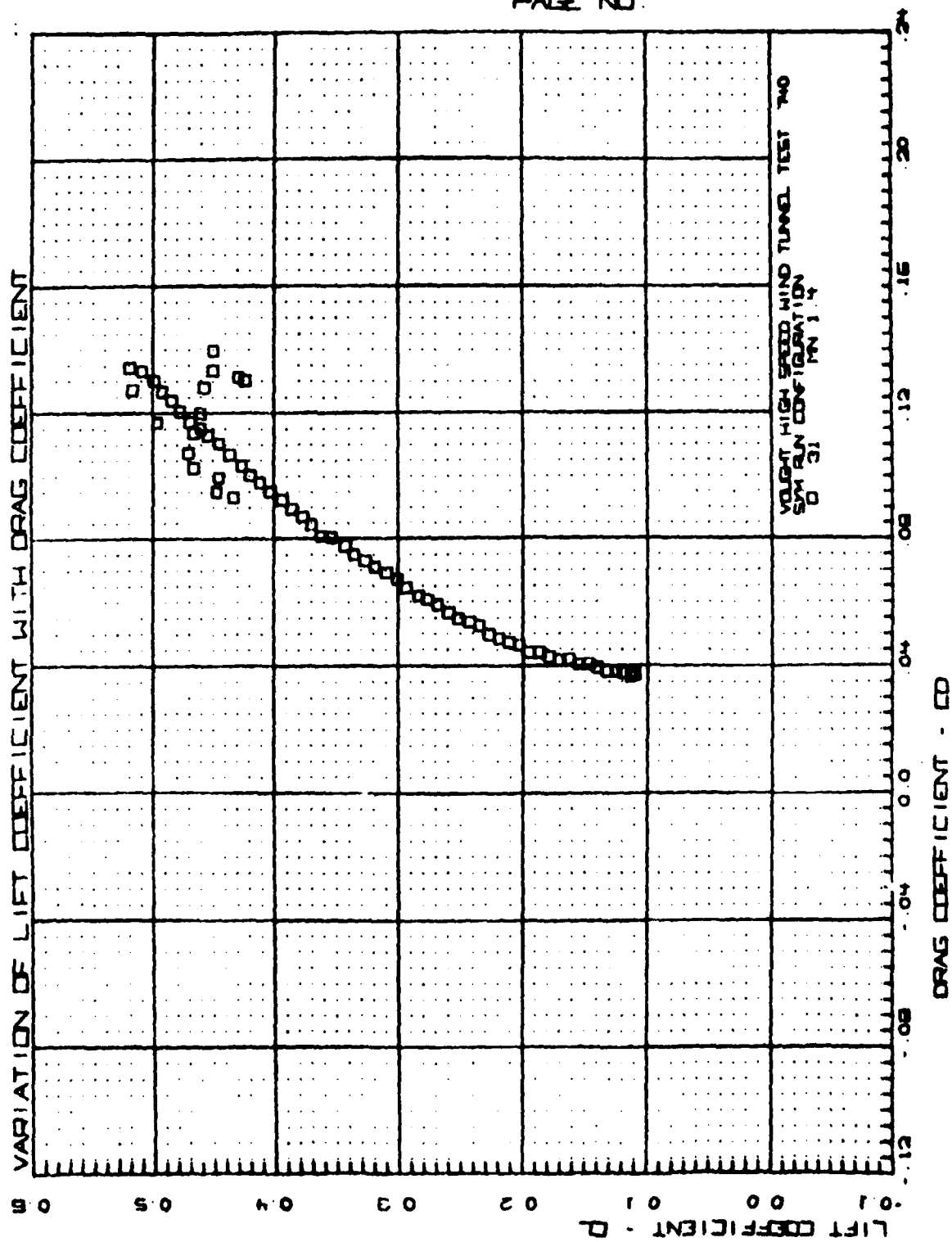


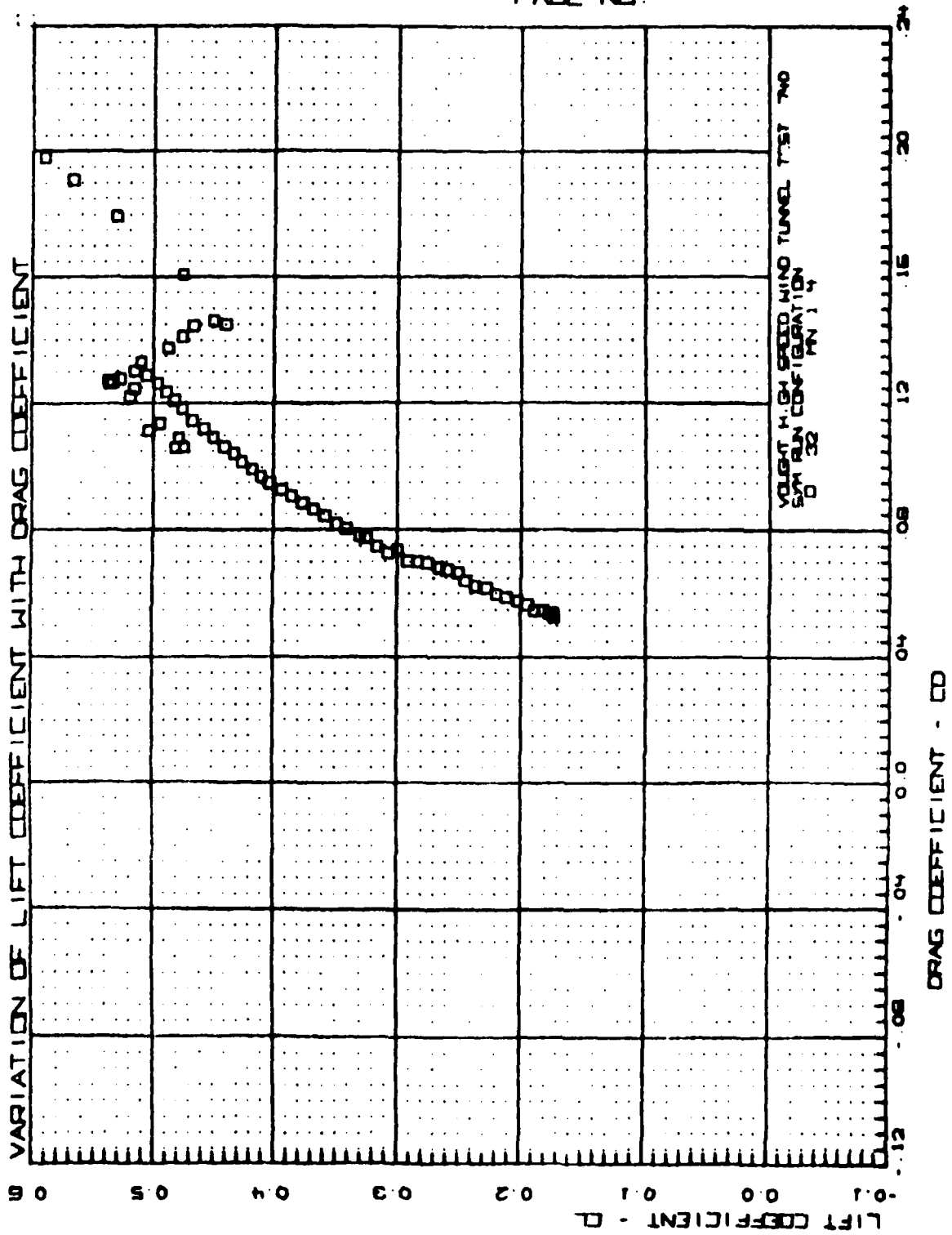
VOUGHT HEWITT TEST 740
PAGE NO.

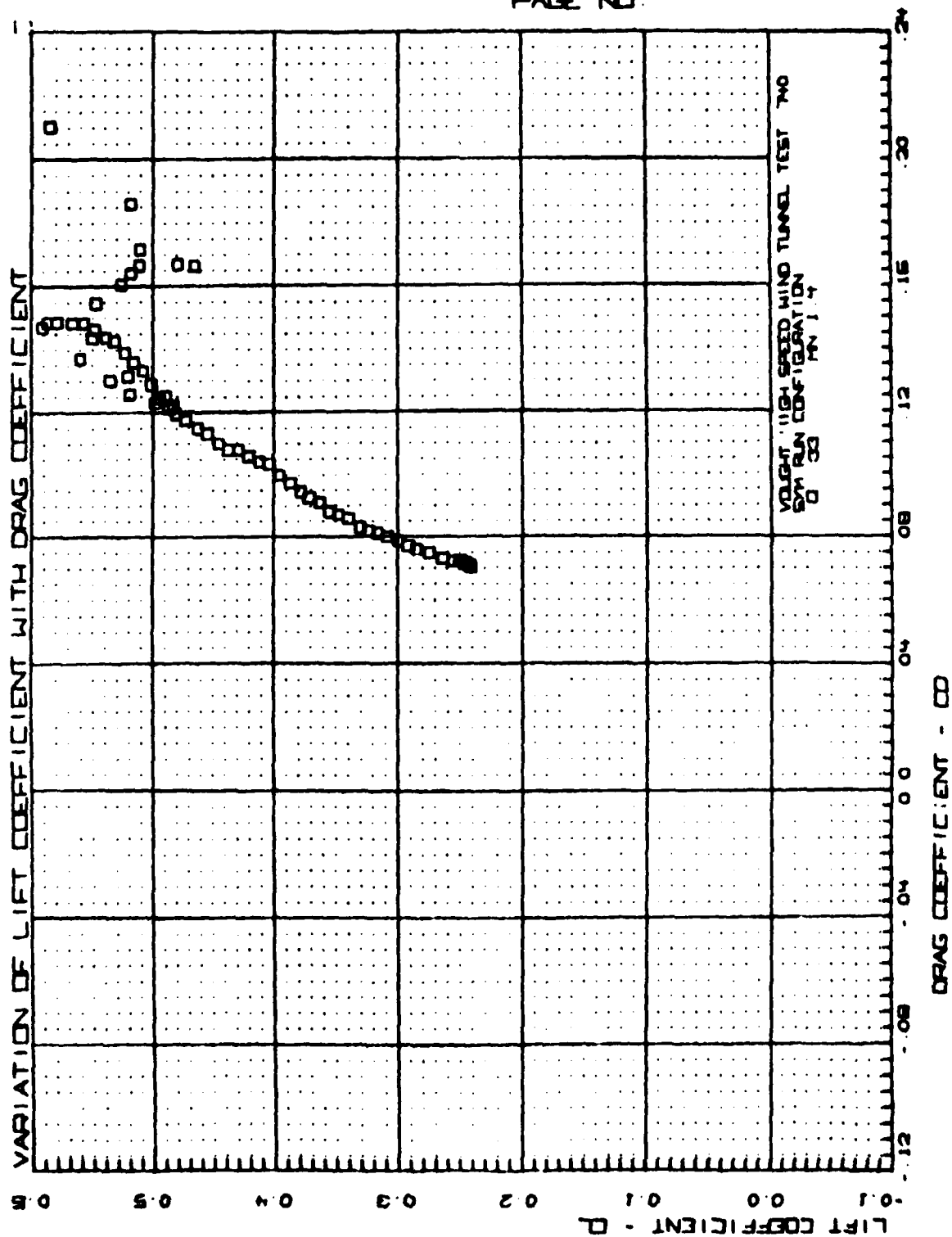


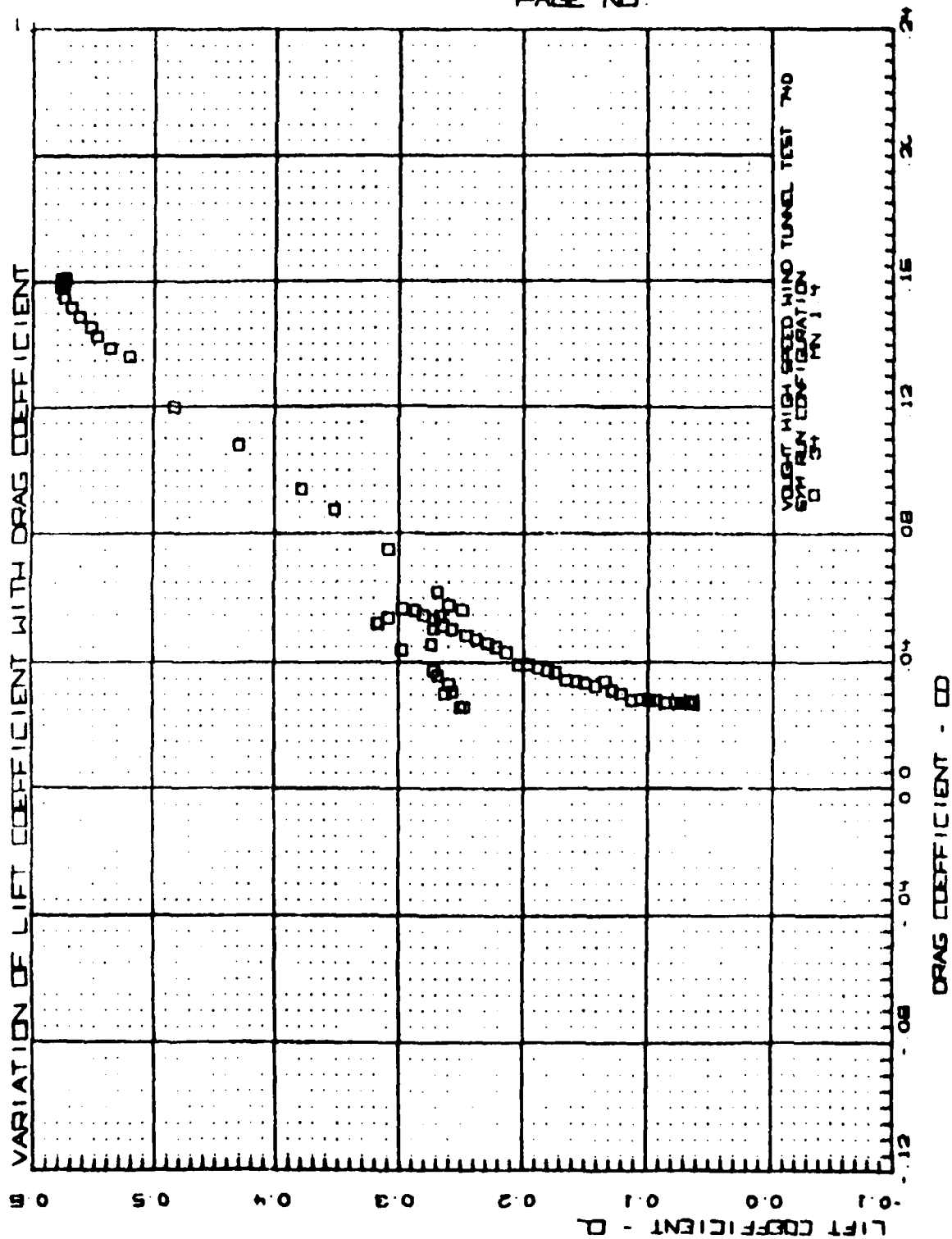
VOLUNTARY TEST TWO
PAGE NO.

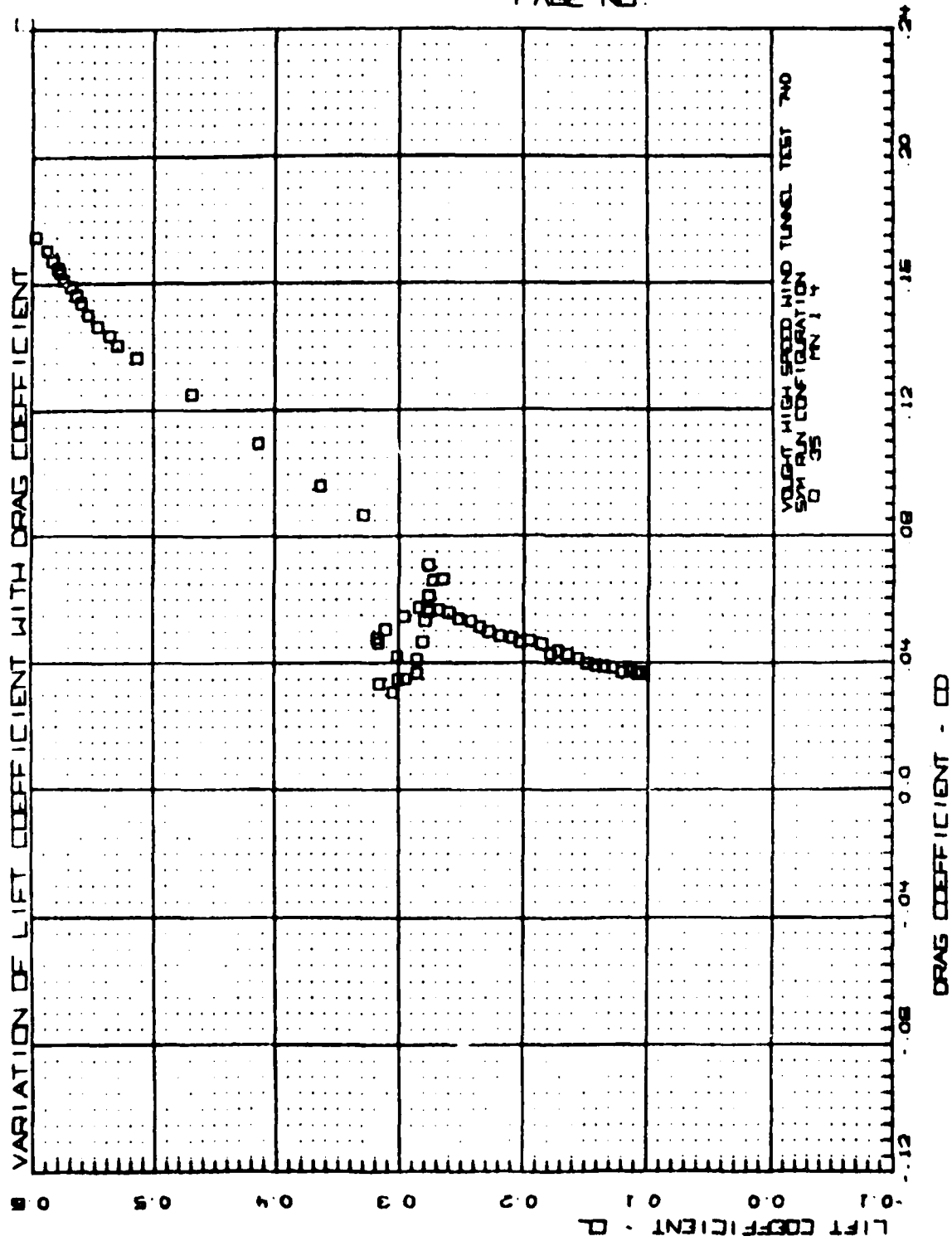


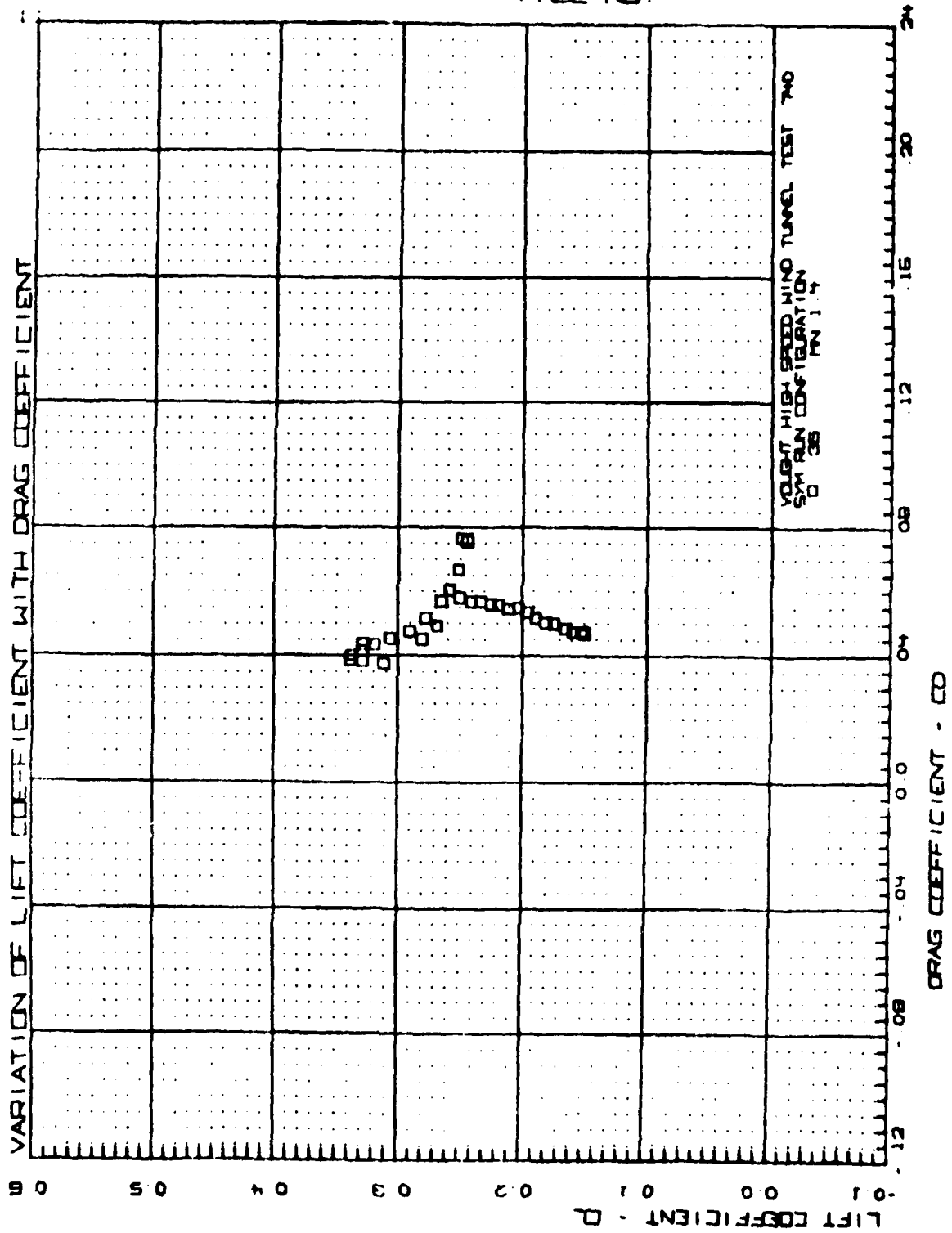


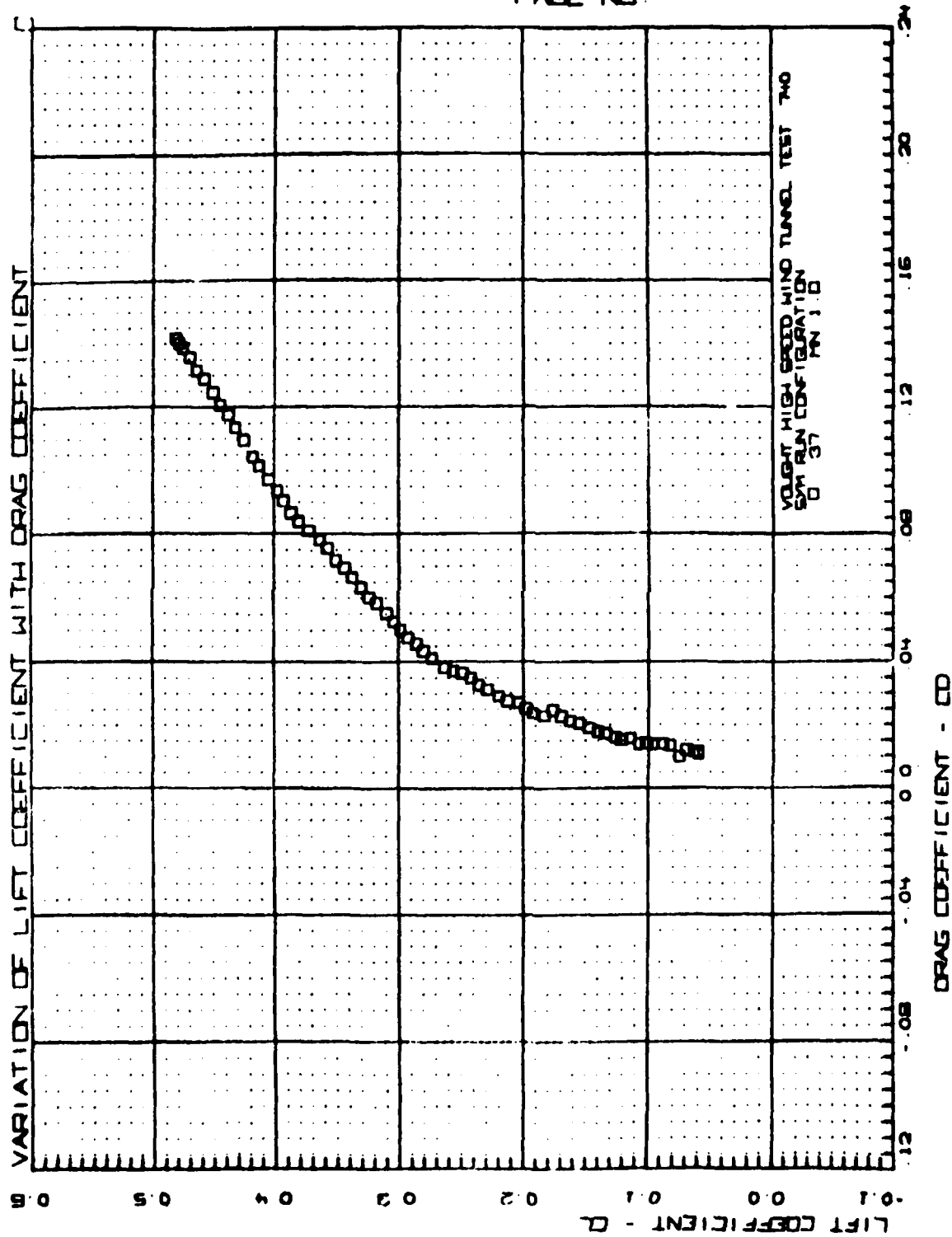


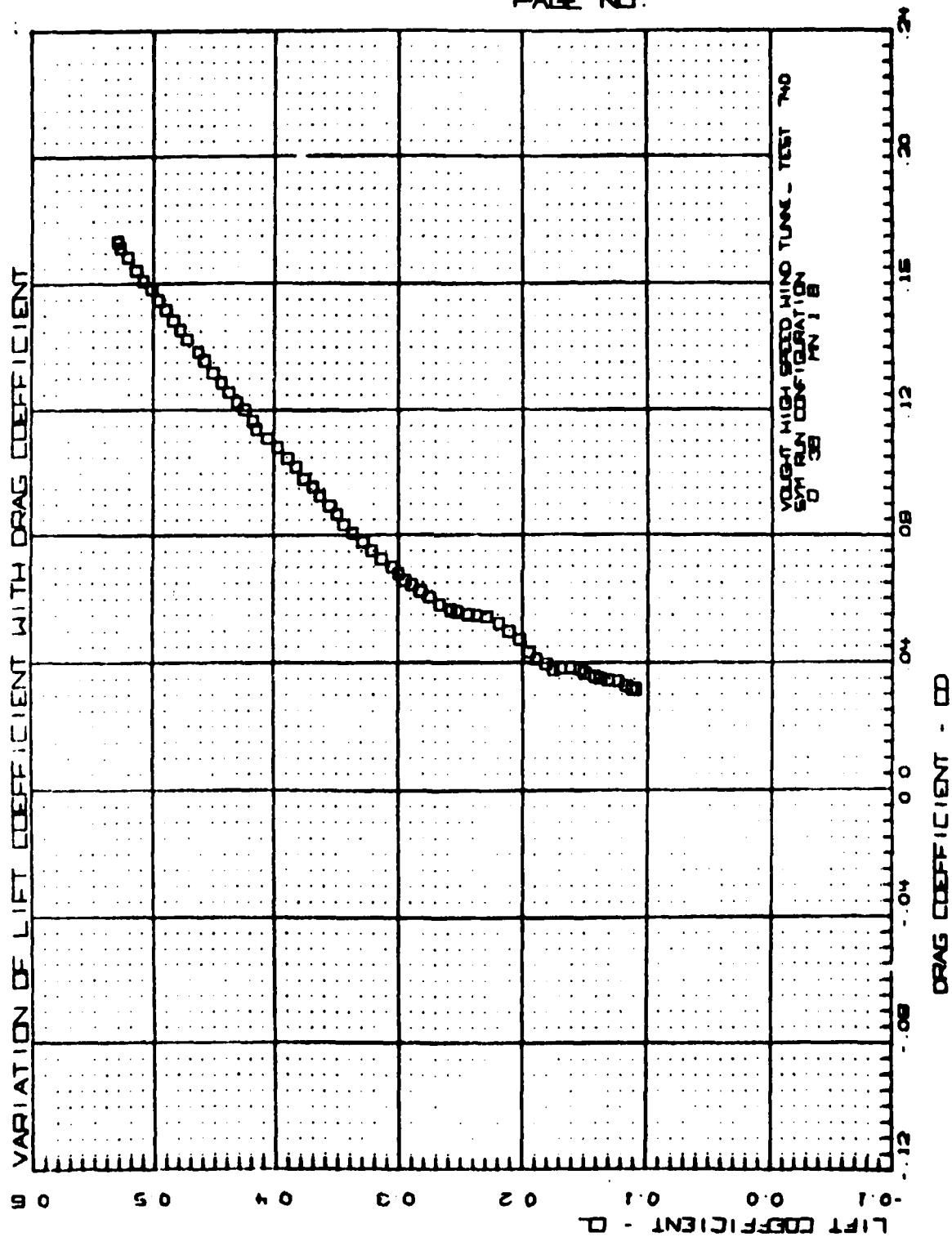




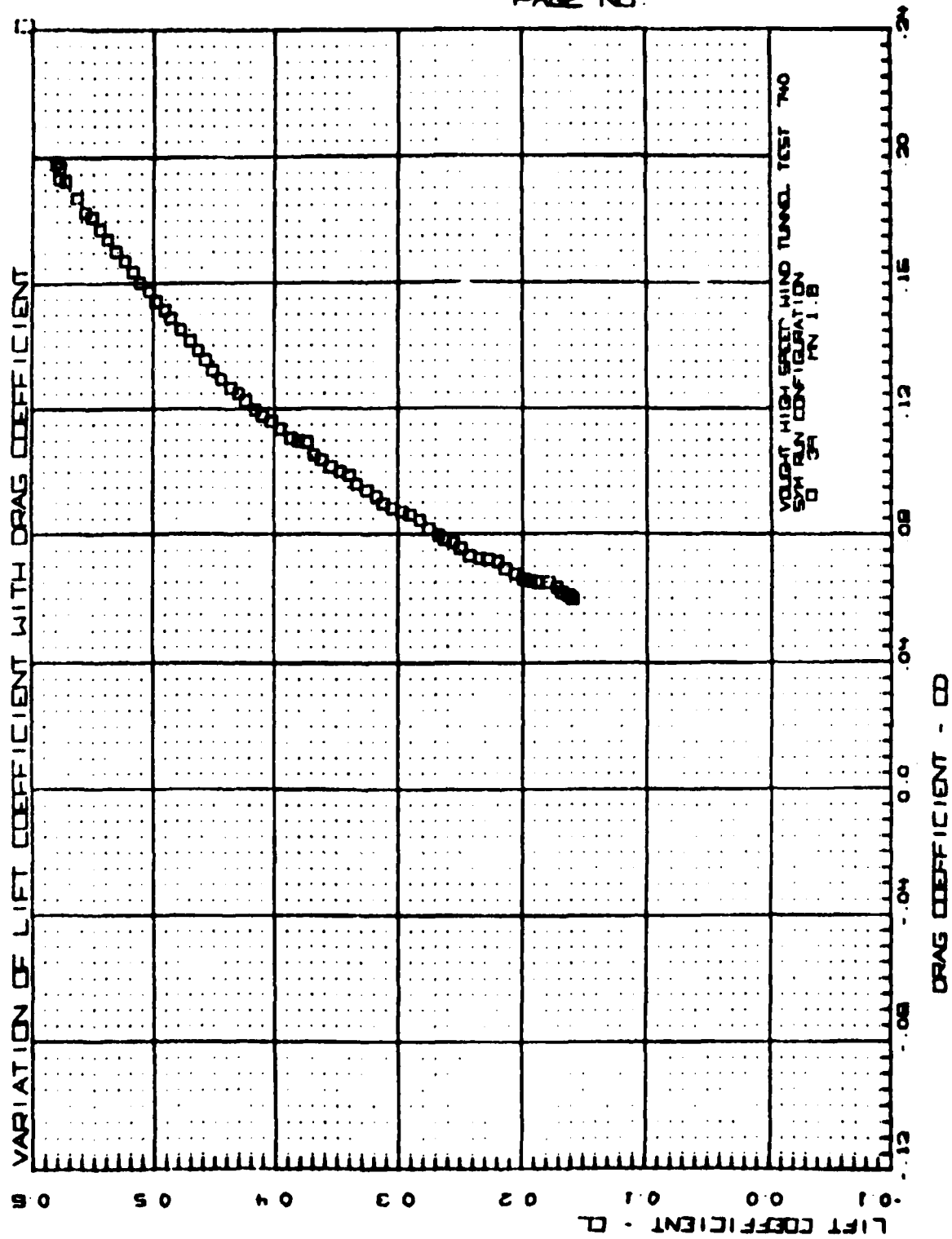


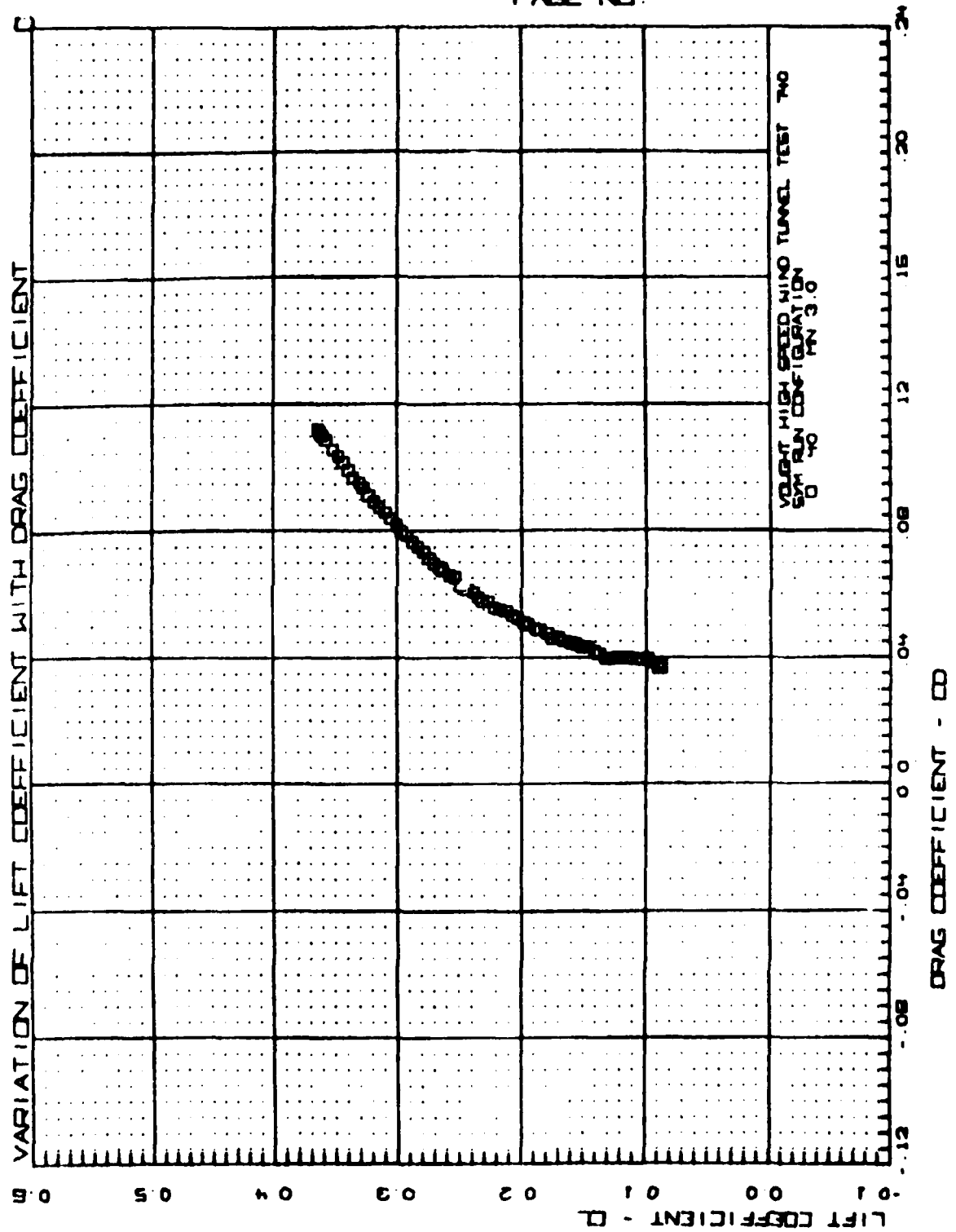


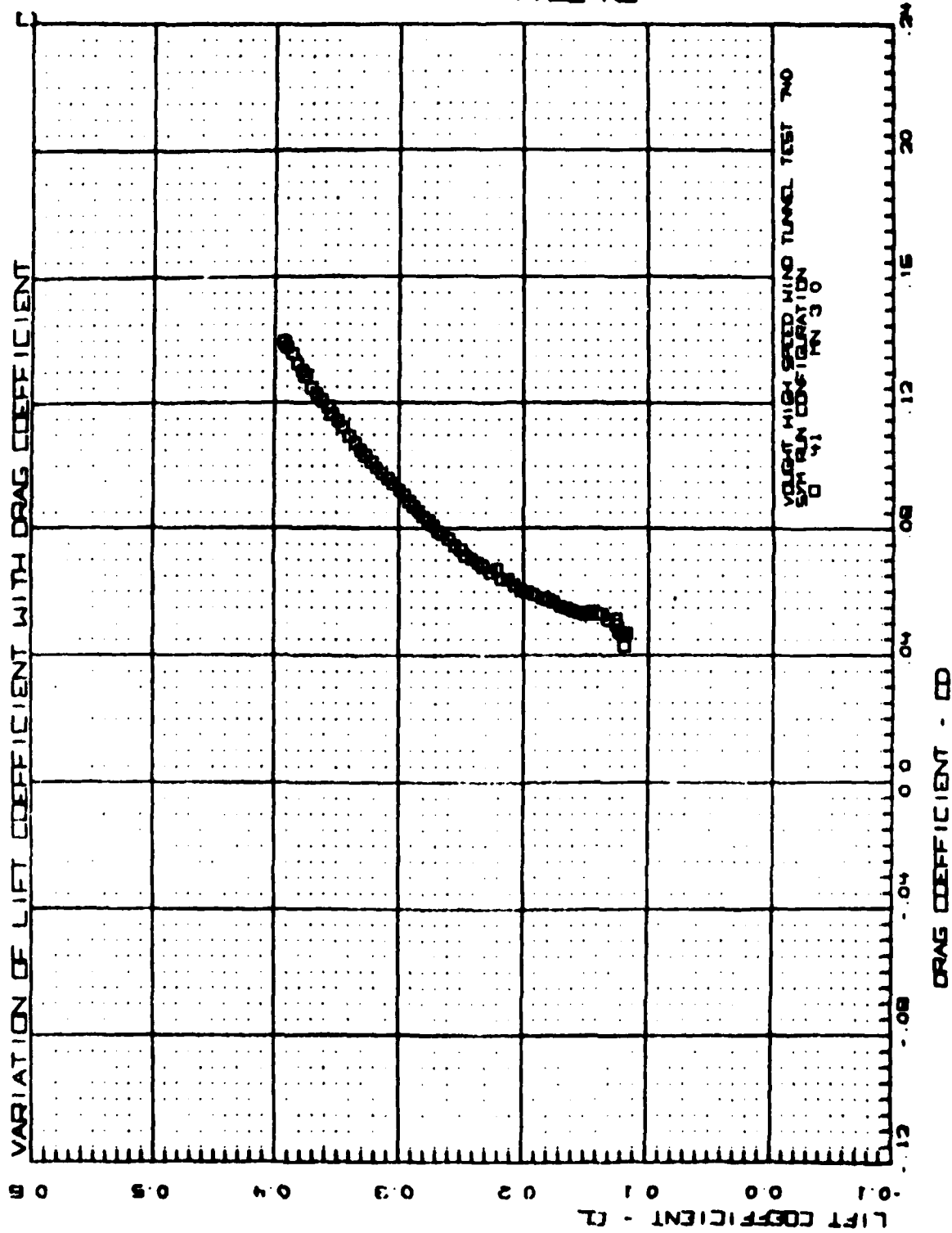


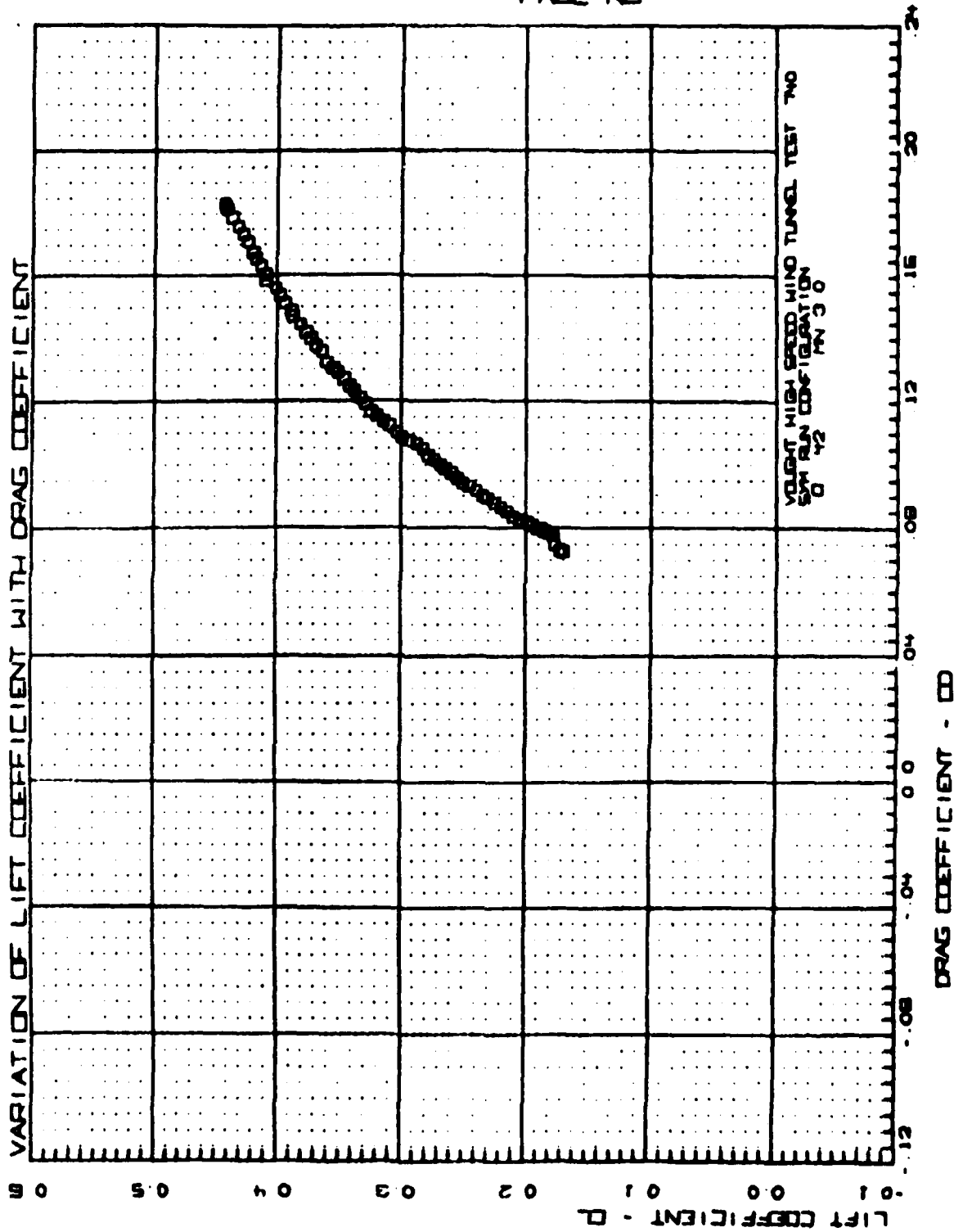


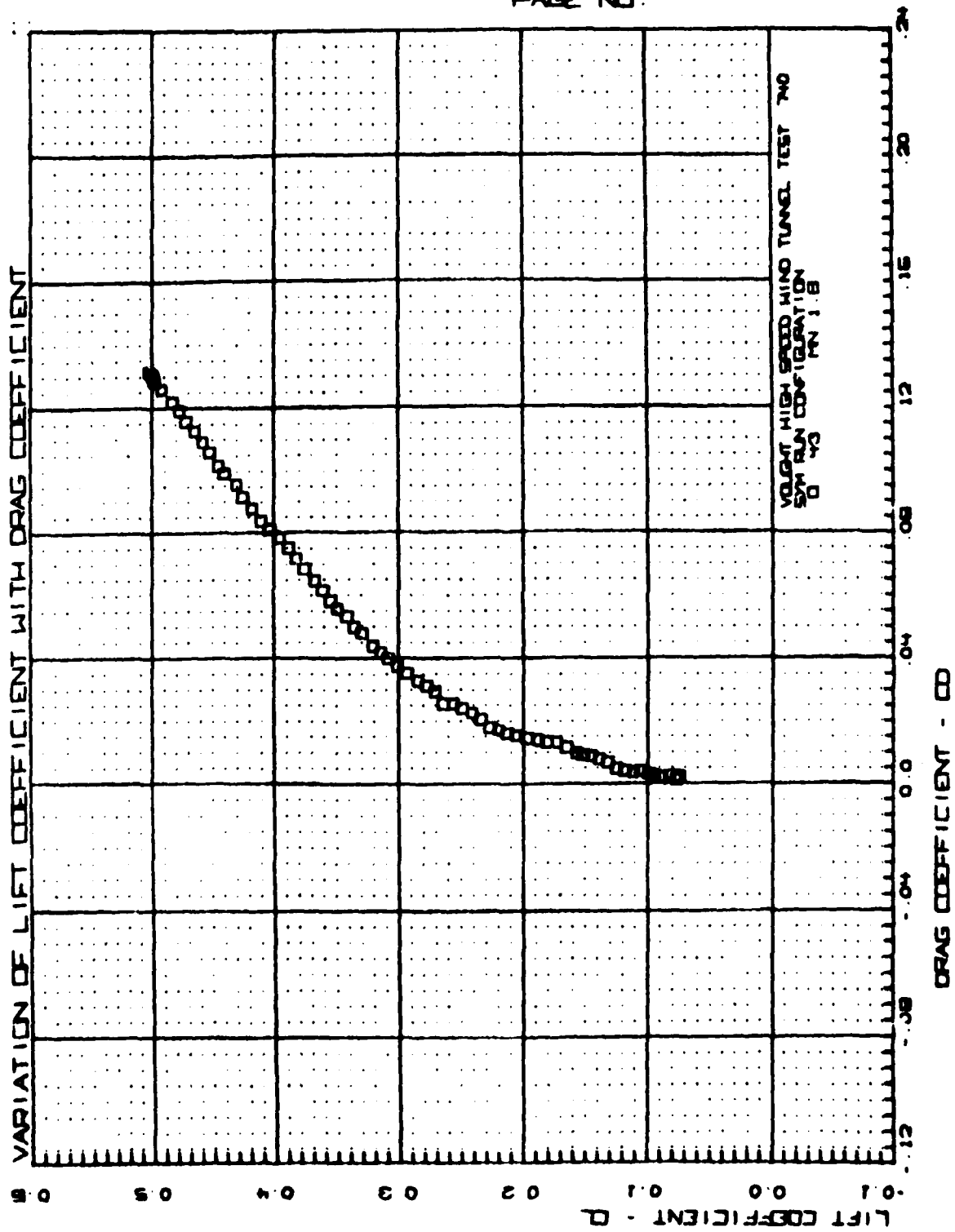
VOLIGHT HEAT TEST TWO
PAGE NO.

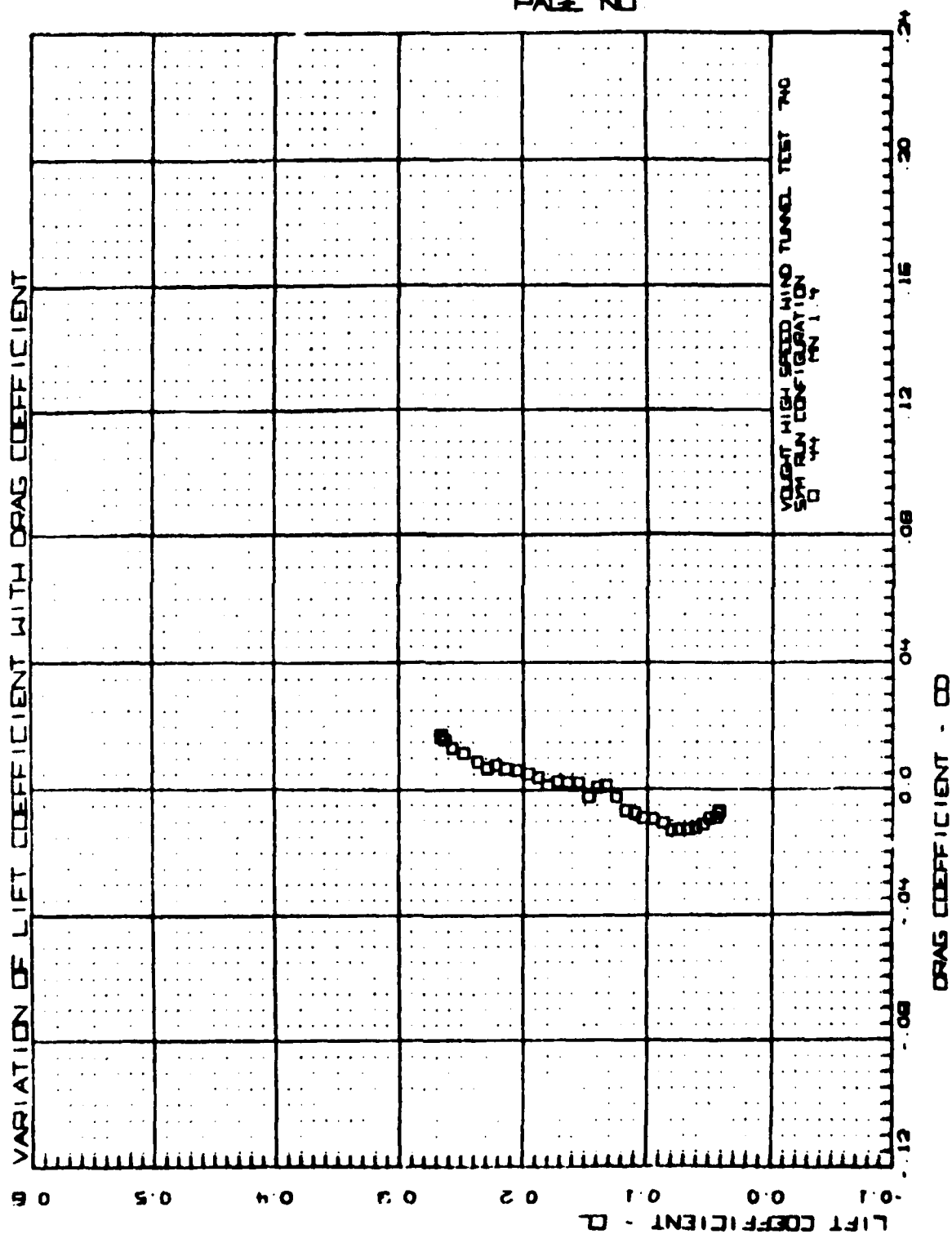


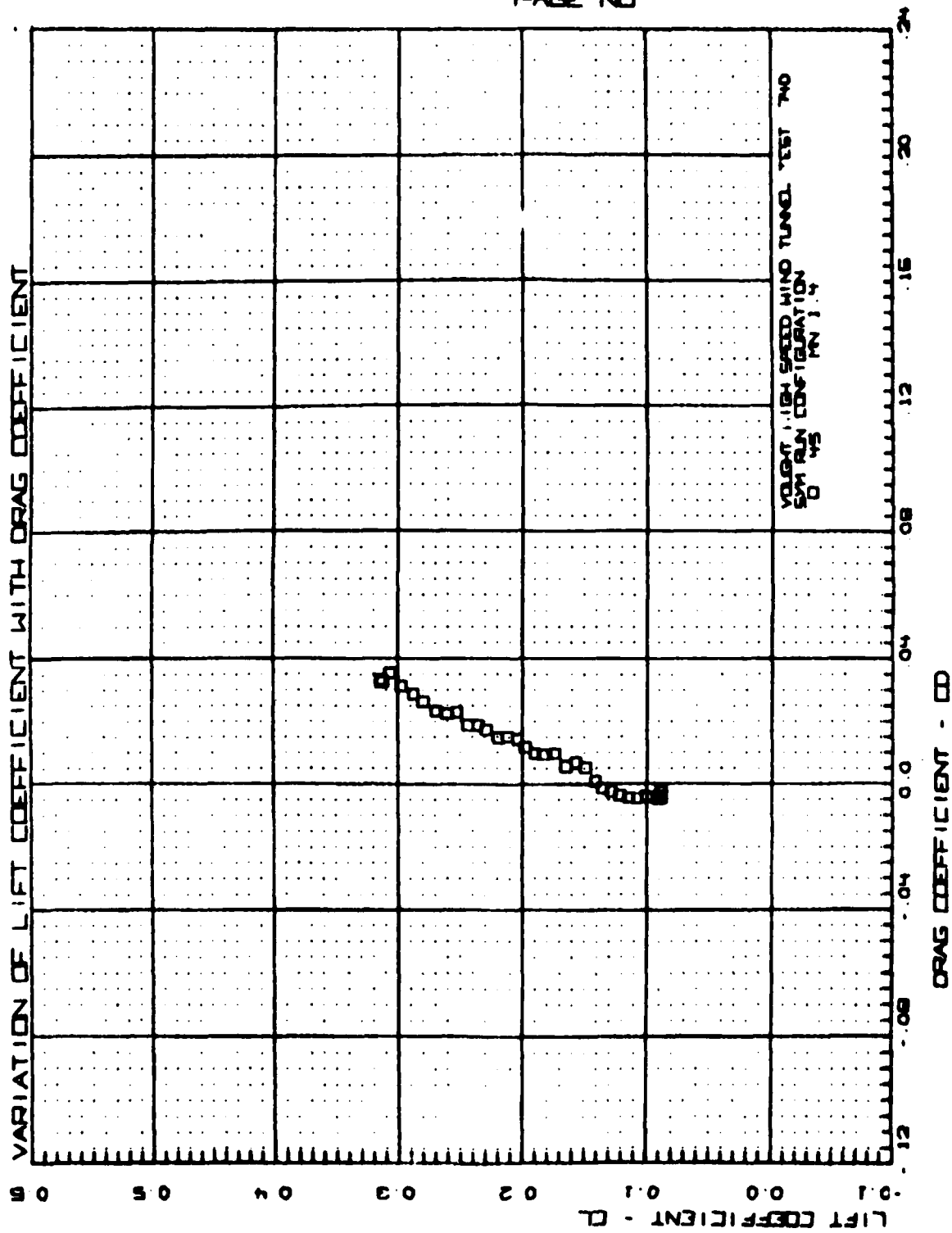


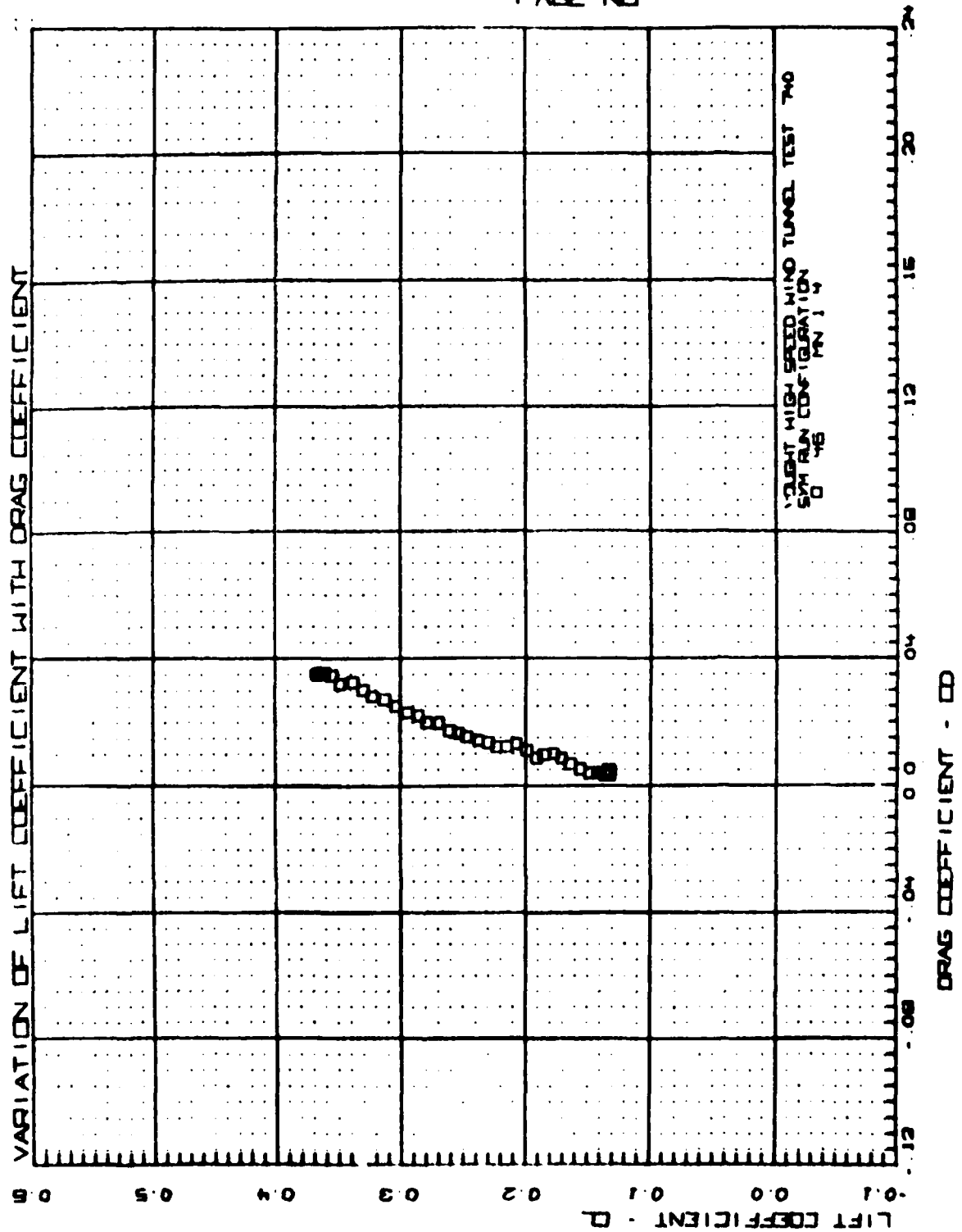


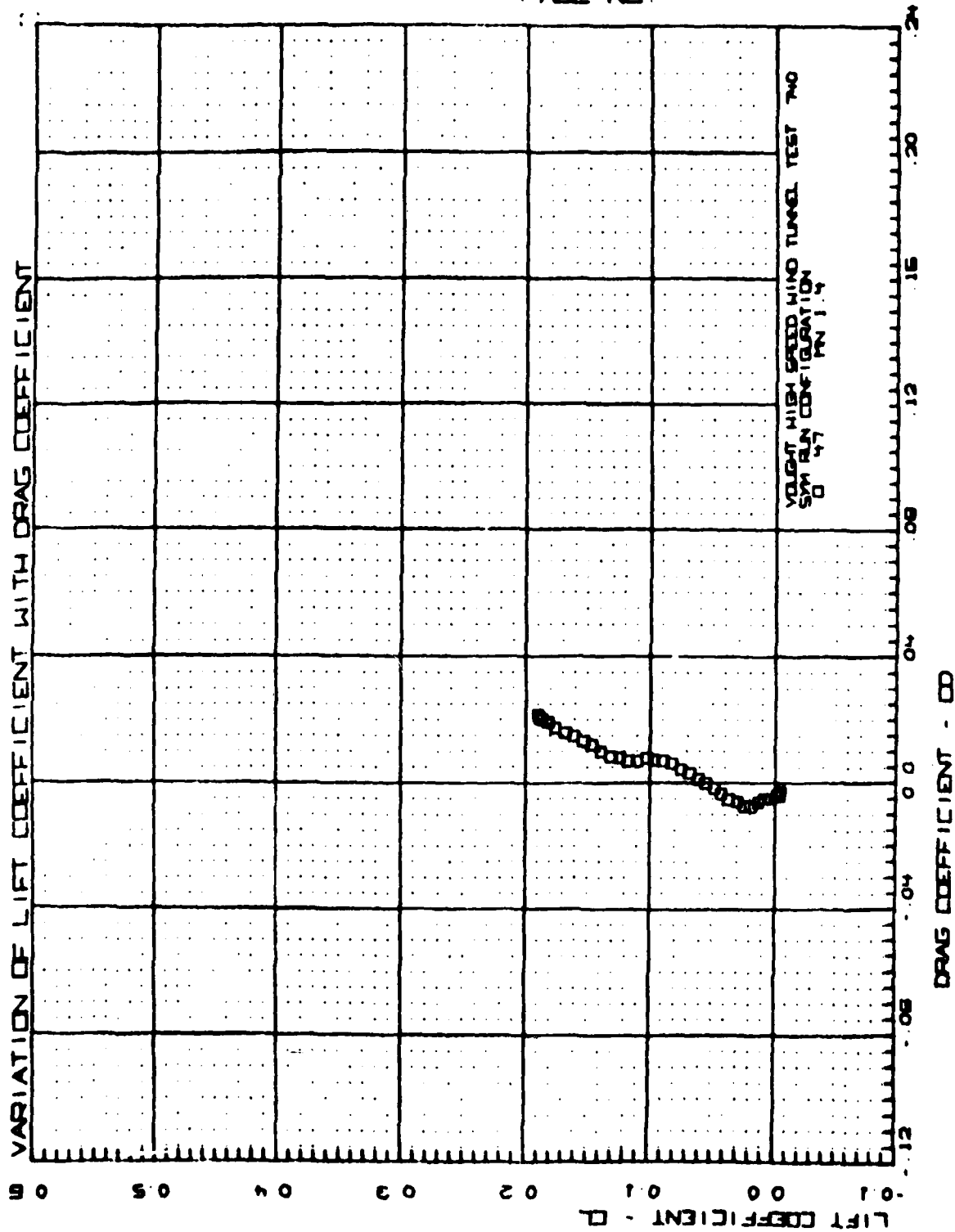


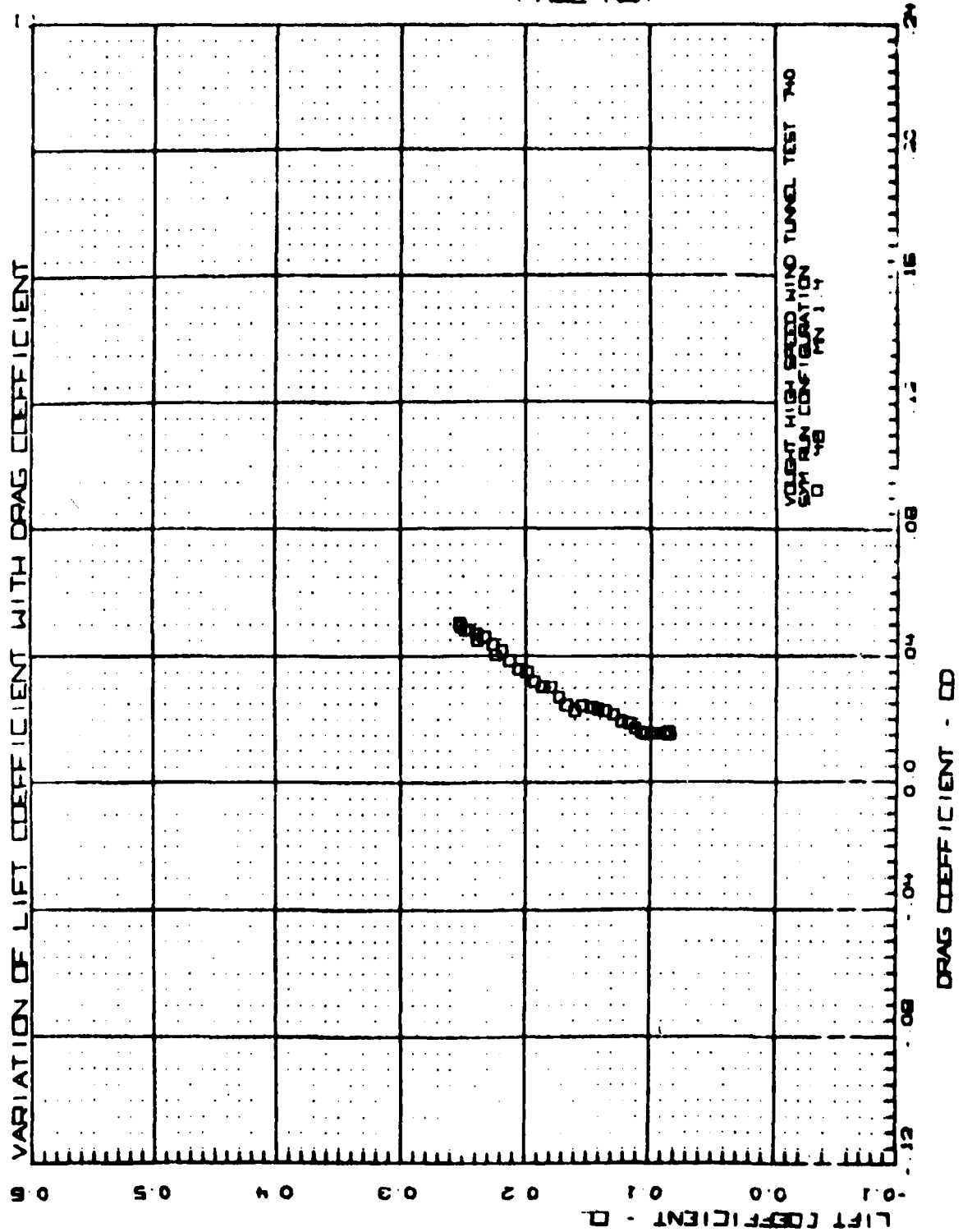


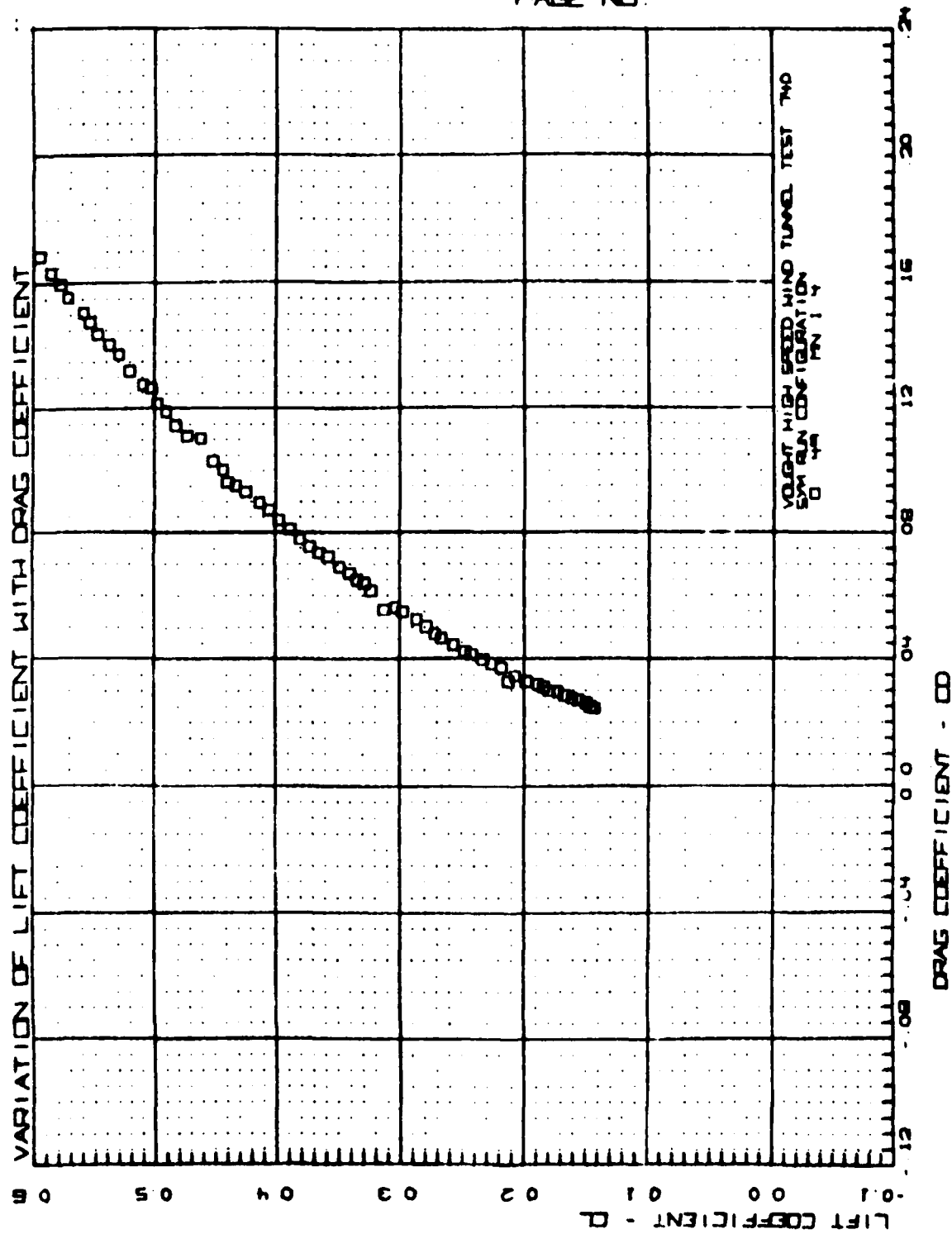


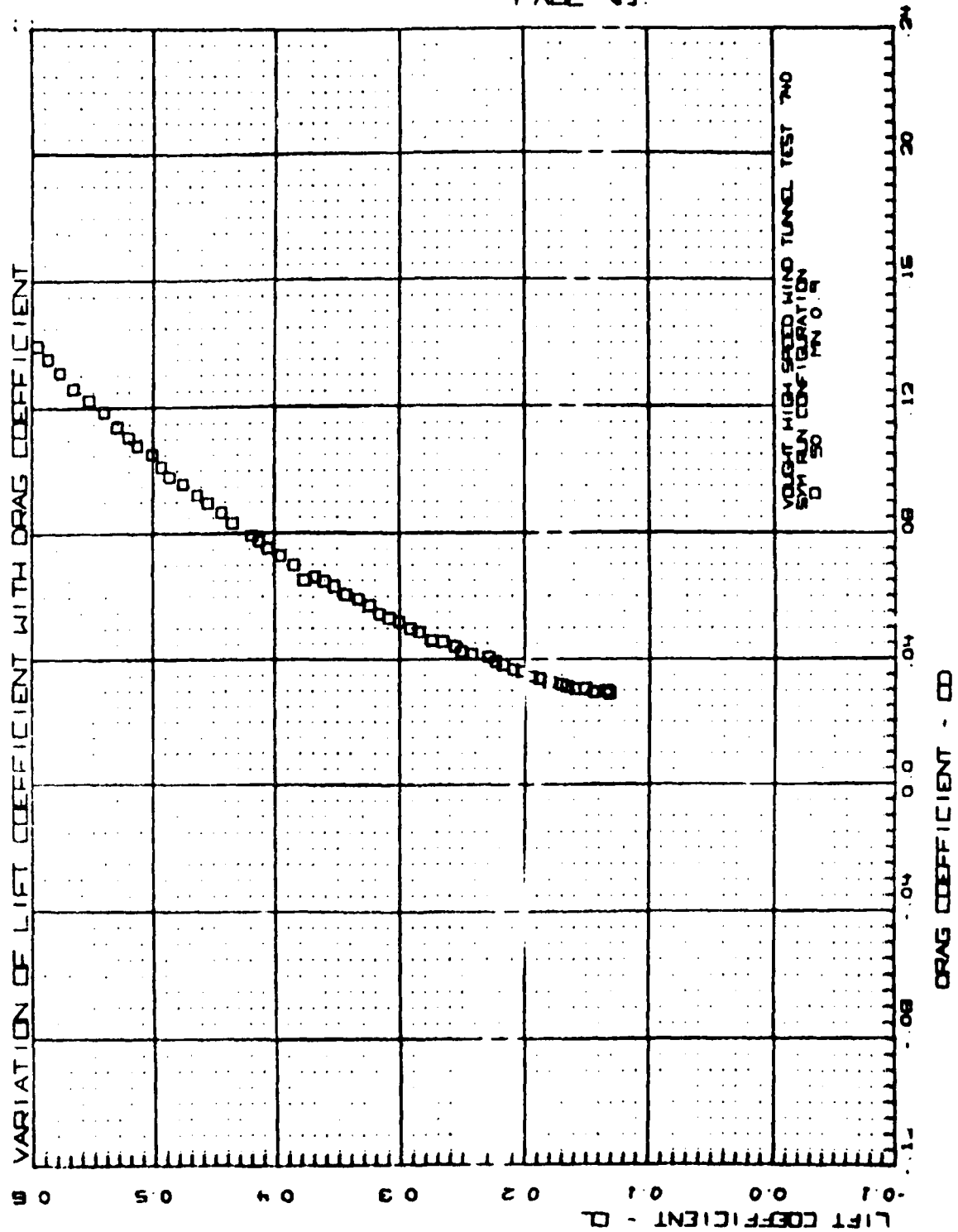


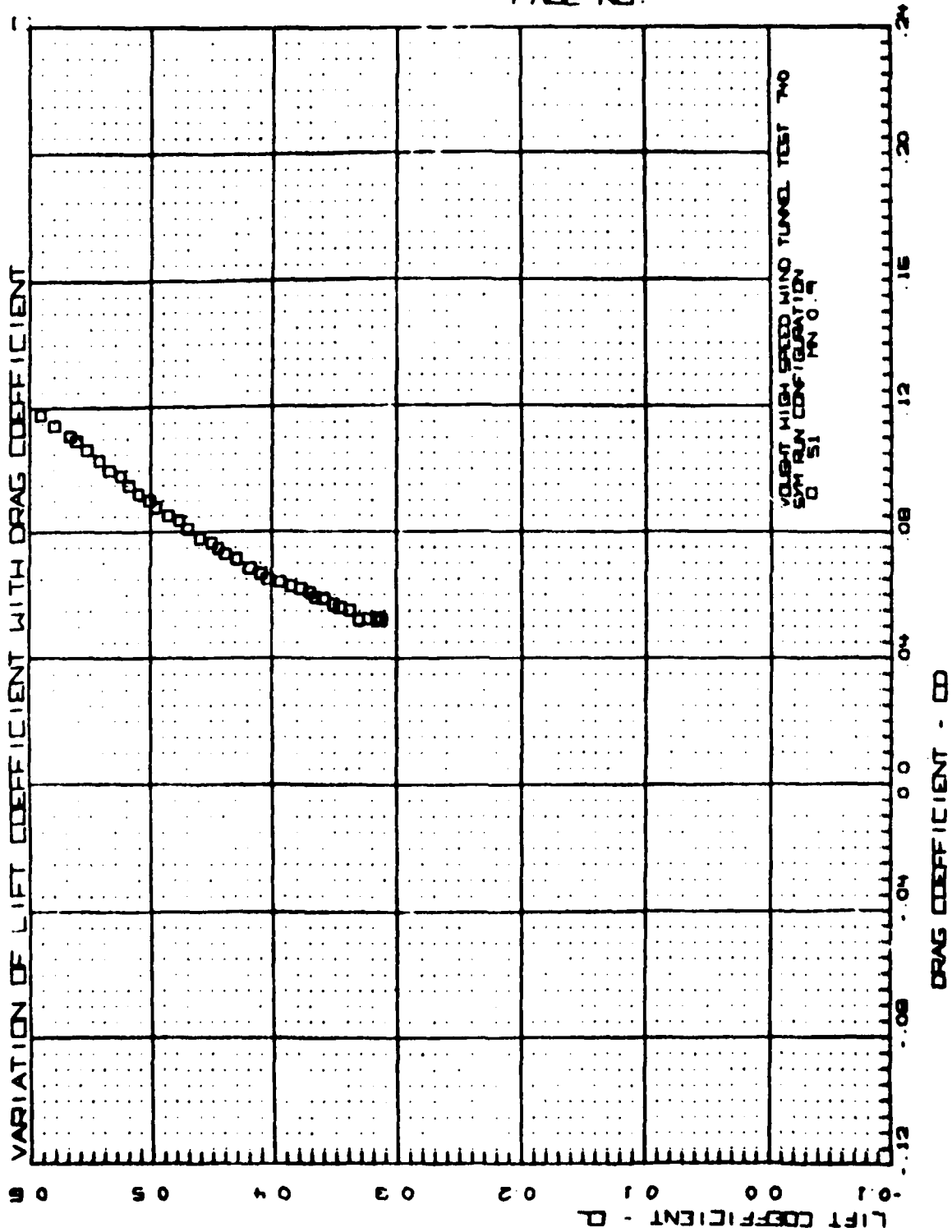


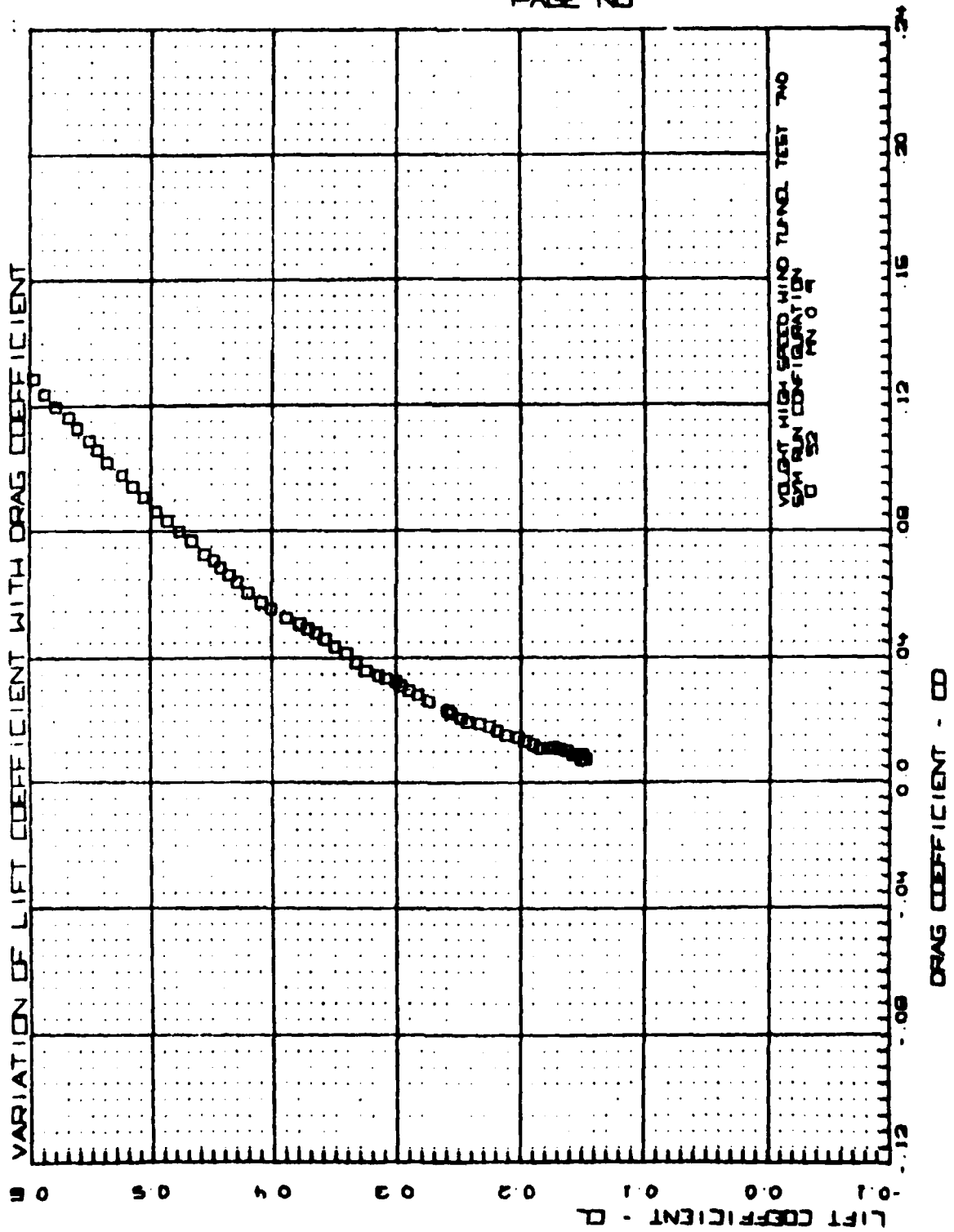




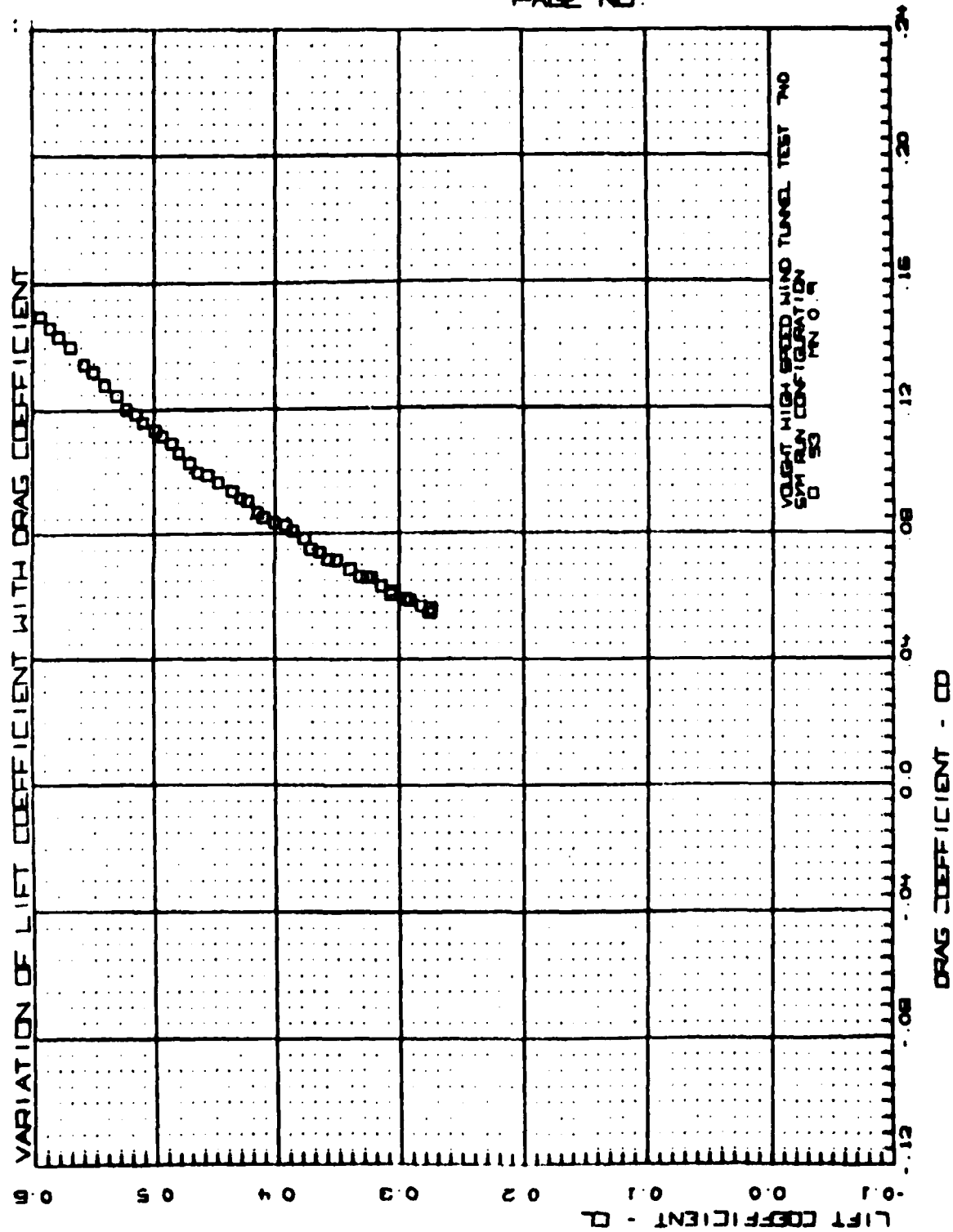


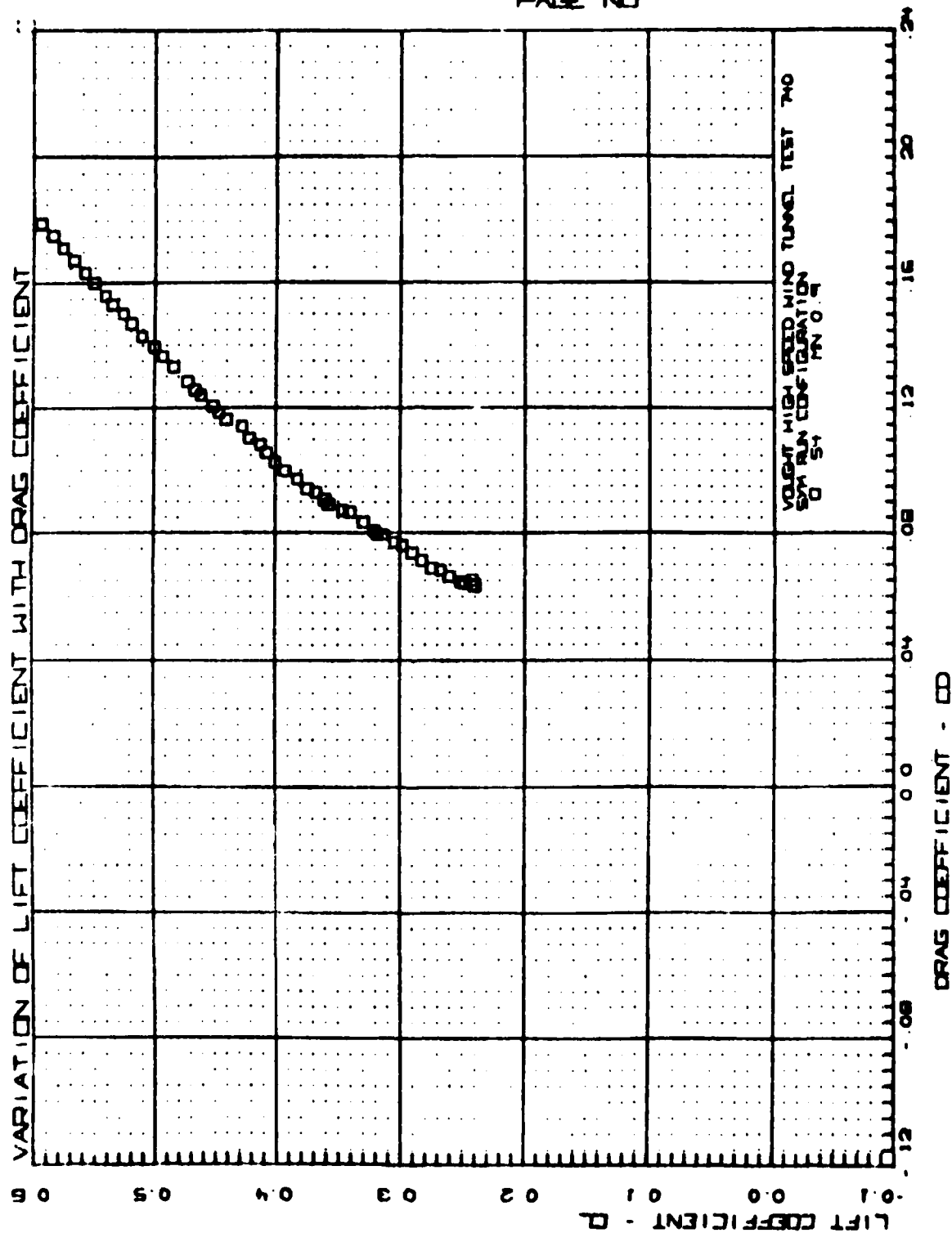


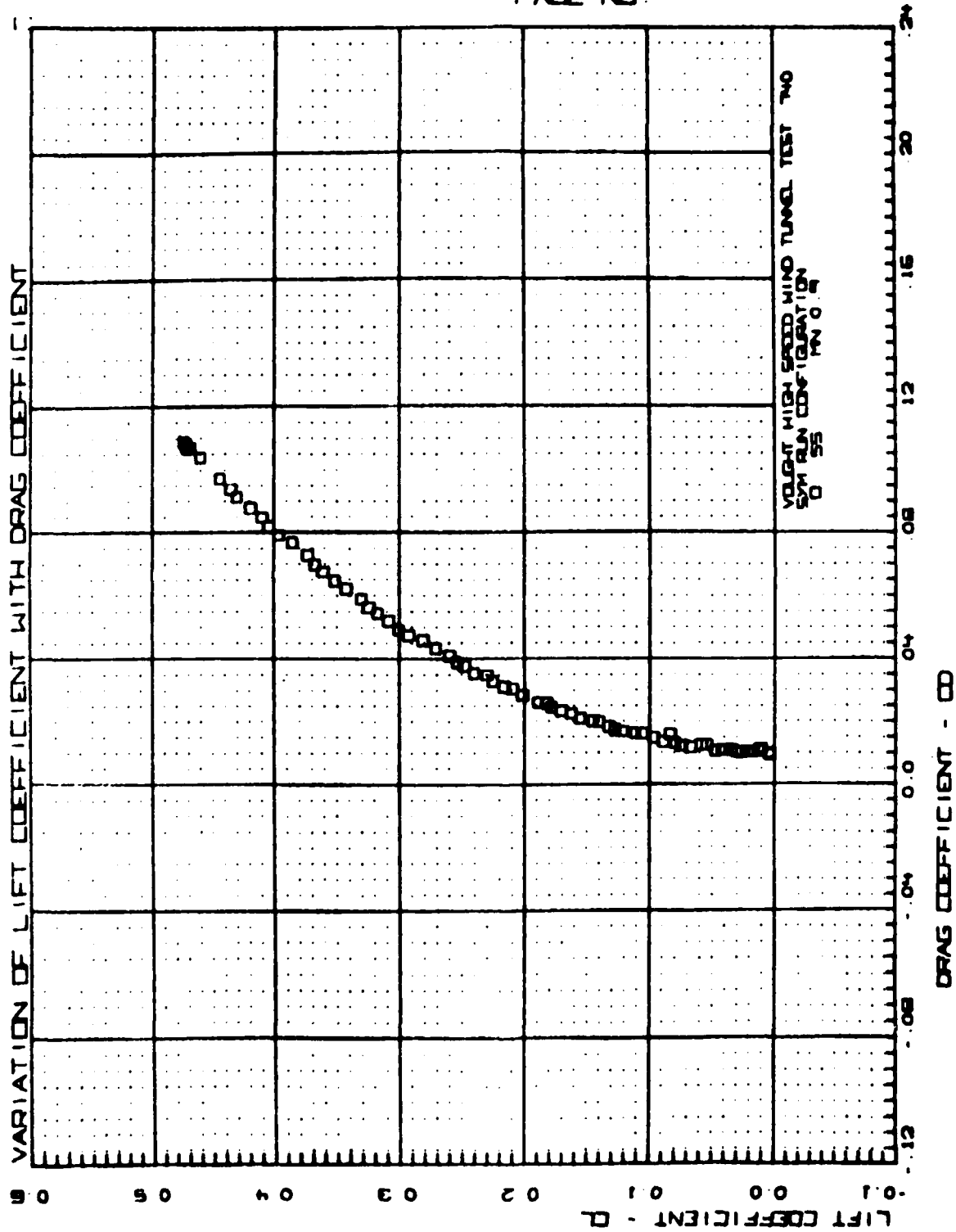


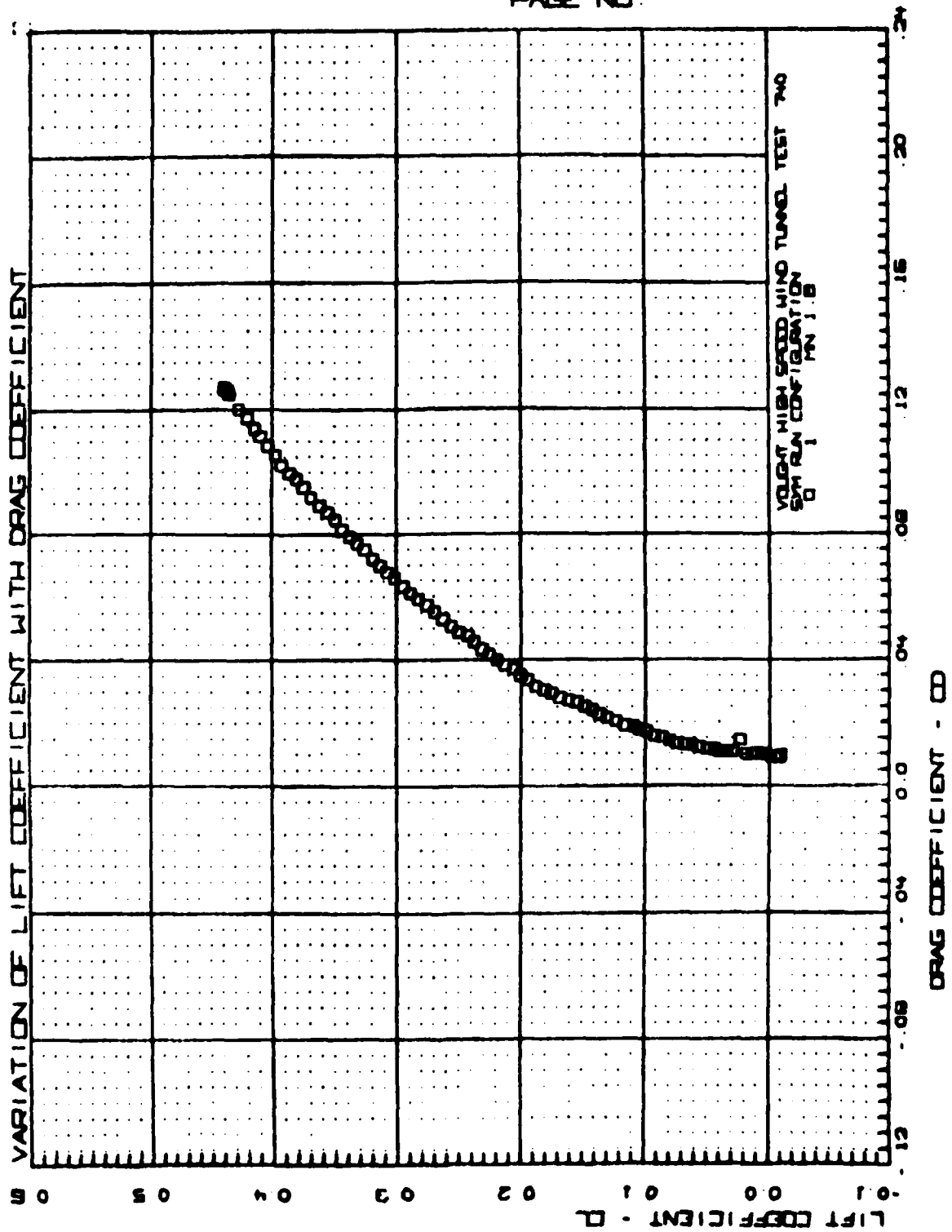


VOUGHT HEAT TEST TWO
PAGE NO.









DISTRIBUTION

Commander
Naval Sea Systems Command
Washington, DC 20360
Attn: SEA-62R41, Mr. L. Pasiuk
Technical Library

Commander
Naval Air Systems Command
Washington, DC 20360
Attn: AIR-320C
Technical Library

Commander
Naval Weapons Center
China Lake, CA 93555
Attn: Mr. Lloyd Smith
Mr. R. E. Smith
Technical Library

Office of Naval Research
800 N. Quincy Street
Arlington, VA 22217
Attn: Dr. R. Whitehead
Technical Library

Commanding General
U. S. Army Missile R and D Command
Redstone Arsenal, AL 35809
Attn: Mr. R. Deep
Dr. D. J. Spring
Technical Library

Commanding General
Ballistic Research Laboratory
Aberdeen Proving Ground, MD 21005
Attn: Mr. C. Nietubicz

NASA Langley Research Center
Langley Station
Hampton, VA 23365
Attn: Dr. R. C. Swanson, Jr.
Mr. C. M. Jackson, Jr.

Defense Technical Information Center
Cameron Station
Alexandria, VA 23314 (2)

GIDEP Operations Office
Corona, CA 91720

Commanding Officer
Air Force Wright Aeronautical Laboratories
(AFSC)
Wright-Patterson Air Force Base, OH 45433
Attn: Technical Library

Officer in Charge
Naval Intelligence Support Center
4301 Suitland Road
Washington, DC 20390
Attn: J. B. Chalk

Commanding Officer
Air Force Armament Laboratory
Eglin Air Force Base, FL 33543
Attn: Dr. D. Daniel
Technical Library

Commanding General
Army Armament Research and Development Command
Picatinny Arsenal
Dover, NJ 07801
Attn: Technical Library

Commanding Officer
Naval Ordnance Station
Indian Head, MD 20640
Attn: Mr. D. Krause

